INFORMATION TO USERS

This manuscript has been reproduced from the microfilm master. UMI films the text directly from the original or copy submitted. Thus, some thesis and dissertation copies are in typewriter face, while others may be from any type of computer printer.

The quality of this reproduction is dependent upon the quality of the copy submitted. Broken or indistinct print, colored or poor quality illustrations and photographs, print bleedthrough, substandard margins, and improper alignment can adversely affect reproduction.

In the unlikely event that the author did not send UMI a complete manuscript and there are missing pages, these will be noted. Also, if unauthorized copyright material had to be removed, a note will indicate the deletion.

Oversize materials (e.g., maps, drawings, charts) are reproduced by sectioning the original, beginning at the upper left-hand corner and continuing from left to right in equal sections with small overlaps.

Photographs included in the original manuscript have been reproduced xerographically in this copy. Higher quality 6" x 9" black and white photographic prints are available for any photographs or illustrations appearing in this copy for an additional charge. Contact UMI directly to order.

Bell & Howell Information and Learning
300 North Zeeb Road, Ann Arbor, MI 48106-1346 USA
800-521-0600

UMI®

Modeling Flow Through Natural Wetlands with a Modified Dynamic Wave Equation

by

DAVID A. STERN

A dissertation submitted to the Graduate Faculty in Engineering in partial fulfillment of the requirements for the degree of Doctor of Philosophy, The City University of New York.

2001

This manuscript has been read and accepted for the graduate faculty in Engineering in satisfaction of the dissertation requirement for the degree of Doctor of Philosophy.

1/26/2001
Date

Dr. Reza Khanbilvardi, Chair of Examining Committee
Director of Center for Water Resources and Environmental Research
Department of Civil Engineering: City College of CUNY

1-26-2001
Date

Dr. Mumtaz Kassir, Executive Officer

Dr. Lin Ferrand,
Department of Civil Engineering: City College of CUNY

Dr. John Fillos,
Chair, Department of Civil Engineering: City College of CUNY

Dr. Victor Goldsmith,
Director of Center for Applied Studies of the Environment
Department of Geology and Geography : Hunter College of CUNY

Dr. Lorraine Janus,
Director of Field Operations, Division of Drinking Water Quality Control,
New York City Department of Environmental Protection

Supervisory Committee

THE CITY UNIVERSITY OF NEW YORK

Abstract

MODELING FLOW THROUGH NATURAL WETLANDS WITH A MODIFIED DYNAMIC WAVE EQUATION

by

David A. Stern

Advisor: Professor Reza Khanbilvardi

This dissertation presents a mathematical model that simulates the hydrodynamics of natural wetlands. The model represents the first attempt to describe wetland flow dynamically with variables and coefficients that can be measured easily in the field.

A considerable amount of field data was collected to describe the hydrodynamics thereby providing a basis for the theory of the model and data for model calibration and verification. Several significant findings were found through dye tracer tests. Wetland type, flooding, and season significantly influenced the flow velocity through the wetland studied.

The model uses the full dynamic wave equation which has been modified to incorporate the effects of wetland stream sinuosity and vegetation. These properties can be related to the U.S. Fish and Wildlife Service's National Wetland Inventory Classification Scheme.

The computer program developed for the model (DYNAWET) is based on the U.S. National Weather Service's FLDWAV program with significant modifications to solve the equations developed in this dissertation. The DYNAWET model replaces the Manning's equation expressions for the flood plain conveyance with new equations that specifically account for the porosity, average vegetative stem diameter, and drag friction that are unique

for flow through vegetation. The calculation of cross-sectional areas also is modified to include a wetland porosity parameter. Comparison of the model output with stage data collected in the field demonstrates a close correspondence between the two.

An important application of the DYNAWET model is to use its output in a transport model to simulate pollutant transport through wetlands. This application could provide information that is essential for water utilities in their protection of water supplies. Water suppliers are particularly interested in the transport and fate of the (oo)cysts from two human parasitic protozoan organisms: *Giardia* spp. and *Cryptosporidium* spp. as they travel through the wetlands of their watersheds. A theoretical particle model is presented to estimate concentrations of particles leaving a wetland in the size range of (oo)cysts. Since reliable particle counting data of natural waters could not be obtained, the theoretical particle model was based on an analytical equation instead of a numerical algorithm.

Acknowledgments

First and foremost I must acknowledge the support and understanding I received from my family throughout my academic education. My family sacrificed my undivided attention to allow me to concentrate on completing this program. My soul mate Barbara, who has shared the best and worst experiences in life with me, used her outstanding research skills and intellect to assist me in finding pertinent literature and edit the dissertation. She also sacrificed my presence at many dinners to encourage progress on my studies, while managing to keep our family thriving. We were fortunate enough to be blessed with my three children Austin, Jamie and Jared during my studies. They have served as an inspiration to set the example of striving to achieve the highest educational accomplishments. I deeply thank my father, Leonard Stern, for not only helping me find time to work on this study, but for encouraging me take advantage of opportunities that were not offered to him. My brothers, Lawrence and Richard, and their families also provided valuable inspiration during this endeavor.

I thank my advisor Reza Khanbilvardi for not just being an advisor but a colleague and friend. His advice and support were critical in completing my studies. He represents the best faculty that City College has to offer in its long tradition of excellence in Engineering. I was fortunate to be able to select an excellent committee. Lin Ferrand supplied indispensable advice on how to develop equations. Lorraine Janus provided insight on data interpretation and presentation. Her encouragement was greatly appreciated. Victor Goldsmith gave enthusiastic support in studying the positive effects of wetlands and provided assistance with understanding the potential utility of using GPS and GIS.

I would also like to thank the Pathogen Program staff I supervise at DEP, who

furnished support in obtaining the information and data to make this research possible.

Table of Contents

Table of Contents (continued)

List of Tables

List of Figures

List of Figures (continued)

List of Figures (continued)

1. INTRODUCTION

Research on describing the mechanisms that define the hydrodynamics and pollutant removal of naturally occurring wetlands has been limited. Almost all the studies in the literature addressing these topics have been in regard to constructed wetlands. Natural wetlands have been described generally through studies that provide percent reduction of various pollutants. Accordingly, there is a large opportunity to study the hydrodynamics and pollutant removal of natural wetlands in further detail.

This study focused on developing techniques to simulate the hydrodynamics and associated removal of particles by natural wetlands. The size of the particles of greatest interest are those in the same range as two human parasitic protozoans of *Giardia* spp. cysts and *Cryptosporidium* spp. oocysts [henceforth referred to collectively as (oo)cysts]. These organisms have been found to be significant waterborne human pathogens that resist conventional disinfection treatment. Accordingly, understanding the hydrodynamics that significantly influence the transport and fate of particles that are in the same size class as (oo)cysts will provide suppliers of drinking water insight into watershed management for particle and (oo)cyst reduction.

1.1. Statement of Problem

Accurate determination of the retention time that a natural wetland provides under different climatic and flow conditions is essential to determine the extent that wetlands provide natural disinfection of pathogenic organisms such as *Giardia* and *Cryptosporidium*. An adequate model to meet this need has an additional constraint that

it must contain parameters that can be obtained with reasonable effort. It is often the case that resources devoted to obtain parameters for model simulations are limited and must be substituted with literature values or determined by best professional judgement. Accordingly, there is a need to develop models for natural wetlands with parameters that can be easily related to existing information or can be obtained without a large commitment of resources. The models also need to be developed with equations that provide adequate detail for the descriptions of the transport mechanisms for natural wetlands. This is especially important with regard to the differences found between natural and constructed wetlands. Natural wetlands often contain stream corridors that can meander. This feature can significantly affect the retention time between base and flood flows.

With accurate predictions of wetland detention time, methods need to be developed that begin to simulate the transport and fate of important human pathogenic protozoans through natural environments. Relatively few methods have been reported in the literature, none of which were developed for the wetland environment.

1.2. Approach

The focus of this dissertation is to provide an improved description of the flow through wetlands so that reliable and easily obtained values of retention time can be simulated. These values are used to determine the theoretical removal of (oo)cysts sized particles within the wetland system. To improve our understanding of the hydrodynamics of a natural wetland, intensive monitoring (including dye tracer tests) and the development of a hydrodynamic model was employed. To demonstrate the utility of this

model, a theoretical particle model was developed.

The hydrodynamic wetland model is based on the full dynamic wave equation to account for all the forces that may be present in a control volume of water within the natural wetland system. The dynamic wave equation included modifications reported in the literature that account for flood plain flow and meandering streams. This dissertation provides additional modifications with regard to the calculation of conveyance through more detailed descriptions of the flood plain cross-sectional area and friction factors. The highlight of these modifications is the incorporation of a new equation (4.23) that determines the conveyance of flow through the vegetated flood plain.

The hydrodynamic model was derived, calibrated and verified with field data collected in a natural wetland. The wetland system that was studied is located near an intake for a reservoir that is a source of drinking water for New York City (Figure 1.1). The watershed above the wetland has been urbanized with commercial and residential development. The discharge from the wetland eventually enters the source water reservoir (Kensico Reservoir) near the intake for an aqueduct that feeds water to New York City. Much of the physical parameters such as wetland boundaries, location and meandering of the stream corridor, and extent of wetland type were determined with a Global Positioning System (GPS) that provided location data for the Geographical Information System (GIS). This system used the GPS derived data to calculate channel and flood plain lengths, channel sinuosity, flood plain widths, and to associate the

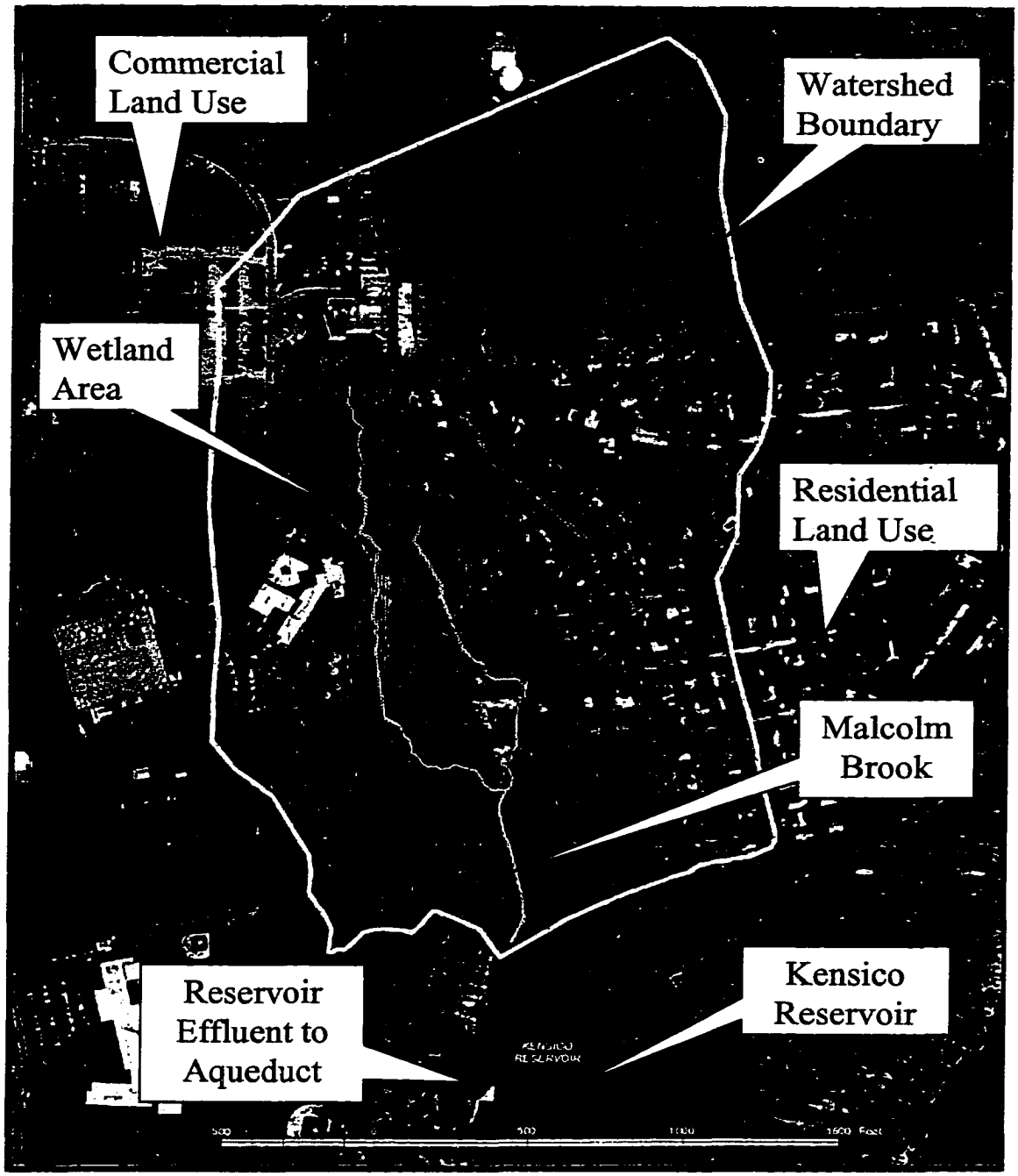

Figure 1.1 Infra-red aerial photograph of the Malcolm Brook watershed. The Malcolm Brook wetland is located on the western branch of Malcolm Brook next to a commercial complex. The watershed is composed of a mix of residential and commercial development and drains to Kensico Reservoir near the effluent aqueduct.

wetland "type" attribute to these features.

The particle model incorporates the theories of Residence Time Distribution (RTD) and treats the wetland as a system consisting of a plug flow reactor followed by a series of continuously stirred tank reactors. The number of continuously stirred tank reactors was determined empirically with the use of dye tracer tests. The particle model assumes a net reduction in particles for the retention times found in the wetland. A demonstration of how particle transport would behave under a reduction assumption is provided by using estimated values for particles based on turbidity data. Reliable particle data needs to be collected to calibrate and verify the particle model and confirm this assumption.

The following chapters review the background information available on wetland modeling and pollutant removal by wetlands, furnish information on the extensive data that was acquired for the study, present a new wetland flow model and provide a discussion on the findings of the study. Additional research is suggested to further improve our understanding on how wetlands remove pollutants. The theoretical particle model and documentation for the hydrodynamic model are provided in appendices.

2. LITERATURE REVIEW

2.1. General Wetland Hydrology

The most important parameter influencing the effectiveness of wetlands in retarding and removing pollutants is the hydrology of the wetland (Mitsch, 1993). How quickly water moves through a wetland system has generally been determined by mass balance analyses of the sources and sinks of the water. The United States Environmental Protection Agency (EPA) recommends determining precipitation, inflow, outflow, evapotransporation, wetland boundaries, slope, channel geometry and Manning's n of a wetland through field measurements and literature values to estimate all inputs and outputs needed to balance the hydrology of a wetland. (Jarosewich 1987; U.S.E.P.A. 1985).

2.2. Existing Hydrodynamic Models For Wetlands

2.2.1. General Information on Wetland Models

Based on the work of Costanza and Sklar (1985) in evaluating the articulation, accuracy, and effectiveness of wetland models, mathematical models for wetlands can be categorized into those that principally simulate hydrologic functions, biomass production, carbon cycling, energy flow, phosphorus cycling or a combination of these. Modeling of hydraulic (i.e., flow movement) properties of wetlands is most often a part of models for the hydrologic, biological and chemical functions of wetlands. The hydraulic properties of wetlands describe how water flows through the system.

Much of the early development of mathematical techniques to model wetland hydraulics was conducted by Federal agencies such as the United States Environmental Protection Agency (EPA) and the Army Corps of Engineers (ACOE) (Kadlec et. al, 1981). Comprehensive hydrologic models such as the ACOE's HEC Series and the EPA's Storm Water Management Model (SWMM) contain subroutines that implicitly and explicitly simulate wetland function. More recent efforts at improving these techniques have evolved from efforts to model specific lake, river or wetland systems (Mitsch and Reeder, 1991) and constructed wetlands for wastewater or stormwater treatment (Hammer, 1989; Kadlec and Knight, 1996; Novotny, 1989). Overall, however, the major hydraulic properties of wetlands have continued to be described through the hydrodynamic flow equations (primarily Manning's Equation) that were put to widespread use through the models of the Federal agencies.

Modeling techniques that simulate the hydraulics of wetlands are an integral component of larger models that simulate the hydrology of watersheds. The hydraulics of wetlands are an important component of hydrology models due to their significant effects on the flow of water through a watershed. In fact, modelers have indicated overland flow as the major forcing function in their models (Mitsch and Reeder, 1991). An accurate model of wetland hydraulics can enable models for entire watersheds to improve predictions of how water will behave in the system.

Determination of specific hydraulic characteristics for wetlands that most significantly influence flow are key to the development of accurate wetland models. is the that are significant enough to explicitly incorporate them into the model. Some insight for determination of these characteristics can be gained by reviewing the basic design

principles that have been published for the use of constructed wetlands to improve water quality of stormwater runoff. These wetland design principals include the size and shape of the system, type of flows (sheet and channel): vegetation type and density, wetland area to watershed area ratio, buffer areas, and land use of wetland watershed (Schueler, 1992, Kadlec and Knight, 1996). These parameters are similar to those needed to model an open channel system. The exceptions are vegetation type and density which are likely to have a large influence on the wetland flood plain hydraulics.

Water moving through a wetland is influenced most by the hydraulic gradient of the water, frictional stress at the bottom, and drag due to obstructions in the water column (Miller, 1987; Jadhav 1995; Kadlec and Knight 1996; Kadlec 1994). In wetlands, obstructions in the water column and surface generally consist of vegetation as indicated in the wetland design principals. The resulting stresses are most often described in hydrologic models through friction factors in general flow formulas. Two general flow formulae have been used most often to describe the hydraulic properties of wetlands: Manning's Equation for surface flow and Darcy's Law for flow through porous media.

2.2.2. Darcy's Law Applied to Wetlands

Models that describe the hydrodynamics of subsurface wetland treatment systems incorporate the general flow equation based on Darcy's Law (Kadlec and Knight, 1996). For Darcy's Law to be applicable, flow must be laminar (i.e., Reynold's number equal to or less than one). Dye-tracer studies of wetlands appear to support a laminar flow mechanism through the detritus zone of the wetland (Kadlec et. al, 1981; Kadlec and Knight, 1996). Darcy's Law is given by the following equation:

$$Q = -KA\frac{dH}{dX} \tag{2.1}$$

where:

Q= the flow across total cross-sectional area including space occupied by porous material;

K= hydraulic conductivity of the wetland and

dH/dX= change of head with respect to distance.

The frictional forces of the wetland are described in Darcy's Law through the hydraulic conductivity (K) variable. Hydraulic conductivity is generally small for wetlands. These values reflect the fact that flow through a wetland's detritus zone is retarded due to the lack of pore spaces caused by the high organic material content of this zone. Although Darcy's Law has been used primarily to describe flow through subsurface wetland treatment systems, its use is not widespread in the mathematical models used to describe natural wetland systems.

2.2.3. Manning's Equation Applied Wetlands

The more commonly used general equation for modeling wetland hydraulics has been Manning's Equation. This equation is used to simulate both turbulent and laminar flows seen in wetland systems although its derivation assumes turbulent flow (Kadlec et. al, 1981). The following formula presents Manning's Equation for surface flow through a

riverine wetland (Mitsch, 1993):

$$Q = \frac{AR^{2/3}S^{1/2}}{n} \qquad (2.2)$$

where:

Q is the surface channelized flow into (i) or out of (o) the wetland in m^3/sec.

A is the cross-sectional area of the channelized flow in m^2.

R is the hydraulic radius in m which equals A/wetted perimeter (P).

S is the dimensionless channel slope.

n is the dimensionless Manning's roughness coefficient

As mentioned above, the major frictional forces within a wetland are produced by vegetation. The Manning's roughness coefficient has been empirically derived for several types of rivers and flood plains. Manning's n values for vegetative flood plains are presented in Table 2.1. This table shows a range of Manning's n values reported

Table 2.1. Range of Manning's n values reported for wetlands.

Manning's n	Wetland type	Reference
0.022	Straighten earth canals	Chow, 1959
0.03-0.07	Natural channels, top width at flood < 100ft	Gupta, 1989
0.035	Winding natural streams with some plants	Lee, 80
0.04-0.10	Natural channels with pools, top width < 100ft	Gupta, 1989
0.040-0.050	Mountain streams with rocky streambed	Lee, 80
0.042-0.052	Winding natural streams with high plants growth	Lee, 80
0.06	Short marsh grass	Miller, 1987
0.065	Sluggish streams with high plant growth	Chow, 1959
0.112	Very sluggish streams with high plant growth	Chow, 1959
0.100	Very weedy reaches	Chow, 1959
0.125	bulrush	Miller, 1987
0.24	dense grasses	Chapman, 1991

between 0.022 and 0.240. By far the most extensive estimation of various Manning's n was done by Chow, (1959). His results range from 0.025 for a short grass flood plain wetland to 0.150 for a very weedy stream. It is important to note, however, that these empirically derived values reflect the relatively large scale river and flood plain systems that they were derived from. On this scale, the depth of flow is often much larger than the depth of vegetation or the detritus zone. Accordingly, the impact from these features is relatively small. In much smaller systems, the impact of vegetation and the detritus zone can result in proportionally much larger frictional forces. Larger Manning's n values would be needed to describe this.

Miller (1987) concluded that "effective" Manning's n values for wetlands are a reflection of both bottom stress and form-drag friction factors. This is evident since Manning's n values for wetlands have been found to be depth dependent (Kadlec and Knight, 1996). As flow depth increases, the n value decreases which results in larger velocities to keep balance in the Manning's equation. This relationship can be described as follows (Kadlec and Knight, 1996):

$$\frac{n}{n_1} = \left(\frac{h_1}{h}\right)^m \tag{2.3}$$

where:

n is the friction factor, n_1 is a known n value for h_1

h is the water depth, h_1 is the water depth known for n_1

m is an empirically derived coefficient

In some studies, (m) has been found to be equal to 1; therefore the relationship was a simple linear proportion (Kadlec and Knight, 1996). For depths greater than 20 cm in wetlands that are sparsely vegetated, the value of m was from 0.33 to 0.50. Smaller depths with the same vegetation had m values from 1.0 to 2.0. Kadlec and Knight (1996) have suggested estimating the friction factor for densely vegetated wetlands by $1.0\ h^{-1.7}$ ($0.1 \leq h \geq 1.0$m) and sparsely vegetated wetlands by $0.2\ h^{-1.7}$ ($0.05 \leq h \geq 1.0$m) based on several studies (Shih et al., 1979; MacVicar,1985; Shih and Rahi,1982; Mierau and Trimble, 1988;Kadlec et al.,1981; Hammer and Kadlec, 1986; Kadlec, 1990; Hall and Freeman,1994).

2.2.4. Kadlec Model for Wetland Velocity

Concerns over errors in accurately modeling wetland flow using Manning's equation with "effective" Manning's n values have led to new forms of the friction equation. Manning's Equation describes turbulent flows affected most by bed friction. Flow through wetlands often tend to fall in the transition zone between laminar and turbulent flow and are strongly affected by vegetative resistance (Kadlec, 1990). To account for the variable nature of the roughness coefficient, vegetative and bottom elevations, Kadlec (1990) has proposed a power law model which modifies the

Manning's equation by relaxing the coefficients in the equation. This equation is as follows:

$$\frac{Q}{W} = K d^{\beta} S^{\alpha} \qquad (2.4)$$

where:

Q is the flow.

W is the width of the wetland.

K is an empirically derived pre-multiplier.

d is depth of flow.

β is an empirically derived depth exponent.

S is slope.

α is an empirically derived slope exponent.

Based on his experience with numerous empirical studies (Kadlec et al., 1981; Hammer and Kadlec, 1983; Hammer and Kadlec, 1986; Roig and King, 1993; Kadlec, 1990), Kadlec recommends using a β value equal to 3, an α value equal to 1 and a K value equal to 1×10^7 for densely vegetated wetlands and 5×10^7 for sparsely vegetated wetlands (Kadlec and Knight, 1996). The limitation of this model is that the coefficients

are empirically derived lumped parameters. Since there have not been extensive empirical studies (such as those for the Manning's n), the model would be site specific to the wetlands that the coefficients were calibrated for and therefore not directly transferable to another wetland system. In addition, a significant amount of time and resources are needed to collect sufficient data to derive the model parameters; this makes practical application of the model an involved process.

2.2.5. Jadhav and Buchberger Model for Wetland Flow

Jadhav and Buchberger (1995) have suggested an alternative model that accounts for the vegetative friction and the reduced area of flow. This model is based on modifications to the full dynamic wave equation as given by the classic Saint-Venant equations (Saint-Venant, 1871). These equations are solved through implicit finite difference approximation methods (Jadhav, 1994). The governing equations for this model are as follows:

The one-dimensional continuity equation is given as:

$$\frac{\partial}{\partial x}Q + \frac{\partial}{\partial x}(\eta A) = 0 \qquad (2.5)$$

and the one-dimensional momentum equation is given as:

$$\frac{\partial}{\partial t}Q+\frac{\partial}{\partial x}\left(\frac{Q^2}{\eta A}\right)+\eta Ag\left(\frac{\partial y}{\partial x}-S_o+\frac{C_{db}P_eQ^2}{g(\eta A)^3}+\frac{C_{ds}DmByQ^2}{2g(\eta A)^3}\right)=0 \tag{2.6}$$

where:

Q is flow in m^3/s.

A is the cross sectional area of wetland channel in m^2.

x is the longitudinal distance along the wetland channel in m.

y is the water depth in m.

t is time in s.

S_o is the longitudinal slope of the wetland channel bottom.

g is gravitational acceleration in m/s^2.

B is the bottom width of the wetland channel in m.

P_e is the effective wetted perimeter in m (for a wide rectangular channel $P_e = \eta B+2y$).

D is the average stem diameter of the wetland vegetation in m.

m is the wetland vegetation density (in number of stems per unit area) in m^{-2}.

η is the porosity which equals $1-\pi/4(mD^2)$.

C_{db} is the drag coefficient associated with bed friction.

C_{ds} is the drag coefficient associated with stem friction.

This approach has been verified through theoretical simulations where vegetation is considered at zero or at a specific density. It is uncertain how well this model would perform on actual field data since wetland vegetation is seldom uniformly dense. In addition, this model includes several new parameters that would require considerable time and resources to obtain.

2.2.6. Development of Models using the Full Dynamic Wave Equation

The use of the full dynamic wave equation to model the hydrodynamics of a system began long before its application by Jadhav and Buchberger. The practical use of the equation for simulating hydrodynamics began several decades ago when digital computers became available to engineers and scientists so that numerical solutions could be applied. Early numerical solutions to the dynamic wave equation included the method of characteristics (Liggett and Cunge, 1975 and Abbott, 1979). However, these solutions were found to be difficult to program (USACOE, 1995).

The most often applied numerical approximation techniques have used finite difference methods. Explicit finite difference has been found to be generally unstable for applications of systems with shallow slopes (Strelkoff, 1970; Price,1974). The most common implicit method used to solve the Dynamic Wave Equation is the four-point

implicit method first applied by Preissmann (1961). Several further modifications were made to improve the method's stability and application (Amein and Chu, 1967; Amein and Fang, 1970; Fread and Harbaugh, 1971; Fread, 1973; Fread and Smith, 1978; DeLong, 1986; DeLong,1989; Fread, Jin and Lewis, 1996). The method resulting from these modifications is used to solve the one-dimensional dynamic wave equation in several United States Agency models. These models include the National Weather Services's Flood Wave Model (FLDWAV), the Army Corps of Engineer's CE-QUAL-RIV model and the United States Geological Survey's Full Equations Model(FEQ). A more detailed description of the application of the weighted implicit, finite difference method is provided below in Chapter 4. (Full Dynamic Wave Wetland Model).

2.3. Water Quality Attributes of Wetlands

Wetlands may remove up to 90% of the total suspended solids portion of turbidity (Schueler, 1992). In addition to pollution reduction, wetlands provide flood protection and critical habitats. However, research on the potential value of wetlands as natural filters is still in the early stages. Research directed at determining the attenuation of pollutants by wetlands has focused on sediment, nutrients (particularly nitrogen and phosphorus), pathogens, heavy metals and trace organic compounds. Much of the data collected has been from wetlands that were constructed for the primary purpose of treating municipal wastewater. However, natural wetlands are expected to yield similar pollution reduction and have done so when such data have been collected (E.P.A., 1988).

The ability of wetlands to improve water quality is derived from the following fundamental processes that occur in wetlands (E.P.A. 1988; Elder, 1987):

1. The low slope, low velocity and long retention time physically trap and settle pollutants suspended in the wetland influent;

2. The high sorptive capacity of wetland sediments entrap pollutants;

3. The diverse microbial community in both anaerobic and aerobic conditions of the sediment allow for significant biotransformation and utilization of influent pollutants; and

4. The high productivity biomass ratio of wetland vegetation consumes significant amounts of nutrients that may be present in the influent.

Table 2.2 presents a qualitative view of the specific removal mechanisms that wetlands provide (including physical, chemical, and biological processes) for contaminants found in wastewater (Stowell, 1979). The range of pollutant removal efficiencies of wetlands is presented in Table 2.3. It is important to note that many contaminants are removed at an efficiency greater than fifty percent and wetlands often

Table 2.2. Removal mechanisms in wetlands for contaminants in wastewater. P = primary effect; S = secondary effect; I = incremental effect (effect occurring incidental to removal of another contaminant). From Stowell, 1979.

Mechanism	Suspended Solids	Colloidal Solids	BOD	N	P	Heavy Metals	Refractory Organics	Bacteria and Virus
PHYSICAL								
Sedimentation	P	S	I	I	I	I	I	I
Filtration	S	S						
Adsorption		S						
CHEMICAL								
Precipitation				P	P			
Adsorption				P	P	S		
Decomposition						P		P
BIOLOGICAL								
Bacterial Metabolism		P	P	P			P	
Plant Metabolism							S	S
Plant							S	S
Adsorption				S	S	S	S	
Natural Die-Off								P

Table 2.3 Pollutant removal efficiencies by wetlands. From E.P.A. 1988

Species	% Removal
Total solids	40-75
Dissolved solids	5-20
Suspended solids	60-90
BOD 5	70-96
TOC	50-90
COD	50-80
N (total as N)	25-96
P (total as P)	10-50 (seasonal)
Heavy metals	65-98
Benzene	95-100
Toluene	98-100
Ethylbenzene	97-100
Chlorobenzene	91-100
Chloroform	94
Chlorodibromomethane	98-100
1, 1, 1-trichloroethane	98-100
Tetrachloroethylene	92
Phenol	81
Butylbenzyl phthalate	81
Diethyl phthalate	75
Isophorone	67
Napthalane	86
1,4-Dichlorobenzene	91-100

meet the removal efficiencies required for treatment plants under Federal and State pollution control programs.

2.3.1 Influence of Wetlands on Suspended Solids and Turbidity

The most significant removal mechanism for suspended solids within wetlands is sedimentation. Wetlands continually settle suspended solids although the rate of sedimentation may vary between wetlands and over time. Sedimentation is enhanced due to the reduced stream velocity through wetlands. Sediment removal in wetlands improves water quality by removing excessive sediments and contaminants, such as some nutrients and heavy metals that have adhered to suspended particles. Table 2.4 presents the cumulative effect wetlands have on water quality within different watersheds (Johnston, 1990.) Based on this table, 23-93% of the sediment found in the watersheds' streams was retained by the wetlands.

2.3.2. Influence of Wetlands on Pathogens

Pathogens include bacteria, parasitic protozoans and viruses. Research conducted to investigate the removal efficiency of bacteria by wetlands indicates approximately a 90% removal rate (E.P.A., 1988). Pathogens in wetlands are removed by the same mechanisms as in ponds; including predation by other microorganisms, sedimentation, absorption and unfavorable environmental conditions. New York City Department of

Table 2.4. Sediment storage in wetlands as a percentage of watershed erosion (from Johnston, 1990.)

Basins	State or Country	Area (km^2)	Sediment Stored in Wetlands, % of Total Erosion	Sediment Leaving Basin, % of Total Erosion	Sediment Stored in Wetlands, % of Suspended Sediment
Lone Tree Creek	CA	1.7	19	62	23
Upper Neuse	NC	1,997	15	14	52
Upper Tar	NC	1,119	21	8	72
Day Creek	NE	52	31	64	33
Coon Creek, 1853-1938	WI	360	58	6	91
Coon Creek, 1938-1975	WI	360	37	7	84
Gullied Basin	SE Australia	340	37	10	79
11 Small Basins	Luxembourg	3.5	14	34	29
Yendacott	Devon, U.K.	1.0	45	93	3

Environmental Protection (NYCDEP) has studied the influence of wetlands on pathogenic protozoans and has discovered that subwatersheds that incorporate larger percentages of wetland areas may discharge lower levels of pathogens (Stern, 1998). However, information on this topic is scant and other studies on the removal of parasitic protozoans and viruses by wetlands have not been found in the literature.

Based on the previous discussion presented in this chapter, there are several weaknesses regarding modeling natural wetlands that have been identified. Among these is the lack of models designed specifically for natural wetlands. Most models available for wetlands were designed for constructed wetlands and therefore, generally model steady state flow conditions. Another weakness is the limited application of dynamic equations to address for the complexity of flow through the vegetated flood plain. The one report on the application of the full dynamic wave equation did not provide consideration of the practicality of data collection to calibrate and verify such an approach. Accordingly, a model to simulate flow through natural wetlands needs to be based on dynamic equations that can account for the changes in flow and depth over time. These equations also need to address the complexities of flow through vegetation and the presence of meandering streams.

3. DATA ACQUISITION

3.1. Description of Study Area

The area studied was situated within the Malcolm Brook watershed which is located in a northern suburb of New York City in the Village of Valhalla, Westchester County, New York. The watershed is 108 acres in size, with slopes ranging from 1 to 25 percent, and with land uses that include commercial, residential and forest. The entire watershed is sewered. Malcolm Brook drains into Kensico Reservoir which is the source water reservoir for approximately 90 percent of the New York City water supply. The proximity of this watershed's discharge to one of the supply intakes has made it one of New York City's most monitored sub-basins.

Figure 3.1 provides a map of the Malcolm Brook watershed and the locations of routine monitoring stations. Monitoring sites were located throughout the watershed. The intensive data needed for model development was collected at the sites located within the wetland area. The upstream boundary was identified as the Malcolm Brook Fork (MBF) site which delineates the area where the flow splits between the two branches of Malcolm Brook. Downstream of MBF, the sites were identified in numbered order from upstream to downstream as Malcolm Brook Wetland sites one, two, three, four, and five (MBW1, MBW2, MBW3, MBW4, MBW5). Two additional sites were located in the flood plain areas of site MBW1 and MBW2 and identified as Malcolm Brook Wetland site one flood plain and Malcolm Brook Wetland site two flood plain (MBW1F, MBW2F). A permanently gaged station (MB1) is located downstream

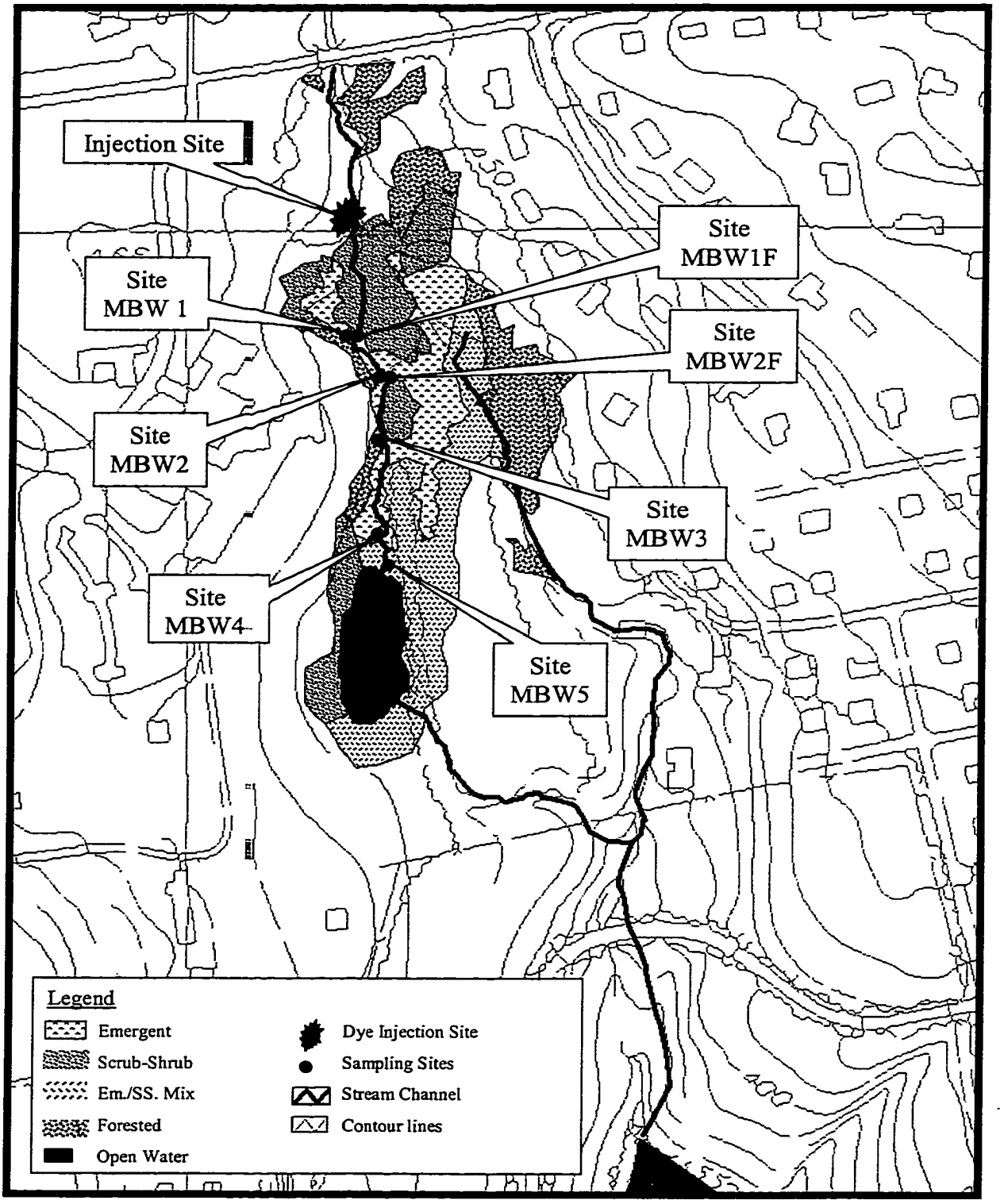

Figure 3.1. Map of segmented wetlands with monitoring sites.

of the location where the two branches of Malcolm Brook rejoin.

The watershed flows in a north-to-south orientation. The headwaters of the Malcolm Brook begin with the drainage from a commercial office development. Approximately 300 feet south of this development, the stream bifurcates. The eastern branch flows through a channelized and suburbanized area. The western branch travels through scrub-shrub, emergent and mixed (scrub-shrub and emergent) wetlands, empties into a shallow pond and flows in its southern reach through a steep channel. The channels rejoin just north of West Lake Drive and flow approximately 600 feet to the reservoir.

The Malcolm Brook watershed is primarily covered with a mix of low-density residential, commercial office and forested land uses. The entire watershed is sewered. It represents a typical watershed found in the suburbanized areas surrounding Kensico Reservoir (Figure 3.1).

3.2. Wetland Delineation and Segmentation

Use of a standardized classification system to describe different wetland characteristics can reduce the variability associated with different sites or different individuals performing the delineation. Accordingly, this study segmented the wetland into polygons with the use of the US Fish and Wildlife's National Wetland Inventory Classification Scheme (Cowardin, 1979). The perimeter of segmented wetland areas formed the boundaries for model input. Accordingly, data to describe the boundary conditions (such as cross sectional areas and stages) were collected at these locations.

3.2.1. Methods

The delineation of the wetland segments was accomplished by utilizing a Global Positioning System (GPS). The specific GPS receiver used was a Trimble model P20XR. This technology allowed identification of specific locations to within a few centimeters through the use of several satellites and correction information supplied by the Federal Government.

3.2.2. Results

Figure 3.2 provides a map of the wetland class delineation that was generated using GPS. The GPS data that was collected was used in a GIS system to generate the map's geographical orientation of the wetland areas. The segmentation of the stream corridor was based on the boundaries of the classified wetland areas. Based on field observations, there was a consistent pattern within a wetland class of similar features that can affect flow. These included primarily the vegetation and its associated friction, and sinuosity of the stream corridor found in the class. Segments classified as Emergent had relatively highly vegetated flood plains and contained stream segments with low sinuosity. Scrub-shrub classified segments had highly meandering streams with relatively low vegetated flood plains. In addition to delineating the boundaries of each of the wetland types, the GPS was used to collect information on the extent of meandering and assist in the location of monitoring stations. The accuracy of these measurements was approximately $\pm$ 0.1 feet.

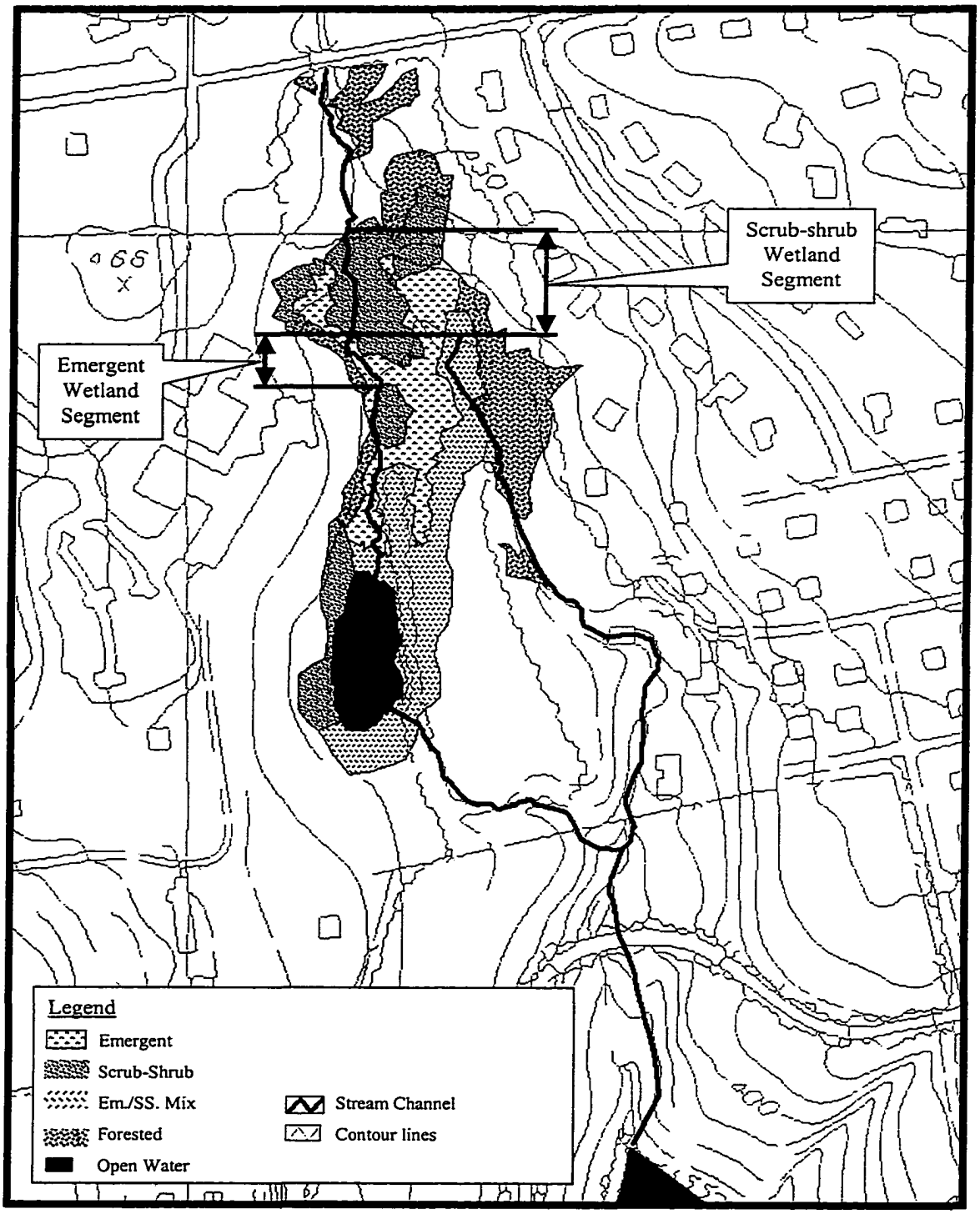

Figure 3.2. Map of delineated wetlands based on NWI classification scheme. Boundaries were determined through the use of GPS. The map was generated with a GIS system.

Conventional surveying equipment was used to delineate the elevations and widths of the stream invert, stream bank and the extent of the flow in the vegetated flood plain. The GPS could not be used to collect this data due to its much lower accuracy in measuring elevations. The accuracy of the Trimble P20XR for elevations is approximately ± 3 feet. The accuracy of surveying equipment was ± 0.01 feet.

Table 3.1 provides a summary of several characteristics found with the wetland types that included surface flows. Wetland type, channel dimensions, flood plain vegetation density, and stem diameters were determined through field surveys. Average stem diameter was determined by measuring stems in randomly placed one-meter plots along a transect through a representative portion of the wetland segment. Stem diameter was measured at three elevations within the maximum flood flow level.

3.2.3. Discussion

Use of the GPS allowed a rapid determination of boundaries and features. Similar information collected solely with conventional surveying equipment would have required a substantially greater amount of time. The GPS does not provide the same level of spatial resolution as conventional equipment. However, this loss of resolution in the horizontal plane is not significant for the scale of the study site when time resources are considered. The GPS was not accurate enough in the vertical plane to allow its use in delineating the elevations of the cross-sectional areas. Conventional surveying equipment was able to provide the needed accuracy of ± 0.01 feet for these measurements.

Table 3.1 Characteristics measured for each classified wetland segment.

Wetland Class	Scrub-Shrub (SS)	Emergent (EM)	Mixed (SS/EM)
Area (acres)	3.26	2.38	1.57
Segment Length (ft)	235.66	105.78	123.29
Average Segment Width (ft)	60.25	97.90	55.35
Average Channel Width (ft)	4.51	2.55	2.63
Stream channel length (ft)	367.14	125.98	154.15
Channel Sinuosity [1]	1.56	1.19	1.25
Relative Floodplain Vegetation Density	Low	High	Moderate
Floodplain Average Stem Diameter[1] (ft)			
Leaf-off	0.15	0.10	0.10
Leaf-on	0.11	0.03	0.12

1. See text for description

3.3. Flow and Stage Measurements

Flow measurements at the upstream boundary were needed for the input to the hydrodynamic model. Flow was measured indirectly through stage measurements. Accordingly, a rating curve was developed for the upstream boundary site MBF. Cross-sectional areas were determined for each site and were interpolated within the wetland hydrodynamic model to calculate the flows. Depth of flow (or stage) measurements at each cross-section was needed to calibrate and verify the hydrodynamic model. Although the measurements were collected continuously through the study period, several problems associated with the use of the automated equipment that collected these measurements required the data to be adjusted, using the stage data collected from a permanent stream gauge station that was located downstream from the study site.

3.3.1. Methods

Flow measurements were obtained at the upstream boundary site with the use of a Doppler Sonar Velocity Meter (Starflow Ultrasonic Doppler Instrument, Unidata Corp). This instrument also includes a pressure transducer to simultaneously measure the depth of the flow. Depth of flow was redundantly measured with an independent pressure transducer (model PDCR 1830, Druck corp.). A data logger (model CR10X Campbell Scientific Inc.) recorded data obtained by both instruments. Stage was recorded during base and flood flow condition as well as during seasons when the vegetation was actively growing or lying dormant. The frequency that the measurements were recorded was generally in fifteen-minute intervals during base flows. During storm flows, the data logger was set to record the measurements more frequently. This was accomplished by

programming the data logger to record more frequently when a pre-determined stage was reached. The stage level that triggered the storm sub-routine in the data logger was set to be at a level approximately ten percent greater than the average base flow stage.

Stage measurements were also collected at the downstream cross sections continuously with pressure transducers (Model 6508, Unidata Corp). Data from these sensors were recorded by individual data loggers (Starlogger Model 6004, Unidata Corp) located at each cross-section. Data was recorded at fifteen-minute intervals. This interval represented the most frequent data collection possible when the limitations of data logger memory and resources to support the data logger were considered.

3.3.2. Results of flow and stage measurements

Flow measurements

Flow was derived from stage measurements and a rating curve. The rating curve for site MBF was developed with the data collected from the pressure transducer and the Doppler Sonar Velocity Meter. Over nine thousand velocity and stage readings were collected over a five- month period to generate the rating curve.

Flow was related to velocity and area with equation 3.1:

$$Q = VA \tag{3.1}$$

Where Q is flow in L^3/T, V is velocity in L^2/T, and A is cross-sectional area in L^2. Velocity measurements were obtained from the Doppler sonar equipment. Area was determined with the use of curves which related the field measured cross-sectional area to stage (Figure 3.3). Two regression lines were drawn through these curves based on whether the stage represented channel (base) or flood flow. Using two regression lines

provided a closer fit than one continuous line. The area was calculated based on the equations for the regression lines. These equations are as follows:

$$h \leq 0.51 \text{ ft:} \quad A = 6.10h \tag{3.2a}$$

$$h > 0.51 \text{ ft:} \quad A = 25.36h - 9.83 \tag{3.2b}$$

Where h is the depth of flow (L), i.e.,stage.

Area was multiplied by the velocity measurements for varying stages to obtain flow data. Figure 3.4 presents the resultant plot of flow data for various stages. This rating curve was used to determine flow for any recorded stage measurements. The rating curve was divided into two lines to represent channel and flood flow. The best fit line for channel flow was a second order polynomial whereas the best fit for the flood flow was a straight line. The algebraic expressions of the lines were calculated by spread sheet software and are presented as equations 3.3a and b. Based on these equations, flow was calculated from stage data. The equations are presented as follows for stages below and above the flood stage.

$$h \leq 0.51 \text{ ft:} \quad Q = 4.63h^2 - 1.50h + 0.13 \tag{3.3a}$$

$$h > 0.51 \text{ ft:} \quad Q = 4.98h - 1.97 \tag{3.3b}$$

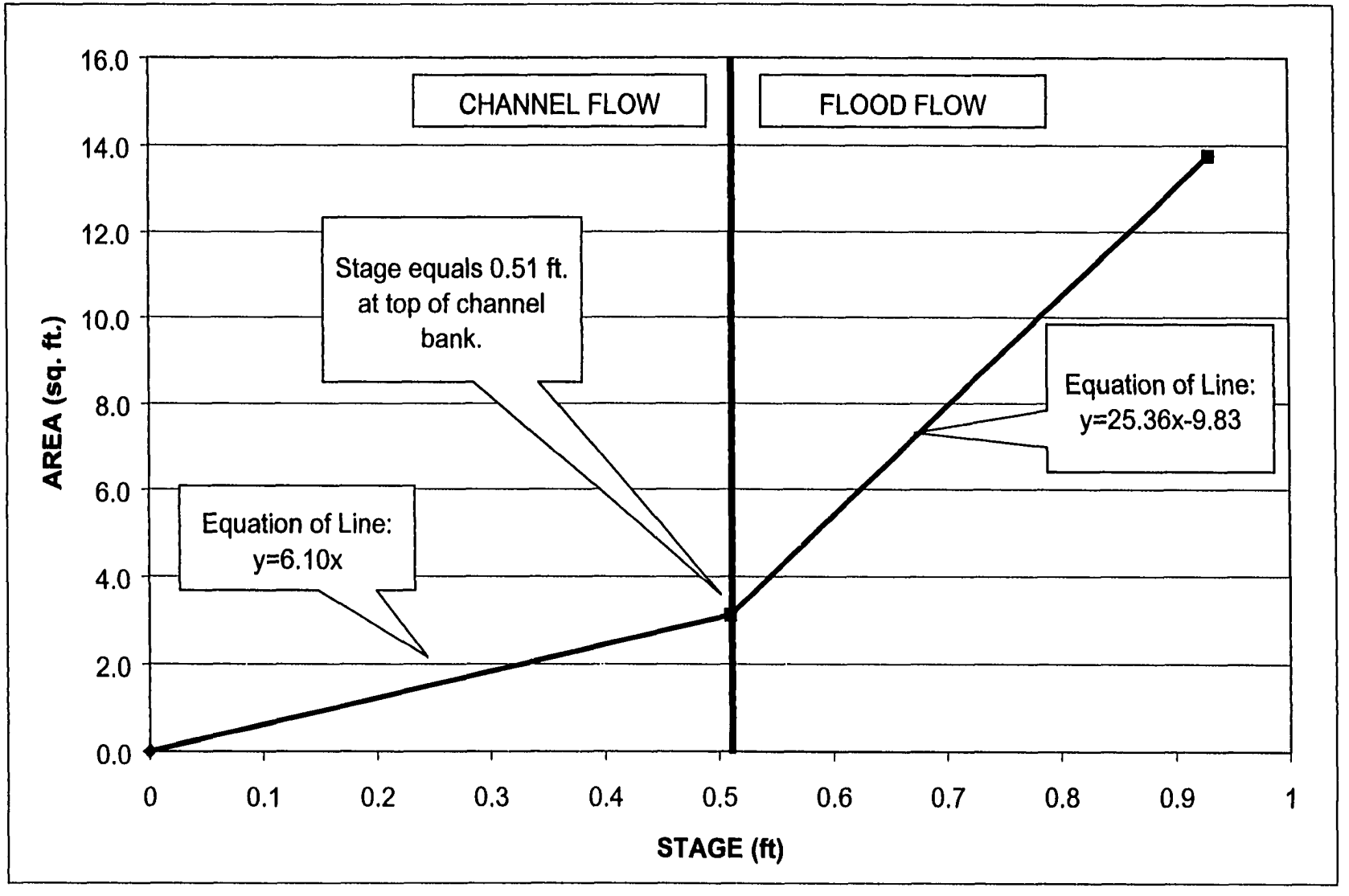

Figure 3.3. Plot of the relationship between stage and cross-sectional area for site MBF. Area increases more dramatically after the stage exceeds the banks of the channel and floods the flood plain.

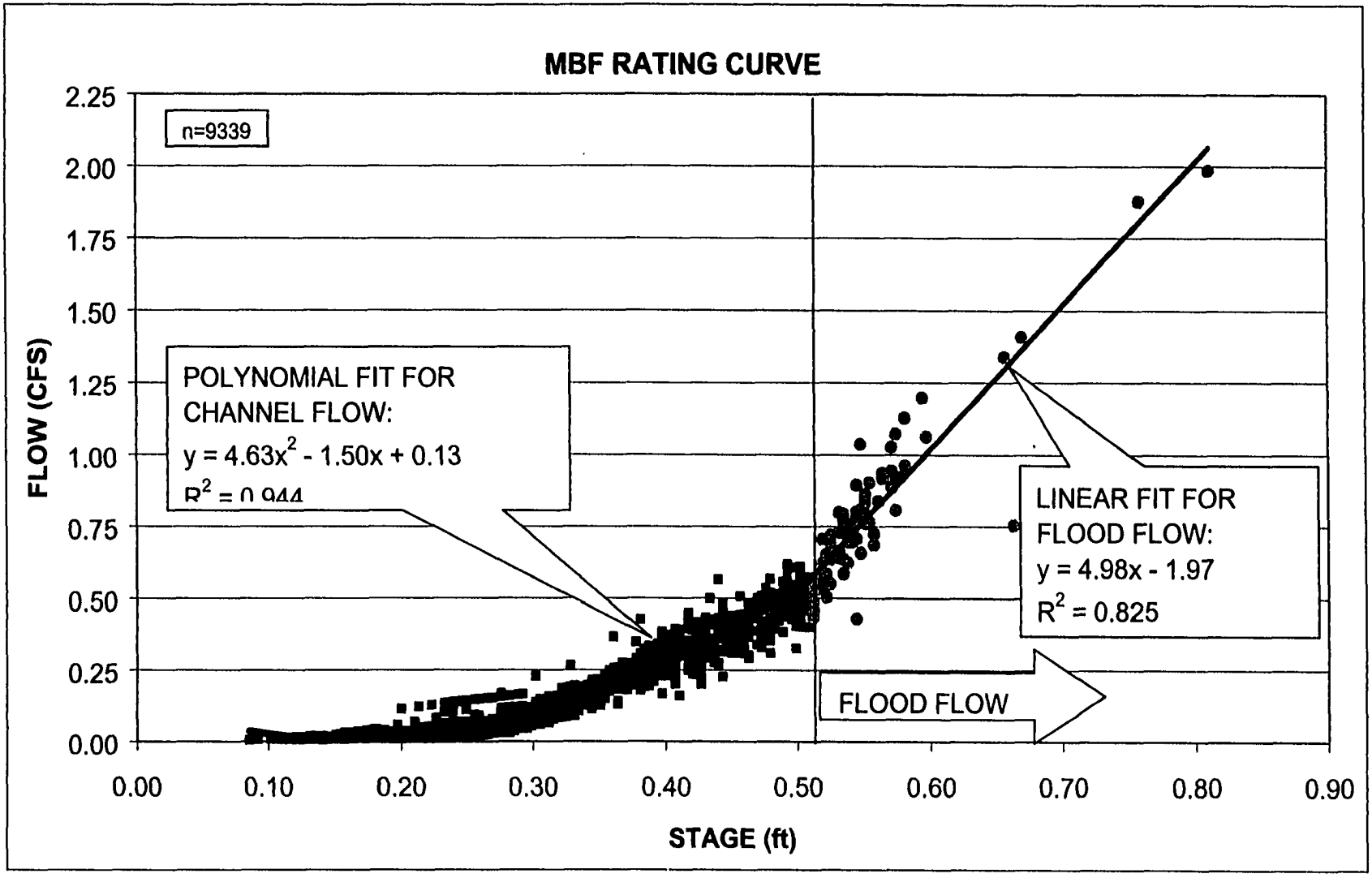

Figure 3.4. Rating curve for site MBF. Best-fit lines were drawn for channel and flood flow conditions.

Stage measurement adjustments

The overall record of stage data collected at each of the sites was compared to the stages observed at a permanently gaged station located downstream of the wetland (site MB1). Figure 3.5 presents the stage readings for the study period for site MB1. Figure 3.6 presents the stage readings for sites MBF, MBW1, and MBW2. A comparison of these plots indicate that there was a gradual decline in the stage readings for wetland sites MBW1 and MBW2 during a period between February and May 1998 (Figure 3.7). This decline was not observed for the gaged site MB1. The cause of the observed decline is unknown. The sedimentation that occurred around the pressure transducers can offer one possible explanation. The drift was significant enough to require the wetland stage data to be indexed to match the magnitude of the storm events observed at site MB1.

To adjust the stages for the wetland sites, the general slope was calculated for the two seasons of interest (leaf-on and leaf-off) for each of the sites. Although storms were included, the general slope reflected primarily base flow conditions since there are relatively few data points collected from storms when compared with the numerous data points collected for base flow. It is also important to note that the storms were approximately evenly spaced in time and did not follow any consistent pattern of increase or decrease in magnitude. The stage data was then adjusted to match the general slope of the stage from gaged station MB1. Figures 3.8a and b provides the plots of these changes. This indexing scheme was applied to all the data of a site within a season regardless of its use for calibration or verification. The indexed data was confirmed with limited stage measurements that were manually collected a few times during the study.

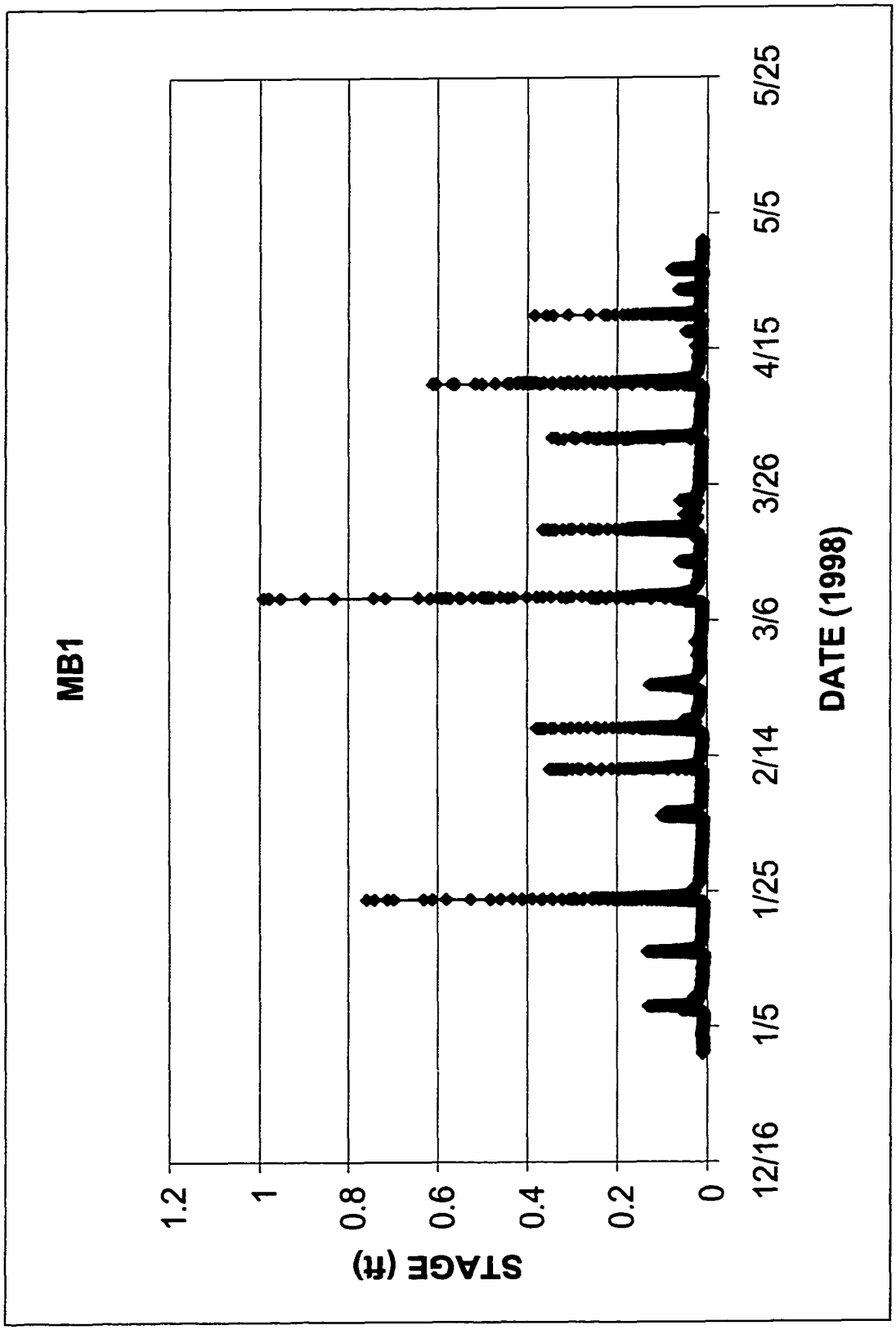

Figure 3.5. Plot of the portion of recorded data for gauged control site MB1.

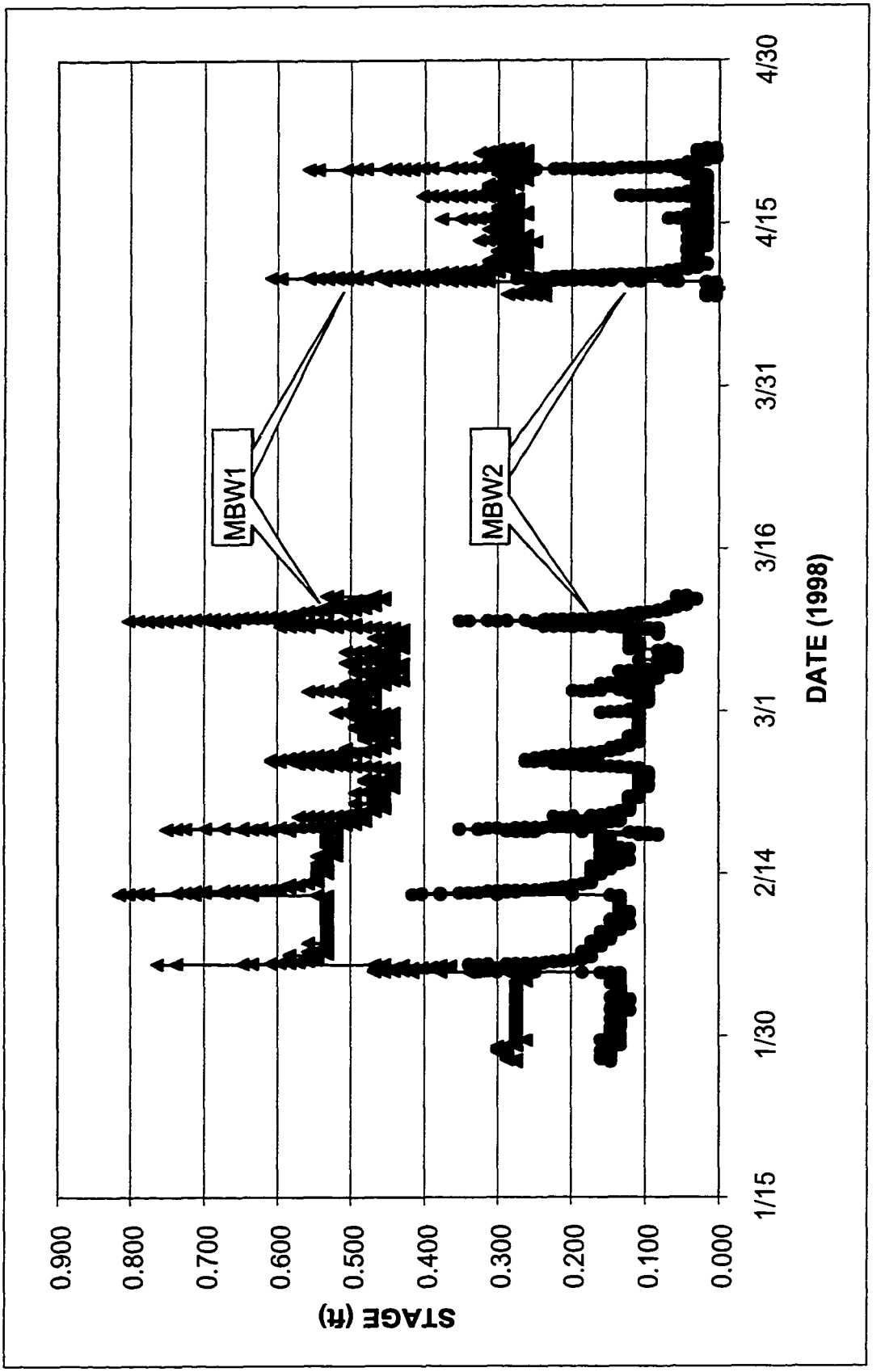

Figure 3.6 Plot of data recorded at sites MBW1 and MBW2

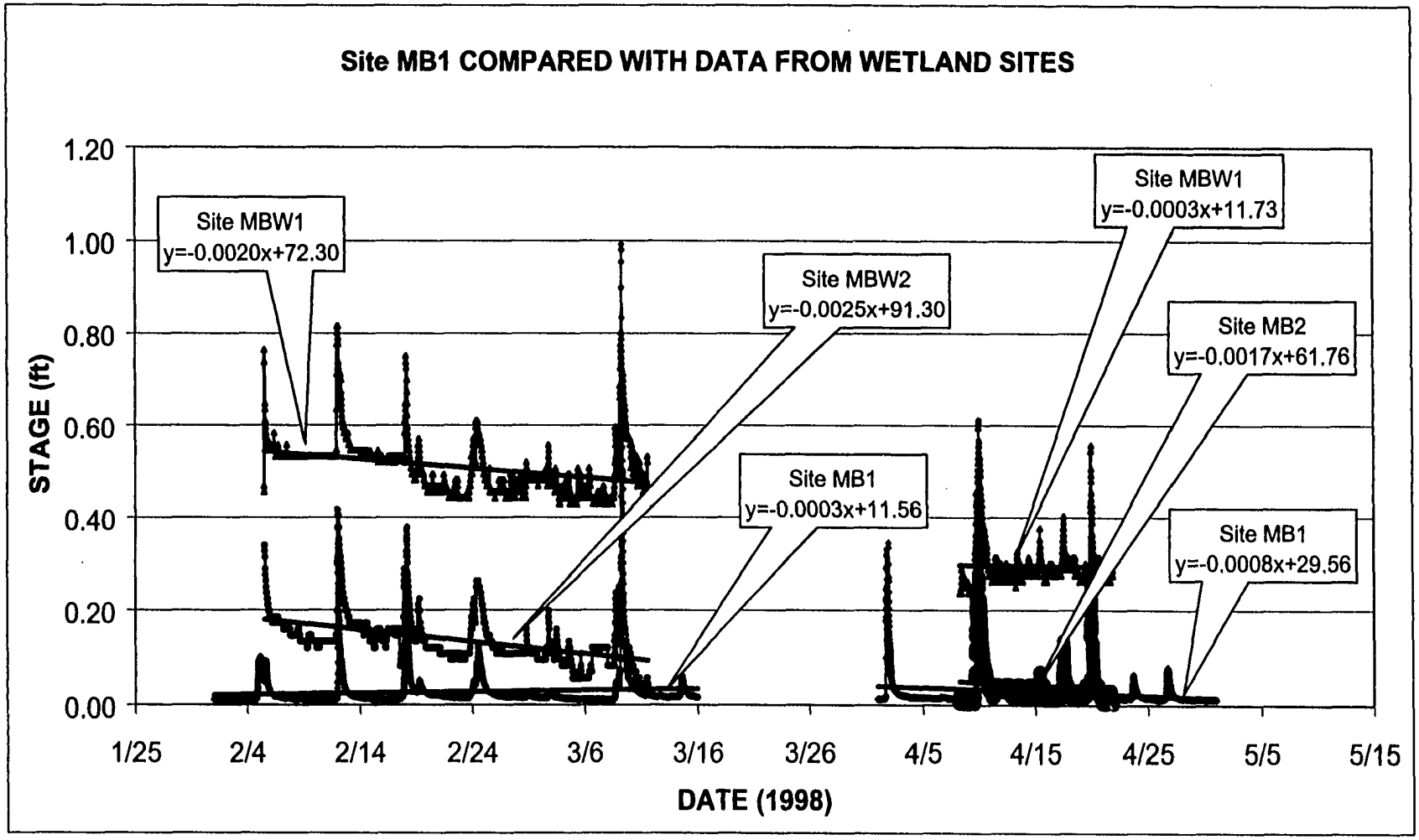

Figure 3.7 Plot of the portion of recorded data for site MB1 compared with data recorded at sites MBW1 and MBW2. The plot provides linear regression lines with associated equations for each of the data sets. Slopes significantly different from the gaged station (MB1) were observed with the data for sites MBW1 and MBW2 during the first three months of 1998.

In addition to adjusting the level of the stage data, it became apparent that the time associated with the data would also need to be indexed. The data loggers were set to record the stage at the minimum time step that logger memory and support resources allowed. This resulted in the data being recorded at fifteen-minute time intervals. Unfortunately, the speed of the flow wave often fell below fifteen minutes. Additionally, there was difficulty in maintaining the clock synchronization between data loggers. To address these deficiencies, the timing of the stage data was adjusted to match the lag times obtained through the dye tracer tests. This was accomplished by shifting the time of the stage data so that the times of the highest peak of the stage between sites was separated by an amount equal to the separation of the centroids of the mass of the dye tracer observed at the sites. The dye tracer tests selected to base these adjustments were of similar magnitude of flow and within the same seasonal conditions.

3.3.3. Discussion

The observed data appears to be a reasonable representation of the actual conditions when the flow and adjusted stage data are compared to the data measurements. With timing and stage adjustments made to the data collected within the wetland, the occurrences of the largest events match those found at the gaged station. Peak stages first appear upstream and pass the downstream stations at times equivalent to those seen with the dye tracer.

The adjustments needed for the wetland data highlight the need to invest the resources to routinely adjust and calibrate pressure transducers and adjust data logger

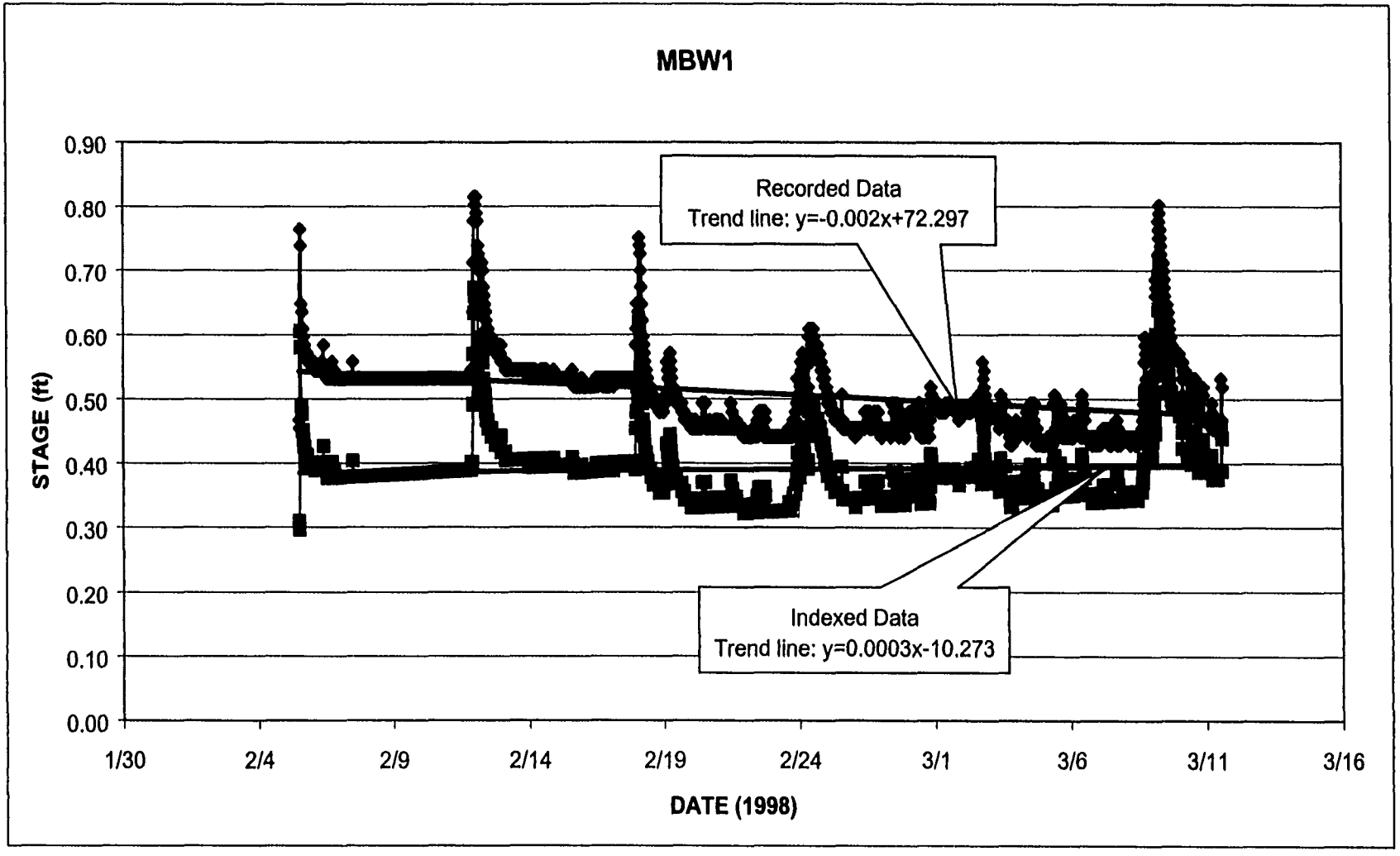

Figure 3.8a. Plot of the portion of recorded data for site MBW1 that was indexed to match the slope observed at the gauged station (MB1). Plot provides linear regression lines with associated equations.

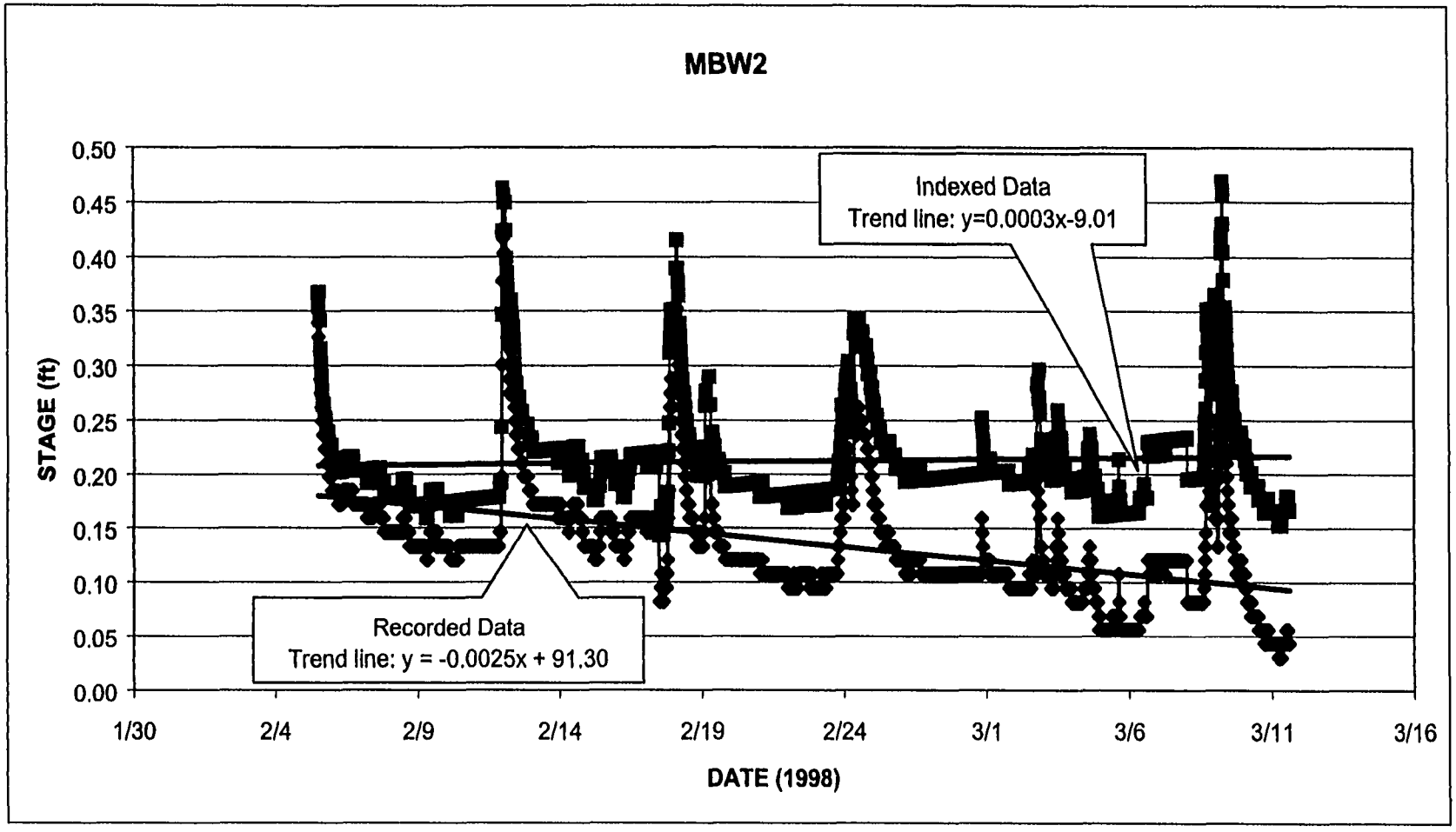

Figure 3.8b. Plot of the portion of recorded data for site MBW2 that was indexed to match the slope observed at the gauged station (MB1). The plot provides linear regression lines with associated equations.

clocks. Although the specifications of the equipment used did not indicate a need for frequent calibrations, the use of the equipment in an urbanized wetland environment appears to increase this need. The larger variation of flow velocities present in an urban wetland increases erosion and sedimentation. Based on this study, data drift appeared after about six months after the placement of the pressure transducers. This suggests at least a quarterly program of adjustments should be made to keep the instruments calibrated.

3.4 Dye Tracer Tests

Dye Tracer Tests were used in this study to obtain several parameters. Since control structures to measure flows accurately did not exist within the wetlands studied in this project, dye tracer tests were needed to determine the one-dimensional average velocities associated with different combinations of wetland types. This was especially important due to the different velocities that exist between stream channel flow and flood plains flow. Accordingly, data obtained from these tracer tests were used to confirm and adjust (if needed) the time of the stage measurements recorded by the data loggers at each cross section.

The dye tracer tests also provided information on the dispersion properties of the flow through different wetland classes. Although specific dispersion coefficients were not calculated for this study, the dispersion information was essential in calculating the number of continuously stirred tank reactors (which indirectly describes dispersion) in the particle model described in appendix A.1.

3.4.1. Methods

To conduct efficient dye studies and obtain the necessary approvals from the regulating authorities, comprehensive and detailed documents providing information on how the studies will be conducted is needed. Accordingly, both a Quality Assurance Plan (QAP) and a Standard Operating Procedure (SOP) document were produced based on the procedures presented in the American Society for Testing and Materials (ASTM), Annual Book of ASTM Standards, Section 11 Water and Environmental Technology (ASTM,1992) and the United States Geological Survey's Fluorometric Procedures for Dye Tracing (Wilson et al., 1986).

The dye test program consists of six major tasks: (1) determine which wetland segments to evaluate; (2) establish the level of flows or stages that are important to be tested; (3) measure the background fluorescence found in the stream prior to the introduction of tracer dye; (4) place dye at the upstream boundary of the wetland system; (5) collect water samples at timed intervals for each cross section of interest and (6) analyze the water samples for the concentration of tracer dye.

The determination of the wetland segments is described above. The level of flow that is important to the wetland system can be broadly separated into two flow regimes: base flow and flood flow. During base flow conditions, the flow is traveling primarily in the wetland channel. Flow during flood flow conditions is traveling in both the wetland channel and its flood plains. The condition of the vegetated flood plain may also have a effect on retention depending whether the vegetation is actively growing or dormant. Since information was needed on these conditions to adequately describe flow through the wetland system, dye tracer tests were performed during varied flow conditions as well

as for the two seasons.

The tracer dye selected for the study was a fluorescent organic compound known as Rhodamine WT (20% solution, Crompton & Knowles Inc., Charlotte, N.C.). This dye is a good tracer because it is: water soluble; strongly flourescent (therefore highly detectable at low concentrations); flourescent in a part of the light spectrum not common to materials generally found in water; inexpensive; reasonably stable in a natural water environment; and relatively harmless in low concentrations (Wilson et al., 1986). Rhodamine WT is the only tracer material that is approved for use within water supply systems. It has also been the most common tracer used for measuring hydraulic properties of wetlands (Shilton and Prasad, 1996; Pilgrim, 1992; Fisher, 1990; Stairs and Moore, 1994).

The initial dye concentration was determined in accordance with the dilution equations developed for large river system tracer tests ASTM (1992). Higher concentrations were used in this study after initial monitoring for the tracer dye indicated that the tracer signal was too weak to be detected in the downstream sites. Fifty milliliters of stock solution of 20% concentrated Rhodamine WT dye was diluted into one liter of de-ionized water to produce a diluted stock solution of ten- parts per thousand. One-hundred to two-hundred milliliters of this diluted stock dye solution was mixed with stream water to fill a 5 gallon plastic container equipped with a 12 volt pump (Shurflo model 2088-534-344). The pump was capable of delivering a flow of approximately 2.5 gallons per minute with one meter of head pressure. The entire volume of the dye tracer solution was injected into the stream channel at the upstream boundary of the wetland system at site MBF within one minute after the pump was energized.

Since flow through a wetland system is rather slow, it was necessary to use auto-sampling equipment to capture the dye tracer downstream over several hours. Accordingly, auto-samplers (Portable Sampler Model 3700, ISCO corp.) were located at each downstream cross-section. The auto-samples were capable of collecting 24 one-liter samples over a programmed period of time. Sample collection began shortly after the introduction of tracer dye to allow time for the auto-samplers to collect samples that reflected the background levels of fluorescence. The auto-samplers were initially programmed to collect a sample every fifteen minutes for the dye tracer tests performed under base flow conditions. The results from the initial tests performed during flood flow conditions indicated that the tracer curves could be captured with improved accuracy through five minute sample intervals. This change was based on the magnitude of the decrease in travel time (hours to minutes) during storm events. As a result, the auto-samplers were programed to collect a sample every five minutes.

A fluorometer (Model 10, Turner Corp., Sunnyvale, CA.) was used to measure the level of fluorescence in the water samples collected by the auto-samplers. Measurement procedures followed those detailed in ASTM (1992), Wilson et al. (1986), and Turner Designs (1981). Also measured was temperature, turbidity (Hach turbiditimeter model 2100 Hach Co., Loveland, Co.) and particles in four ranges between 2 and 50 microns (Hach Log Easy 400 particle counter, Hach Co., Loveland, Co.). Results for each tracer test were recorded along with related information on a data form (Figure 3.9). This form included the fluorometer readings, their conversion into concentrations in parts per billion (ppb), temperature, and turbidity.

Time of travel was calculated by the difference in the times when the centroid of

tracer dye mass passed from one site to the next. Average velocities for each wetland segment were calculated by dividing the length between monitoring stations by the time of travel.

3.4.2. Results for Dye Tracer Tests

Over a one year period from September 1997 to October 1998, thirty-four dye tracer tests were performed during varying base and flood stages. Table 3.2 provides an outline of the data collected for the tests. From the thirty-four tests, six tests failed to produce any data and seven tests failed to produce data at critical sites. These failures were due to equipment failure for either the auto-injection of dye tracer or the autosamplers. A total of Twenty-one tests produced results for both sites MBW1 and MBW2 which represented the sites of most interest. Of these tests, ten represented the leaf-on period (May 1 to October 15) and eleven represented the leaf-off season (October 16 to April 30). The results of the dye tracer tests produced the expected response curves for a non-ideal flow system. The dye did not travel as a single non-spreading slug (as would be the case for plug flow) nor did it instantaneously disperse (as with completely mixed flow). The observations supported the concept that the dye traveled under conditions somewhere between the two idealized regimes. Figure 3.10 provides a typical dye tracer response curve observed for the Malcolm Brook wetland system. The response

Time-Of- Travel Study On Malcolm Brook
Sample Site _____; Date/Time (Inj.)_____(tested)_____;
Dye injected at _____; Type of dye **Rhodamine WT**; Amt. Inj._____;
Conc. (%) _____; Sampling section discharge _____cfs;
Width _____; Mean depth _____; Other_____

Sample #	Sample Time*	Bottle Number	Turb. (ntu)	Temp. (°C)	Corr. Value		Fluorometer Readings X3.16	X10	X31.6	[Dye] (ppb)

*Military Time

- Misc._____

_____

_____

_____

Figure 3.9 Data entry form used during the collection of data for the dye tracer tests and particle counting.

Table 3.2. Dates, flow conditions, season and data collected for dye tracer tests.

Date	Flow Type	Season	Sites with Dye Data
9/23/97	Base	Leaf-on	Missed Dye due to timing
10/2/97	Base	Leaf-on	1
10/8/97	Base	Leaf-on	3, 4, 5
10/16/97	Base	Leaf-off	1, 2, 3, 4, 5
10/27/97	Base	Leaf-off	2, 3, 4, 5
10/31/97	Base	Leaf-off	1, 2, 3, 4, 5
11/6/97	Base	Leaf-off	1, 2, 3, 4, 5
11/20/97	Base	Leaf-off	1, 2, 3, 4, 5
12/1/97	Base	Leaf-off	1, 2, 3, 4, 5
12/3/97	Base	Leaf-off	1, 1F, 2, 2F, 3, 4, 5
12/5/97	Base	Leaf-off	1, 1F, 2, 3, 5
12/12/97	Base	Leaf-off	1,1F, 2,2F, 3, 4, 5
12/18/97	Base	Leaf-off	1,1F, 2,2F, 3, 4, 5
1/29/98	Base	Leaf-off	1,1F, 2, 2F, 3, 4, 5
3/9/98	Storm	Leaf-off	1,1F, 2F, 3, 4, 5
3/19/98	Storm	Leaf-off	1, 1F, 2, 3, 4, 5
4/7/98	Base	Leaf-off	1
5/6/98	Base	Leaf-on	1, 2, 3, 4
5/7/98	Storm	Leaf-on	2, 2F
6/5/98	Base	Leaf-on	1, 2, 3, 4, 5
6/12/98	Storm	Leaf-on	1, 1F, 2, 2F, 3, 4, 5
6/25/98	Base	Leaf-on	1,2,3,4,5,mb3
7/1/98	Base	Leaf-on	1,2,3,4,5
7/17/98	Base	Leaf-on	1,2,3,4
7/23/98	Storm	Leaf-on	Failed auto-dye injection
7/30/98	Storm	Leaf-on	Failed auto-dye injection
8/4/98	Base	Leaf-on	Failed auto-dye injection
8/13/98	Base	Leaf-on	1, 2, 3, 4
8/18/98	Storm	Leaf-on	Failed auto-dye injection
8/26/98	Storm	Leaf-on	1, 1F, 2, 2F, 3, 4
8/28/98	Storm	Leaf-on	Failed auto-dye injection
9/2/98	Storm	Leaf-on	1, 2F
10/1/98	Base	Leaf-on	1, 2, 3, 4
10/8/98	Storm	Leaf-on	1, 1F, 2, 2F, 3, 4

observed at each monitoring site is represented by an asymmetric curve characterized by a right-skewed distribution. Decreasing peak concentrations were observed as the flow traveled further from the injection point. Minimal adsorption of dye was observed based on the relatively rapid return of dye concentrations to background levels. The greatest recovery of dye was observed at sites MBW1 and MBW2 which were closest to the injection point. Accordingly, this study focused on these sites, which also had the least variability. In addition, both these sites were nearly homogenous within their own wetland classification.

Figures 3.11a and 3.11b show typical response curves between base and flood flow conditions respectively at the sites representing the scrub-shrub segment (site MBW1 and site MBW1F) and the emergent segment (site MBW2 and site MBW2F). The same concentration of dye was injected during both tests although a larger volume of flow was present during flood flow conditions. The storm flow results (6/12/98 test) indicate that their response curves have sharper peaks and occur sooner than for the base flow results (6/25/98 test). Figure 3.11b also provides the tracer curves observed in the flood plains (i.e., sites MBW1F and MBW2F) during flood flows. The dye was not observed at the flood plain sites during base flow but was detected during flood flow. These results agree with field observations that indicated that during base flow conditions, the water was channelized and surface flow in the flood plains was observed only during flood flow conditions. It is important to note that this response was observed during the leaf-off season as well as the leaf-on season.

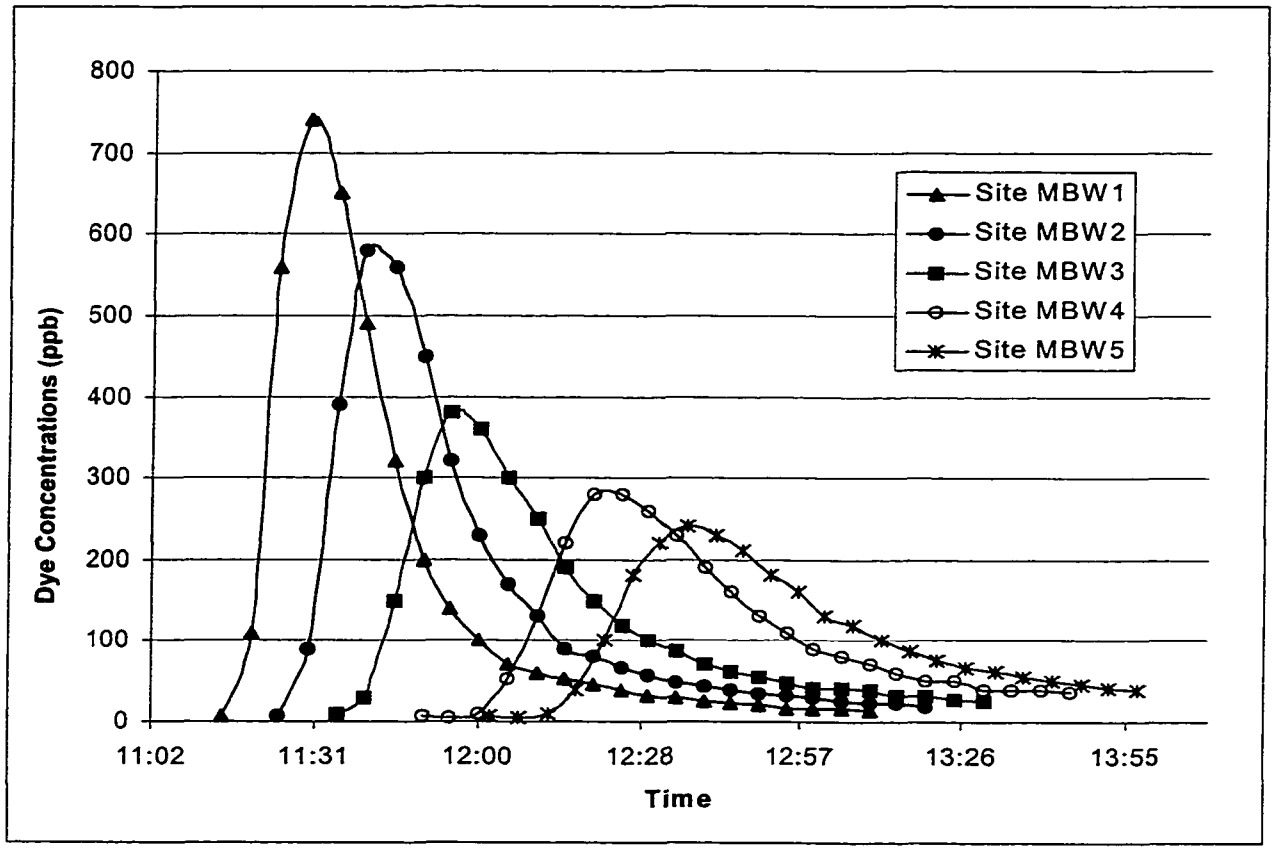

Figure 3.10. Malcolm Brook wetland dye test for 7/1/98 representing typical dye tracer response curves resulting from Malcolm Brook wetland monitoring.

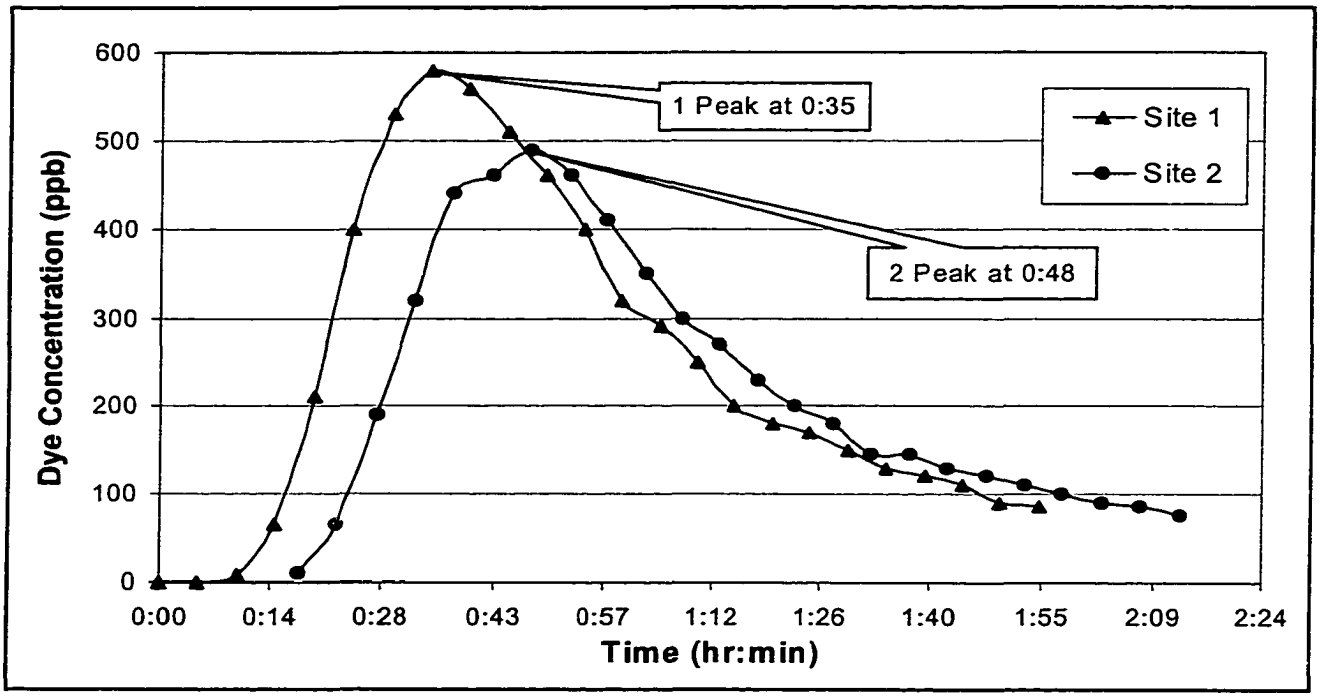

Figure 3.11a. Dye tracer response curves for base flow conditions during 6/25/98 test. Dye was not detected in the flood plain sites (1F and 2F).

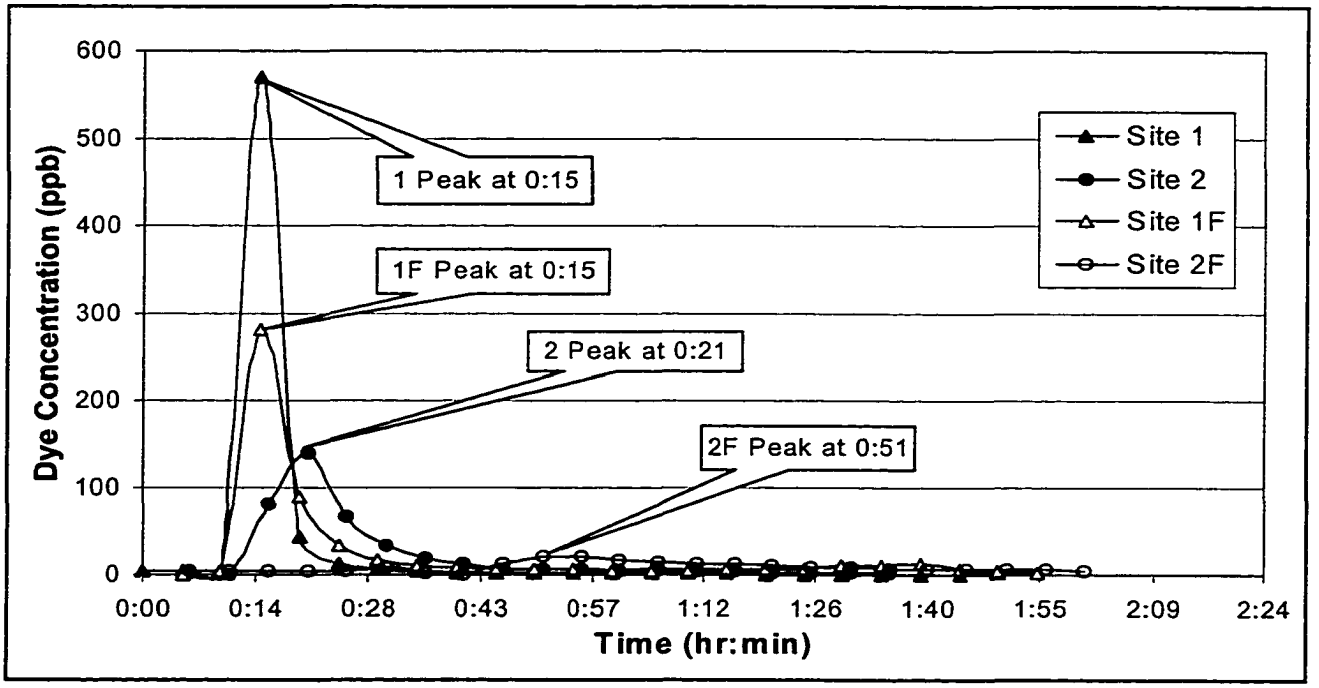

Figure 3.11b. Dye tracer response curves during flood flow conditions during 6/12/98 storm event.

Increasing scatter was observed for sites furthest from the injection point. Explanations for this scatter include increased fluorometer variability for samples with lower concentrations and increased dispersive flow paths as the tracer dye moved from one wetland segment to the next. The least scatter was observed at sites MBW1 and MBW2 which were closest to the tracer dye injection. Therefore, evaluation of the velocity differences between wetland types was based on the less variable data associated with these two sites.

Data obtained from the twenty-one successful tracer tests was used to calculate average flow velocities. The velocities associated with each wetland classification were compared to determine the behavior of the flow in each classified segment under a range of flow conditions.

Figures 3.12 and 3.13 provides a comparison in velocities during different stages of flow for the two predominant types of wetlands during the leaf-on and leaf-off seasons respectively. Site MBW1 represents the discharge of a scrub-shrub type wetland whereas site MBW2 represents the discharge of an emergent type. The range of velocities observed for scrub-shrub-classified segment was from 3.44 to75.71 ft/min during the leaf-on season and from 1.47 to 37.09 ft/min during the leaf-off season. For the emergent-classified segment, the range of velocities was from 4.14 to 20.43 ft/min during the leaf-on season and from 1.28 to 25.07 ft/min during the leaf-off season.

During the leaf-on season, the scrub-shrub type wetland exhibited approximately 20 percent lower flow velocities than the emergent type wetland during base flow conditions (Figure 3.12). However, during flood flow conditions, the scrub-shrub

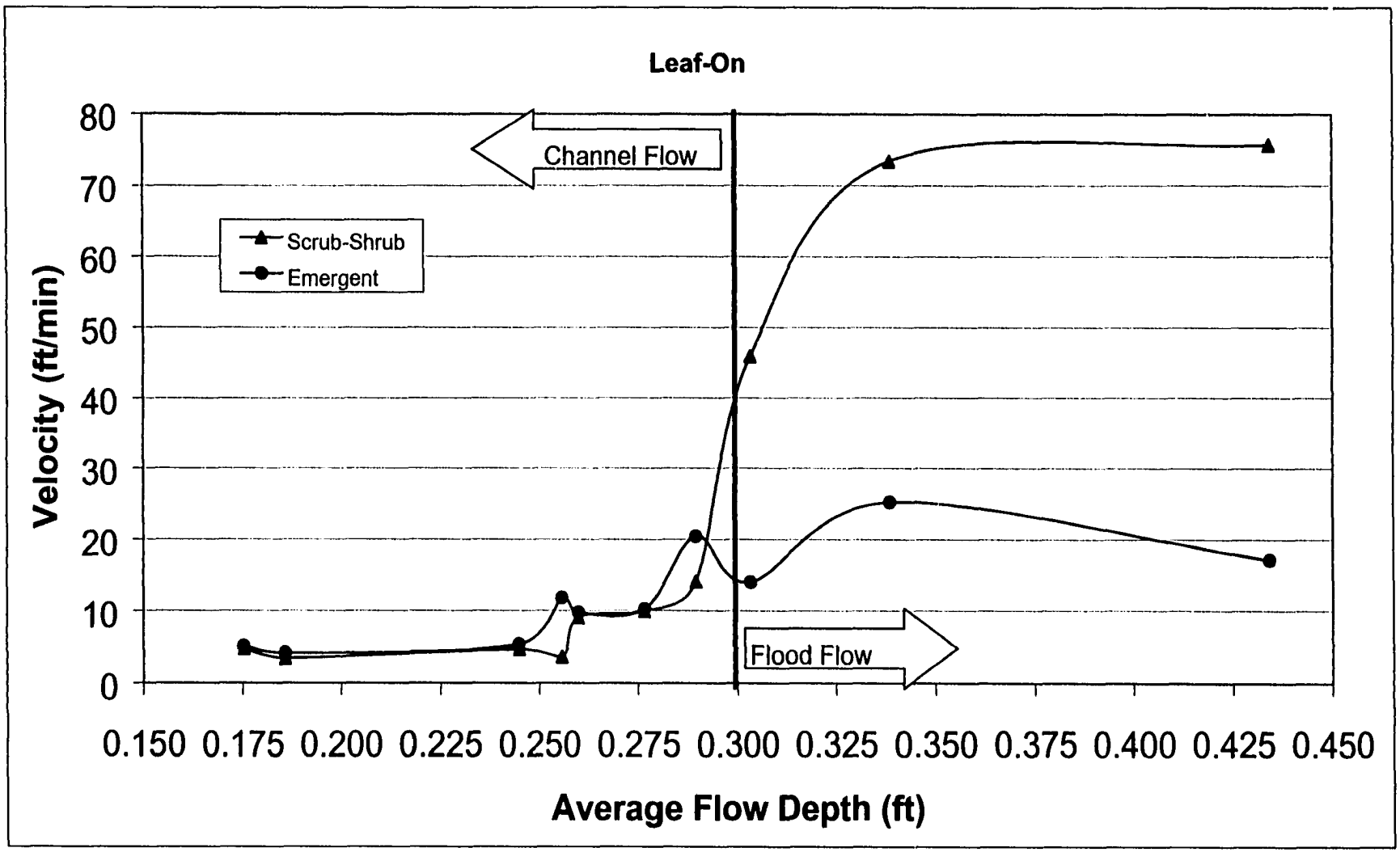

Figure 3.12. Velocities observed from dye tracer tests for two types of wetland segments during leaf-on period. Flood flow existed when the flow depth exceeded the top of the banks of the channel at 0.290 feet.

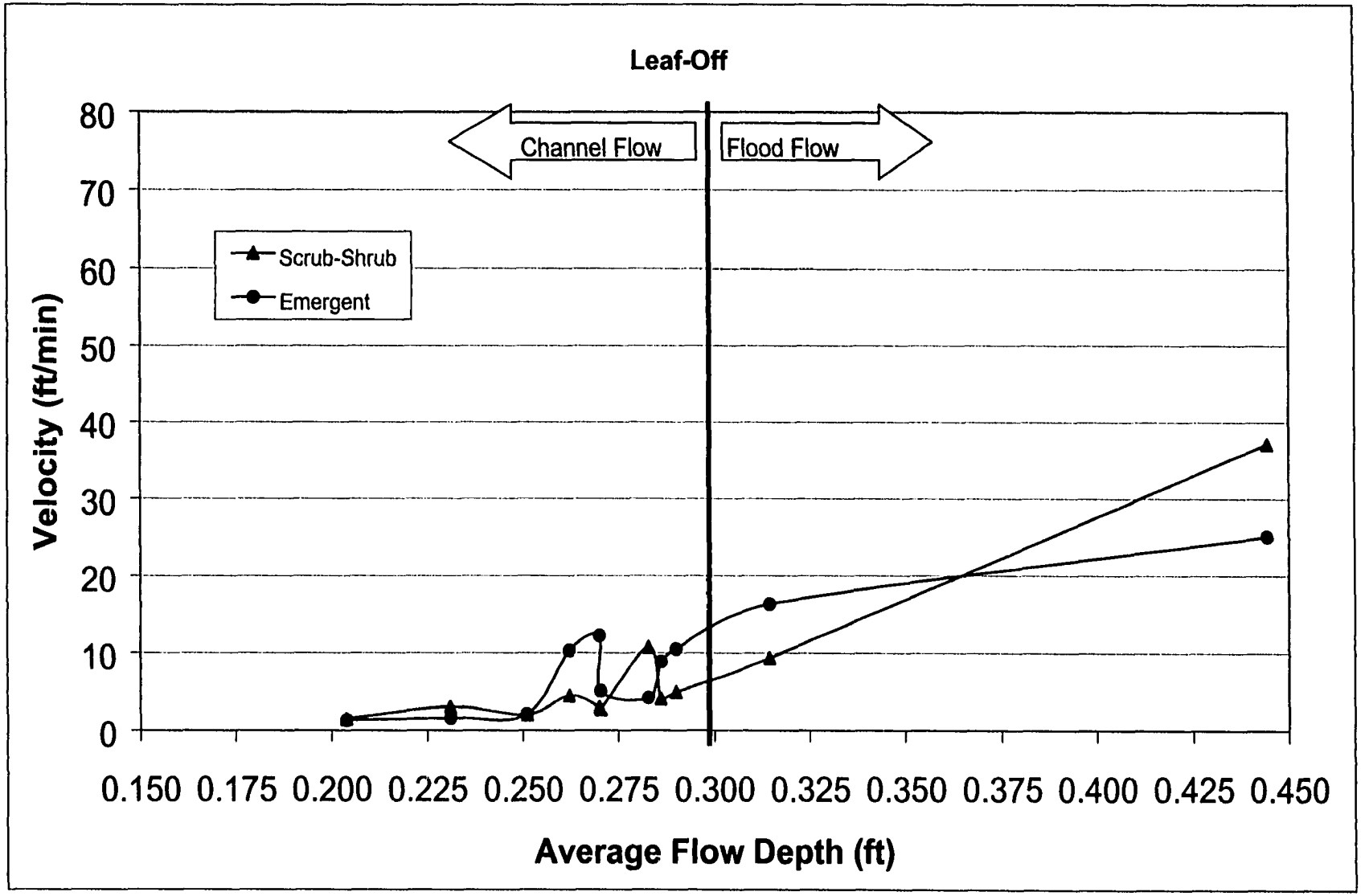

Figure 3.13. Velocities observed from dye tracer tests for two types of wetland segments during leaf-off period. Flood flow existed when the flow depth exceeded the top of the banks of the channel at 0.290 feet.

type wetland had approximately 70 percent greater flow velocities than the emergent type. For the leaf-off season, the scrub-shrub type wetland exhibited approximately 2 percent lower flow velocities (on average) than the emergent type wetland during base flow conditions (Figure 3.13). However, during flood flow conditions, the scrub-shrub type wetland had approximately 3 percent greater flow velocities than the emergent type.

Figure 3.13 indicates a noticeable decrease in velocities observed during the leaf-off season. Averaged together, the leaf-on velocity for all the dye tracer tests was 24.46 ft/min and 12.30 ft/min for the scrub-shrub type wetland and the emergent type wetland respectively. During the leaf-off period these values decreased to 7.52 ft/min and 8.84 ft/min for the scrub-shrub type wetland and the emergent type wetland, respectively. The more dramatic decrease for the scrub-shrub type wetland was most reflected in the flood flow conditions.

3.4.3. Discussion

The successful capture of dye along with the reproducibility of the results indicated that the test methods used in this study were adequate in describing flow through natural wetlands. The use of Rhodamine WT as the tracer material adequately delineated the movement of water through the natural wetlands. The results did not indicate significant adsorption of this dye tracer. The dye tracer signal measured at the downstream monitoring stations indicated similar patterns under comparable flow velocities. Part of this consistency can be attributed to the riverine nature of the wetland system studied. During base flow conditions, the presence of the stream channel directed the flow to travel in a well-defined path. Without the channel, the flow could travel

through several paths depending on only slight modifications of the micro-channels commonly found in wetlands. Accordingly, the methods used in this study are not adequate for wetland systems that are stagnant or exhibit multidirectional flow such as those that are found in the headwaters of a watershed. In these wetlands, flow needs to be described in at least two dimensions.

The results also support the use of the USFWS NWI classification scheme as a method to distinguish the hydrodynamic properties associated with different types of natural wetlands. Although this classification scheme was developed primarily for the purposed of inventorying wetlands found in the United States to support regulatory management (Cowardin, et.,al., 1979), its dependence on vegetation for classification allows it to be applicable to hydrodynamic features as well. One explanation for this applicability of the USFWS NWI classification scheme is that the presence of particular wetland vegetation is a reflection of the hydrology of the area it inhabits. Relating the USFWS NWI classification scheme to wetland hydrology has been part of the recent activities of several federal agencies in the United States. These activities include the refinement to the USFWS NWI classification scheme by adding hydrogeomorphic (HGM) characteristics. These characteristics classify hydrodynamic properties indirectly through relationships with the geographical setting of the wetland (Brinson 1993, Tiner 1997). The HGM refinements describe several wetland functions including water storage and transport.

Unfortunately, this study was only able to evaluate two classifications within one wetland system. Future study is needed to determine the hydraulic characteristics of additional classifications and to determine the variability of the hydraulic properties

within each classification. This can be best accomplished through additional dye tracer studies at a range of natural wetland sites at different locations.

In addition to the changes in the hydraulics observed between different classified wetland segments, there were measurable differences in average velocities between base and flood flow conditions. In this context, two wetland characteristics appear to have a profound effect on the flow velocity, stream sinuosity and vegetation density. The combined effect of these two characteristics resulted in the velocity pattern presented in Figures 3.12 and 3.13. The sinuosity of the stream significantly affects the length of the flow path and therefore the average flow velocity through a segment. During base flow conditions, most of the flow is channelized within the stream corridor of the wetland segments. Since the stream channel in the scrub-shrub type wetland exhibited a higher level of sinuosity, the average flow velocity was lower relative to the emergent type wetland. As the flow increased during a storm event it began to overtop the banks of the channel. Within the scrub-shrub type wetland, the overtopping significantly shortened the distance the flow must travel to transverse the segment (Figures 3.14a and b). Instead of following the meandering stream channel, the portion of flow above the channel banks traveled in a straight path through the wetland's flood plain. The greater sinuosity observed within the scrub-shrub type wetland was due to the vegetative features found with this classification. The woody roots and stems of the vegetation found in scrub-shrub type wetlands act as semi-permanent obstructions in the flow path of the stream channel. These obstructions aid in the development of meanders.

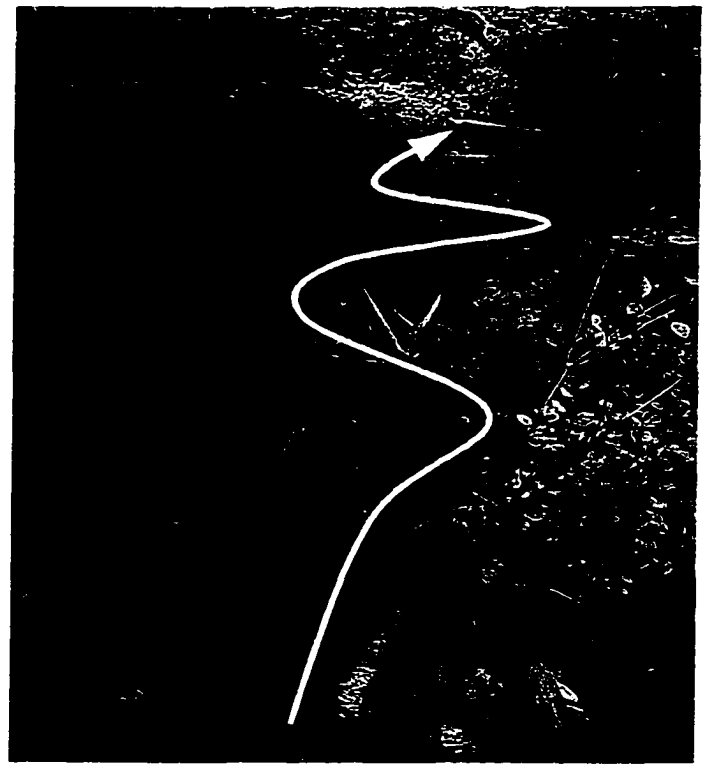

Figure 3.14a. Photograph of Scrub-Shrub type wetland during base flow. Flow travels within a meandering stream channel in one direction downstream. Note photograph was taken during dye tracer test.

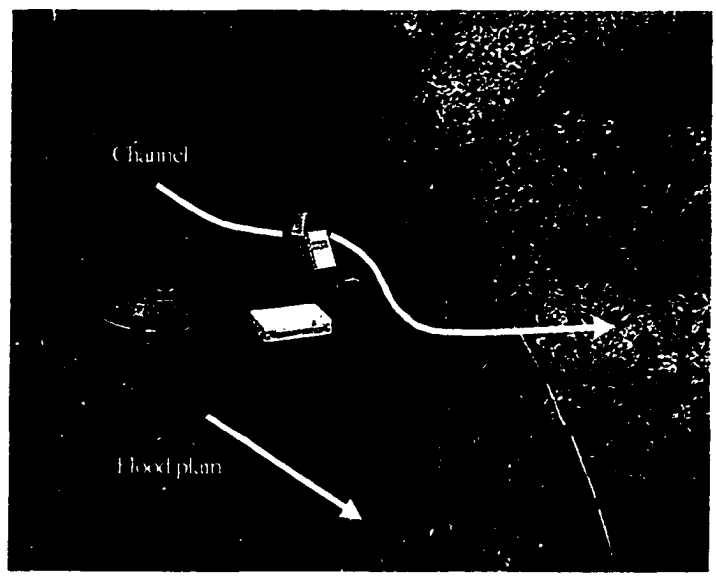

Figure 3.14b Photograph of Scrub-Shrub type wetland during flood flow. Flow has over-topped the meandering stream and is traveling in one direction downstream.

Exhibiting different vegetative features, the emergent type wetland segment contained a relatively straight stream channel that allowed direct conveyance of flow during base flow (Figure 3.15). This wetland type consisted of mostly grasses and sedges which did not form the semi-permanent obstructions found with the woody vegetation. When the flow overtopped the stream banks of this segment, the travel path did not change as much as the scrub-shrub type wetland.

Another wetland characteristic that significantly influenced the flow velocity was the density of the vegetation in the wetland's flood plain. The scrub-shrub type wetland had relatively low vegetation density with large stem diameters. This is reflective of the dominance of the woody vegetation found in this class. During flood flow, the low density, large stem diameter vegetation tends to provide a relatively low resistance to flow. In contrast, the emergent type wetland had high vegetation density with small stem diameters which is reflective of the dominance of grasses and sedges. The vegetation in the emergent type wetland provided greater resistance during flood flow.

The differences observed in the velocities between the two seasons also supports the concept that the vegetation has a significant effect on the hydrodynamics of the wetland. Both types of wetlands had lower velocities during the leaf-off season for the same flow levels when compared to the leaf-on season. Debris from deciduous vegetation may create more obstructions in the stream channel during the leaf-off season. In addition, the scrub-shrub wetland was observed to have an approximately 50 percent reduction in velocities under similar peak stage conditions. An explanation for this can be that the woody vegetation creates a denser detritus zone. This zone represents the area that most of the flood flow travels through.

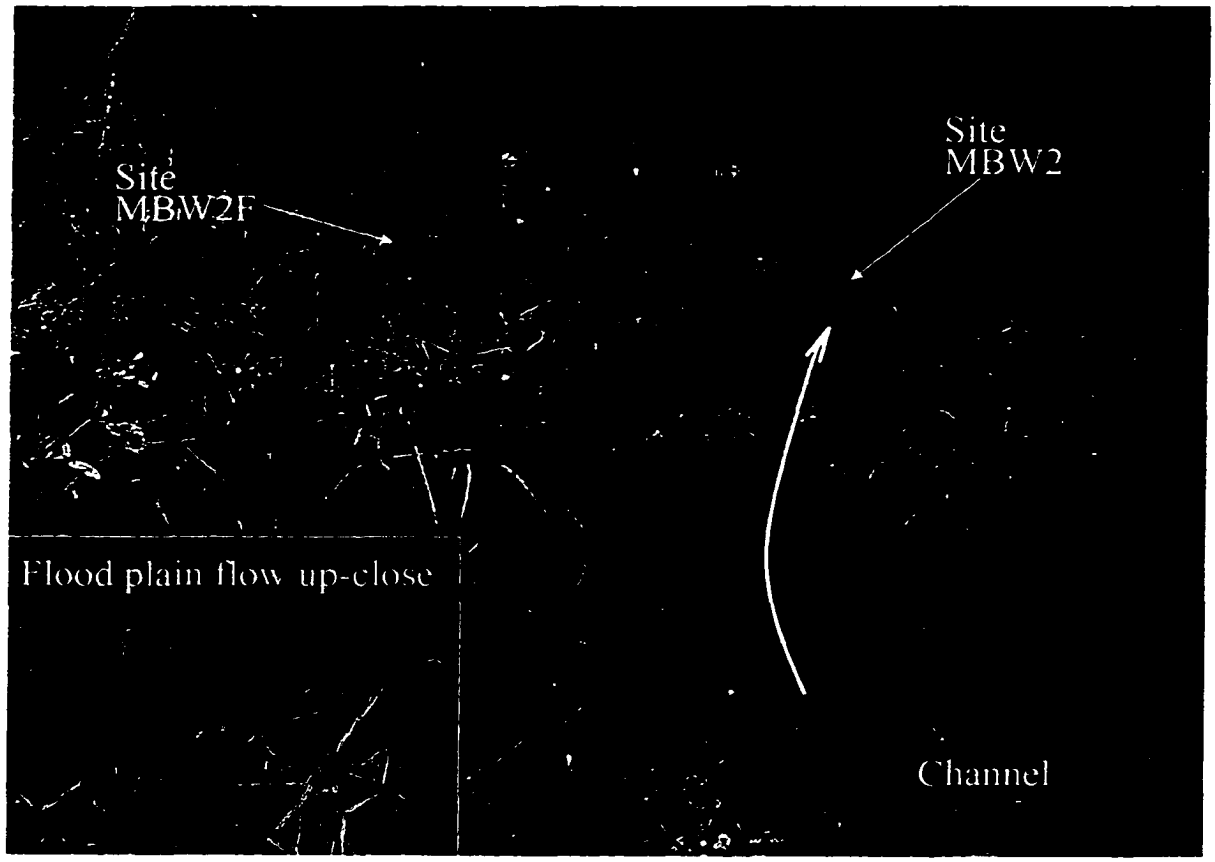

Figure 3.15. Photograph of emergent type wetland during base and flood flow. Flow has over-topped the stream channel and is traveling in one direction downstream through the vegetated flood plain.

In addition to describing the hydrodynamics of the wetland, the dye tracer tests provided a more absolute check on retention time than stage measurements at specific locations. The tests were also used to adjust the stage and flow data to account for large time steps and clock irregularities. The results from the initial tests performed during flood flow conditions indicated that the tracer curves could be captured in a shorter duration. This was due to the significant decrease in travel time (hours to minutes) during storm events. The collection time was re-programmed for every ten minutes for flood flow conditions after the initial storm event results.

Data from the dye tracer tests also were used to describe the level of dispersion to use in the particle model. The difference between the time of the peak dye concentration and the centroid of the mass of dye equated to dispersion. The time differences were used directly as input data for the particle model.

3.5. Particle Measurements

The particle counts were collected to provide data for the input of the particle model and provide the information needed to calibrate and verify the model. Particle counting is an emerging technology with respect to its use in monitoring watersheds. Accordingly, there is a lack of information on the quality control measures that are needed to obtain accurate measurements. This is especially pertinent with regard to samples of stream water where particles are present in large concentrations. Regardless of these limitations, this study collected particle count data in an effort to calibrate and verify the theoretical particle model.

3.5.1. Methods

Aliquots of the water samples collected for the dye tracer tests were analyzed for particles in several size classes. These classes ranged from 2 microns to 50 microns to capture the size ranges where *Giardia* cysts and *Cryptosporidium* oocysts would be found. The particle counter used for this study was the Hach Log Easy 400 particle counter (Hach Co., Loveland, Co.).

The Hach Log Easy 400 particle counter counts and sizes individual particles by light obscuration (blockage). Figure 3.16 provides a schematic on how this type of particle counter operates. The light source is a solid state laser diode used to cast a narrow beam. Light obscuration (which is equated to particle size) is based on the amount of light that was obscured by the particle. Light that is not obscured is measured with a photo-diode to produce a small electrical signal. This signal is then transmitted to a computer processor for data interpretation. The amount of the intensity of light decreased due to the scattering and absorption produced by the particle is a function of the particle's projected area and refractive index (Hargesheimer and Lewis, 1992). Accordingly, each decreased pulse represents a counted particle with its size determined by the magnitude of the decrease.

Samples were analyzed using Standard Methods procedures (Proposed Method 2560, Particle counting and size distribution, APHA, 1998). This method was developed for generic particle counting and included limited information on quality control procedures for natural waters.

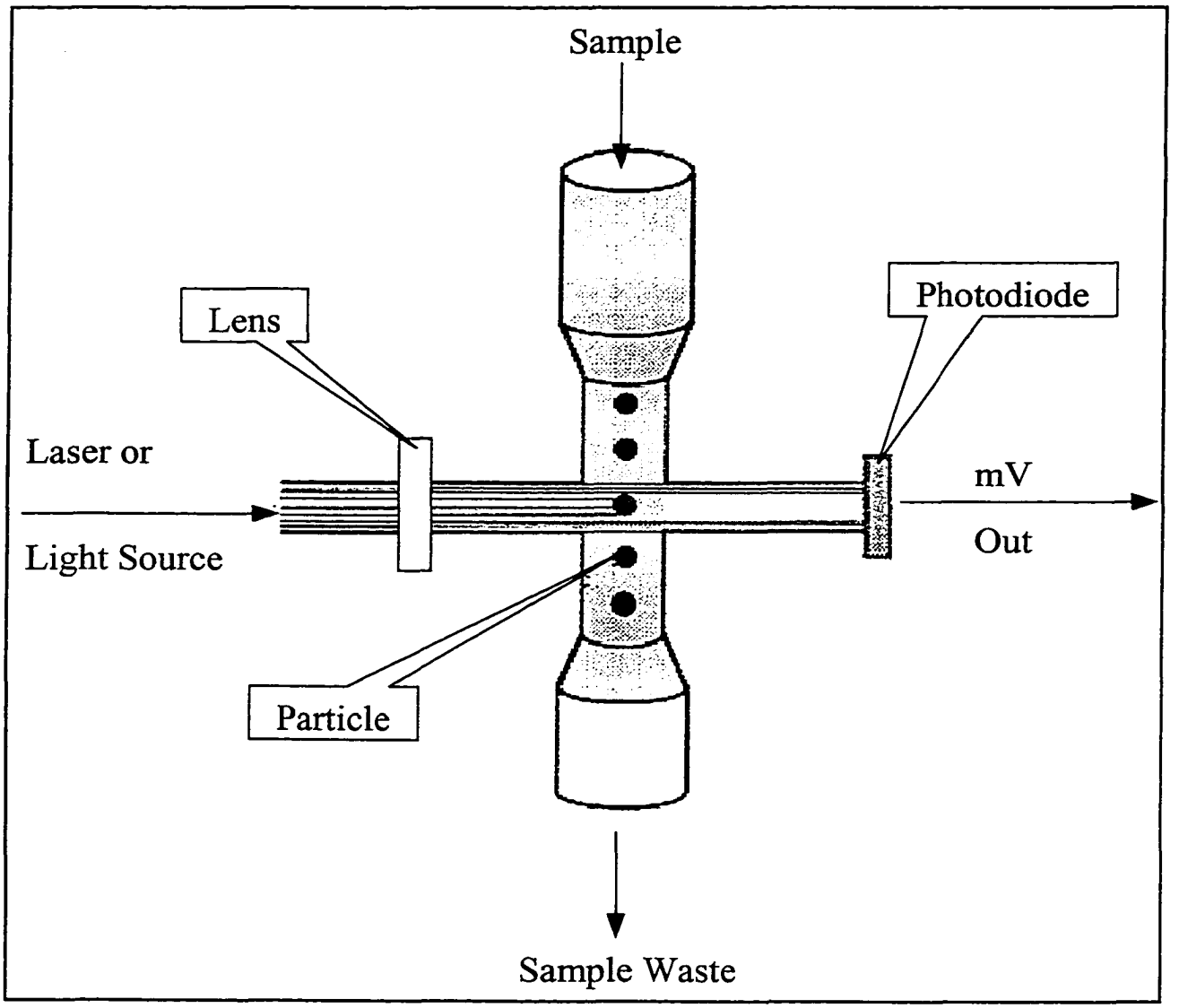

Figure 3.16. Schematic of a particle counter. (From Hargeshiemer and Lewis, 1992).

3.5.2. Results for Particle Measurements

Review of the data obtained from the particle counters indicate that the counts were too variable to be used for model development. Table 3.3 provides the typical results found for samples collected at several sites during base flow (or steady state) conditions. Under these conditions, flow and velocity remain relatively constant at each site. As indicated in Table 3.3, the variability in particle counts was considerable. Precision as measured by standard deviation (Barthov and Brown, 1994) was often as large as 50 percent of the mean. The lack of precision allowed sample variability between samples to overlap by as much as 40 percent. Turbidity measured in the same samples indicated much less variability. Table 3.4 presents the turbidity data for the same base flow event as present in Table 3.3 Several studies have related turbidity to particle counts in the (oo)cysts size range for the water quality found in water treatment plants. These studies indicate that the number of particles in the stream could have been three orders of magnitude larger than measured. A typical turbidity reading for baseflow conditions was in the order of 10 NTU. Based on extrapolating the regression line presented by Hargesheimer and Lewis, (1992), this turbidity level is equivalent to a particle count of approximately 10,000. During base flow conditions, the turbidity was reduced by approximately fifty percent. Based on the turbidity measured during the dye tracer tests an estimate of the magnitude of (oo)cyst sized particles would be approximately ten to fifteen thousand. This provides supporting information that the particles were undercounted.

Table 3.3. The particle counts and associated statistics for the July 1,1998 base flow event. Each site had 5 samples collected. The table presents the highest and lowest values along with the mean and standard deviation.

SITE	Maximum	Minimum	Mean	Standard Deviation
MBW1	510.5	195.3	352.9	157.6
MBW2	2349.9	486.1	1418.0	931.9
MBW3	1288.8	349.6	819.2	469.6

Table 3.4. Turbidity values in NTU with associated statistics for the July 1,1998 base flow event (same event as presented in Table 3.3). Each site had 5 samples collected. The table presents the highest and lowest values along with the mean and standard deviation.

Site	Maximum	Minimum	Mean	Standard Deviation
MBW1	10.7	1.8	6.3	4.5
MBW2	6.2	2.1	4.1	2.0
MBW3	1.7	1.5	1.6	0.1

3.5.3. Discussion of Particle measurements

The most extensive evaluation of particle counting variability for its application to drinking water has been presented in AWWA's report on the Evaluation of Particle Counting (Hargesheimer and Lewis, 1992). Hargesheimer and Lewis (1992) evaluated the precision of particle measurements with the Coefficient of Variation (CV). This coefficient is calculated by "dividing the standard deviation by the mean of replicate analyses and multiplying by 100" (Hargesheimer and Lewis, 1992). The coefficient of variation is presented as a percent. As calculated in Table 3.5, the CV for a typical particle count for base flow conditions was between forty-five and fifty-seven percent. The CV values reported by Hargesheimer and Lewis were no greater than fifteen percent for various types of waters. A possible explanation for the variability measured could be the effect of over-concentration of particles. Figure 3.17 illustrates how a high concentration of particles can either block the detection of other particles, or pack the particles so that they are measured as larger single particles.

Based on these results, the particle count data was determined to be too variable to be used for model calibration and verification. However, an estimate of the magnitude of particles in the (oo)cyst size range was made based on turbidity measurements. This estimate was used to demonstrate the particle model.

Table 3.5. Values for the coefficient of variation for particle counts for the July 1, 1998 base flow event.

Site	Coefficient of Variation (%)
MBW1	4464.9
MBW2	6571.8
MBW3	5732.6

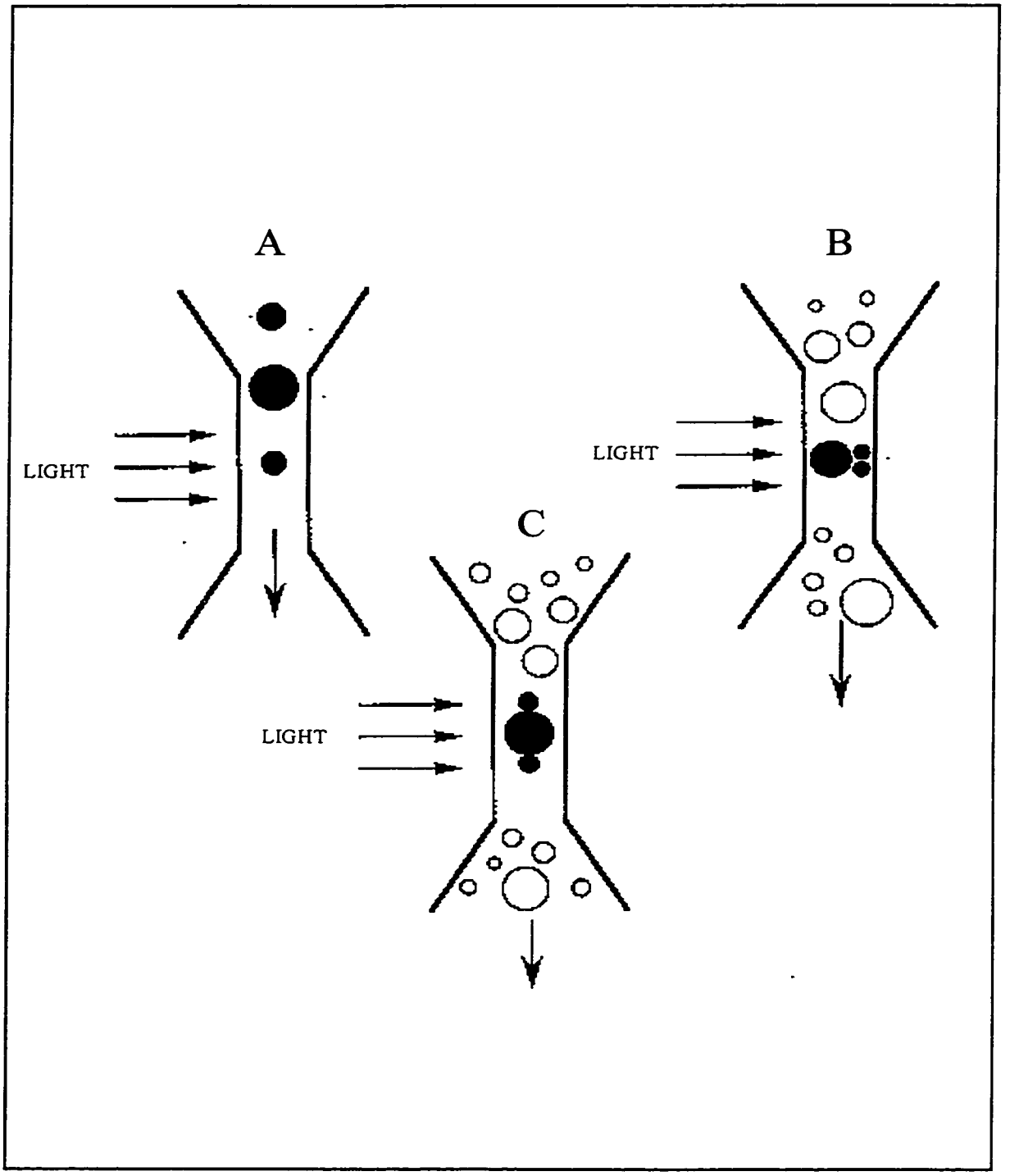

Figure 3.17. The effects of high concentrations of particles in creating counting errors. (A) Three particles correctly counted and sized, (B) only one of three particles are detected due to blockage, and (C) only one, incorrectly sized particle is detected for three particles due to the close proximity of the other particles. (From Hargesheimer and Lewis, 1992).

4. FULL DYNAMIC WAVE WETLAND MODEL (DYNAWET)

The DYNAWET model was created as part of this study. The following chapter provides a description of this model. The description includes a thorough discussion of the theory underlying the equations that are solved by the model and provides an outline of the computer code used to run the model. The highlight of this chapter is the presentation of a new equation (4.23) that determines the conveyance of flow for the vegetated flood plain in terms of porosity, average stem diameter, and a friction factor related to National Wetland Inventory (NWI) wetland classifications.

4.1. Conceptual Model

Wetlands can have a significant impact on pollutant levels because of their ability to detain the flow of water that transports these pollutants allowing physical processes (such as settling) to reduce them. Accordingly, the goal of the proposed wetland model is to provide reliable predictions of retention time by accurately simulating the flow and stage within the wetland.

4.1.1. Existing approaches to wetland modeling

As discussed in the literature presented in Chapter Two, the classic approach to modeling wetland flow is to assume steady flow and apply either Manning's Equation (2.2) or some variation of this equation. Not only does this approach assume that the variations in flow are minor, it provides a limited description of how wetland characteristics affect flow. Equation (2.4) proposed by Kadlec and Knight (1996)

replaces the coefficients associated with the Manning's Equation with empirically derived coefficients. The deficiency of this approach is that its coefficients are site specific and not related to any wetland classification scheme. Therefore application of their approach to a new location requires substantial field work.

Jadhav and Buchberger (1995) proposed a model which included a reformulation of the Saint-Venant equations (2.5 and 2.6) to provide a more detailed description of how flow passes through constructed wetlands under dynamic flow conditions. There are several deficiencies associated with their approach. Their model assumes the wetland is homogenous and lacks any channels or streams. It includes a large number of coefficients, most of which are not easy to obtain for natural wetlands. This approach was not tested under actual field conditions. It used data obtained from experiments that measured flow through steel wires in a laboratory test flume (Fenzl, 1962). Considerable resources would need to be devoted to obtain the model coefficients, especially if the wetland to be modeled is large and the vegetation heterogenous.

4.1.2. Description of a Natural Wetland System

Since all of the wetland models presented in the literature have been developed primarily for constructed wetlands they all lack some consideration of the features that are often present in natural wetlands. Figure 4.1 provides an idealized natural wetland system. Important features found in many natural wetlands (but generally missing in constructed wetlands) include the presence of nonhomogeneous vegetation, irregular

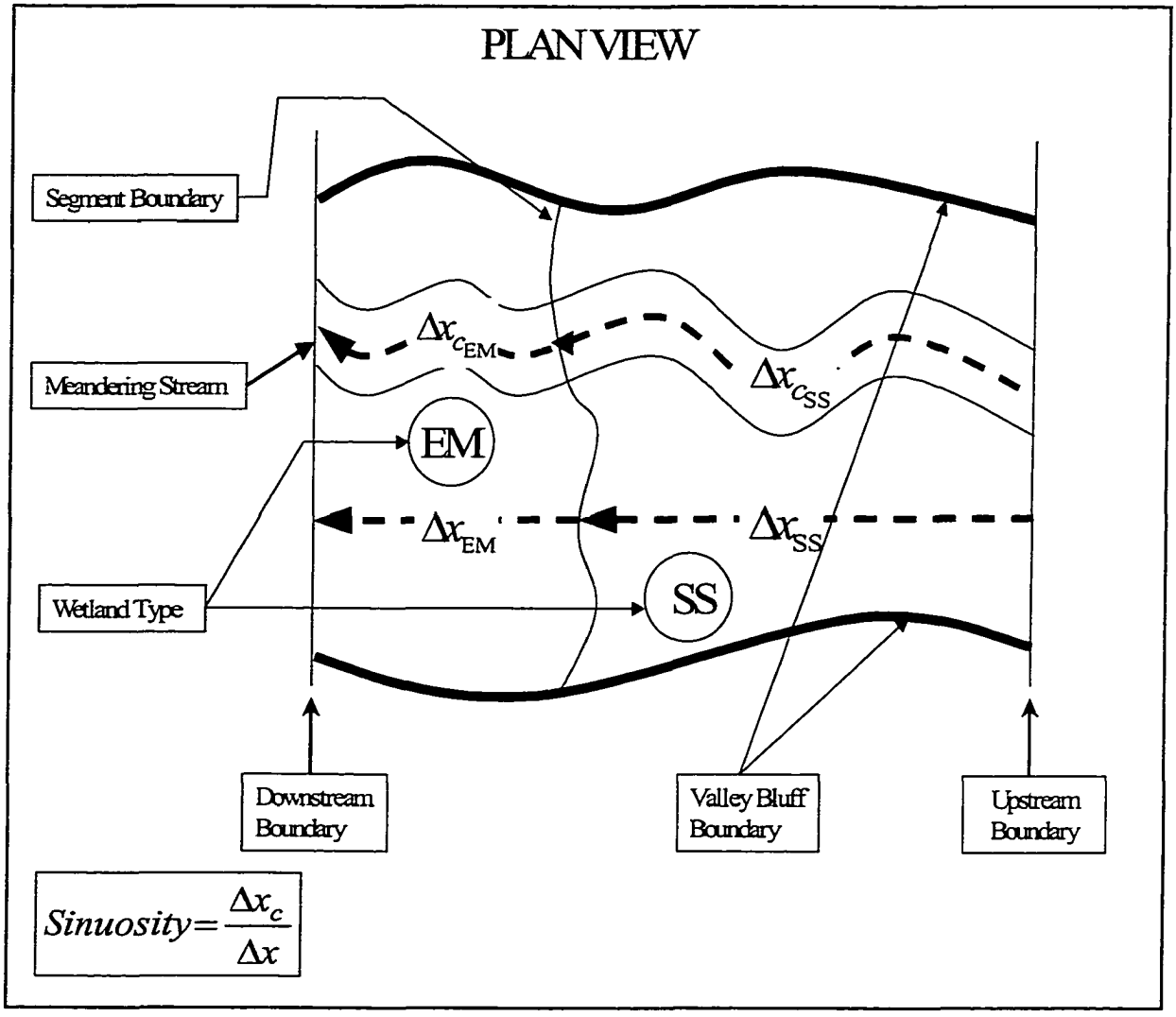

Figure 4.1. Idealized wetland system. SS is scrub-shrub and EM is emergent; the subscript "c" refers to channel.

boundaries, and meandering streams. Chapter Three provided techniques to delineate and classify the nonhomogeneous vegetation of a natural wetland system into smaller nearly homogenous segments. Information obtained through the flow monitoring and dye tracer tests conducted for this study also provide some insights on how to conceptualize the wetland hydrodynamic model. These field studies suggested that each class of wetland type has its own unique response to flood flows. They also showed that the meandering of the stream channel has significant effects on the retention time of a wetland segment. The presence of these characteristics requires that the modeling approach for a natural wetland system be general enough to account for them.

In addition to the considerations discussed above, natural wetlands can differ from constructed wetlands by the condition of the flow that pass through them. Natural wetlands lack control structures to moderate unsteady flow conditions resulting from storm event surges. Flow entering a constructed wetland is generally controlled so that it is as steady as possible. This suggests that the steady-state approaches provided by applying Manning's equation (2.2) is deficient in simulating flow through a natural wetland.

4.1.3. Modeling Approach

As stated in the introduction, an overall goal of this study was to develop a model that provides an improved description of flow through a natural wetland and utilizes variables and coefficients that can be measured easily in the field. With consideration to the description of the natural wetland system provided above, a one dimensional, distributed hydrodynamic model can be used to meet this goal. Figure 4.2 summarizes

the different types of distributed hydrodynamic models based on the Saint Venant equations (4.1 and 4.9). All of these models route unsteady flow through open channels. The continuity equation (4.1) for each type is identical and is described in detail in the next section. The form of the momentum equation (4.9) used in each hydrodynamic model differs by the level of inclusion of different forces. Figure 4.2 presents the terms of the momentum equation with general descriptions for the purpose of discussing the selection of the most appropriate hydrodynamic model. Detailed descriptions of each term of the momentum equation are presented in the next section. The kinetic wave model is the simplest of these models. It assumes that the momentum forces resulting from gravity are balanced with those resulting from friction. The diffusion wave model balances the momentum gravity forces with friction and pressure. Inclusion of the pressure term accounts for the force resulting from changes in depth along the longitudinal axis of the channel. The full dynamic wave model includes both frictional and pressure force terms and incorporates inertial force terms as well. The inertial forces are separated into the local and convective acceleration terms. Local acceleration describes changes in velocity over time whereas the convective acceleration describes changes in velocity along the longitudinal axis of the channel.

Only the full dynamic wave model considers the inertial forces that exist in a wetland due to the presence of vegetation. Accordingly, the model proposed here includes the complete description provided by the full dynamic wave model but with a reformulation that incorporates coefficients that can be determined without extensive

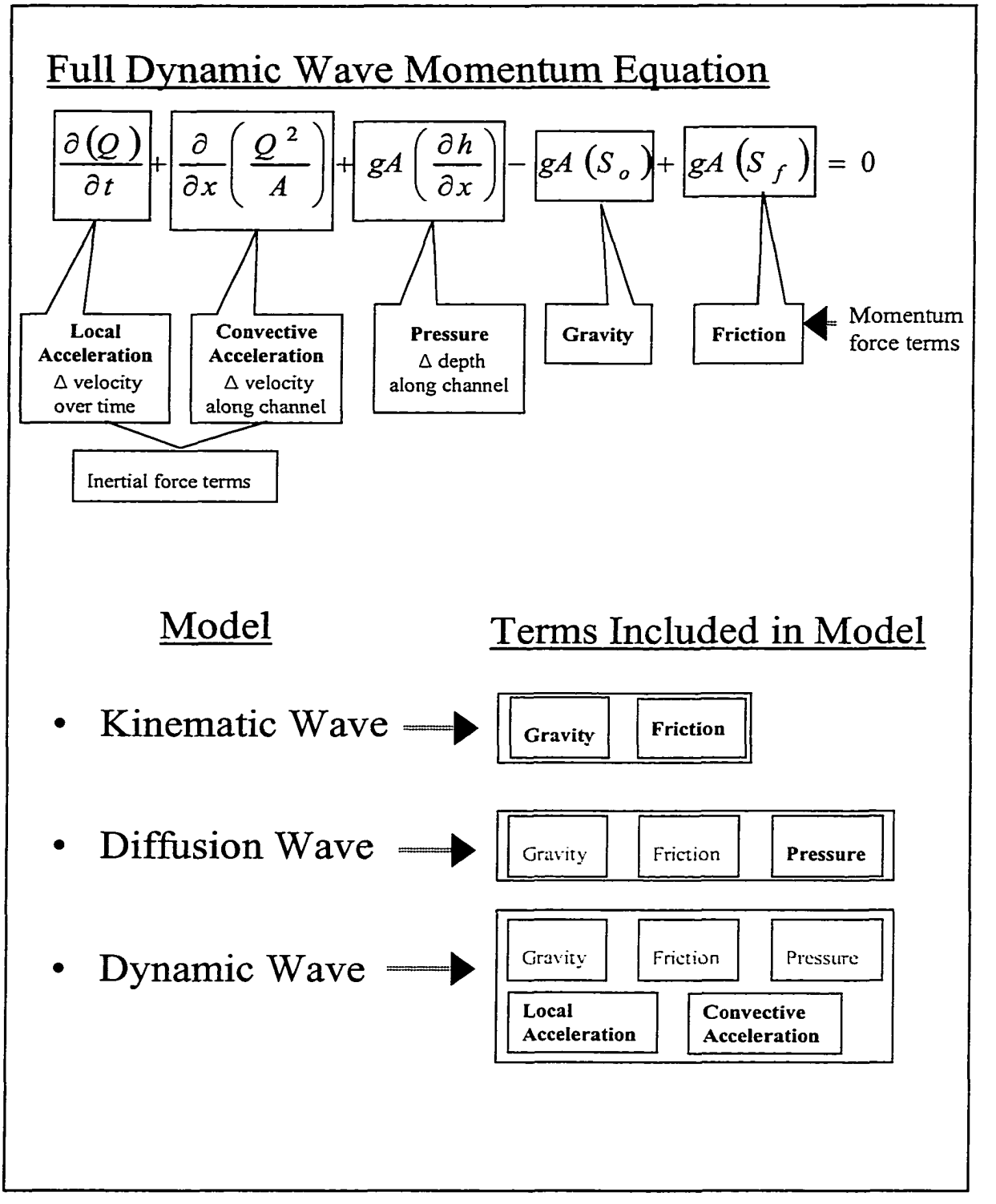

Figure 4.2. General description of the types of distributed hydrodynamic models along with the forces that are considered within each type. The dynamic wave equation represents the most inclusive model.

field investigations. The model is also based on an improved mathematical description of the mechanisms that influence flow through natural wetlands.

Based on these findings, the overall modeling approach presented here is to treat the wetland as a one-dimensional system which is segmented by different classes of vegetation. The Saint-Venant equations (4.1 and 4.9) are modified to specifically account for the reduced cross-sectional area of flow due to the presence of vegetation. The modifications also include a new equation to provide a more accurate description of the frictional forces from the drag caused by the presence of vegetation.

The forcing function for the model is the nominal flow rate. Slope, width, hydraulic radius, wetland porosity, average stem diameters and a friction coefficient based on the wetland classification are the state variables. The model solves the modified Saint-Venant equations (4.2 and 4.10) to provide the flow rate and water level simultaneously at each node along the wetland.

4.2. Governing Equations

The governing equations that are used in the DYNAWET model are a modified form of the Saint Venant equations (4.1 and 4.9), described as the full dynamic wave equations or the complete equations of unsteady flow. These equations are one dimensional, hyperbolic partial differential equations. They were first described by Barre' de Saint-Venant in 1871. Several texts and references provide a full derivation of these equations through the use of the control volume method (Liggett, 1975; Roberson and Crowe, 1990; USACOE, 1995). The Saint Venant equations (4.1 and 4.9) were modified in this study to incorporate the sinuosity of the wetland stream, the reduction in

cross section flow area due to vegetation and a new expression for describing the conveyance of flow through the vegetated flood plain of the wetland. The resultant equations are presented below.

The continuity equation (mass balance) equation describes the balance between the time rate of storage in the system and the net mass efflux through the system's control surface. The unmodified continuity equation is:

$$\frac{\partial Q}{\partial x} + \frac{\partial A}{\partial t} - q = 0 \qquad (4.1)$$

Where:

Q is the total flow (L^3/T);

x is the increment distance along the longitudinal axis (L);

A is the the cross-sectional area (L^2)

t is the time increment (T); and

q is the flow per unit channel length (L^2/T) of minor inputs (+) and outputs (-), such as evapotranspiration, precipitation and ground water gains or losses.

To better represent mass flow through natural wetlands, this equation was modified to account for several additional characteristics found in a natural wetland system. The total cross-sectional area is reduced by the level of porosity that exists in the vegetated flood plains. Following Fread (1974), off-channel storage (A_0) is separated

from the total flow area. A sinuosity term (S_A) is included to account for the differences in length of the flow path between the channel and its flood plains. This modification was proposed by DeLong (1986,1989) when previous attempts to describe one-dimensional flow for a meandering stream and its flood plains (Smith 1978; Fread 1976; Chow et al.,1988) were found not to conserve mass. Accordingly, the modified continuity equation developed for the DYNAWET model is as follows:

$$\frac{\partial Q}{\partial x} + \frac{\partial \left[S_A \left(A_T + A_o \right) \right]}{\partial t} - q = 0 \qquad (4.2)$$

Where:

Ao is the off channel area (L^2); and

A_T is the total cross-sectional area (L^2) which equals:

$$A_T = A_c + A_l + A_r \qquad (4.3)$$

This equation allows inclusion of the flood plain areas when considering the total flow area. In addition, consideration of the reduction in the effective cross-sectional areas caused by vegetation is represented by including porosity in the calculation of the cross-sectional areas for the vegetated flood plains. Porosity (φ) is defined as the portion of the cross-sectional area occupied by the voids between the vegetation divided by the entire cross-sectional area of the flood plain. The typical values of porosity are between 85 and 98 percent (Fenzl, 1962; Jadhav, 1994; Jadhav and Buchberger, 1995; Kadlec and Knight,

1996). The three components of the total cross sectional area (A_T) are calculated as follows:

$$A_c = hB_c \tag{4.4}$$

$$A_l = \phi_l hB_l \tag{4.5}$$

$$A_r = \phi_r hB_r \tag{4.6}$$

Where:

A_c is the cross-sectional area of flow of the channel (L);

A_l is the cross-sectional area of flow of the left flood plain (L);

A_r is the cross-sectional area of flow of the right flood plain (L);

h is the water depth (L);and

B_c is the top width of flow through channel (L);

B_l is the top width of flow through left flood plain (L);

B_r is the top width of flow through right flood plain (L);

φ_l is the wetland porosity of the left flood plain; and

φ_r is the wetland porosity of the right flood plain.

The sinuosity term (S_λ) in the modified continuity equation (4.2) is area-weighted. This equation was derived by Fread and Lewis, (1998) using Delong's (1986, 1989) evaluation of incorporating sinuosity in one-dimensional models. It is calculated as follows:

$$S_A = \frac{sA_c + A_l + A_r}{A_c + A_l + A_r} \tag{4.7}$$

Where:

s is the sinuosity of the channel calculated as:

$$s = \frac{\Delta x_c}{\Delta x} = \frac{x_{ci+1} - x_{ci}}{x_{i+1} - x_i} \quad , \tag{4.8}$$

x is the length of the flow path for the flood plain for a reach (L),

x_c is the length of the flow path for the meandering channel for the same reach as x (L), and.

i is the incremental distance in the x direction.

The momentum equation describes the balance between the net force acting on the system's control volume with the time rate change of momentum in the control volume plus the net rate change of the efflux of momentum through the control volume. The unmodified Saint Venant momentum equation is:

$$\frac{\partial Q}{\partial t} + \frac{\partial}{\partial x}\left(\frac{Q^2}{A_T}\right) + gA_T\left(\frac{\partial h}{\partial x} + S_f - S_o\right) = 0 \tag{4.9}$$

Where:

g = acceleration of gravity (L/T^2);

S_f = friction slope caused by shear and drag forces; and

S_o = bed slope.

This equation was also modified in several ways. The bed slope (S*o*) is assumed to be minor because slopes in wetlands are small. The sinuosity of the channel is considered as well as a momentum correction factor to address the velocity distribution across the cross-sectional area. Both these considerations follow the modifications proposed by Fread and Lewis (1998). Momentum changes resulting from the gain or loss from lateral flows are also included as a term. A new mathematical expression (derived below) is introduced to improve the description of flow through the vegetated flood plains. Accordingly, the modified momentum equation developed for the DYNAWET model is as follows:

$$\frac{\partial(S_K Q)}{\partial t} + \frac{\partial}{\partial x}\left(\frac{\beta Q^2}{A_T}\right) + gA_T\left(\frac{\partial h}{\partial x} + S_{fD}\right) - qv_x = 0 \qquad (4.10)$$

Where:

qv_x is described by USCOE (1995) as the momentum in direction of flow resulting from the lateral inflows or outflows (L^3/T^2). This term is the product of the lateral flow (q) and its associated velocity (v_x) in the x direction (L/T).

The term S_{fD} represents the friction slope (S_f) that is uniquely calculated for the

DYNAWET model. The friction slope is calculated by equation 4.11:

$$S_{fD} = \frac{Q^2}{K_T^2} \tag{4.11}$$

Where K_T represents the total conveyance of the channel and the two flood plains (L^3/T). Total conveyance is calculated as:

$$K_T = K_c + K_l + K_r \tag{4.12}$$

Where K_c, K_l, and K_r represent the conveyance for the channel, left vegetated flood plain and right vegetated flood plain respectively. The expression to calculate the conveyance for a non-vegetated channel is based on Manning's Equation (2.2) as presented in several references (Chow et al., 1988; Gupta,1989 . Fread and Lewis, 1998). Accordingly, the conveyance for the channel is represented by:

$$K_c = 1.49 \frac{A_c R_c^{2/3}}{n_c S_K^{1/2}} \tag{4.13}$$

Where:

n_c is the Manning's friction factor ($T/L^{1/3}$) for the channel,

R_c is the hydraulic radius for the channel (L) which is calculated as

$$R_c = A_c / P_c \text{ , and} \tag{4.14}$$

P_c is the wetted perimeter (L) for the channel, which is :

$$P_c = 2h + B_c, \tag{4.15}$$

S_k is the sinuosity term found in the DYNAWET momentum equation (4.10) and the equation for channel conveyance (4.13). It was derived by Fread and Lewis, (1998) using Delong's (1986, 1989) evaluation of incorporating sinuosity in one-dimensional models. The term is weighted by conveyance. Accordingly, the momentum sinuosity coefficient is calculated as follows.

$$S_K = \frac{sK_c + K_l + K_r}{K_c + K_l + K_r} \tag{4.16}$$

Equation 4.13 has also been used to describe the conveyance for the vegetated flood plains in other dynamic wave models (Fread and Lewis, 1998). However, as discussed in Chapter Two, Manning's equation (2.2) provides a poor description of flow through vegetation because it does not consider the drag forces from the vegetation nor the laminar and transitional flow regime that often exists in a wetland. It assumes all the frictional forces are generated by the shear forces between the flowing water and the wetted perimeter of the channels bottom and sides. Also, the coefficients associated with Manning's Equation are based on empirical studies of flow through channels under turbulent flow conditions (Kadlec and Knight, 1996). These assumptions do not accurately describe the flow through vegetation.

An alternative description provided here includes an expression that does not

assume the flow is turbulent and considers the presence of vegetation. The Darcy-Wiesbach Equation provides the basis for this new description.

$$Q = A\sqrt{\frac{8g}{f}RS_f} \tag{4.17}$$

Where:

f is a dimensionless friction factor.

Equation (4.17) relates flow and friction regardless of whether the flow is turbulent or laminar. Accordingly, it is appropriate to use it to describe the wetland hydrodynamics which has been found to exhibit flow in the transition zone between turbulent or laminar flow conditions (Kadlec and Knight, 1996).

Considering equation (4.11) with equation (4.17) provides the expression for conveyance (K) :

$$K = A\left(\frac{8g}{f}\right)^{1/2} R^{1/2} \tag{4.18}$$

The characteristics associated with vegetated wetland flood plains are incorporated in the friction factor (f) and the hydraulic radius (R) terms in equation (4.18). Since the friction factor is related to flow through a wetland, it is identified as

C_{wetl} and C_{wetr} for the left and right floodplain respectively.

The hydraulic radius (R) is calculated using equation (4.14) but replacing the Area (A) and wetted perimeter (P) terms to reflect the characteristics of a vegetated channel. Figure 4.3 provides a schematic of a cross section of flow through vegetation to assist in the description of the Area (A) and wetted perimeter (P) terms for a wetland flood plain. The area of flow was described before with equations (4.5) and (4.6) for the left and right flood plains respectively.

The wetted perimeter (P) is approximated with the following expression:

$$P_w = P_u + P_s \qquad (w = l,r) \tag{4.19}$$

Where:

P_u is the wetted perimeter for the un-vegetated portion and is represented by the porosity(φ_w) over the width of the floodplain(B_w):

$$P_u = \phi_w B_w \qquad (w = l,r) \qquad \text{and,} \tag{4.20}$$

P_s is the wetted perimeter of the stems for the vegetated portion and is represented as:

$$P_s = 2h\left[N_v\right] \qquad (w = l,r) \tag{4.21}$$

Where:

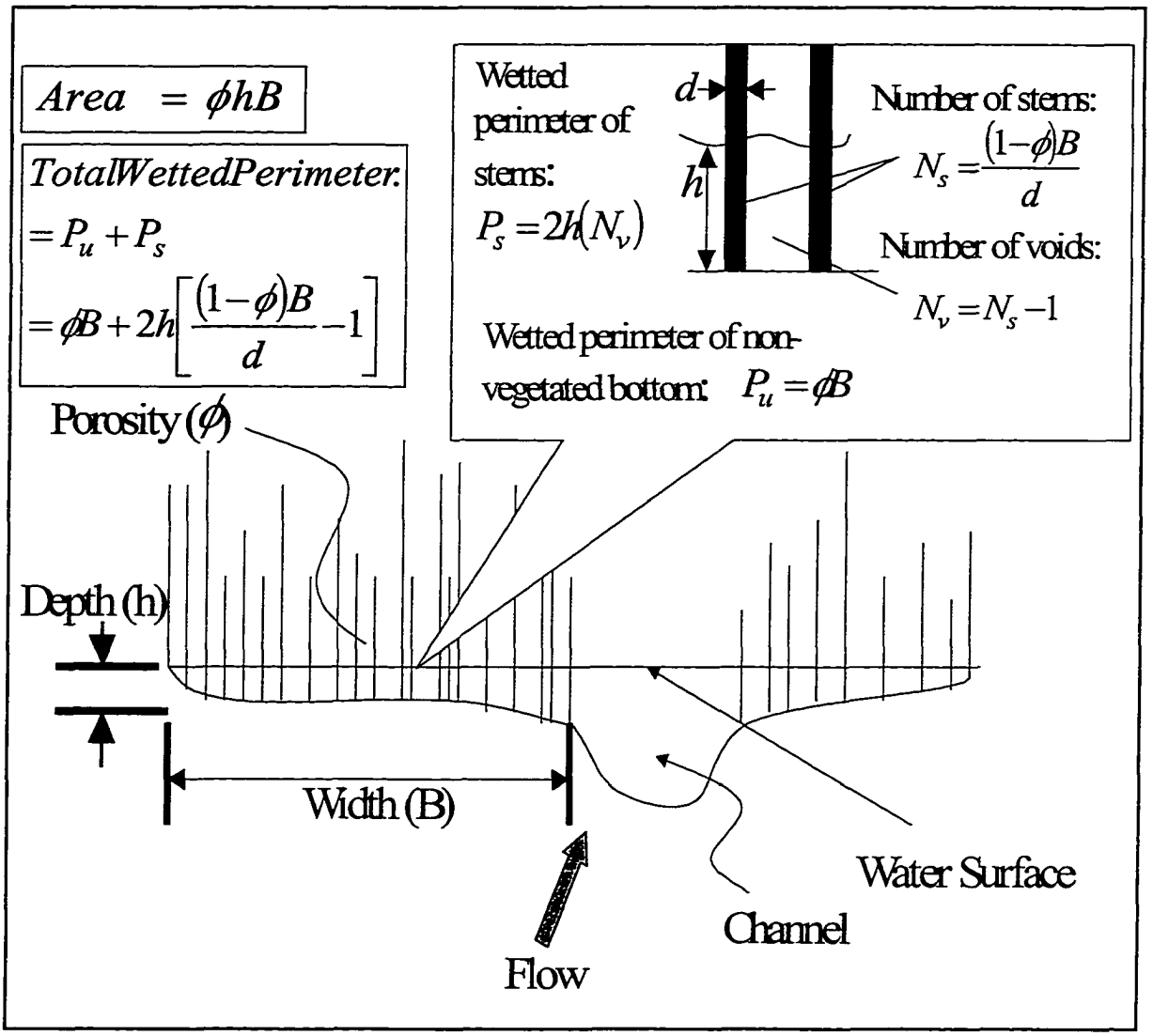

Figure 4.3. Cross-sectional view of flow through the vegetated portions of a wetland. Area and wetted perimeters are calculated with consideration of the presence of vegetation. The average diameter of the stems is represented by (d) in units of length. Flow through the channel portion of the wetland is calculated with Manning's equation.

N_v represents the number of voids between the stems of the vegetation and is equal to the number of stems minus one (N_s-1). The number of stems (N_s) is calculated as:

$$N_s = \frac{(1-\phi_w)B_w}{d_w} \qquad (w = l,r) \qquad (4.22)$$

where:

d is the average stem diameter (L).

Based on the description provided above in equations 4.18 through 4.22, a new equation that describes the conveyance through a vegetated flood plain of a wetland is presented as follows:

$$K_w = A_w\left(\frac{8g}{C_{WET_w}}\right)^{1/2}\left(\frac{A_w}{\phi_w B_w + 2h\left[\frac{(1-\phi_w)B_w}{d_w} - 1\right]}\right)^{1/2} \qquad (w = l,r) \qquad (4.23)$$

Equation 4.23 represents an improved description of conveyance for the vegetated flood plains of a natural wetland.

In addition to the terms described above, there is a momentum correction factor (β) in the DYNAWET momentum equation (4.10). With the assumption that the flow is

predominantly one-dimensional, velocity is averaged over the cross-sectional area. To address the variations in velocity across the cross-section of a reach, a momentum correction factor (β) suggested by Fread and Lewis (1998) is calculated as follows:

$$\beta = \frac{\left(\frac{K_c^2}{A_c} + \frac{K_l^2}{A_l} + \frac{K_r^2}{A_r}\right)}{\left(\frac{K_T^2}{A_T^2}\right)} \tag{4.24}$$

4.3. Numerical Solution

The governing equations are solved through the use of an implicit finite difference approximation. The numerical solution follows the "weighted four-point" scheme that has been developed over the last several decades (Preissmann, 1961; Baltzer and Lai, 1968; Amein and Fang, 1970; Strelkoff, 1970; Fread and Harbaugh, 1971; Chaudhry and Contractor, 1973; Fread, 1974; Fread, 1976; Liggett and Cunge, 1975; Fread and Smith,1978; Chow et. al.,1988; Fread and Lewis 1998). This scheme has been widely applied in solving the Saint Venant equations since it allows the use of unequal spatial and time steps and its stability and convergence properties can be conveniently controlled (Fread, 1974).

Figure 4.4 provides the time-distance solution domain. The domain represents the region where the solution for depth (h) and flow (Q) are sought at the nodes of the rectangular net. The nodes are determined by the intersection of parallel axes representing time (t) and position (x). Time and spatial increments are represented by Δt_j and Δx_i respectively and may be variable.

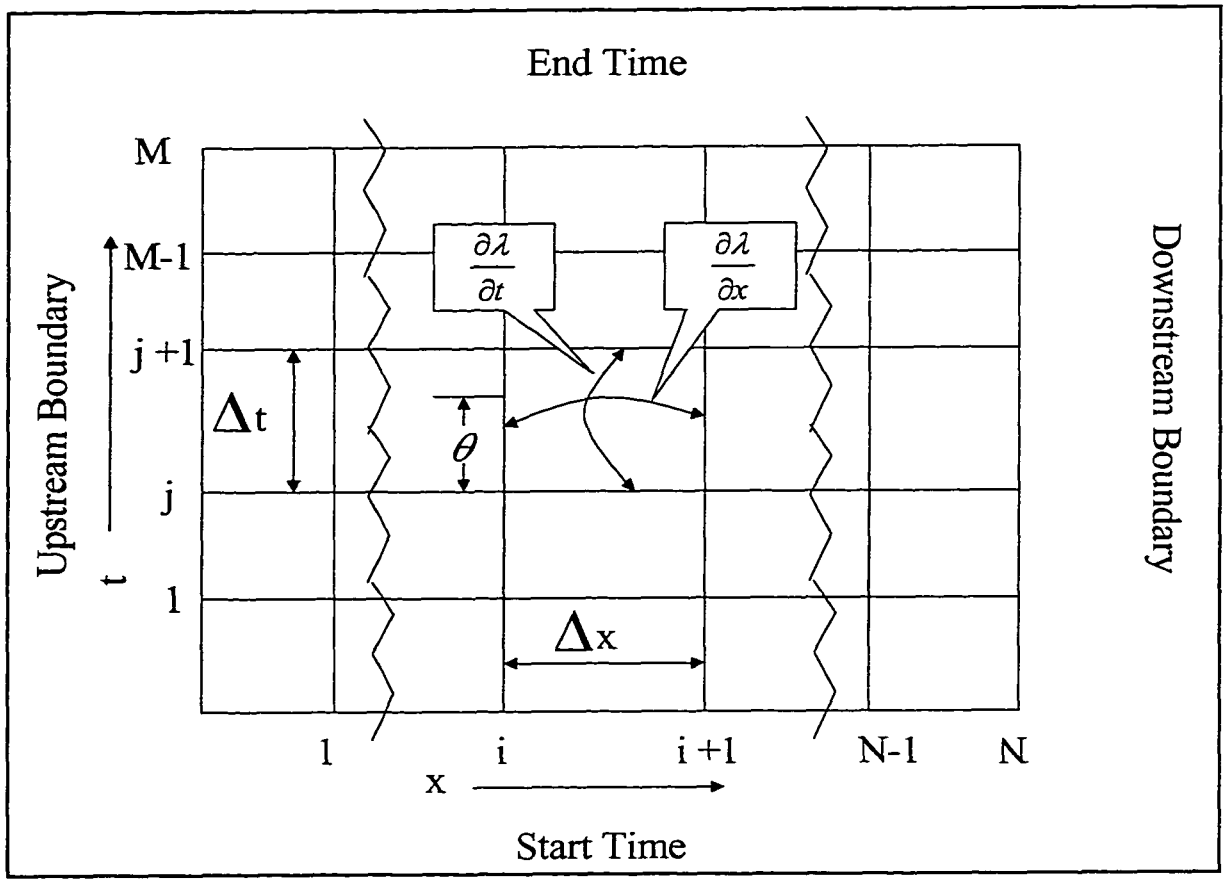

Figure 4.4. The time-distance solution domain for the DYNAWET model.

The finite difference expressions for the governing equations (4.2 and 4.10) are derived with the use of three approximation equations. These equations transform the elements of the partial differential equations into algebraic expressions that can be solved using a numerical technique.

The time derivatives are approximated by a forward-difference equation centered between nodes *i* and *i*+1 on the spatial axis:

$$\frac{\partial(\lambda)}{\partial t} = \frac{\lambda_i^{j+1} + \lambda_{i+1}^{j+1} - \lambda_i^j - \lambda_{i+1}^j}{2\Delta t_j} \tag{4.25}$$

where λ represents an unknown variable (i.e., Q, h, A).

The spatial derivatives are approximated by a time-weighted forward-difference equation.

$$\frac{\partial(\lambda)}{\partial x} = \theta\left[\frac{\lambda_{i+1}^{j+1} - \lambda_i^{j+1}}{\Delta x_i}\right] + (1-\theta)\left[\frac{\lambda_{i+1}^{j} - \lambda_i^{j}}{\Delta x_i}\right] \quad (0 < \theta \le 1) \tag{4.26}$$

Where:

θ is the weighting factor.

Equation (4.26) represents the fully implicit (backward difference) scheme when the weighting factor equals one. The box scheme results when the weighting factor is equal to 0.5 (Amein and Fang, 1970). Instability was observed with the box scheme by Baltzer and Lai, 1968, and Chaudhry and Contractor, 1973. Fread, 1974 examined the

effects of different values of the weighting factor and determined that a value between 0.55 and 0.60 minimizes the loss of accuracy associated with larger values while avoiding the instability found with the box scheme.

The parameters that are not derivatives are approximated at each time step at the same weighted location as the spatial derivatives with the following expression:

$$\lambda = \theta\left[\frac{\lambda_i^{j+1} + \lambda_{i+1}^{j+1}}{2}\right] + (1-\theta)\left[\frac{\lambda_i^{j} + \lambda_{i+1}^{j}}{2}\right] \tag{4.27}$$

Equations (4.25, 4.26, and 4.27) are used to transform equation (4.2) into the weighted, finite-difference form of the continuity equation (4.28).

$$\theta\left[\frac{Q_{i+1}^{j+1} - Q_i^{j+1}}{\Delta x_i}\right] + (1-\theta)\left[\frac{Q_{i+1}^{j} - Q_i^{j}}{\Delta x_i}\right] - \left[\theta q_i^{j+1} + (1-\theta) q_i^{j}\right] + \tag{4.28}$$

$$\left[\frac{S_{Ai}^{j+1}\left(A_T + A_o\right)_i^{j+1} + S_{Ai}^{j+1}\left(A_T + A_o\right)_{i+1}^{j+1} - S_{Ai}^{j}\left(A_T + A_o\right)_i^{j} - S_{Ai}^{j}\left(A_T + A_o\right)_{i+1}^{j}}{2\Delta t_j}\right] = 0$$

Equation (4.29) represents the four-point implicit, weighted, finite-difference form of the

momentum equation (4.10).

$$\left[\frac{\left(S_{Ki}Q_i\right)^{j+1}+\left(S_{Ki}Q_{i+1}\right)^{j+1}-\left(S_{Ki}Q_i\right)^{j}-\left(S_{Ki}Q_{i+1}\right)^{j}}{2\Delta t_j}\right]+ \tag{4.29}$$

$$\theta\left[\frac{\left(\beta Q^2/A_T\right)_{i+1}^{j+1}-\left(\beta Q^2/A_T\right)_{i}^{j+1}}{\Delta x_i}\right]+(1-\theta)\left[\frac{\left(\beta Q^2/A_T\right)_{i+1}^{j}-\left(\beta Q^2/A_T\right)_{i}^{j}}{\Delta x_i}\right]+$$

$$(\theta)\left[g\overline{A}_T^{j+1}\left(\frac{h_{i+1}^{j+1}-h_i^{j+1}}{\Delta x_i}+\overline{S}_{fD}^{j}\right)\right]+(1-\theta)\left[g\overline{A}_T^{j}\left(\frac{h_{i+1}^{j}-h_i^{j}}{\Delta x_i}+\overline{S}_{fD}^{j}\right)\right]+$$

$$\theta\left[qv_{x_i}^{j+1}\right]+(1-\theta)\left[qv_{x_i}^{j}\right]=0$$

Where:

$$\overline{A}_T=\left(\frac{A_{Ti}+A_{Ti+1}}{2}\right), \tag{4.30}$$

$$\overline{S}_f=\left(\frac{\overline{Q}|\overline{Q}|}{\overline{K}_T^2}\right), \tag{4.31}$$

$$\overline{Q} = \left(\frac{Q_i + Q_{i+1}}{2} \right), \text{ and} \tag{4.32}$$

$$\overline{K}_T = \left(\frac{K_i + K_{i+1}}{2} \right) \tag{4.33}$$

Following Fread and Lewis, 1998:,

S_K is evaluated at the upstream node of the reach it represents,

β is evaluated at the same node as Q, and

qv_x is evaluated at the upstream node.

The finite-difference forms of the continuity and momentum equations (4.28, 4.29) constitute a system of algebraic equations that are nonlinear with respect to the dependent variables (Q and h) . These variables are unknown at nodes *i* and *i*+1 at time line *j*+1 (Q_i^{j+1}, h_i^{j+1} ; $i = 1, \ldots, N$) but are known at the *j*th time line from either the initial conditions (Q_i^1, h_i^1 ; $i = 1, \ldots, N$) or from the solution of the equations (4.28, 4.29) from the previous computation.

When equations (4.28, 4.29) are written for each of the nodes of the solution grid, there is a total of 2N-2 equations with 2N unknowns. The two equations needed to complete the solution are given by the upstream and downstream boundary conditions. Figure 4.5 provides an outline of the resulting system of equations in functional form at time level *j*+1. The system of 2N equations is solved for each time step with a iterative

method developed by Amein and Fang (1970) which uses a Newton-Raphson approximation.

The Newton-Raphson method begins with the assigning of trial values for ($Q_i^j, h_i^j ; i = 1,\ldots, N$) to the 2N unknowns at the time step being evaluated. Using the trial values in the system of equations (4.28, 4.29) yields a set of 2N residuals. This system can be expressed in vector form as:

$$f(x) = 0 \tag{4.34}$$

where: $x = \left(Q_1, h_1, Q_2, h_2, \ldots\ldots, Q_N, h_N\right)$ is the vector of the unknown values for flow and stage during time step j+1. At iteration k,

$$x^k = \left(Q_1^k, h_1^k, Q_2^k, h_2^k, \ldots\ldots, Q_N^k, h_N^k\right) .$$

Following Fread, 1976 and Chow et. al., 1988, this non linear system is linearized to:

$$f\left(x^{k+1}\right) \approx f\left(x^k\right) + J\left(x^k\right)\left(x^{k+1} - x^k\right) \tag{4.35}$$

where $J\left(x^k\right)$ is a Jacobian coefficient matrix composed of the first partial

Functional Form of Equation	Description
$UB\left(h_1^k, Q_1^k\right) = RUB^k$	Upstream boundary condition
$C_1\left(h_1^k, Q_1^k, h_2^k, Q_2^k\right) = RC_1^k$	Continuity for node x_1
$M_1\left(h_1^k, Q_1^k, h_2^k, Q_2^k\right) = RM_1^k$	Momentum for node x_1
.	.
.	.
.	.
$C_i\left(h_i^k, Q_i^k, h_{i+1}^k, Q_{i+1}^k\right) = RC_i^k$	Continuity for node x_i
$M_i\left(h_i^k, Q_i^k, h_{i+1}^k, Q_{i+1}^k\right) = RM_i^k$	Momentum for node x_i
.	.
.	.
.	.
$C_{N-1}\left(h_{N-1}^k, Q_{N-1}^k, h_N^k, Q_N^k\right) = RC_{N-1}^k$	Continuity for node x_{N-1}
$M_{N-1}\left(h_{N-1}^k, Q_{N-1}^k, h_N^k, Q_N^k\right) = RM_{N-1}^k$	Momentum for node x_{N-1}
$DB\left(h_N^k, Q_N^k\right) = RDB^k$	Downstream boundary condition

Figure 4.5. The system of finite difference equations expressed in function form for time line $j+1$ and the k^{th} iteration of the Newton-Raphson method. (After Fread,1976). RC and RM represent the residuals from the solution of the continuity and momentum equations, respectively.

derivative of $f(x)$ evaluated at x^k. The vector of residual errors is represented by $f(x^{k+1})$. When this vector is set equal to zero, equation 4.35 (with some rearranging) is equivalent to:

$$J(x^k)(\Delta x^k) = -f(x^k) \tag{4.36}$$

where: $\Delta x^k = (x^{k+1} - x^k)$, and (4.37)

$-f(x^k)$ is the vector of the negatives of the residuals. For each iteration (k), the system is solved for Δx^k by Gaussian elimination to estimate the values for x^{k+1}. The process is repeated until Δx^k is smaller than some specified tolerance (Chow et. al., 1988).

Figure 4.6 provides a summary of solution for the system of equations for each time step using the Newton- Raphson method. The values for the unknowns at iteration k+1 are obtained from the solution for Δx^k by equations 4.38 and 4.39.

$$h_i^{k+1} = h_i^k + dh_i \tag{4.38}$$

$$Q_i^{k+1} = Q_i^k + dQ_i \tag{4.39}$$

Where dh_i and dQ_i are components of vector Δx^k.

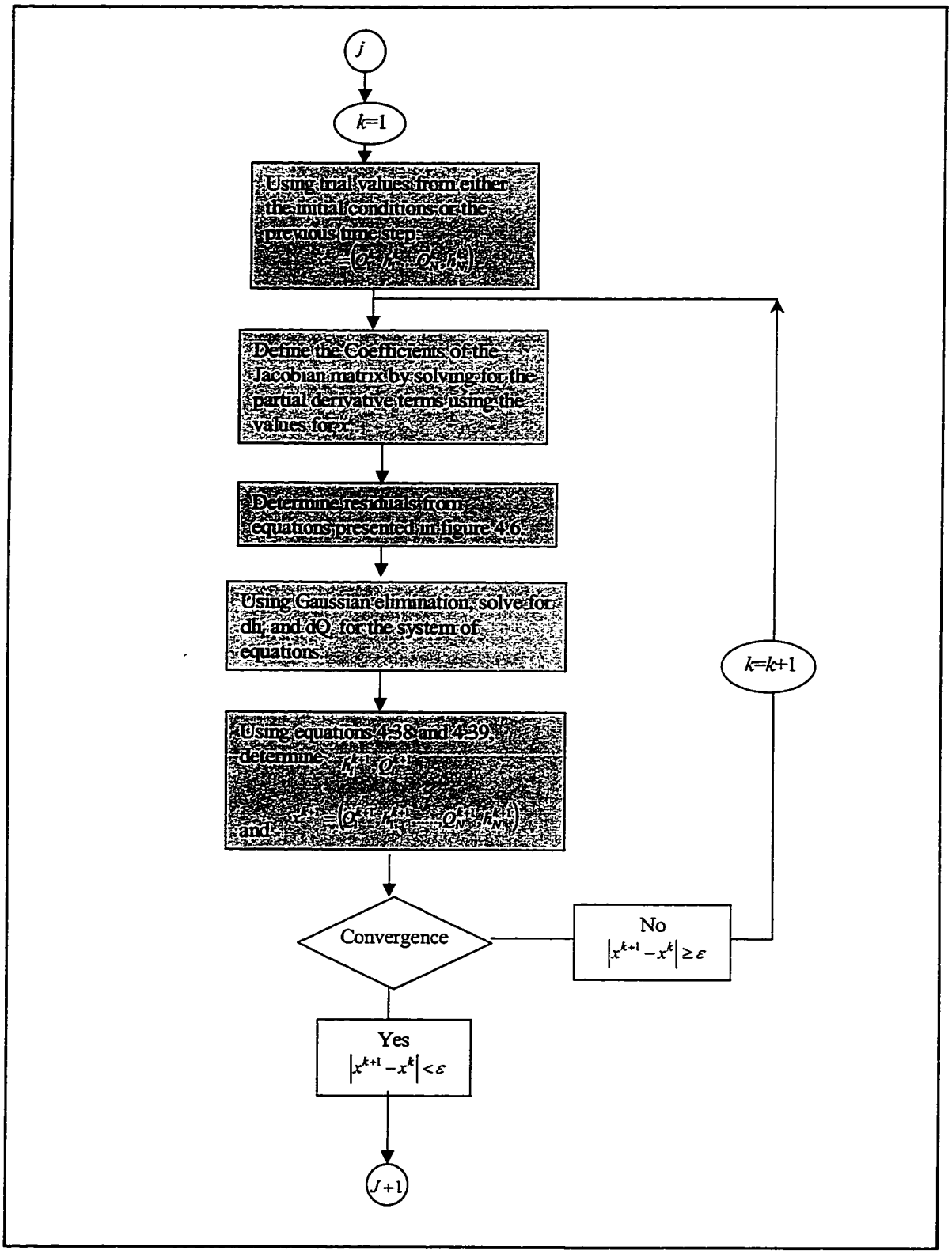

Figure 4.6. Procedure for the solution at each time step for the system of equations that are incorporated in DYNAWET model using the Newton-Raphson method. (Adapted from Chow et.al., 1988)

4.4. Initial and Boundary Conditions

As described in the previous section, the solution for the continuity and momentum equations requires initial and boundary conditions. Initial conditions need to be known for all nodes to solve the governing equations. Boundary conditions for the upstream and downstream boundary are needed to complete the solution grid.

The initial condition is usually provided as a specific flow(Q) and depth(d) for each node. Under steady flow conditions, the initial condition of downstream nodes can be calculated by using the upstream boundary initial conditions in conjunction with any associated lateral flows between downstream nodes. Equation (4.40) provides the formula for steady state conditions (Fread and Lewis, 1998).

$$Q_i = Q_{i-1} + q_{i-1}\Delta x_{i-1} \quad i = 2,3,\ldots N \tag{4.40}$$

The boundary conditions influence the flow behavior of the system being simulated. The upstream boundary is usually provided as a hydrograph of flow (Q) or depth(h) for the most upstream cross-section. The upstream boundary condition may also be provided from a synthesized hydrograph in the mathematical form of a gamma function (Fread,1974). The function is based on initial base flow (Q_o), the time (T_p) from base flow to peak flow (Q_p),the ratio of Q_o to Q_p given as (ρ),and the ratio between the time of the centroid (ratio from the initial steady flow to the centroid of the hydrograph) to T_p, which is given as γ. The gamma function as provided by Fread (1974) is as follows.

$$Q(t) = Q_o + (\rho - 1)\left(\frac{t}{T_p}\right)^{\frac{1}{\gamma-1}} e^{\left(\frac{1}{\gamma-1}\right)\left(1-\frac{t}{T_p}\right)} \tag{4.41}$$

The downstream boundary is located at the point where the system discharges its flow. The downstream boundary can be represented by a rating curve equation that relates flow (Q) with depth (h) at the downstream cross section. Other equations representing the downstream boundary are available. Fread and Lewis (1998) provide five additional equations to calculate the downstream boundary for the FLDWAV model. These equations include (in addition to the single-value rating equation described above), two dynamic loop rating equations, a critical flow rating equation, a known depth time series and a known flow time series.

4.5. Computer Program

The following section provides information on the computer program that was developed to solve the equations presented in the previous sections. The hydrodynamic model presented here was developed by significantly modifying an existing program designed for simulating flood waves resulting from a dam break.

4.5.1. Program Selection

A computer program is needed to utilize the numerical solution for the hydrodynamic flow equations described in section 4.2. As discussed in the Chapter Two Literature Review, there are several models that solve the Saint Venant equations with the weighted four-point finite difference method. These models include the National Weather Services's Flood Wave Model (FLDWAV), the Army Corps of Engineer's CE-QUAL- RIV model and the United States Geological Survey's Full Equations Model (FEQ). Within these models, only the FLDWAV Model incorporates in its formulation

consideration to flood plain flow and channel sinuosity. In addition to these features, the FLDWAV model includes several other features which allow much greater flexibility than either the CE-QUAL- RIV or FEQ models provide.

The NWS FLDWAV model was released in late 1998 and represents the NWS's most advanced model to address the flood waves associated with dam breaks. Earlier models developed by the NWS to address this issue include the DWOPLER model for unsteady flows and the Dam Break model (DAMBK). The FLDWAV model program is written in FORTRAN 77. It includes several external files that must be included to execute the program. The model is able to calculate stage and flows under a large range of conditions. Time and distance steps are adjustable to describe any scale of a system. The most sensitive coefficients (i.e., friction factors) are incorporated in the model to be variable with depth to more precisely model the effects of different depths of flow.

4.5.2. Description of DYNAWET Program Subroutines

The DYNAWET program significantly modifies the NWS FLDWAV model to solve the modified governing equations described in section 4.2. It solves the dynamic wave equation for a wetland system composed of distinct wetland types with associated porosities, friction factors and average stem diameters. The output of the model includes retention times for each segment of wetland which is used in the wetland particle model to analytically calculate particle reduction.

The subroutines of the DYNAWET model that were used to modify the FLDWAV model to account for wetland mechanisms are provided in appendix A.2.

These changes include modifying the read subroutines to rename the flood plain friction factors and include two new parameters describing the porosity and average stem diameter of the flood plains. Since FLDWAV incorporates dynamic arraying, files and subroutines that allocate space for arrays had to be modified to accommodate the new parameters.

The subroutine that calculates the cross-sectional area of the flood plain (SECTF) was modified to include the porosity term (PORE) for each flood plain (right side and left side). Two new subroutines (PORESL and PORESR) were written to allow interpolation of porosities between different depths prior to their use in calculations. These new subroutines maintain an important feature of the FLDWAV program. This feature is the incorporation of depth varying parameters.

The interpolated porosity terms along with the wetland friction factor terms (C_{WET}) and the average stem diameter parameters (DIAL and DIAR) are incorporated into the modification of the subroutine that calculates conveyance (COMPK). The new equation (4.23) presented in Section 4.2 that describes the conveyance in the vegetated flood plains of a wetland is incorporated in this subroutine. The wetland friction factor terms (C_{WETL} and C_{WETR}) are interpolated between depths by two subroutines (FRICTL and FRICTR) which were originally used to interpolate Manning friction factors (CML and CMR) in the FLDWAV program. The average stem diameter parameters (DIAL and DIAR) are interpolated between depths by two new subroutines (STEMSL and STEMSR)

Two subroutines that generate the output of the model (OUTPUT and SUMARY) were modified to provide information that could be used in the particle model. The

formatting for several existing output parameters was modified to allow for enough significant figures to be written in scale with the magnitude associated with the small wetland systems to be modeled. In addition to formatting, three new terms were calculated and written (VTC, XTC and RTTC) to provide information on the average velocity, distance and retention time for each wetland segment. These additional parameters required modification to an additional dynamic arraying subroutine (SIZE) to provide space for the arrays. This subroutine (SIZE) dynamically allocates space for the size of arrays that are calculated within the program.

The DYNAWET model was compiled with the Compaq Visual Fortran (version 6.0) compiler. As with the FLDWAV model, six external files (datafile, lcs, los, mxvl, opfil and unts) are required to execute the program. The program prompts the operator to provide the location and name of the input and output files (Figure 4.7). The start time is provided at the beginning of the execution. A run time is displayed at the end of the execution.

The input file is constructed in free format and follows the FLDWAV model scheme as presented by Fread and Lewis (1998). The parameters utilized in the input file for the DYNAWET simulations of flow through a wetland system is provided in Appendix A.3. Each data group is represented in the input file as a line.

The output of the DYNAWET model is a text file which contains information on input, operation and output of the model (Appendix A.4). The input data is echoed back in the output file to insure the intended parameters were included in the input file. Presentation of model operation information is retained from the FLDWAV model. Specific information is provided for each time step to determine whether the program

successfully converged on a solution. If non-convergence occurs, a notation is made and the time step is reduced automatically in an attempt to reach a solution. If the reduced time steps fail to provide convergence on a solution, a value is provided based on an interpolation between two successful time steps. Output parameters are provided in six tables. The first table provides the peak stage, flow and velocity for each node along the longitudinal axis of the wetland. The next table provides the stage (in feet) for each time step and station located at each cross section. This table is followed by a similarly formatted table with flow (in cubic feet per second) presented instead of stage. The last three tables provide information on the retention times calculated for each time step for each segment.

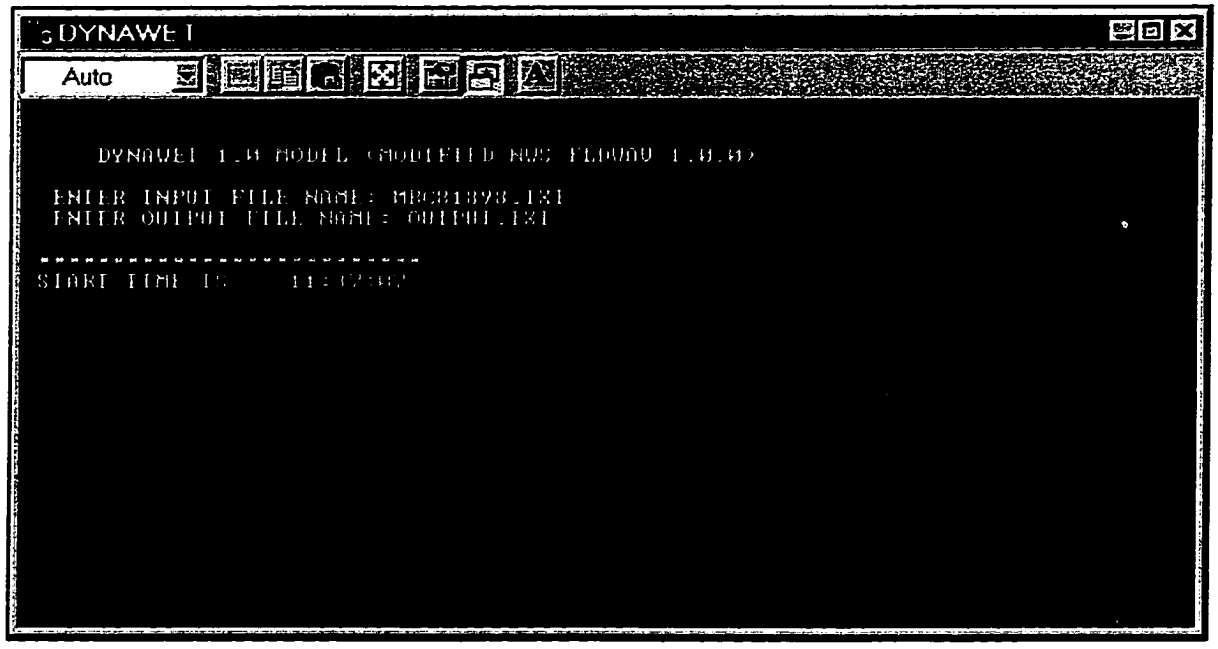

Figure 4.7. The prompt screen for the DYNAWET model. An input and output file name is requested to run the model. The start time (11:37:07) is displayed to provide the user with a measure of actual run time.

5. DYNAWET MODEL APPLICATION

The Dynawet model was applied to the Malcolm Brook wetland site for several storm events to calibrate and verify the hydrodynamic module. An evaluation of how well the model fit the observed data was conducted and is provided in the following sections.

5.1. Data Selection

Information on the depth of flow (or stage) for the upstream boundary site MBF was used to determine which storms were to be modeled in order to calibrate and verify the DYNAWET model. Stage data was collected over approximately eighteen months. Within this time period there were intervals where the record was incomplete due to various types of equipment failure. A full discussion of collection of this data is provided in Chapter Three Data Acquisition. Figure 5.1 presents the level of stage measured at the upstream boundary at site MBF over the most complete portion of the duration of stage data collection. This continuous data set was separated into the two seasons i.e., when the vegetation was growing (leaf-on) and when the vegetation was dormant (leaf-off). Specific storm events were selected to represent varying flow conditions. For each season, the highest and lowest storm event which had a complete data set (i.e.,stage measurements for cross sections at MBF, MBW1, and MBW2) was chosen to calibrate the DYNAWET model. A storm event with a magnitude of stage somewhere between the two calibration events for a specific season was chosen to verify the DYNAWET model for that season.

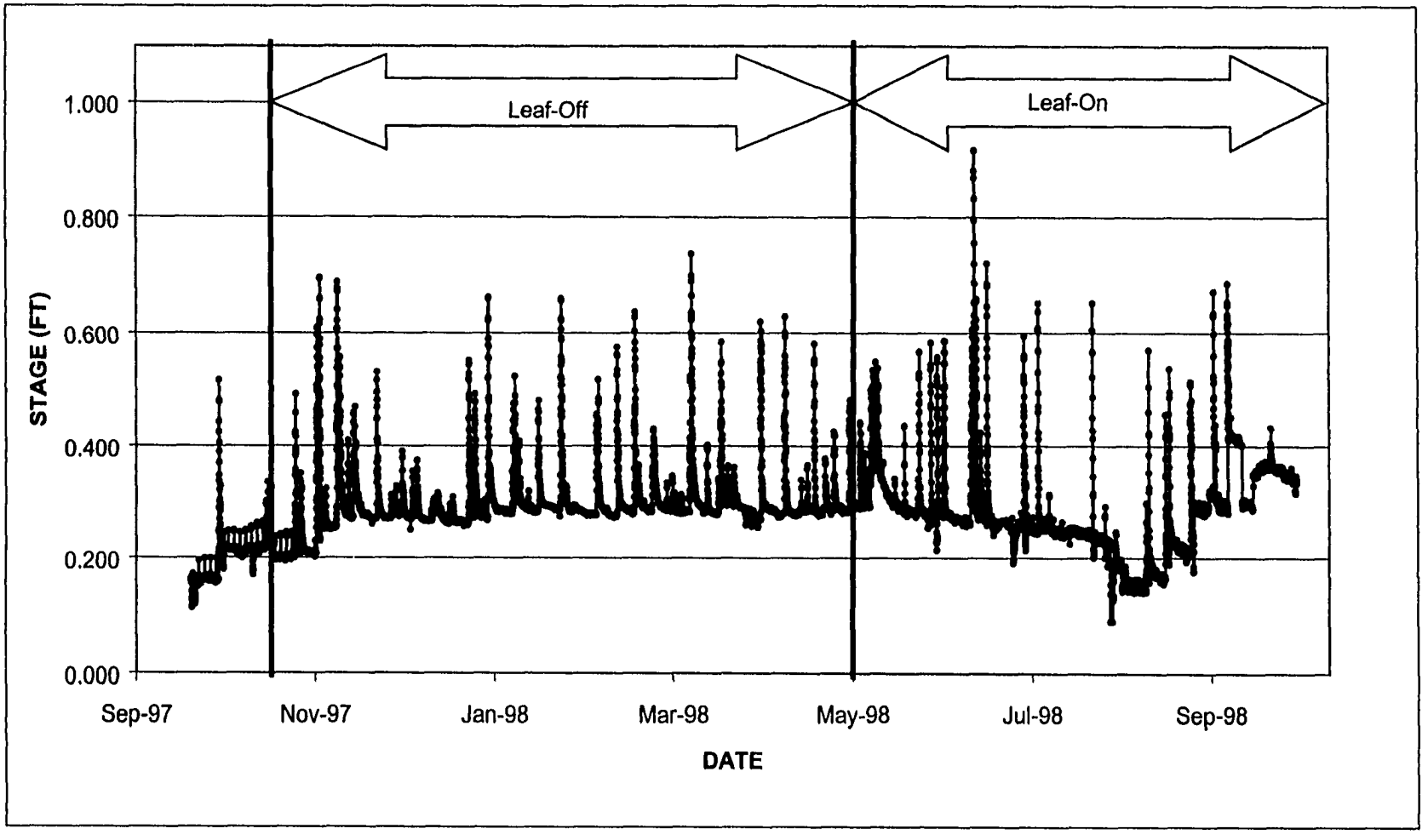

Figure 5.1. Record of stage data for site MBF. Seasons are indicated as leaf-off for October 16 through April 30 and the leaf-on period for May 1 through October 15.

The calibration and verification of the DYNAWET model was based on stage at three cross sections (MBF,MBW1 and MBW2). Although the model could have been calibrated and verified based on flow, these measurements would need to be derived through rating curves with stage data. Such a derivation would likely introduce the error associated with the development of the rating curve. The stage measurements represented a more direct observation of actual field conditions.

The parameters used for calibration were those parameters that are difficult to measure in the field (e.g., wetland porosity and friction coefficients). Simple optimization was accomplished by taking the average high and low flow calibration values as recommended by fread and Lewis (1998). The DYNAWET model has the flexibility to vary these parameters depending on depth of flow. This feature was developed as an important option of the FLDWAV model and remained incorporated in the DYNAWET model.

Figure 5.2 provides the model's sensitivity to these parameters with regard to conveyance. Conveyance represents the capacity of a segment to transmit flow through it and is described mathematically by equations 4.13 and 4.23 in Section 4.2. The DYNAWET model calculates flow for each time step. To compare model sensitivity to the parameters most efficiently, the conveyance calculation for just one segment and time interval was used. Based on Figure 5.2, the general sensitivity of the model to each parameter is implied by the degree of its slope. Accordingly, the model was most sensitive to porosity. Manning's roughness coefficient for the channel, and the friction factor associated with vegetated wetland flood plains resulted in similar sensitivity

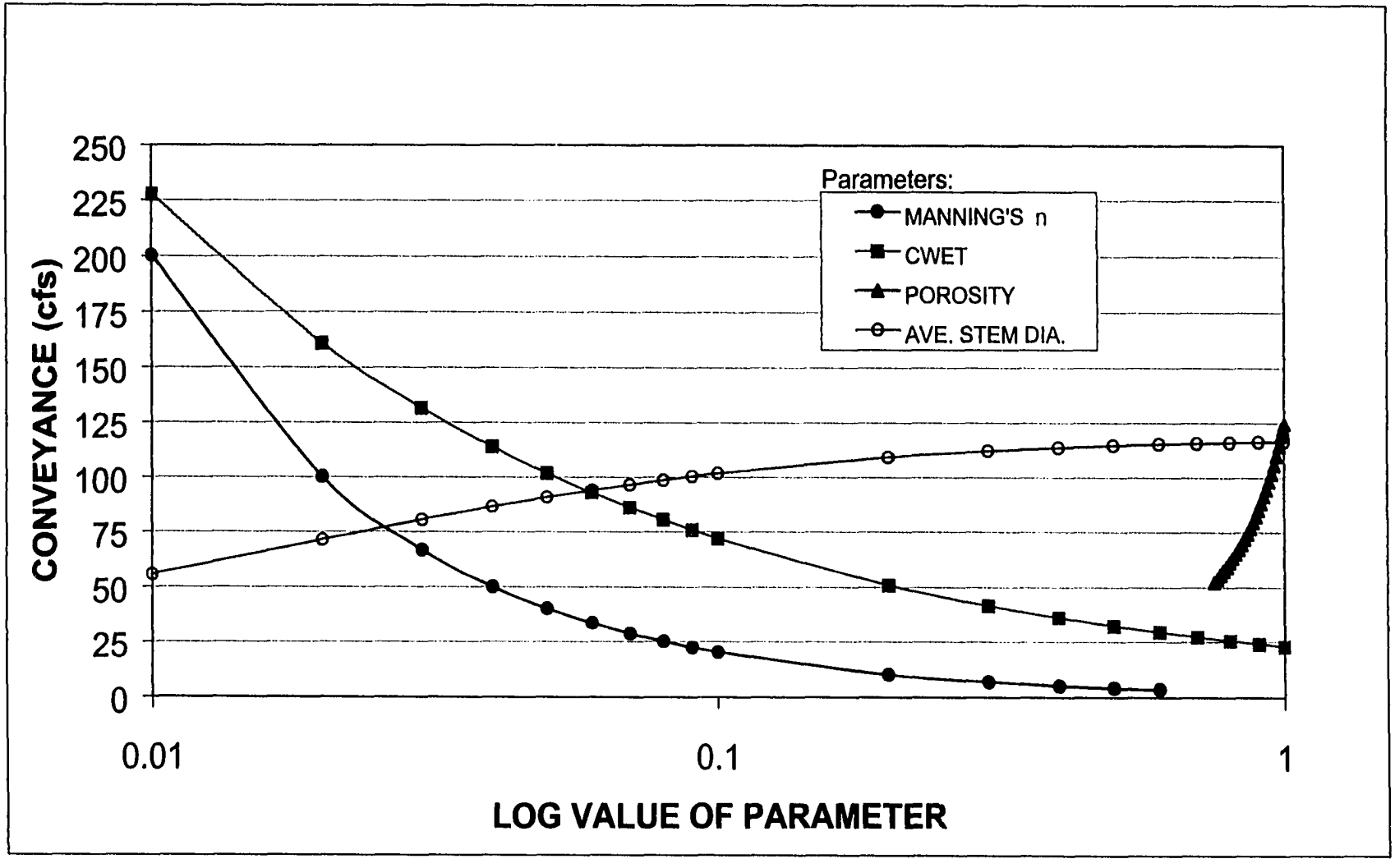

Figure 5.2. Plot of conveyance verses several parameters. Based on the slopes of the lines, sensitivity from highest to lowest is inflow hydrograph, porosity, Manning's n, Cwet and average stem diameter.

with less sensitivity than flow depth or porosity. The model was least sensitive to the average stem diameter parameter.

5.2. Calibration

5.2.1. Leaf-off conditions

Figure 5.3 provides the stage measurements for site MBF for the leaf-off period between January 1, 1998 and May 15, 1998. Within this range of dates, two storm events were selected for the calibration of the DYNAWET model. These dates and how they were used in the calibration and verification process are identified on Figure 5.3. The highest stage producing storm for this period occurred on March 9, 1998. The smallest storm that included flood flow through the vegetated flood plains of the wetland, occurred on April 19, 1998. The DYNAWET model was run on these two events to calibrate the parameters for the two extremes of the range of flow observed for the leaf-off period.

Several model runs were required to find the best fit of the friction and porosity coefficients. The Model's predictions of stage were plotted with the observed stages at each of the sites using these calibrated coefficients and are presented on Figures A.6a through A.7c in Appendix A.5. The model closely matched the observed data for most of each event. The error in stage predictions for both events did not exceed 0.05 feet.

The coefficients resulting from the leaf-off calibration model runs are presented in Table 5.1. The coefficients were associated to different depths numbered one to four.

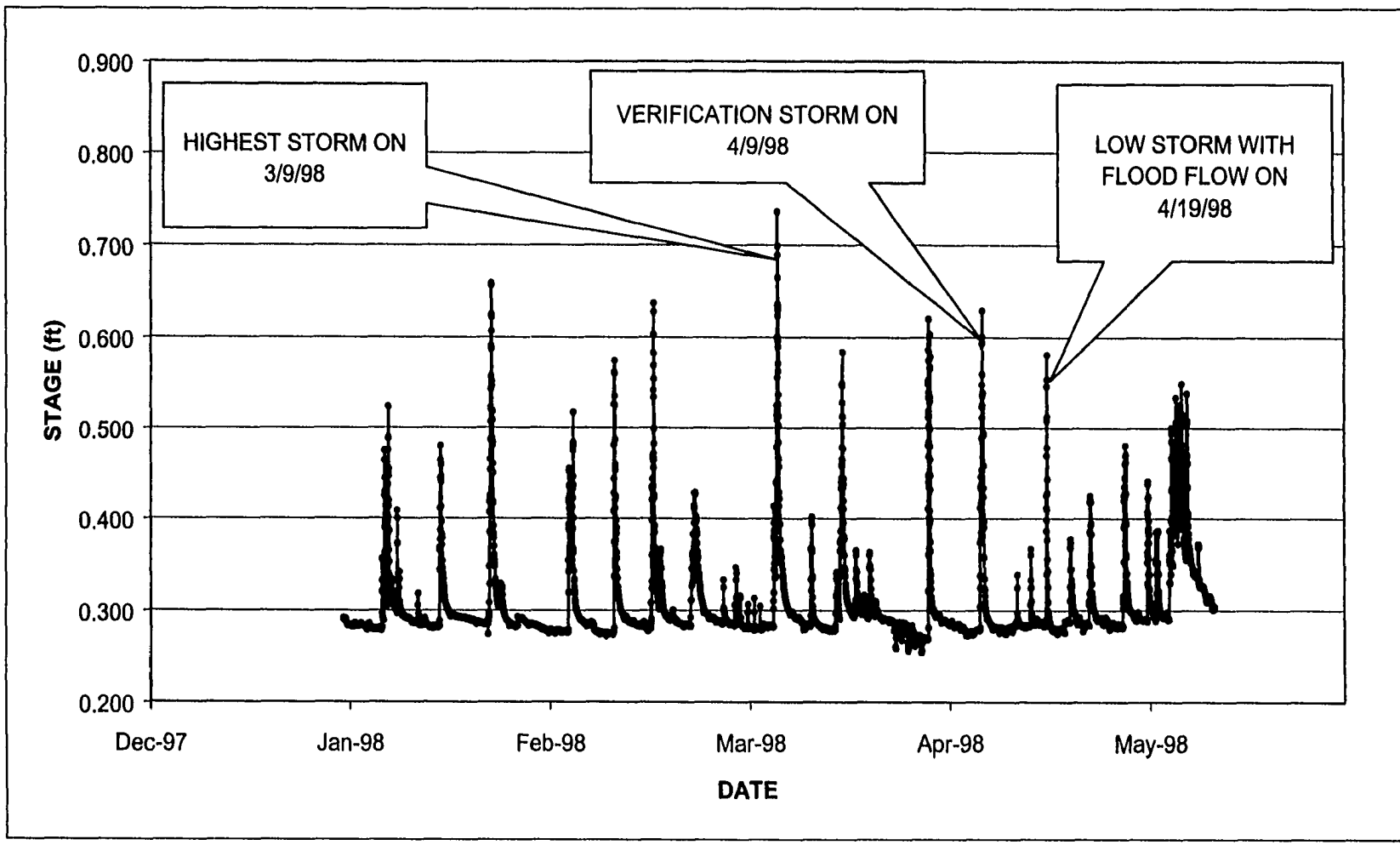

Figure 5.3. Stage measurements during leaf-off period for upstream site MBF. Storm events selected for calibration and verification are indicated on the plot.

Table 5.1. Table of calibrated coefficients for DYNAWET model.

Segment	Coeff	Leaf-off			Leaf-on		
		High	Average	Low	High	Average	Low
		9-Mar	9-Apr	19-Apr	5-Jul	18-Aug	26-Aug
MBF-MBW1	CM1	0.400	0.425	0.450	0.570	0.570	0.570
	CM2	0.400	0.425	0.450	0.570	0.535	0.500
	CM3	0.380	0.355	0.330	0.400	0.375	0.350
	CM4	0.410	0.370	0.330	0.570	0.410	0.250
	CWETL1	0	0	0	0	0	0
	CWETL2	0	0	0	0	0	0
	CWETL3	0.030	0.030	0.030	0.002	0.002	0.002
	CWETL4	0.030	0.030	0.030	0.002	0.002	0.002
	CWETR1	0	0	0	0	0	0
	CWETR2	0	0	0	0	0	0
	CWETR3	0.030	0.030	0.030	0.002	0.002	0.002
	CWETR4	0.030	0.030	0.030	0.002	0.002	0.002
	POREL1	1	1	1	1	1	1
	POREL2	1	1	1	1	1	1
	POREL3	0.95	0.95	0.95	97	97	97
	POREL4	0.96	0.96	0.96	98	98	98
	PORER1	1	1	1	1	1	1
	PORER2	1	1	1	1	1	1
	PORER3	0.95	0.95	0.95	97	97	97
	PORER4	0.96	0.96	0.96	98	98	98
	DIAL1	0	0	0	0	0	0
	DIAL2	0	0	0	0	0	0
	DIAL3	0.150	0.150	0.150	0.110	0.110	0.110
	DIAL4	0.150	0.150	0.150	0.110	0.110	0.110
	DIAR1	0	0	0	0	0	0
	DIAR2	0	0	0	0	0	0
	DIAR3	0.15	0.15	0.15	0.11	0.11	0.11
	DIAR4	0.15	0.15	0.15	0.11	0.11	0.11
MBW1-MBW2	CM1	0.650	0.525	0.400	0.250	0.250	0.250
	CM2	0.650	0.525	0.400	0.250	0.200	0.150
	CM3	0.950	0.710	0.470	0.260	0.180	0.100
	CM4	0.980	0.765	0.550	0.250	0.200	0.150
	CWETL1	0	0	0	0	0	0
	CWETL2	0	0	0	0	0	0
	CWETL3	0.027	0.027	0.027	0.005	0.005	0.005
	CWETL4	0.027	0.027	0.027	0.005	0.005	0.005
	CWETR1	0	0	0	0	0	0
	CWETR2	0	0	0	0	0	0
	CWETR3	0.027	0.027	0.027	0.005	0.005	0.005
	CWETR4	0.027	0.027	0.027	0.005	0.005	0.005

Table 5.1. Table of calibrated coefficients (continued).

Segment		Leaf-off			Leaf-on		
		High	Average	Low	High	Average	Low
		9-Mar	9-Apr	19-Apr	5-Jul	18-Aug	26-Aug
MBW1-MBW2 (cont.)	POREL1	1	1	1	1	1	1
	POREL2	1	1	1	1	1	1
	POREL3	0.86	0.86	0.86	0.96	0.96	0.96
	POREL4	0.87	0.87	0.87	0.97	0.97	0.97
	PORER1	1	1	1	1	1	1
	PORER2	1	1	1	1	1	1
	PORER3	0.86	0.86	0.86	0.96	0.96	0.96
	PORER4	0.87	0.87	0.87	0.97	0.97	0.97
	DIAL1	0	0	0	0	0	0
	DIAL2	0	0	0	0	0	0
	DIAL3	0.100	0.100	0.100	0.025	0.025	0.025
	DIAL4	0.100	0.100	0.100	0.025	0.025	0.025
	DIAR1	0	0	0	0	0	0
	DIAR2	0	0	0	0	0	0
	DIAR3	0.100	0.100	0.100	0.025	0.025	0.025
	DIAR4	0.100	0.100	0.100	0.025	0.025	0.025
MBW2-MBW3	CM1	0.040	0.085	0.130	0.130	0.090	0.050
	CM2	0.040	0.085	0.130	0.130	0.090	0.050
	CM3	0.040	0.043	0.045	0.050	0.030	0.010
	CM4	0.010	0.010	0.010	0.010	0.010	0.010
	CWETL1	0	0	0	0	0	0
	CWETL2	0	0	0	0	0	0
	CWETL3	0.010	0.010	0.010	0.002	0.002	0.002
	CWETL4	0.010	0.010	0.010	0.002	0.002	0.002
	CWETR1	0	0	0	0	0	0
	CWETR2	0	0	0	0	0	0
	CWETR3	0.027	0.027	0.027	0.005	0.005	0.005
	CWETR4	0.027	0.027	0.027	0.005	0.005	0.005
	POREL1	1	1	1	1	1	1
	POREL2	1	1	1	1	1	1
	POREL3	0.95	0.95	0.95	0.97	0.97	0.97
	POREL4	0.96	0.96	0.96	0.98	0.98	0.98
	PORER1	1	1	1	1	1	1
	PORER2	1	1	1	1	1	1
	PORER3	0.86	0.86	0.86	0.96	0.96	0.96
	POREL4	0.87	0.87	0.87	0.97	0.97	0.97
	DIAL1	0	0	0	0	0	0
	DIAL2	0	0	0	0	0	0
	DIAL3	0.150	0.150	0.150	0.100	0.100	0.100
	DIAL4	0.150	0.150	0.150	0.100	0.100	0.100
	DIAR1	0	0	0	0	0	0
	DIAR2	0	0	0	0	0	0
	DIAR3	0.100	0.100	0.100	0.100	0.100	0.100
	DIAR4	0.100	0.100	0.100	0.100	0.100	0.100

Depths one to two were associated with channel flow and depths three to four were associated with flood flow (Figure 5.4). For leaf-off conditions, the channel friction factor (Manning's n) varied between 0.330 and 0.980 amongst the three segments. The wetland flood plain friction factor (C_{wet}) varied between 0.01 and 0.03. The porosity varied between 0.86 and 0.96 and the average stem diameter varied between 0.10 and 0.15. Within a segment, the variation of these coefficients was much smaller (within the same order of magnitude).

5.2.2 Leaf-on conditions

The same procedure was followed for the leaf-on conditions as was performed for the leaf-off calibration. The highest stage producing storm for this period and the smallest storm that included flood flow through the vegetated flood plains of the wetland, were selected from the stage measurements for site MBF. The leaf-on period with a continuous data record was between May 16, 1998 and September 30, 1998 (Figure 5.5). The largest storm with a complete stage record occurred on July 5,1998. The smallest event with flood flow and a complete data record occurred on August 26, 1998. The data from these two events were used to calibrate the friction and porosity coefficients of the DYNAWET model for the two extremes of the range of flow observed for the leaf-on period. The leaf-on calibration also required several model runs to find the coefficients that provided the best model fit to the observed data. Figures A.8a through A.9c in appendix A.5 provide plots of the model's prediction of stage using these calibrated coefficients along with the observed stages for each site. The simulated stage matched the observed stage within 0.075 feet.

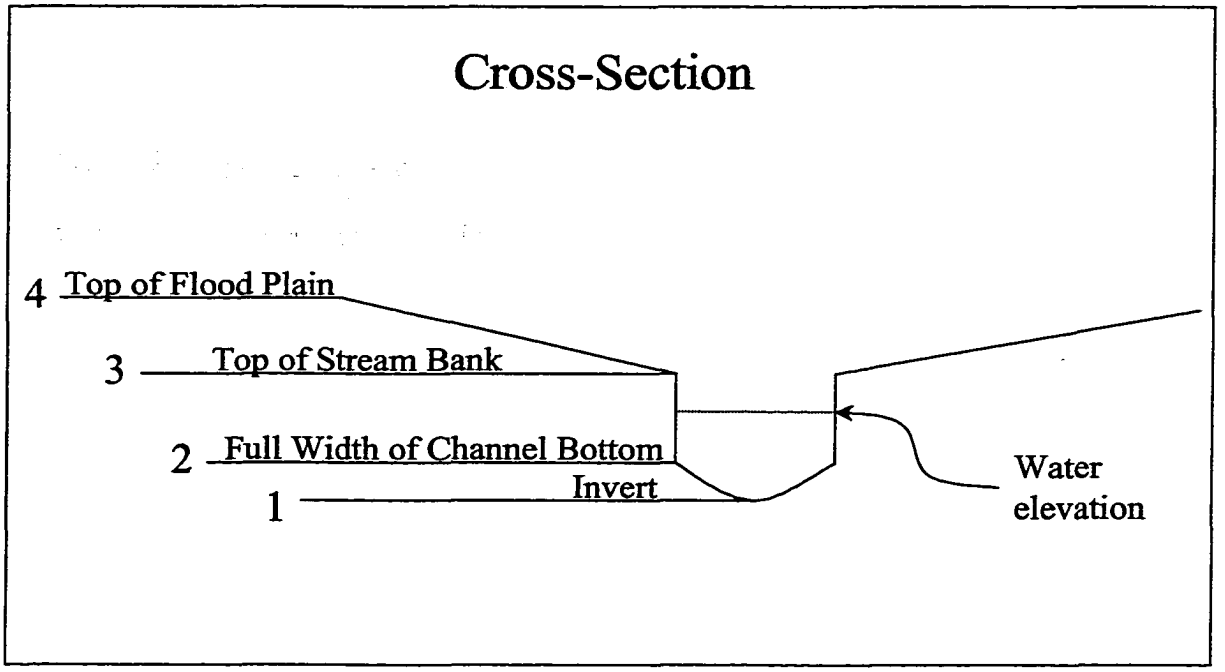

Figure 5.4. Schematic of the cross-section of a wetland segment identifying the location of the elevations used for the calibration coefficients.

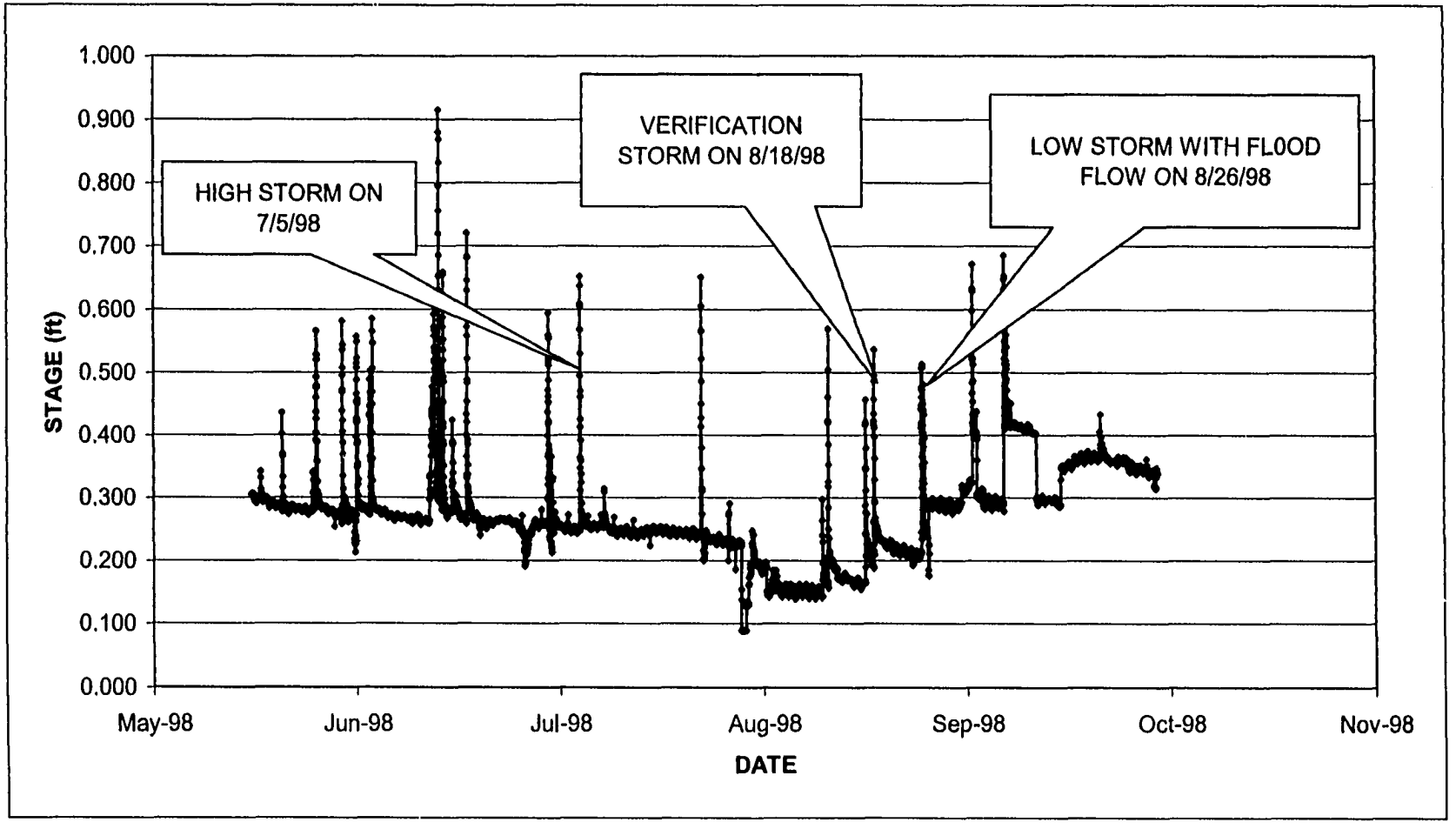

Figure 5.5. Stage measurements during leaf-on period for upstream site MBF. Storm events selected for calibration and verification are indicated on the plot.

The calibrated coefficients for leaf-on conditions are presented in Table 5.1. Amongst the three segments, the channel friction factor (Manning's n) varied between 0.010 and 0.570. The wetland flood plain friction factor (C_{wet}) varied between 0.002 and 0.025. The porosity varied between 0.96 and 0.98 and the average stem diameter varied between 0.110 and 0.025. As with the leaf-off calibration, this variation was much smaller within a segment.

5.3 Verification

5.3.1 Coefficients used in verification runs

The model was applied to a total of six events. Four events, covering two seasons (3/9/98, 4/19/98,7/5/98 and 8/26/98) were simulated to calibrate the model. Two events, covering two seasons (4/9/98 and 8/18/98) were simulated to verify the model. Table 5.1 provides the value of the coefficients calibrated through the calibration runs. The coefficients used for model verification were based on the average of the coefficients calibrated during each of the two calibration events modeled for a season.

Changes in the calibration coefficients support the observations seen during the dye tracer tests. Generally there is a decrease in porosity and an increase in the friction coefficients during the leaf-off period. The porosity of the emergent segment decreased to a larger extent than for the scrub-shrub segment. The wetland friction factor was much greater with the scrub-shrub segment (fifteen times larger than for the leaf-on season) than the emergent segment (six times larger than for the leaf-on season). These changes support the findings from the dye tracer tests that the retention times increase during the leaf-off season.

5.3.2 Leaf-off conditions

A storm that reflected flow conditions between the two storm events used for the calibration was selected for verification under leaf-off conditions. The intermediate storm event chosen to represent leaf-off conditions occurred on April 9, 1998. The coefficients used for the verification run was equal to the average of the coefficients determined through the leaf-off calibration runs. These average values are presented in Table 5.1.

The stages predicted by the model for verification were plotted along with the observed data. These plots are presented in Figures 5.6a through 5.6c. The model was able to match most of the observed data within 0.100 feet. Site MBW2 over-predicted the peak of the hydrograph (not exceeding 0.100 feet). How well the model fit the observed data is discussed in section 5.4, Model Performance.

5.3.3 Leaf-on conditions

A similar procedure was followed to verify the DYNAWET model for leaf-on conditions. The intermediate storm event chosen for the leaf-on season occurred on August 18, 1998. The verification used coefficients that represented the average value between the coefficients used for the calibration storm events. Figures 5.7a through 5.7c provide the plots for the stages predicted by the model and those observed in the field. The predicted values matched the observed values well (in terms of matching the pattern of the stage without missing peaks or lows). The simulations indicated less error (not exceeding 0.040 feet) for the simulations of sites MBF and MBW2 than for the leaf-off verification. However, there was greater error for site MBW1. The simulated data for site MBW1 under-predicted the observed data for all of the hydrograph by 0.100 to 0.150

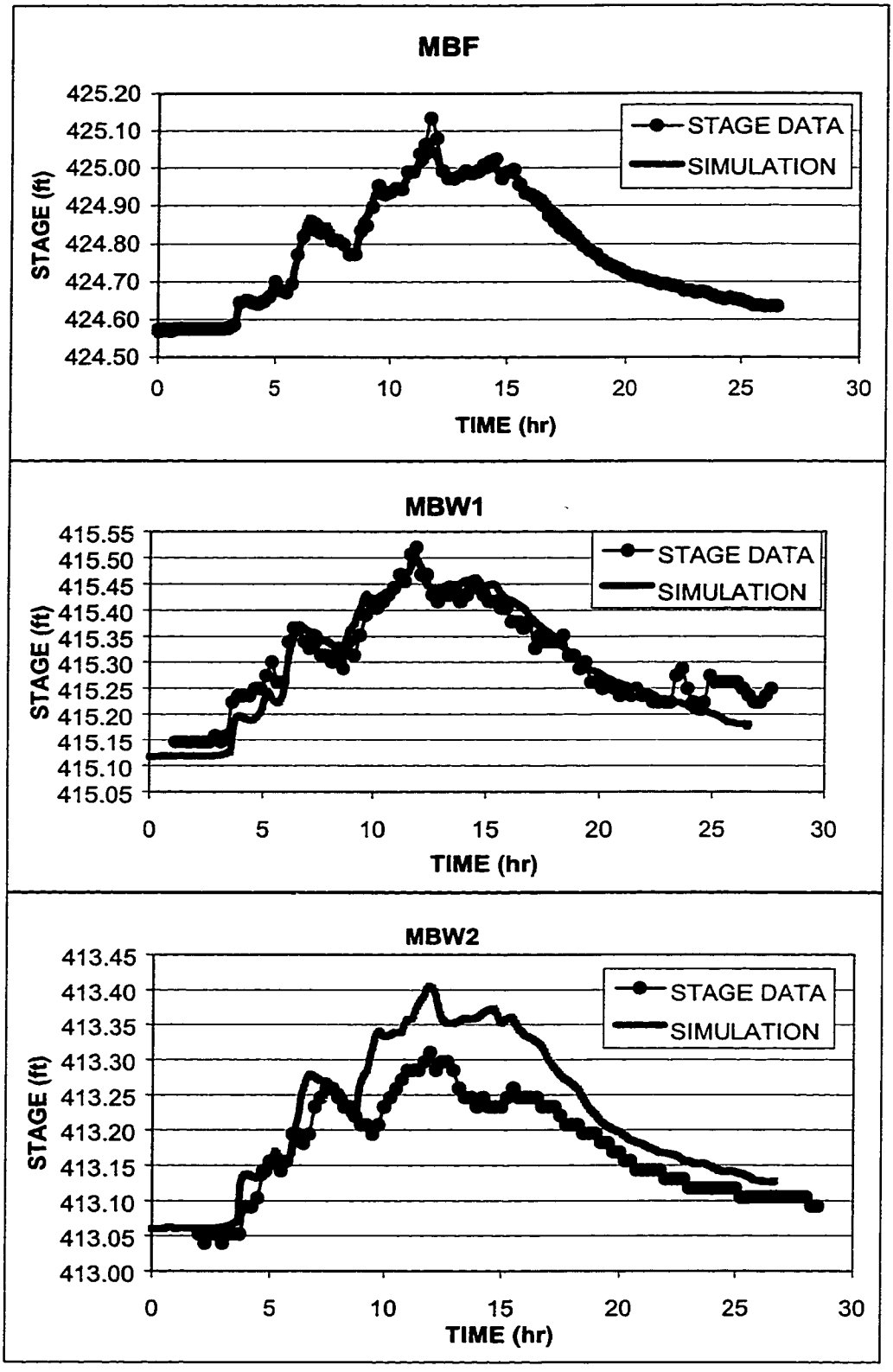

Figures 5.6 a,b,c. Plots of simulation and stage data at each monitoring station for leaf-off storm event validation on 4/9-10/98.

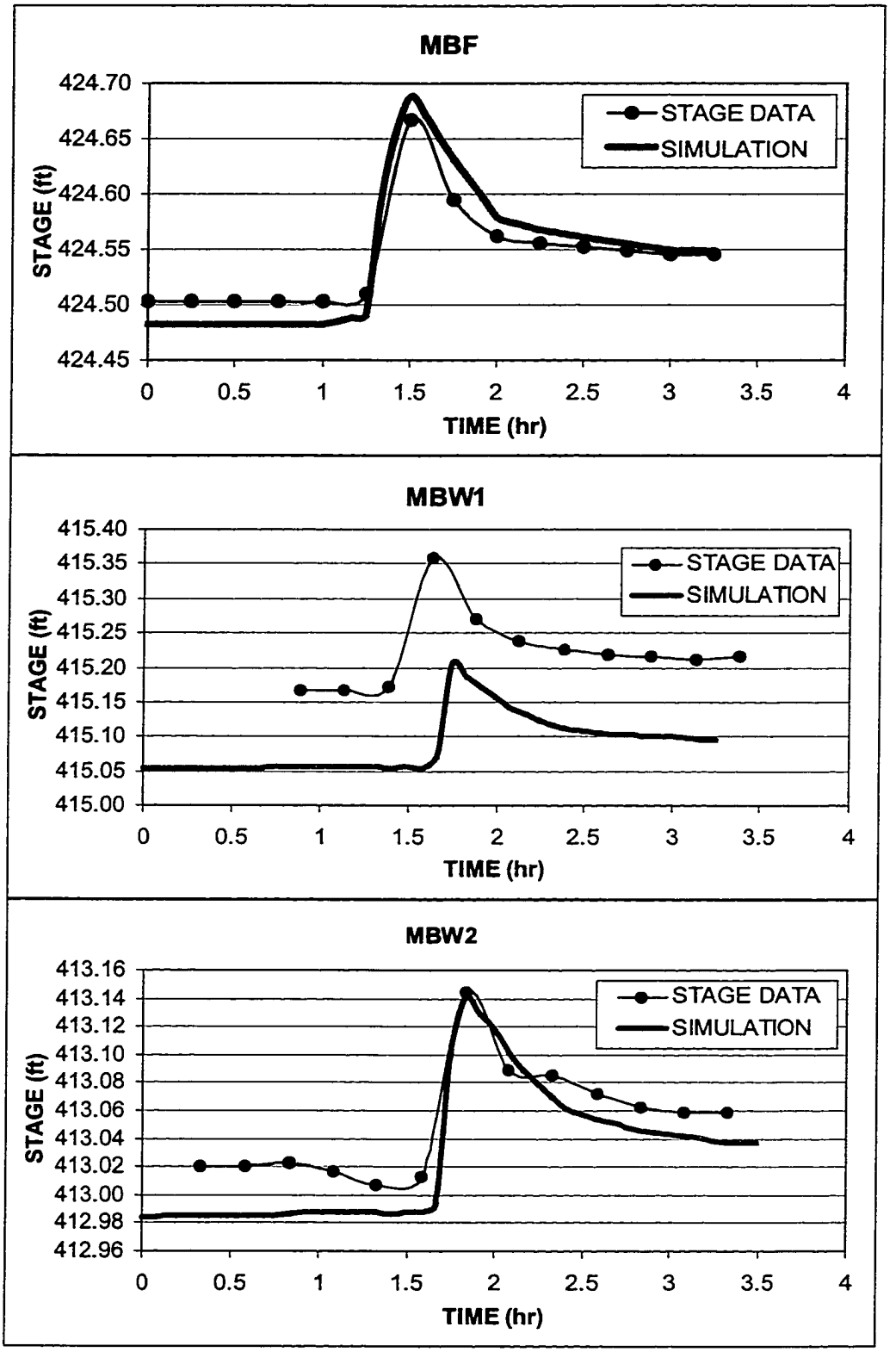

Figures 5.7 a,b,c. Plots of simulation and stage data at each monitoring station for leaf-on storm event verification on 8/18/98.

feet. Section 5.4, Evaluation of DYNAWET model provides a discussion on how well the model fit the observed data for the leaf-on season.

5.4 Model Performance

The DYNAWET model is based on equations that describe the physics of water flowing through a wetland system. Mechanistic relationships were used in place of empirically derived equations where possible. Model performance is therefore a measure of how well these mathematical expressions describe the mechanics of the system. The equations used in the DYNAWET model were able to converge on a solution due to the model's flexibility in accepting any time and distance step as well as its level of detail regarding the system's physical parameters (i.e., channel and flood plain width, sinuosity, and segment lengths).

The model was able to simulate the stage, for a large range of conditions. The adequacy of these simulations can be evaluated through the results presented in the Figures of the previous sections. These figures indicate that the model is capable of simulating stages at different cross-sections that matched the pattern of stages observed with field equipment. This pattern not only describes the magnitude of the flow wave but also its timing. The events used for the calibration and verification of the model had varying patterns, including single sharp peak events (i.e., 7/5/98, 4/19/98 and 8/18/98), and multiple peak events (i.e., 3/9/98,4/9/98 and 8/26/98). The model's ability to match this variety of events demonstrates its adequacy in simulating the physical processes that occur in a natural wetland. This ability also indicates that the model is robust (i.e., applicable to a wide range of conditions).

Another approach to evaluate model performance is to plot the simulated data

against the observed data at each observation station. Figures 5.8a through 5.9c provide the scatter plots for the simulations used to verify the model (the 4/9/98 and 8/18/98 storm events). Most of the sites closely match the 1:1 line. This information was also used to determine the correlation coefficient (r^2) to measure the degree of closeness between simulated and observed data, its significance (F), and the Root Mean Square Error (RMSE). The RMSE is a statistic that describes the accuracy of the model with an estimate of the average error (which includes both random and systematic error). Table 5.2 provides these values for the verification simulations under leaf-on (8/18/98) and leaf-off (4/9/98) conditions. Based on this table, almost all the simulated data matched the observed data with r^2 values at or greater than 0.900, with high confidence (i.e., F was small) and low RMSE (less than 5 %). The exceptions were for site MBW2 for the leaf-off period (which had a r^2 value of 0.895 and a RMSE of 6.32 percent) and site MBW1 for the leaf-on period (which had a r^2 value of 0.060 and a RMSE of 13.00 percent).

The slightly larger error associated with the model run for site MBW2 for the leaf-off period indicated that the model over-predicted the peak stage and receding limb of the hydrograph. The lower observed stage may have been the result in a reduction in the debris found in the flow path. The event represented the later part of the leaf-off season when early spring flows could have flushed debris out. Such a change could influence the values of porosity and friction which was not reflected in the coefficients (which were based on the average of the coefficient values estimated for the two calibration events).

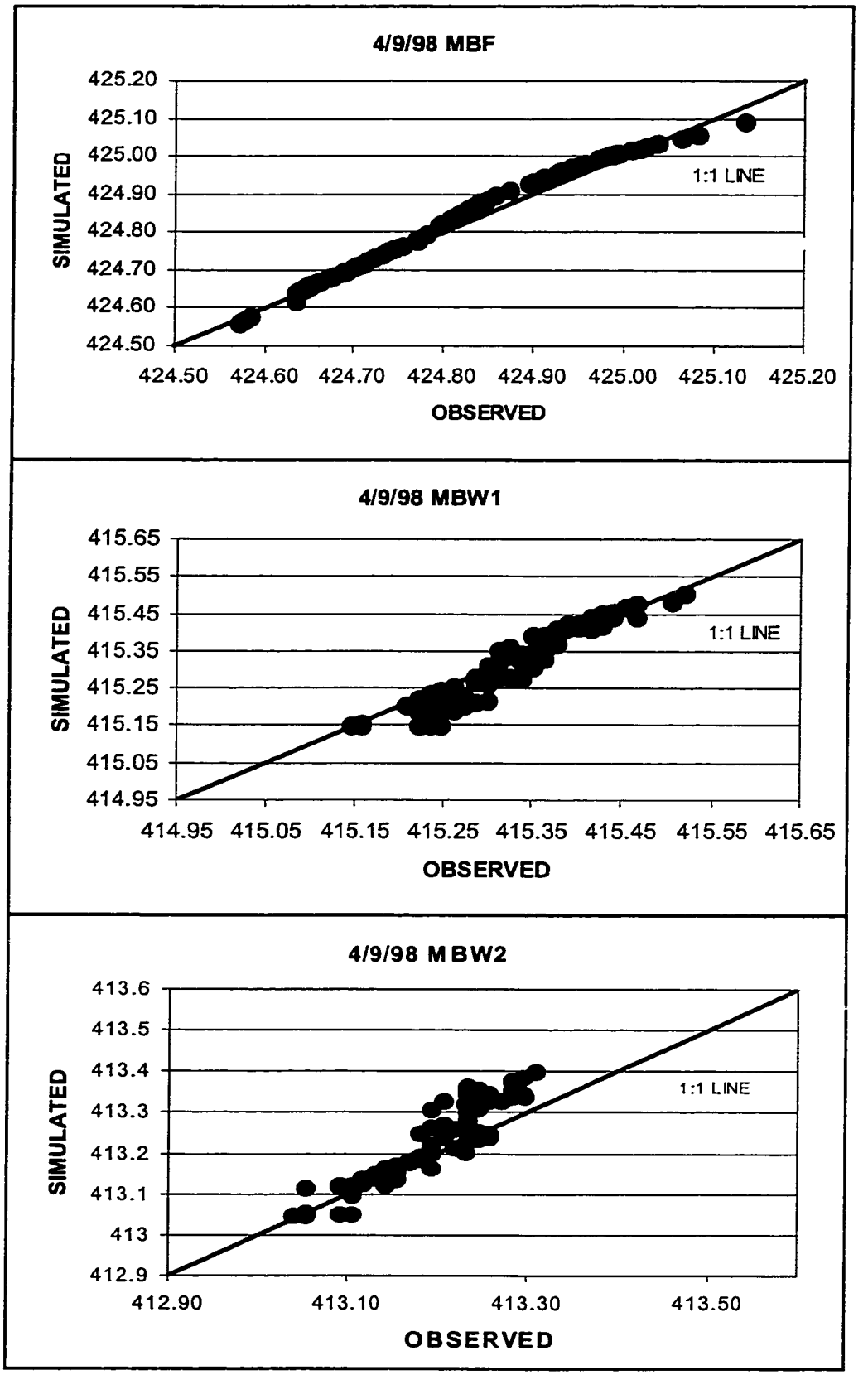

Figures 5.8.a,b,c. Scatter plots comparing simulated model results with observed stage values for leaf-off conditions.

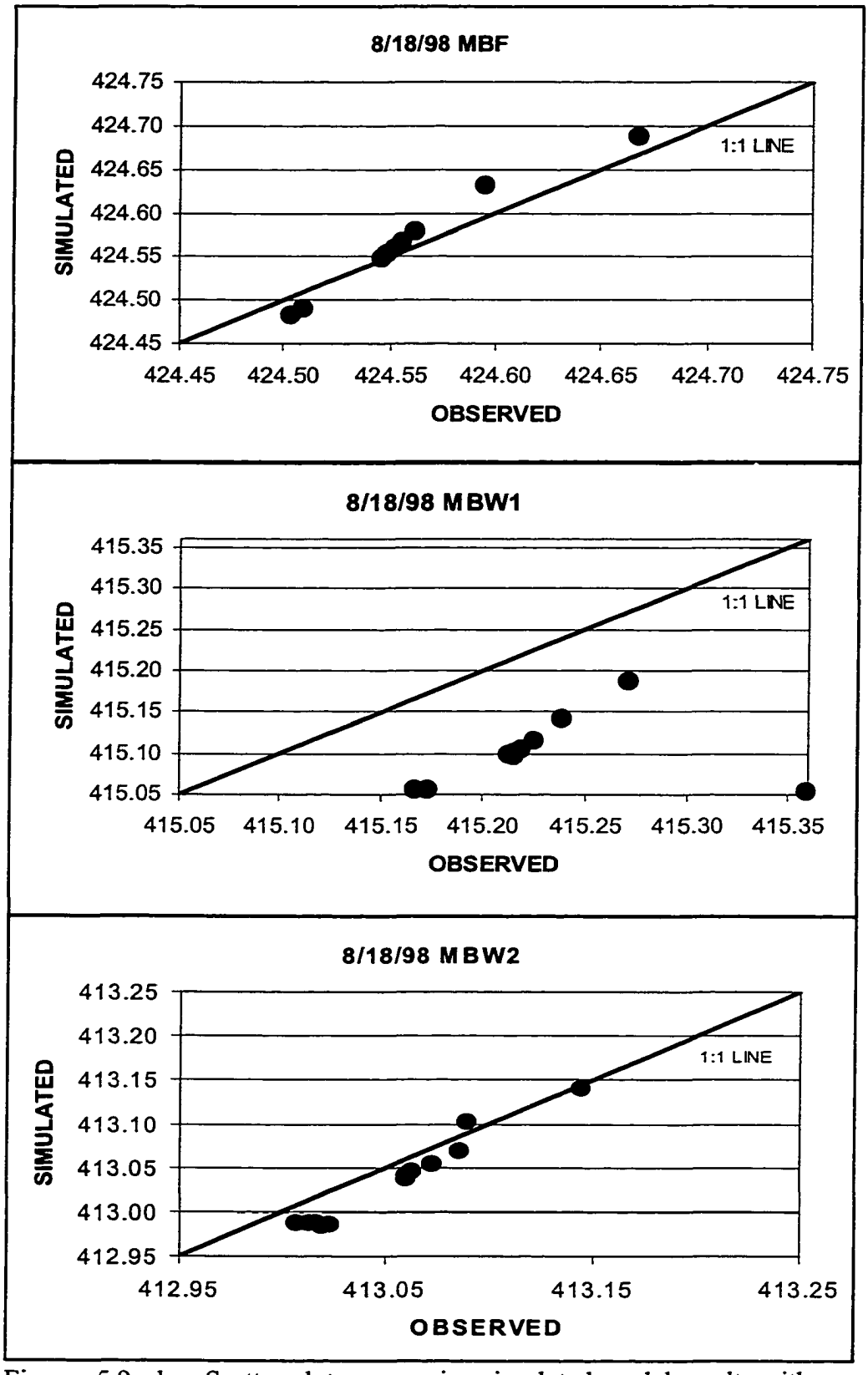

Figures 5.9 a,b,c. Scatter plots comparing simulated model results with observed stage values for leaf-on conditions.

Table 5.2. Table of statistical values evaluating DYNAWET model performance.

Leaf-off				
4/9/98	R Square	Standard Error	Significance F	RMSE
MBF	0.994	0.012	1.73E-119	1.22%
MBW1	0.925	0.031	6.09E-58	3.46%
MBW2	0.895	0.032	2.96E-49	6.31%
Leaf-on				
8/18/98	R Square	Standard Error	Significance F	RMSE
MBF	0.975	0.011	6.03E-11	1.86%
MBW1	0.060	0.043	4.67E-01	13.00%
MBW2	0.967	0.010	1.74E-09	2.40%

The largest error was seen at site MBW1 for the leaf-on period. Figure 5.7b indicates that the model not only under-predicted the magnitude throughout the hydrograph, but it also lagged the hydrograph by a few minutes. This shift may have been the result of short circuiting of the flow through the first segment, which resulted in the observed stage peaking before the predicted peak. The timing issues associated with the data loggers as discussed in Chapter 3 could also have been the cause of this error. Explanations for the under-prediction include the errors inherent with the relatively few data points used for the comparison. In this case, the observed data could have missed the peak stage. Another explanation for the under-prediction is that there was a reduction in the cross-sectional area due to sedimentation. In this case, the model input data would have assumed a larger cross-sectional area than what would have existed at the site.

6. SUMMARY AND CONCLUSIONS

Since wetlands can have a positive influence on water quality, there has been a growing interest in developing models that can simulate the flow and water quality changes that occur when stream flow travels through these systems. This dissertation represents a first attempt to evaluate and model the hydrodynamic behavior of natural wetlands. Published studies on wetland flow have focused almost exclusively on constructed wetlands. Study of the hydrodynamics and particle transport through natural wetlands has been limited because natural wetlands are irregularly shaped, can be composed of heterogenous vegetation and tend to include meandering stream channels. These features cause the flow characteristics associated with natural wetlands to be more dynamic than those for constructed wetlands. Models developed to simulate the flow through wetlands have generally lacked the inclusion of influences from stream sinuosity, porosity, and seasonal changes in vegetation (which are included in the DYNAWET model). This dissertation presents a mathematical model, based on field observations, that explicitly accounts for the occurrence of meandering streams, vegetation density, and friction. These features, influence wetland retention times which in turn affects particle fate and transport. The overall goal of the development of this model was to provide an improved description of flow through a natural wetland that is based on variables that can be measured in the field without extraordinary resources.

A considerable amount of field data was collected and analyzed to describe the hydrodynamics of natural wetlands and provide a basis for the theory of the model. This information also enabled the model to be calibrated and verified. Dye tracer tests were

used in this study to develop a description for the hydrodynamics of different wetland types during different seasons. This description included the influence of different classified wetland segments on average velocities between base and flood flow conditions. Through dye tracer studies of two types of wetlands (scrub-shrub and emergent), two wetland characteristics were found to have a profound effect on the flow: stream sinuosity and vegetation density.

In addition to the changes in the hydraulics observed between different classified wetland segments, there were differences in average velocities between the leaf-on and leaf-off seasons. Generally, the dye tracer tests indicated that velocity is slower during the leaf-off season. This finding was also predicted through the modeling results. While counter-intuitive, this finding may be explained by the fact that flow through a natural wetland is generally shallow and during the leaf-off period there is a greater amount of leaf litter in the zone of flow.

To model the hydrodynamics of natural wetlands, the governing equations need to account for the characteristics mentioned above. The mathematical model developed in this study (DYNAWET) describes the variations of flow in natural wetlands under different seasons and weather conditions by using the full dynamic wave equation to account for the inertial forces that are found in wetlands due to the effects of vegetation. This equation has been modified to incorporate the sinuosity of the wetland stream, the reduction in cross section flow area due to the presence of vegetation, and the additional reduction in conveyance due to increased drag at the wetted perimeter of the vegetation. These modifications provide a detailed description of flow through a wetland that can be

related to wetlands classified within the National Wetland Inventory Classification Scheme.

The new full dynamic wave equation is theoretically applicable to almost any type of wetland class. In this study, it was applied to two different classes of wetlands (scrub-shrub and emergent). As a result, the model was able to simulate wetland stage, flow, and retention time for various segments over a wide range of storms event types.

The computer program developed for the model (DYNAWET) is based on the United States National Weather Service's FLDWAV model with significant modifications to solve the equations developed in this dissertation. The DYNAWET model replaces the Manning's equation expressions for the flood plain conveyance with equations that specifically account for the porosity, average vegetative stem diameter, and drag friction that are unique for flow through vegetation. The calculation of cross-sectional areas also is modified to include a wetland porosity parameter.

Comparison of the model with stage data collected in the field demonstrates a reasonable fit. The accuracy of the model was dependent, in part, on the accuracy of the measurements of the cross sectional areas and upstream flow. Field data accuracy could be improved with greater quality control and maintenance of equipment.

The DYNAWET model should be very flexible in its application for wetlands. Theoretically, the model can be applied to any riverine wetland system where the upstream flow is known, information is available on the width of flow at different depths, wetland types have been delineated, and stage data is available for calibration. In addition to this flexibility, the model's resolution may be applied over a wide range of

time and space. This is due to the emphasis placed on basing the model on the mathematical description of the physics of water movement rather than on empirical relationships. The flexibility in resolution theoretically allows the model to be applicable from the largest river-flood plain system to the smallest system that contains channelized flow.

Although the DYNAWET model is extremely flexible in its application for wetlands there are some shortcomings. In particular, the model is not applicable to wetland systems that require their hydrodynamics to be described in more than one dimension (i.e., upland and pothole wetlands). The DYNAWET model also requires numerous input settings to run a simulation. A relatively high level of sophistication in running Fortran-based models is required. This task could be made much easier with the incorporation of a user interface subroutine. Table 6.1 provides a summary of the model's strengths and shortcomings.

This study found that the scrub-shrub wetlands act hydraulically similar to a shallow detention basin where flow is detained during base flow conditions then released more rapidly during flood flow conditions. Emergent wetlands appear to have a reverse effect. During low flows an emergent wetland behaves hydraulically similar to an open channel and at high flows it behaves similar to a retention tank with a large storage capacity during high flows. The arrangement of wetland types observed in Malcolm Brook may be ideal for controlling pollution from the first wash-off of a storm. In Malcolm Brook, the first flush is detained mostly by scrub-shrub wetlands whereas the peak flow is retarded by the emergent wetland.

Table 6.1 Information on the strengths and shortcomings of the DYNAWET model.

Model Strengths	Model Shortcomings
Theoretically applicable to a wide range of riverine wetland systems.	One-dimensional flow is assumed therefore the model is not applicable to certain wetlands (i.e.,upland and pothole wetlands).
The time and space resolution of the model is highly flexible.	Many input settings are required to run the model.
The governing equations of the model are based on a mathematical description of the physics of water movement through a wetland instead of empirical relationships.	A sophisticated level of understanding of the model input is required to operate the model.
The model includes wetland parameters such as a porosity and friction coefficient in its mathematical description.	The model lacks a graphical user interface to improve usability.
The wetland parameters are associated with an existing classification scheme.	Only two wetland classes have been characterized. Only one location has been characterized.

In addition to the hydrodynamic differences between different types of wetlands, there were differences observed in this study between seasons. The greater detention time observed during the leaf-off season through the dye tracer tests and confirmed with the modeling results, highlights the importance in the detritus zone in wetlands. During the leaf-off season, porosity decreases and friction increases in the zone of flow of the vegetated wetland flood plain. This zone of flow incorporates most of the detritus zone. Management of wetland areas for their water quality function should consider the importance of flow retention during the leaf-off season. Promotion of selected vegetation should include consideration to their detritus building ability in addition to their nutrient uptake capabilities.

In conclusion, improving our understanding of how natural wetlands modify flow through a watershed can lead to improvements in water resource management. Characterizing the hydraulic function of natural wetlands can lead to improvements to water quality remediation and provide justification for wetland creation. Particularly, the DYNAWET model can be used to select the most appropriate type and arrangement of wetland vegetation to result in the optimization of the water quality and quantity functions of a wetland system. Such optimization could result in the replacement of concrete and steel structures with wetlands composed of different types of wetlands in order to provide water quality and quantity improvements.

7. RECOMMENDATIONS FOR FUTURE STUDIES

This study has presented a model capable of simulating the hydrodynamics of one wetland system. It was tested on a single wetland system. Future research should include investigating the model's performance for other wetland systems. Since the development of the DYNAWET model minimized the use of empirically derived equations, it is hoped that the model will prove to be robust, i.e., applicable to a wide range of new sites.

Additional research should also explore the variability in the wetland friction factor (C_{WET}) and wetland porosity (φ). Although this study determined these parameters for the scrub-shrub and emergent type wetlands, a determination is needed for the other NWI classifications to allow for the general application of DYNAWET. The coefficients for the known wetland types should also be applied to another location under different hydrodynamic conditions to determine their variability.

In addition to testing the model for different locations, it should be tested for a greater variety of seasonal conditions. The data available for calibration and verification was for the late leaf-off season and the middle of the leaf-on season. The seasons were separated based on plant growth. Since the depth of flow through the vegetated flood plains is shallow, the amount of detritus on the flood plain bottom may play a greater role in the hydrodynamics of the wetland than the vegetative growth. The depth of this detrital zone may also vary throughout these seasons resulting in a significant difference in the friction and porosity parameters. Accordingly, future studies should measure the variability of these parameters within the leaf-on and leaf-off seasons.

The DYNAWET model is compiled as a DOS-based program and accordingly its input and operation are esoteric. To improve its general use, a user-friendly interface should be developed. This will eliminate the need to decode the input file with the written text provided in appendix A.3. In addition, the interface could provide an output that is already formatted for use in a spreadsheet or graphics software package.

To demonstrate the progressive improvement provided by the DYNAWET model, the model along with a model based on Manning's equation needs to be applied to a wetland with similar vegetation as the Malcolm Brook wetland. The robustness of the DYNAWET coefficients should provide better predictions of flow. Such a demonstration could also test the hypothesis that the DYNAWET coefficients are characteristic of the NWI classified wetland types.

APPENDICES

A.1. Theoretical Wetland Particle Model

The following section provides a description and demonstration of a theoretical Wetland Particle Model to highlight the applicability of the results from the DYNAWET model.

A.1.1 Theory for Wetland Particle Model (WPM)

The most significant impact wetlands have on pollutants are their ability to detain the flow of water that transports these pollutants and allows physical processes (such as settling) to reduce them. Accordingly, the DYNAWET model is designed to provide the best predictions of retention time. The residence times in wetlands are often variable due to the non-ideal flow associated with wetlands. To address this variability, the particle model presented in this section is based on the same theories regarding reaction time for non-ideal flow that are often used in chemical engineering. Application of these theories to wetlands have been presented by Kadlec and Knight (1996) as a more exact approximation of the chemical reactions that occur in wetlands than using nominal residence time based on the geometry of the wetland.

The non-ideal flow of a material in the fluid of a reactor was first described by its Residence Time Distribution (RTD) by Danckwerts (1953). The RTD represents the age distribution of the fluid (Levenspiel, 1999). The difference in age of various portions of the flow is the result of the channeling and recycling of the flow under non-ideal conditions. The RTD can be considered the probability density function for the contact time between the flow and the wetland. To obtain the RTD, dye tracer studies are used

to measure the tracer concentration as a function of time at the wetland outlet (Kadlec and Knight, 1996). The RTD represents the fraction of dye tracer that resides in the wetland between time (t) and some change in time (Δt). The RTD for a tracer is given by equation A.1 as presented by Kadlec and Knight (1996).

$$f(t) = \left(\frac{C(t)}{\int_0^\infty C(t)dt} \right) \quad \textbf{(A.1)}$$

Where:

f(t) = Residence time distribution for time (t)

C(t) = tracer concentration at outlet at time (t)

The RTD theory is applied to modeling a wetland system by averaging the concentrations of particles over the distribution of residence times (Kadlec and Knight, 1996). This yields the equation A.2.

$$\frac{C_{out}}{C_{in}} = \int_0^\infty f(t)e^{(-kt)dt} \quad \textbf{(A.2)}$$

Where:

C_{out} = Concentration of particles at the outlet;

C_{in} = Concentration of particles at the inlet;

k = a constant representing the rate of the reaction; and

t = time

This application allows construction of models that incorporate reaction kinetics for non-ideal flow. The most common use of this application is to model a non-ideal flow system with a series of reactor tanks. The reactor tanks are classified into two types of ideal mixing. A Plug Flow Reactor (PFR) is a reactor without any mixed zones. A Continuously Stirred Tank Reactor (CSTR) is a reactor with completely mixed zones. Non-ideal transport is simulated through a combination of both type of reactor tanks. Figure A.1 provides the tracer response curve at some time $t+\Delta t$ for an idealized plug flow. Due to the lack of mixing, the shape of the original impulse is maintained as it passes through the system. Figure A.2 represents the tracer response curves for one idealized CSTR and three idealized CSTRs in series. For one CSTR, mixing occurs immediately and a fully mixed condition is approached rapidly. With three CSTRs, mixing begins gradually as the impulse travels from one reactor to the next. A peak is reached and the system slowly approaches a fully mixed condition. Figure A.3 provides the tracer response curve for a theoretical combination of one PFR and three CSTRs. The PFR provides a delay and the multiple CSTRs provide gradual mixing. This curve provides a good representation of the response curves observed for the dye tracer tests.

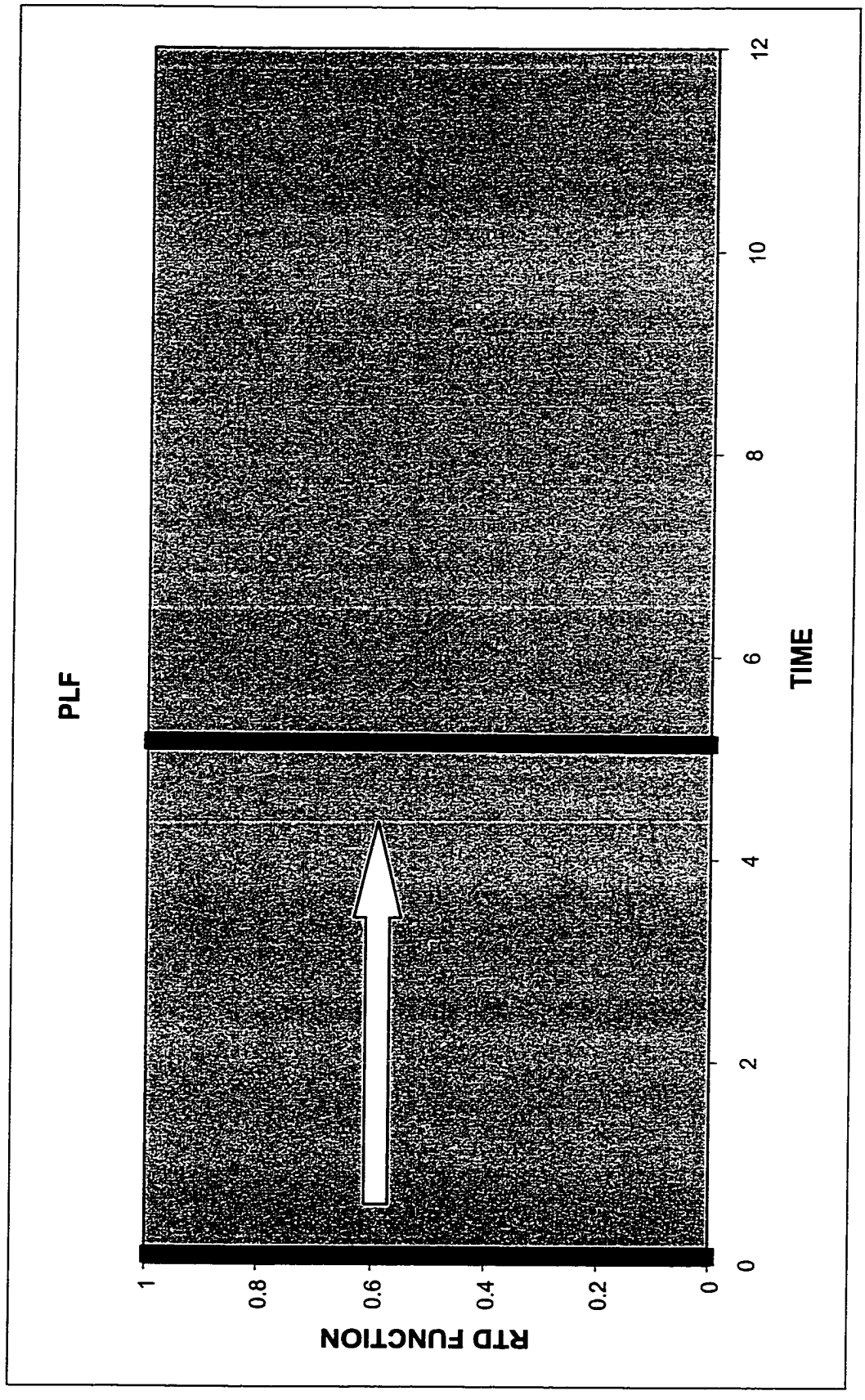

Figure A.1. The response curve for an idealized Plug Flow Reactor.

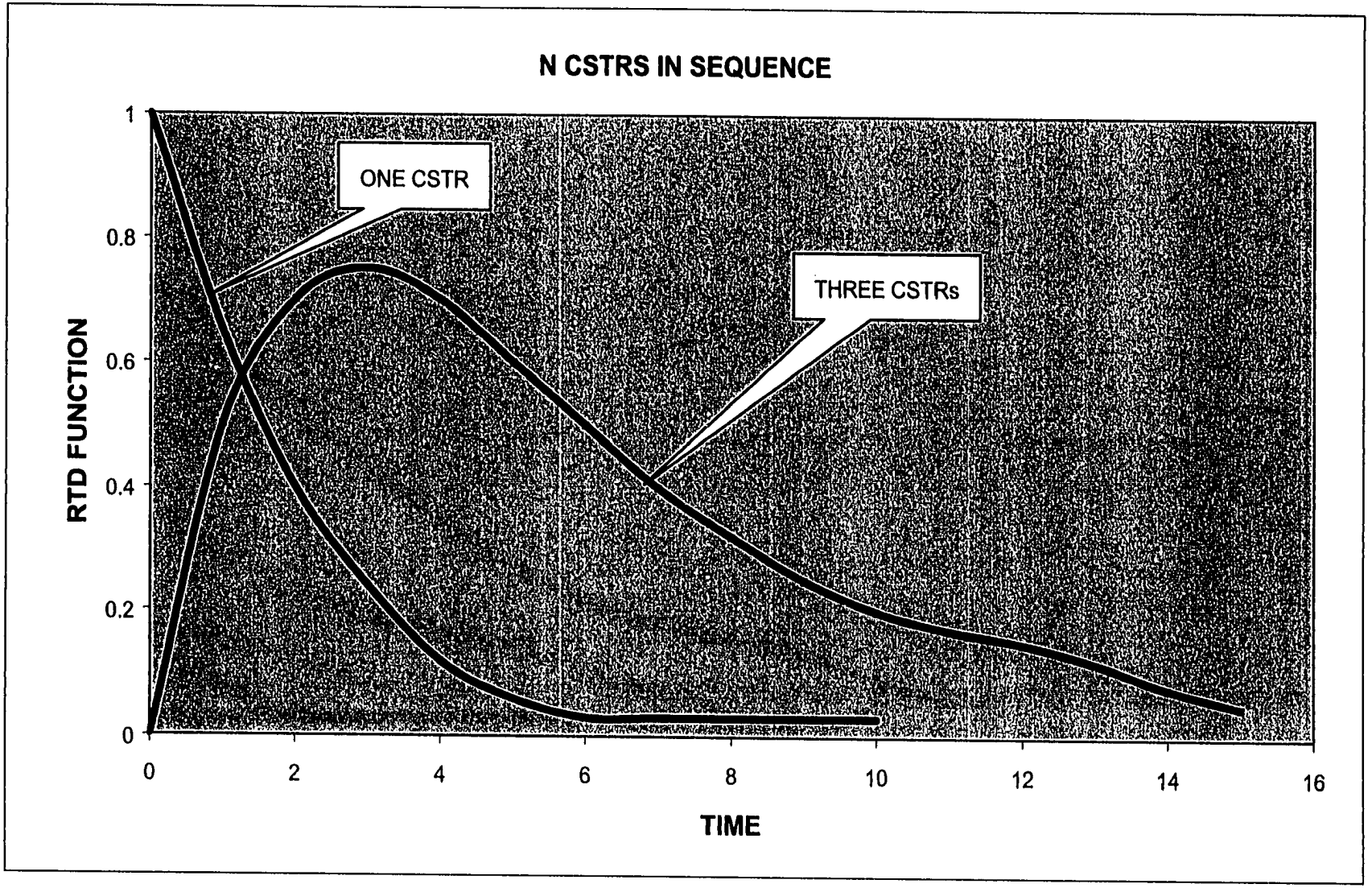

Figure A.2. The response curves for one and three idealized Continuously Stirred Tank Reactors.

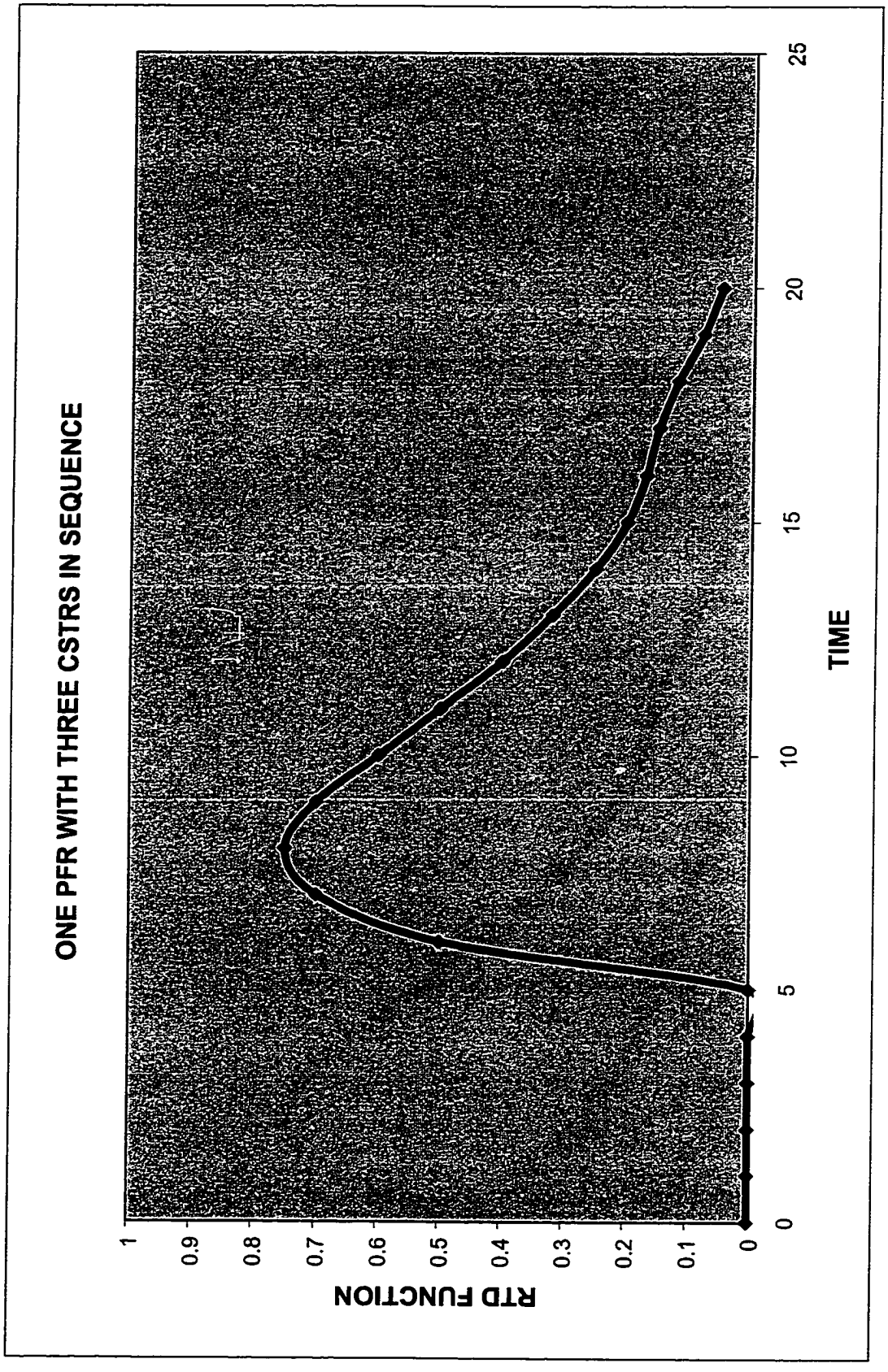

Figure A.3. The response curve for a system with one PFR and three CSTRs in series.

The equations associated with the RTD approach for wetland modeling were derived by Kadlec and Knight (1996) and are presented as follows. Some slight modifications were made to present the equations in the context of volumetric reactions instead of areal reactions. The equations are presented to provide the outflow concentration for each type of reactor and then a combination of the two types of reactor.

Concentration at the outflow is calculated in a plug flow reactor experiencing a first-order reaction (in this case a reduction due to settling) with equation A.3.

Plug Flow Reactor (PFR):

$$C_{out} = C_{in} e^{(-Da)} \qquad \textbf{(A.3)}$$

Damkohler number for volumetric reaction (Da):

$$Da = kt \qquad \textbf{(A.3a)}$$

The concentration at the outflow of a single CSTR experiencing a first-order volumetric reaction is provided by :

$$C_{out} = \frac{C_{in}}{1 + Da} \qquad \textbf{(A.4)}$$

Equation A.5 calculates the concentration of particles at the outflow of a number (N) of CSTRs in series. All the CSTRs are experiencing a first-order volumetric reaction.

$$C_{out} = \frac{C_{in}}{\left[1 + \frac{Da}{N}\right]^{N}} \qquad \textbf{(A.5)}$$

The equations associated with the RTD approach for wetland modeling were derived by Kadlec and Knight (1996) and are presented as follows. Some slight modifications were made to present the equations in the context of volumetric reactions instead of areal reactions. The equations are presented to provide the outflow concentration for each type of reactor and then a combination of the two types of reactor.

Concentration at the outflow is calculated in a plug flow reactor experiencing a first-order reaction (in this case a reduction due to settling) with equation A.3.

Plug Flow Reactor (PFR):

$$C_{out} = C_{in} e^{(-Da)} \qquad \textbf{(A.3)}$$

Damkohler number for volumetric reaction (Da):

$$Da = kt \qquad \textbf{(A.3a)}$$

The concentration at the outflow of a single CSTR experiencing a first-order volumetric reaction is provided by :

$$C_{out} = \frac{C_{in}}{1 + Da} \qquad \textbf{(A.4)}$$

Equation A.5 calculates the concentration of particles at the outflow of a number (N) of CSTRs in series. All the CSTRs are experiencing a first-order volumetric reaction.

$$C_{out} = \frac{C_{in}}{\left[1 + \frac{Da}{N}\right]^{N}} \qquad \textbf{(A.5)}$$

Determination of the number of CSTRs to use is based on the shape (as expressed by variance) of the tracer response curve (Levenspiel, 1999). One CSTR (N = 1) represents the idealized flow condition of a completely mixed system. The resultant tracer response curve from such a system has a variance equal to one. Infinite CSTRs (N = ∞) represent the plug flow condition. The resultant tracer curve from this system has a variance equal to zero. Equations A.6a and A.6b provide the relationship between N and the shape of the tracer curve as presented by Levenspiel (1999) and Kadlec and Knight (1996).

For short crest shapes:

$$\frac{1}{N} = \frac{\tau_{centroid} - \tau_{peak}}{\tau_{centroid}} \qquad \textbf{(A.6a)}$$

For broad crest shapes:

$$\frac{1}{N} = \sigma^2_{RTD} \qquad \textbf{(A.6b)}$$

Combining equations A.3 and A.5 provides an equation that describes a tracer response that has the shape resulting from CSTRs but is delayed for some length of time. This equation partitions the type of reactor with a weighting factor (λ) which is based on an estimate of the influence exerted by the PFR or CSTR reactors. Equation A.7 provides the calculation to determine concentration of a mixed system composed of a PFR and a number (N) of CSTRs.

$$C_{out} = \frac{C_{in}^{\left(-Da/\lambda\right)_{PFR}}}{\left[1 + \frac{\left(Da/(1-\lambda)\right)_{CSTR}}{N}\right]} \qquad \textbf{(A.7)}$$

The results from the dye tracer tests presented in Chapter 3 indicate that the wetland system exhibits the behavior that can be represented by equation A.7, the combined formula. The wetland particle model is accordingly based on a combination of a PFR coupled with a number (N) CSTRs. With this algorithm, particle transport is determined at various locations and times along a one-dimensional wetland through each iteration of time and location.

A.1.2. Description of Wetland Particle Model (WPM) Program

The Wetland Particle Model (WPM) is an original algorithm developed as part of this study to describe particle transport through wetlands. The model is based on the theories presented in the Section A.1.1. It is designed to use the retention times calculated by the DYNAWET model to estimate particle concentrations for specific time steps and locations.

The WPM model is composed of one main program subroutine consisting of approximately one-hundred lines of code. The space allocated for the arrays is 1000

elements for each dimension. The program code was written in Fortran 77 and was compiled with the Compaq Digital Fortran compiler. Appendix A.6 provides the entire source code for the WPM program.

The program begins with statements to report a start time and to open the input file (named INPUT.TXT). The input file is a comma delimited text file located in the same directory as the executable code. At the same time, an output file is opened in the same directory with the name OUTPUT.TXT. The program next reads in the input data and prints it out as an echo to be used for input verification. The integer parameters for the number of time steps (NT) and wetland segments (NX) are read first. Next, the real numbers representing the reduction rate coefficients for each type of reactor (RKP and RKC) are read in. The array representing the particle concentrations at the upstream segment (CIN) is read in next. This is followed by reading a set of arrays for each segment. Three of these arrays provide data on the proportion of type of reactor (PORT), time of centroid (TC) and time of peak (TP) for each segment. These arrays are followed by a two-dimensional array that provides the retention times for each time step over each segment. This last array is obtained from the output table generated from the DYNAWET model.

The program uses the input data to calculate the parameters needed to solve equation A.7. This includes calculating the Damkohler numbers for each type of reactor (PDA and CDA), and the number of CSTRs (RN) from the given data on the behavior of the dye tracer tests. With these variables calculated, the particle concentration for each segment and time (COUT) is determined.

The output consists of a table which provides the concentration, and number of

CSTRs used in the calculations for each segment at each time step. The units of the time are equal to the retention time units. The units for the concentration are equal to the units of the input concentration. Appendix A.7 provides an example printout of the input and output for the WPM program.

A.1.3. Wetland Particle Model Demonstration

Data needed to run the Wetland Particle Model (WPM) includes several parameters. Retention times were obtained from the DYNAWET model run for the August 18, 1998 storm event that was used to verify the model under leaf-on conditions. To evaluate the model for leaf-off conditions, the upstream flow for the August 18, 1998 storm event was used however, the friction and porosity coefficients were set to match the calibrated values for the leaf-off conditions.

As presented in Chapter 3, section 3.5, the measured particle data was too variable to be used for model calibration or verification. In order to demonstrate the particle model, a simulated data set was constructed. The magnitude of the level of particles is based on a extrapolation of the relation between particle counts and turbidity presented by Hargesheimer and Lewis (1992). Accordingly, the level of particles used for the model demonstration was between 10,000 and 15,000 particles. The lower estimate is extrapolated from the average turbidity reading for the baseflow conditions during the August 18, 1998 storm event which was in the order of 10 NTU. The higher value was based on a typical peak of turbidity. The simulated data for the peak of particles preceded peak stage by one time step to simulate a first-flush effect.

The proportion of type of reactor (PORT) was set equal to fifty percent for PFR

and CSTR. Since data for calibration was not available, the extent of the delay for the response curve (as reflected by the influence of the PFR) was unknown.

Based on several dye tests with similar flows, the time between the peak dye tracer concentration and the centroid was estimated to be approximately a four minute difference for the scrub-shrub segment and approximately six minutes for the emergent segment. The same parameters were used to determine the number of CSTR for the leaf-off demonstration.

The retention times were provided by the output from the DYNAWET hydrodynamic model. The output for the August 18,1998 event included over forty values of retention time for each segment. Nine values for each segment were selected to reduce the size of the input and output files so that they could be presented in a reasonable amount of space. These values provided enough information to characterize the response curve from the storm event and were equivalent to the number of values available from the stage measurements.

The WPM program was applied to two examples. Both examples used the flow and resultant retention time for the August 18, 1998 storm event. Figures A.4 and A.5 provide the results from these simulations. During leaf-off conditions there was a twenty-three percent reduction of the peak particle count in the first segment and an addition three percent reduction from the second segment. During leaf-on conditions the reduction was fifteen percent and an additional four percent for the first and second segments respectively. In this simulation, these results reflect the influence of retention time on the output. The difference in reduction is due to the differences in the retention times between leaf-on and leaf-off conditions. All other parameters were kept constant.

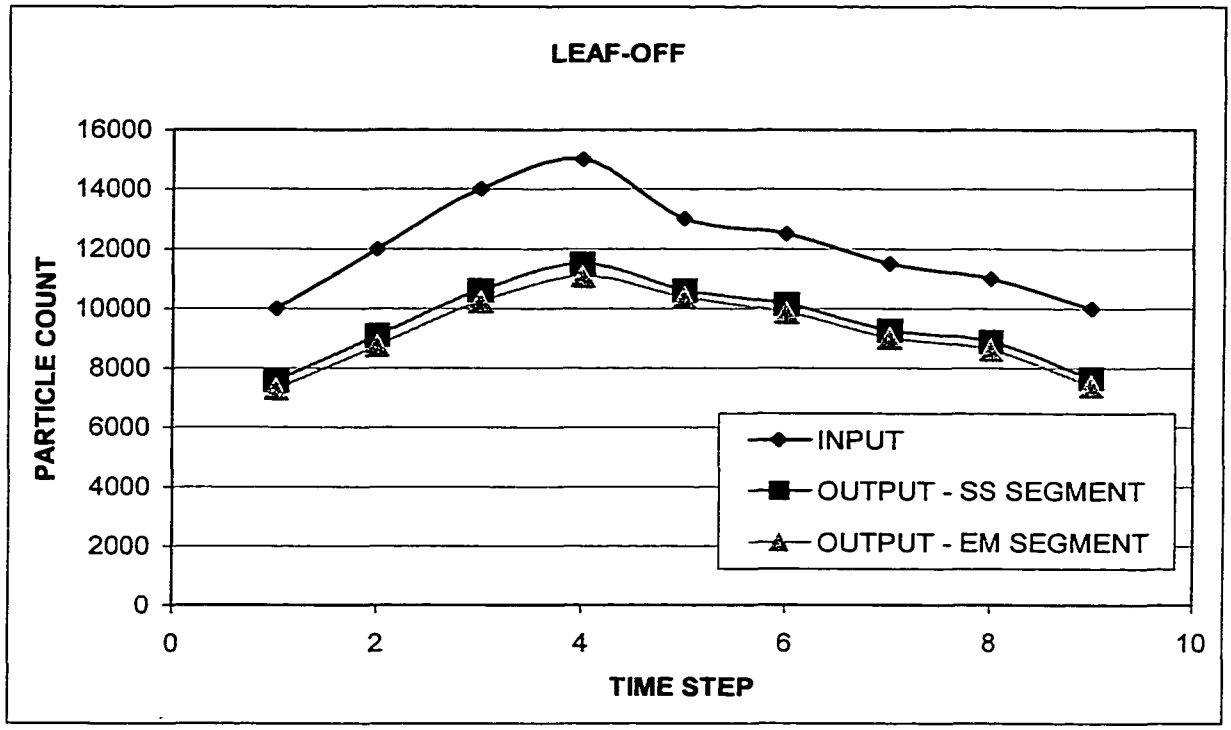

Figure A.4. Demonstration output from Wetland Particle Model for leaf-off conditions.

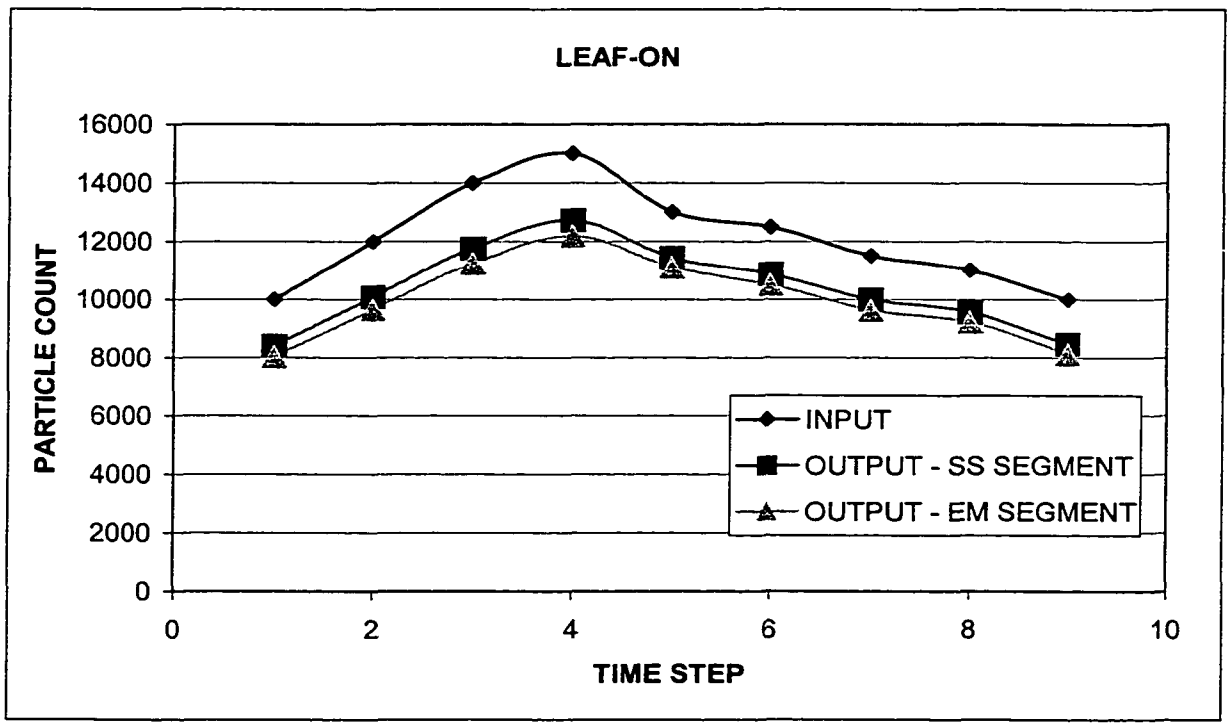

Figure A.5. Demonstration output from Wetland Particle Model for leaf-on conditions.

Factors other than the retention time may significantly alter these results. Differences in the reduction rate or dispersion other than those used for the demonstration can result in different particle counts.

Due to the lack of observed data, the WPM could not be evaluated further with regard to calibration and verification. Accordingly, only a demonstration of the model has been discussed. The relationship between particle concentration and retention time must be defined in order to apply this model.

A.1.4 Summary and Conclusions

An important application of the DYNAWET model is to simulate the migration of particles in streamflow. Water suppliers are particularly interested in water quality changes that affect the transport and fate of two human parasitic protozoan organisms *Giardia* spp. and *Cryptosporidium* spp. as they travel through the wetlands of their watersheds. These organisms presumably can be modeled as particles. The flows simulated by the DYNAWET model were used to determine residence times of wetland segments composed of mixes of differently classified wetlands. These residence times in turn were used in determining the theoretical resultant changes in concentration of particles in the size range of *Giardia* spp. cysts and *Cryptosporidium* spp. oocysts. Since reliable particle counting data of natural waters could not be obtained, the theoretical particle model presented was based on an analytical equation instead of a more complex numerical algorithm. The theoretical Wetland Particle Model represents a starting point in modeling particle transport through a natural wetland. The problems associated with counting particles in high concentrations (as is found in natural waters) need to be

resolved before further model development can occur. The temporal and spatial accuracy that can be achieved by the hydrodynamic model DYNAWET may warrant a numerical approach for the particle model. However, the approach chosen will be dependent on the availability of accurate and reliable measurements of particles.

A.1.5 Recommendations

To test the Wetland Particle Model, additional data needs to be collected on the transport and fate of particles. The collection of such information should address the problems associated with counting the high concentrations of particles often found in natural waters. It is likely that the particle counters available today will need to be modified to allow for the dilution of the sample stream with particle free water. Special attention should be given to the routine calibration, cleaning and associated maintenance of the particle counters. Placement of the inlet tubes for the particle counters need to consider the effects of sedimentation and erosion that could bias the results.

With adequate particle data, the Wetland Particle Model could be calibrated and verified. Assuming that the model can simulate the particle data, it should be applied to different wetlands under different conditions to test its general applicability.

Calibration and verification of the Wetland Particle Model may find that the analytical approach used in developing the module is an over-simplification of the mechanisms that determine particle transport and fate. In this case a numerical approach should be applied. Since the hydrodynamic module of the DYNAWET model is already numerical, a numerical particle model would only need to solve the equations describing contaminant transport.

A.2. DYNAWET Hydrodynamic Module Subroutines

The following Fortran code represents the modifications made to the FLDWAV model to create the DYNAWET model. Modifications made as part of this study are identified through highlighting and with comments starting with "CDSC". To save space, approximately five lines of code before and after the modification is provided.

A.2.1. SUBROUTINE AAMAIN

```
C       SUBROUTINE AAMAIN

CDSC    DYNAMIC ROUTING MODEL
CDSC    FOR NATURALLY OCCURRING WETLANDS
CDSC    WITH FLOOD PLAINS AND MEANDERING STREAMS
C
C       THE ONE-DIMENSIONAL (ST. VENANT) UNSTEADY FLOW EQUATIONS ARE SOLVED
C       BY AN IMPLICIT FINITE DIFFERENCE METHOD-'WEIGHTED FOUR-POINT SCHEME'
C
C       THE FRICTION SLOPE AND CROSS SECTIONAL AREAS FOR THE LEFT OVERBANK
C       FLOOD PLAIN, MAIN RIVER CHANNEL AND RIGHT OVERBANK FLOOD PLAIN ARE
C       CALCULATED TO PRESERVE THEIR FLOW LENGTHS,ROUGHNESS, AND GEOMETRIC
C       PROPERTIES
C
C       DEVELOPED BY DAVID A. STERN BY MODIFYING THE NWS FLDWAV MODEL:
C       FLDWAV PROGRAM VERSION 2.0.0  (DATE: JUNE 1, 2000)
C
C       MAIN PROGRAM
C       FLDWAV PROGRAM VERSION 2.0.0 (DATE: JUNE 1, 2000)
C       Note: Version (X.Y.Z) reflects 3 levels of changes:
C               X - Major update (new enhancements)
C               Y - Major changes (errors)
C               Z - minor changes (errors)

        CHARACTER*20 FILIN,FILOUT
        COMMON/ZZ/Z(5000000),LOC(500)
        COMMON/TSIZE/ISIZE
        COMMON/IONUM/IN,IPR
        INCLUDE 'COMMON\OPFIL'
        PRINT 1
CDSC    ************************************************************************
1       FORMAT(//5X,'DYNAWET 1.0 MODEL (MODIFIED NWS FLDWAV 1.0.0) '/)
CDSC    ************************************************************************
        ISIZE=5000000
        DO 10 I=1,ISIZE
        Z(I)=0.
10      CONTINUE

8       OPEN(IN,FILE=FILIN)
        OPEN(IPR,FILE=FILOUT)
        IF(ITRM.EQ.2) FILOUT='DUMMY'
```

```
      IF(FILOUT.EQ.'') FILOUT='DUMMY'
      CALL OPNFIL(FILOUT,LTTL)

CDSC  ***** STERN ADDED FOR STAGE OUTPUT FILE *********************************
      OPEN(100,FILE='ZZSTGOUT.TXT')
CDSC  ***************************************************************************
      WRITE(*,*)
      CALL GETTIM(IHR1,IMIN1,ISEC1,I100TH)
      WRITE(*,50)
50    FORMAT(1X,'*************************')
      WRITE(*,55) IHR1,IMIN1,ISEC1
55    FORMAT(1X,'START TIME IS   ',I2.2,1H:,I2.2,1H:,I2.2)
```

A.2.2. SUBROUTINE COMPK

```
      QKCH0=QKCH
      DQKLF=0.0
      QKLF=0.
      IF(BL.LT.0.2) AL=0.01
      IF(BL.LT.0.2) GO TO 14
CDSC  ** ADDED TWO NEW SUBROUTINES TO INTERPOLATE PORE VALUES *************
      CALL PORESL(NCML,Z(LOPOREL),Z(LOYQCM),J,I,YN,PORENL,DCML,K7,K8)
      CALL PORESR(NCML,Z(LOPORER),Z(LOYQCM),J,I,YN,PORENR,DCMR,K7,K8)
CDSC  ** ADDED TWO NEW SUBROUTINES TO INTERPOLATE STEM DIAMETER VALUES **
      CALL STEMSL(NCML,Z(LODIAL),Z(LOYQCM),J,I,YN,DIANL,DCML,K7,K8)
      CALL STEMSR(NCML,Z(LODIAR),Z(LOYQCM),J,I,YN,DIANR,DCMR,K7,K8)
CDSC  **** REPLACED LEFT FLOOD PLAIN CALCULATION WITH NEW EXPRESSION *****
C     OLD EXPRESSION:  QKLF=1.49/CMNL*AL*(AL/BL)**E23
      QKLF=AL*((8*G/CMNL)**0.5)*((AL/((PORENL*BL)+
     .(Y*2*((1-PORENL)*BL)/DIANL)-1))**0.5)DQKLF=QKLF-QKLF0
CDSC  ***************************************************************************
      QKLF0=QKLF
14    QKRF=0.
      DQKRF=0.0
      IF(BR.LT.0.2) AR=0.01
      IF(BR.LT.0.2) GO TO 15
CDSC  **** REPLACED RIGHT FLOODPLAIN CALCULATION WITH NEW EXPRESSION ****
      QKRF=AR*((8*G/CMNR)**0.5)*((AR/((PORENR*BR)+
     .(Y*2*((1-PORENR)*BR)/DIANR)-1))**0.5)
CDSC  ***************************************************************************
      DQKRF=QKRF-QKRF0
      QKRF0=QKRF
15    IT=IT+1
CC    IF(IT.GT.K2) IT=K2
      ITM=IT-1
```

A.2.3. SUBROUTINE CONVRT

```
      LOC(222)=LOQKC
      LOC(223)=LOFLST
      LOC(224)=LOCML
      LOC(225)=LOCMR
      LOC(227)=LOEPQJ
CDSC  ***** FOLLOWING STATEMENTS ADDED BY STERN ****************************
      LOC(426)=LOPOREL
      LOC(427)=LOPORER
      LOC(428)=LODIAL
      LOC(429)=LODIAR
CDSC  ********************************************************************************
      LOC(231)=LOSNM
      LOC(239)=LOTPG
      LOC(240)=LORHO
      LOC(241)=LOGAMA
      LOC(242)=LOYQI

      LOC(421)=LCVPK
      LOC(422)=LCBKT
      LOC(423)=LCQKT
      LOC(424)=LCERQX
      LOC(425)=LCSNMT
CDSC  ***** FOLLOWING STATEMENTS ADDED BY STERN ***************************
      LOC(430)=LCVTC
      LOC(431)=LCXTC
      LOC(432)=LCRTTC
CDSC  ********************************************************************************
C     LOCATIONS 433-500 ARE NOT CURRENTLY BEING USED
      RETURN
```

A.2.4. SUBROUTINE FIRST

```
      LOBSS=1
      LOCGD=1
      LOCLL=1
      LOCML=1
      LOCMR=1
CDSC  ***** FOLLOWING STATEMENTS ADDED BY STERN ****************************
      LOPOREL=1
      LOPORER=1
      LODIAL=1
      LODIAR=1
CDSC  ********************************************************************************
      LOCRL=1
      LOCSD=1
      LODXM=1
      LOFKC=1
```

```
      LOFKF=1

      LCVLSV=1
      LCWDSN=1
      LCYDIT=1
      LCYINT=1
      LCYUMN=1
CC    ***** FOLLOWING STATEMENTS ADDED BY STERN **************************
      LCVTC=1
      LCXTC=1
      LCRTTC=1
CDSC  ********************************************************************************
      RETURN
      END
```

A.2.5. SUBROUTINE OUTPUT

```
      IF (NGAG.LE.0) GOTO 920
      DO 915 K=1,NGAG
      IG=NGS(K,J)
      STC(KTIME,K,J)=YD(IG,J)+(YU(IG,J)-YD(IG,J))*DTX
      QTC(KTIME,K,J)=QD(IG,J)+(QU(IG,J)-QD(IG,J))*DTX
CDSC  ********************************************************************************
CDSC  *** STERN CHANGE TO ALLOW OUTPUT VELOCITY VTC AND LOCATION XTC****
      IGG=IG+1
      VTC(KTIME,K,J)=VU(IG,J)
      XTC(KTIME,K,J)=ABS(X(IG,J)-X(IG-1,J))*((NPT(2,J)-1)/(MXNBT-1))
       *XFACT
      RTTC(KTIME,K,J)=(XTC(KTIME,K,J)/VTC(KTIME,K,J))/60
CDSC  ********************************************************************************
915   CONTINUE
920   CONTINUE
      KTIME=KTIME+1
      IF (KTIME.GT.K3) GOTO 1000
      GOTO 900
```

A.2.6. SUBROUTINE PORESL

```
      SUBROUTINE PORESL (NCML,POREL,YQCM,I,L,YQ,POREM,DCM,K7,K8)
      DIMENSION POREL(K8,K7,1),YQCM(K8,K7,1)
CDSC  ************ THIS SUBR INTERPOLATES PORER ***
C     ** (LOW DEPTH LIMIT)IF DEPTH (YQ) LT MANN TBL DPTH (YQCM) ***
      IF(YQ.LT.YQCM(1,L,J)) POREM=POREL(1,L,J)
      IF(YQ.LT.YQCM(1,L,J)) GO TO 20
C     ** (HIGH DEPTH LIMIT) IF DEPTH (YQ) GT END OF MANN TBL (N0 YQCM = NCS)**
      IF(YQ.GT.YQCM(NCML,L,J)) POREM=POREL(NCML,L,J)
      IF(YQ.GT.YQCM(NCML,L,J)) GO TO 20
C     ** (BETWEEN DEPTH LIMITS) ***
```

```
      DO 10 KK=2,NCML
      KT=KK
      IF (YQ.LE.YQCM(KT,L,J)) GO TO 12
10    CONTINUE
12    KL=KK-1
      DH=YQCM(KT,L,J)-YQCM(KL,L,J)
      IF(ABS(DH).LE.0.01) DH=0.01
      DPORE=(POREL(KT,L,J)-POREL(KL,L,J))/DH
      POREM=POREL(KL,L,J)+DPORE*(YQ-YQCM(KL,L,J))
20    IF(POREM.LT.0.001) POREM=0.01
      RETURN
      END
```

A.2.7. SUBROUTINE PORESR

```
      SUBROUTINE PORESR (NCML,PORER,YQCM,J,L,YQ,POREM,DCM,K7,K8)
      DIMENSION PORER(K8,K7,1),YQCM(K8,K7,1)

CDSC  ********** THIS SUBR INTERPOLATES PORER ***
C     ** (LOW DEPTH LIMIT)IF DEPTH (YQ) LT MANN TBL DPTH (YQCM) ***
      IF(YQ.LT.YQCM(1,L,J)) POREM=PORER(1,L,J)
      IF(YQ.LT.YQCM(1,L,J)) GO TO 20
C     ** (HIGH DEPTH LIMIT) IF DEPTH (YQ) GT END OF MANN TBL (N0 YQCM = NCS)**
      IF(YQ.GT.YQCM(NCML,L,J)) POREM=PORER(NCML,L,J)
      IF(YQ.GT.YQCM(NCML,L,J)) GO TO 20
C     ** (BETWEEN DEPTH LIMITS) ***
      DO 10 KK=2,NCML
      KT=KK
      IF (YQ.LE.YQCM(KT,L,J)) GO TO 12
10    CONTINUE
12    KL=KK-1
      DH=YQCM(KT,L,J)-YQCM(KL,L,J)
      IF(ABS(DH).LE.0.01) DH=0.01
      DPORE=(PORER(KT,L,J)-PORER(KL,L,J))/DH
      POREM=PORER(KL,L,J)+DPORE*(YQ-YQCM(KL,L,J))
20    IF(POREM.LT.0.001) POREM=0.01
      RETURN
      END
```

A.2.8. SUBROUTINE RDRCH

```
      WRITE(IPR,100) J,J
100   FORMAT(/' XT(I,',I2,') I=1,NB(',I2,')')
      READ(IN,'(A)',END=1000) DESC
      READ(IN,*) (XT(I,J),I=1,N)
      WRITE(IPR,1005) (XT(I,J),I=1,N)
```

```
CDSC  ****** MODIFIED FORMAT TO 5 BY STERN FOR SMALLER DISTANCES**********
1005  FORMAT(8F10.5)
CDSC  ************************************************************************
C.....
C     DXM  -- MINIMUM COMPUTATIONAL DISTANCE INTERVAL BET SECTIONS
C.....
      WRITE(IPR,101) J,J
101   FORMAT(/' DXM(I,',I2,') I=1,NB(',I2,')')
```

A.2.9. SUBROUTINE READ2

```
      WRITE(IPR,110)
110   FORMAT(/' RIVER NO.  NBT NPT1 NPT2     EPQJ     COFW     VWIND
     . WINAGL')
      WRITE(IPR,2030) 1,NBT(1),NPT(1,1),NPT(2,1),Z(LOEPQJ),Z(LOCOFW),
     . Z(LOVWND),Z(LOWAGL)
CDSC  ****** MODIFIED FORMAT TO 10.4 BY STERN ********************************
2030  FORMAT (I5,5X,3I5,4F10.4)
CDSC  ************************************************************************
      ELSE
      WRITE(IPR,111)
111   FORMAT(/' RIVER NO.  NBT NPT1 NPT2  MRV NJUN      ATF     EPQJ
     .  COFW    VWIND   WINAGL')
      WRITE(IPR,2040) 1,NBT(1),NPT(1,1),NPT(2,1),Z(LOEPQJ),Z(LOCOFW),
     . Z(LOVWND),Z(LOWAGL)
CDSC  ****** MODIFIED FORMAT TO 10.4 BY STERN ********************************
2040  FORMAT (I5,5X,3I5,20X,4F10.2)
CDSC  ************************************************************************
      ENDIF
      MXNBT=NBT(1)
      MRV(1)=0
      IORDR(1)=1
      EPSQ=Z(LOEPQJ)
```

A.2.10. SUBROUTINE READ3

```
IUSE=LONCM+JN*MXNCM1
      LOYQCM=1
      LOCM=1
      LOCML=1
      LOCMR=1
CDSC  ***** FOLLOWING STATEMENTS ADDED BY STERN ***************************
      LOPOREL=1
      LOPORER=1
      LODIAL=1
      LODIAR=1
CDSC  ************************************************************************
```

```
      IF(KFLP.LT.2) THEN
      LOYQCM=IUSE
      LOCM=LOYQCM+JN*MXNCM1*MXNCML
      IUSE=LOCM+JN*MXNCM1*MXNCML
      IF(KFLP.EQ.1) THEN
      LOCML=IUSE
      LOCMR=LOCML+JN*MXNCM1*MXNCML
      IUSE=LOCMR+JN*MXNCM1*MXNCML
CDSC  ***** FOLLOWING STATEMENTS ADDED BY STERN ****************************
      LOPOREL=IUSE
      LOPORER=LOPOREL+JN*MXNCM1*MXNCML
      IUSE=LOPORER+JN*MXNCM1*MXNCML
      LODIAL=IUSE
      LODIAR=LODIAL+JN*MXNCM1*MXNCML
      IUSE=LODIAR+JN*MXNCM1*MXNCML
CDSC  ***************************************************************************
      ENDIF
      ENDIF
      CALL CHECK(IUSE,LEFT,NERR)
      IF(NERR.EQ.0) GO TO 650
      WRITE(IPR,9010)

      Z(37)=LONCM+0.01
      Z(81)=LOYQCM+0.01
      Z(186)=LOSNC+0.01
      Z(224)=LOCML+0.01
      Z(225)=LOCMR+0.01
CDSC  ***** FOLLOWING STATEMENTS ADDED BY STERN ****************************
      Z(426)=LOPOREL+0.01
      Z(427)=LOPORER+0.01
      Z(428)=LODIAL+0.01
      Z(429)=LODIAR+0.01
CDSC  ***************************************************************************
      Z(231)=LOSNM+0.01
      IF(NODESC.EQ.0)THEN
      WRITE(IPR,330)
330   FORMAT(//
      .10X,'NCM = CROSS SECTION NUMBER JUST D/S OF A MANNING N REACH'/
      .10X,'SNM  = SINUOSITY COEFFICIENT'/
      .10X,'FKEC = EXPANSION OR CONTRACTION COEFFICIENT'/
CDSC  ***** FOLLOWING STATEMENTS ADDED BY STERN ****************************
      .10X,'CWETL  = WETLAND FRICTION FACTOR FOR LEFT FLOODPLAIN'/
      .10X,'CWETR  = WETLAND FRICTION FACTOR FOR RIGHT FLOODPLAIN'/
      .10X,'POREL  = WETLAND POROSITY FOR LEFT FLOODPLAIN'/
      .10X,'PORER  = WETLAND POROSITY FACTOR FOR RIGHT FLOODPLAIN'/
      .10X,'DIAL  = MEAN DIAMETER OF VEGETATION FOR LEFT FLOODPLAIN'/
      .10X,'DIAR  = MEAN DIAMETER OF VEGETATION FOR RIGHT FLOODPLAIN'/
CDSC  ***************************************************************************
      .10X,'YQCM = WSEL OR DISCHARGES ASSOCIATED WITH MANNING N'/)
      ENDIF
C.....
```

```
C       NCM  = CROSS SECTION NUMBER JUST U/S OF A MANNING N REACH
C       SNM  = SINUOSITY COEFFICIENT
C       FKEC = EXPANSION OR CONTRACTION COEFFICIENT
C       CML  = WETLAND FRICTION FACTOR FOR LEFT FLOODPLAIN
C       CMR  = WETLAND FRICTION FACTOR FOR RIGHT FLOODPLAIN
C       YQCM = WSEL OR DISCHARGES ASSOCIATED WITH MANNING N
CDSC    ***** FOLLOWING STATEMENTS ADDED BY STERN **************************
C         POREL=POROSITY OF LEFT FLOODPLAIN
C         PORER=POROSITY OF RIGHT FLOODPLAIN
C         DIAL  = MEAN DIAMETER OF VEGETATION FOR LEFT FLOODPLAIN
C         DIAR  = MEAN DIAMETER OF VEGETATION FOR RIGHT FLOODPLAIN
CDSC    ************************************************************************
C-----------------------------------------------------------------
        DO 870 J=1,JN
        N=NBT(J)
        NM=N-1
        WRITE(IPR,2010) J

        IF(NQCMJ.NE.0) GO TO 764
C       NQCM<>0, USE MANNING EQUATION, IMPLY KFLP=0
        IF(KFLP.EQ.0) GO TO 769
        LCML=LOCML+(J-1)*MXNCM1*MXNCML+(II-1)*MXNCML-1
        LCMR=LOCMR+(J-1)*MXNCM1*MXNCML+(II-1)*MXNCML-1
CDSC    ***** FOLLOWING STATEMENTS ADDED BY STERN ***************************
        LPOREL=LOPOREL+(J-1)*MXNCM1*MXNCML+(II-1)*MXNCML-1
        LPORER=LOPORER+(J-1)*MXNCM1*MXNCML+(II-1)*MXNCML-1
        LDIAL=LODIAL+(J-1)*MXNCM1*MXNCML+(II-1)*MXNCML-1
        LDIAR=LODIAR+(J-1)*MXNCM1*MXNCML+(II-1)*MXNCML-1
CDSC    ************************************************************************
        READ(IN,'(A)',END=1000) DESC
        READ(IN,*) (Z(LCML+K),K=1,NCML)
        READ(IN,'(A)',END=1000) DESC
        READ(IN,*) (Z(LCMR+K),K=1,NCML)
        WRITE(IPR,2092) II,J,(Z(LCML+K),K=1,NCML)
        WRITE(IPR,2093) II,J,(Z(LCMR+K),K=1,NCML)
CDSC    ***** FOLLOWING STATEMENTS ADDED BY STERN TO READ NEW PARAMETERS**
        READ(IN,'(A)',END=1000) DESC
        READ(IN,*) (Z(LPOREL+K),K=1,NCML)
        READ(IN,'(A)',END=1000) DESC
        READ(IN,*) (Z(LPORER+K),K=1,NCML)
        WRITE(IPR,2192) II,J,(Z(LPOREL+K),K=1,NCML)
        WRITE(IPR,2193) II,J,(Z(LPORER+K),K=1,NCML)
        READ(IN,'(A)',END=1000) DESC
        READ(IN,*) (Z(LDIAL+K),K=1,NCML)
        READ(IN,'(A)',END=1000) DESC
        READ(IN,*) (Z(LDIAR+K),K=1,NCML)
        WRITE(IPR,2194) II,J,(Z(LDIAL+K),K=1,NCML)
CDSC    ************************************************************************
        GO TO 769
764     LYQCM=LOYQCM+(J-1)*MXNCM1*MXNCML+(II-1)*MXNCML-1
        READ(IN,'(A)',END=1000) DESC
```

```
      READ(IN,*) (Z(LYQCM+K),K=1,NCML)
      IF(NQCMJ.LT.0) WRITE(IPR,2094) II,J,(Z(LYQCM+K),K=1,NCML)
```

A.2.11. SUBROUTINE READN

```
      WRITE(IPR,2010) LEFT
      LIMIT=IUSE
      GO TO 5000

CC    610 Z(155)=LOSLFI+0.01
      610 Z(173)=LOIFXC+0.01
CDSC  ************** PASS NEW PARAMETERS ************************************
      CALL READ3(Z,IUSE,LEFT,LIMIT,Z(LONBT),Z(LONGAG),Z(LONQCM),
     * Z(LONCM1),Z(LOIFXC),Z(LONGS),Z(LOXT),Z(LOSLFI),XFACT,JN,NCS,NP,
     * NODESC,K1,K2,K4,K9,K23)
CDSC  ***************************************************************************
      IF(LIMIT.GT.0) GO TO 5000
C.....
C     MESSAGE -- 80-CHARACTER MESSAGE DESCRIBING DATA SET
C.....
      READ(IN,'(A)',END=1000) DESC
      READ(IN,2090) MESAGE
2090  FORMAT(20A4)
```

A.2.12. SUBROUTINE SECTF

```
      DY=Y-HS(KL,I,J)
      DBL=(BSL(KT,I,J)-BSL(KL,I,J))/DH
      DBR=(BSR(KT,I,J)-BSR(KL,I,J))/DH
      BL=BSL(KL,I,J)+DBL*DY
      BR=BSR(KL,I,J)+DBR*DY
CDSC  **** REPLACED FLOODPLAIN AREA CALCULATIONS TO INCLUDE POROSITY *****
CC    ****  OLD TERM: AL=ASL(KL,I,J)+0.5*(BSL(KL,I,J)+BL)*DY  ****
CC    ****  OLD TERM: AR=ASR(KL,I,J)+0.5*(BSR(KL,I,J)+BR)*DY  ****
      AL=ASL(KL,I,J)+0.5*(BSL(KL,I,J)+BL)*DY*POREL(KL,I,J)
      AR=ASR(KL,I,J)+0.5*(BSR(KL,I,J)+BR)*DY*PORER(KL,I,J)
CDSC  ***************************************************************************
      IF(BL.LT.0.01) BL=0.01
      IF(BR.LT.0.01) BR=0.01
      RETURN
      END
```

A.2.13. SUBROUTINE SIZE

```
      LCIRGM=LCVPK+K1*K2
      LCBKT=LCIRGM+K13
```

```
      LCQKT=LCBKT+501
      LCERQX=LCQKT+501
      LCSNMT=LCERQX+500
CDSC  *** STERN CHANGE TO ADD SPACE FOR RETENTION TIME ARRAYS ************
CC    IUSE=LCSNMT+501
      LCVTC=LCSNMT+501
      LCXTC=LCVTC+K1*K4*K3
      LCRTTC=LCXTC+K1*K4*K3
      IUSE=LCRTTC+K1*K4*K3
CDSC  ********************************************************************
C---------- KALMAN FILTER AND EXPLICIT SPACE SETTING ----------
      KALMAN=0
      DO 500 J=1,K1
      IF (KFTR(J).EQ.1) KALMAN=1
500   CONTINUE

      Z(399)=LCPR+0.01
      Z(402)=LCNFLO+0.01
      Z(406)=LCFLAG+0.01
      Z(408)=LCWDSN+0.01
      Z(421)=LCVPK+0.01
CDSC  *** STERN CHANGE TO ADD SPACE FOR RETENTION TIME ARRAYS *************
      Z(430)=LCVTC+0.01
      Z(431)=LCXTC+0.01
      Z(432)=LCRTTC+0.01
CDSC  ********************************************************************
2010  FORMAT(//2X,'**ERROR** AMOUNT OF STORAGE (',I12,') EXCEEDED WHILE
     *ALLOCATING TEMPORARY SPACE ... PROGRAM TERMINATED.')
5000  RETURN
      END
```

A.2.14. SUBROUTINE STEMSL

```
      SUBROUTINE STEMSL (NCML,DIAL,YQCM,J,L,YQ,DIAM,DCM,K7,K8)
      DIMENSION DIAL(K8,K7,1),YQCM(K8,K7,1)

CDS   ************ THIS SUBR INTERPOLATES DIAL ***
CDS   ** (LOW DEPTH LIMIT)IF DEPTH (YQ) LT MANN TBL DPTH (YQCM) ***
      IF(YQ.LT.YQCM(1,L,J)) DIAM=DIAL(1,L,J)
      IF(YQ.LT.YQCM(1,L,J)) GO TO 20
CDS   ** (HIGH DEPTH LIMIT) IF DEPTH (YQ) GT END OF MANN TBL (N0 YQCM = NCS)**
      IF(YQ.GT.YQCM(NCML,L,J)) DIAM=DIAL(NCML,L,J)
      IF(YQ.GT.YQCM(NCML,L,J)) GO TO 20
CDS   ** (BETWEEN DEPTH LIMITS) ***
      DO 10 KK=2,NCML
      KT=KK
      IF (YQ.LE.YQCM(KT,L,J)) GO TO 12
10    CONTINUE
12    KL=KK-1
```

```
      DH=YQCM(KT,L,J)-YQCM(KL,L,J)
      IF(ABS(DH).LE.0.01) DH=0.01
      DDIA=(DIAL(KT,L,J)-DIAL(KL,L,J))/DH
      DIAM=DIAL(KL,L,J)+DDIA*(YQ-YQCM(KL,L,J))
20    IF(DIAM.LT.0.001) DIAM=0.01
      RETURN
      END
```

A.2.15. SUBROUTINE STEMSR

```
      SUBROUTINE STEMSR (NCML,DIAR,YQCM,J,L,YQ,DIAM,DCM,K7,K8)
      DIMENSION DIAR(K8,K7,1),YQCM(K8,K7,1)
CDS   ************ THIS SUBR INTERPOLATES DIAR ***
CDS   ** (LOW DEPTH LIMIT)IF DEPTH (YQ) LT MANN TBL DPTH (YQCM) ***
      IF(YQ.LT.YQCM(1,L,J)) DIAM=DIAR(1,L,J)
      IF(YQ.LT.YQCM(1,L,J)) GO TO 20
CDS   ** (HIGH DEPTH LIMIT) IF DEPTH (YQ) GT END OF MANN TBL (N0 YQCM = NCS)**
      IF(YQ.GT.YQCM(NCML,L,J)) DIAM=DIAR(NCML,L,J)
      IF(YQ.GT.YQCM(NCML,L,J)) GO TO 20
CDS   ** (BETWEEN DEPTH LIMITS) ***
      DO 10 KK=2,NCML
      KT=KK
      IF (YQ.LE.YQCM(KT,L,J)) GO TO 12
10    CONTINUE
12    KL=KK-1
      DH=YQCM(KT,L,J)-YQCM(KL,L,J)
      IF(ABS(DH).LE.0.01) DH=0.01
      DDIA=(DIAR(KT,L,J)-DIAR(KL,L,J))/DH
      DIAM=DIAR(KL,L,J)+DDIA*(YQ-YQCM(KL,L,J))
20    IF(DIAM.LT.0.001) DIAM=0.01
      RETURN
      END
```

A.2.16. SUBROUTINE SUMARY

```
1450  CONTINUE
1500  CONTINUE
C .....
C PRINT THE CONTENTS OF THE COMPUTE WSEL & FLOW ARRAYS AT
C EACH PLOTTING STATION
      WRITE(IPR,1001)
CDSC  ***** STERN CHANGE TO WRITE STG TBL AT LT 3 WAS ORINGNALLY LT 9 ******
      IF(JNK.LT.3) GO TO 1700
CDSC  ********************************************************************************
      DO 1660 J=1,JN
      NGAG=NGAGE(J)
      IF(NGAG.EQ.0) GO TO 1660
      DO 1650 K=1,NGAG
```

```
          KST=1
          WRITE(IPR,1693) J,(NGS(KK,J),KK=KST,KND)
1693      FORMAT(/6H KTIME,2X,10HTII(KTIME),5X,
         & 'COMPUTED STAGES FOR RIVER=',I2,2X,'SECTION=',8I5/)
          DO 1640 KT=1,KTIME
          WRITE(IPR,2124) KT,TII(KT),((STC(KT,KK,J)/FT),KK=KST,KND)
CDSC      ***** STERN ADDED TO OUTPUT STAGE FILE *********************************
          WRITE(100,2124) KT,TII(KT),((STC(KT,KK,J)/FT),KK=KST,KND)
CDSC      ***************************************************************************
1640      CONTINUE
          WRITE(IPR,1315)
          WRITE(IPR,1694) J,(NGS(KK,J),KK=KST,KND)
1694      FORMAT(/6H KTIME,2X,10HTII(KTIME),5X,
         & 'COMPUTED DISCHARGE FOR RIVER=',I2,2X,'SECTION=',8I5/)
          DO 1641 KT=1,KTIME
          WRITE(IPR,2125) KT,TII(KT),((QTC(KT,KK,J)/CFS),KK=KST,KND)
1641      CONTINUE
CDSC      ******** STERN ADDED TO WRITE RETENTION TIMES *************************
CDSC      ******** WRITE VELOCITIES *********************************************
          WRITE(IPR,1315)
          WRITE(IPR,3300) J,(NGS(KK,J),KK=KST,KND)
3300      FORMAT(/6H KTIME,2X,10HTII(KTIME),5X,
         & 'COMPUTED VELOCITY (FT/SEC) FOR RIVER=',I2,2X,'SECTION=',8I5/)
          DO 3310 KT=1,KTIME
          WRITE(IPR,2125) KT,TII(KT),(VTC(KT,KK,J),KK=KST,KND)
3310      CONTINUE
CDSC      ******** WRITE DISTANCES **********************************************
          WRITE(IPR,1315)
          WRITE(IPR,3400) J,(NGS(KK,J),KK=KST,KND)
3400      FORMAT(/6H KTIME,2X,10HTII(KTIME),5X,
         & 'COMPUTED DISTANCES (FT) FOR RIVER=',I2,2X,'SECTION=',8I5/)
          DO 3410 KT=1,KTIME
          WRITE(IPR,2125) KT,TII(KT),(XTC(KT,KK,J),KK=KST,KND)
3410      CONTINUE
CDSC      ******** WRITE RETENTION TIMES XTC/VTC *********************************
          WRITE(IPR,1315)
          WRITE(IPR,3500) J,(NGS(KK,J),KK=KST,KND)
3500 FORMAT(/6H KTIME,2X,10HTII(KTIME),5X,
         & 'RETENTION TIMES (MIN) FOR RIVER=',I2,2X,'SECTION=',8I5/)
          DO 3510 KT=1,KTIME
          WRITE(IPR,2125) KT,TII(KT),(RTTC(KT,KK,J),KK=KST,KND)
3510      CONTINUE
CDSC      ***************************************************************************
          IF(KND.GE.NGAG) GO TO 1660
          KST=KND+1
          KND=KST+8
          GO TO 1645
1650      CONTINUE
1660      CONTINUE
1700      CONTINUE
1315      FORMAT(1X)
```

```
2123    FORMAT(I3,I5,2A1,F12.3,F12.2,F12.5,F12.2,F12.5,F12.4,3F10.4)
CDSC    ** MODIFIED FORMATED TO F15.8 **********************************
2124    FORMAT(I6,F12.3,8F15.8)
2125    FORMAT(I6,F12.3,8F15.8)
CDSC    ********************************************************************************
        RETURN
        END
```

A.3. DYNAWET Hydrodynamic Module Input Parameters

A.3.1 Example of input

The following text is the actual input file used for the 8/18/98 event used for modeling. To understand this file, a labeled print echo of the input data (which is part of one of the output files) is provided on pages 174 to 176.

Input file:

```
PROBLEM MBV81898 LEAF-ON STORM FLOW VERIFICATION 8/18/98
EOM
NO    DESC
0.01   0.5   0.6   5280    0    0    0
1    14    10    3    1    0    0    0    0    0
0    0    0    0
4    2    5    0    0
0    0    0    0    0
4   0.004166  0.08330  0.05    0    0
0    0    0
4    1    31    0.100    0    0    0
2    4    0    4    3    0    0    0    0    0
2    0    0    1    0    0    0    0    0    0
0.044632576  0.06466667  -0.5  1
0    0.044632576  0.06466667  0.088017045
0.0044632576  0.0020034091  0.0023350379
0  0  0
1      MI 0
```

2 MI 0.045

3 MI 0.065

4 MI 0.088

0.0318 0.0318 0.0318 0.0318 0.0318 0.0363 0.2634 0.1308
0.0865 0.0788 0.0751 0.0715 0.0680 0.0680

0.0000 0.2500 0.5000 0.7500 1.0000 1.2500 1.5000 1.7500
2.0000 2.2500 2.5000 2.7500 3.0000 3.2500

0 0 0.0318 0

424.27 424.65 424.78 425.20

0 6.13 6.13 6.13

0 0 0 0.81

0 0 0 7.92

0 0 0 0

0 0 0 0

414.91 415.06 415.21 416.23

0 2.9 2.9 2.9

0 0 0 68.6

0 0 0 34.15

0 0 0 0

0 0 0 0

412.83 413.12 413.41 413.77

0 2.2 2.2 2.2

0 0 0 47.6

0 0 0 40.3

0 0 0 0

0 0 0 0

410.76 411.07 411.37 411.52

0 3.0 3.0 3.0

0 0 0 5.5

0 0 0 12.10

0 0 0 0

1.56 1.56 1.56 1.00

1.19 1.19 1.19 1.00

1.25 1.25 1.25 1.00

0 0 0

1 2 3

0.57 0.54 0.38 0.41

0 0 .002 .002

0 0 .002 .002

1 1 0.97 0.98

1 1 0.97 0.98

0. 0. 0.11 0.11

0. 0. 0.11 0.11

.25 .20 .18 .20

0 0 .005 .005

0 0 .005 .005

1 1 .96 .97

1 1 .96 .97

0. .0 .025 .025

0. .0 .025 .025

0.09 0.09 0.03 0.01

0 0 .002 .002

0 0 .005 .005

```
1  1   0.97   0.98

1  1    .96  .97

.1  .1   .1  .1

.1  .1   .1  .1

0

SUB/SUP/TEST   RUN    (MB)

MB-8 18 98   RIVER
```

A.3.2. Input parameter descriptions

Table A.1 provides the description of the parameters needed to prepare the input file for running the DYNAWET model. This table has been adapted from input description provided for the FLDWAV model (Fread and Lewis, 1998).

Table A.1 Definition of input variables for DYNAWET model (from Fread and Lewis, 1998)

DATA VARIABLE	INPUT LINE	DEFINITION OF THE VARIABLE
MSG	1	Up to 80 character description of data set
DESC	2	Type of output display; set DESC=NO DESC
EPSY	3	Depth tolerance in Newton-Raphson iteration scheme. Range 0.001-1.0 ft; recommend ESPY=0.01
THETA	3	Acceleration factor to solve tributary junction problem Range 0.5-1.0; recommend THETA=0.8
F1	3	Weighting factor in finite difference technique. Range 0.5-1.0; recommend F1=0.6
XFACT	3	Units conversion factor for location of computation points Miles=5280; km=1000; ft=1
DTHYD	3	Time interval of all input hydrographs. If time interval is not constant, set DTHYD=0.
DTOUT	3	Time interval (hrs) of all output hydrographs; set DTHYD=0.
METRIC	3	Parameter for units of input/output (English=0 or Metric=1).
JN	4	Total number of rivers.
NU	4	Number of values associated with observed hydrographs.
ITMAX	4	Maximum number of iterations allowed in the Newton-Raphson iteration scheme. Recommend ITMAX=10
KWARM	4	Number of time steps used for warm-up procedure. Recommend KWARM=2.
KFLP	4	Flood plain (conveyance) parameter; Set KFLP = (0 for no flood plain) or (1 for flood plain)
NET	4	Channel network option currently unavailable; set NET=0
ICOND	4	Type of initial conditions for NWS. Set ICOND=0.
IFUT	4	Future input; set = 0 0 0 0
NYQD	5	Number of values in rating curve at downstream boundary
KCG	5	Points in spillway gate control curve; set KCG=0.
NCG	5	Dummy parameter; set NCG=0.
KPRES	5	Parameter for method of computing hydraulic radius. Set KPRES= (0 for R=A/B) or (1 for R=A/P).
NCS	6	Number of values in table of topwidth vs. elevation.
KPL	6	Parameter for type of hydrograph to be plotted. Set KPL= 0: nothing; 1: h hydrographs; 2 : Q hydrographs; 3:both.

DATA VARIABLE	INPUT LINE	DEFINITION OF THE VARIABLE
JNK	6	Output print parameter. Set JNK= 0:nothing; >0: various information printed. Recommend JNK= 5
KREVRS	6	Parameter for use of the low flow filter. KREVRS= 0: low flow filter activated; 1:reverse flow allowed.
NFGRF	6	Parameter for generating data for NWS's FLDGRF program. NFGRF= 0: data generated; 1: no data generated.
IOBS	7	Parameter indicating if observed data are available. IOBS= 0: no flow data; 1: inflow available; -1: use math function.
KTERM	7	Parameter to print terms in equation of motion. KTERM= 0:no print; 1: print. Recommend KTERM= 0.
NP	7	Parameter for use of Automatic Calibration option. NP= 0:no calibration; 1: auto-calibration. Recommend. NP= 0.
NPST	7	First value in the computed stage hydrograph used in the statistics (calibration). Recommend NPST=0.
NPEND	7	Last value in the computed stage hydrograph used in the statistics (calibration). Recommend NPEND=0.
TEH	8	Time at which routing computations will terminate. (HR)
DTHII	8	Initial computational time step (HR)
DTHPLT	8	Plotting/printing time interval (HR)
FRDFR	8	Window for critical Froude number. Set FRDFR= 0.05.
DTEXP	8	Computational time step for explicit routing. DTEXP= 0.
MDT	8	Divisor for determining the time step. Set MDT= 0.
NLEV	9	Total number of section reaches in the system with levees.
DHLV	9	Difference between max and min levee crest elevations.
DTHLV	9	Computational time step after levee overtopping/failure
NBT(J)	10	Total number of cross sections.
NPT(1,J)	10	Beginning cross-section number for which debug information will be printed.
NPT(2,J)	10	Final cross-section number for which debug information will be printed.
MRV(J)	10	Number of river into which river J flows.
NJUN(J)	10	Number of section along the main river immediately upstream of tributary confluence.
ATF(J)	10	Acute angle tributary makes with main river at its confluence.
EPQJ(J)	10	Discharge tolerance in tributary iteration scheme.
COFW(J)	10	Coefficient of wind stress. Range:1.1 E-06 to 3.0 E-06.

DATA VARIABLE	INPUT LINE	DEFINITION OF THE VARIABLE
VWIND(J)	10	Wind velocity. (ft/s); (+ upstream); (- downstream).
WINAGL(J)	10	Acute angle that wind makes with channel axis. (degrees).
KU(J)	11	Type of upstream boundary condition parameter. KU= 1: stage hydrograph; 2: discharge hydrograph.
KD(J)	11	Parameter for the type of downstream boundary condition. KU= 1: stage hydrograph; 2: discharge hydrograph; 3:single valued rating curve; 4: looped rating curve.
NQL(J)	11	Total number of lateral flows on river.
NGAGE(J)	11	Total number of observed hydrographs on river.
NRCM1(J)	11	Total number of Manning n reaches on river.
NQCM(J)	11	Total number of values in the Manning table. Set NQCM= 0: Manning n is a function WSEL; NQCM=NCS.
IFUT(4)	11	Future input; set IFUT= 0 0 0 0
MIXF(J)	12	Parameter for the flow regime. MIXF(J)= 0: subcritical; 1: supercritical; >1 mixture of subcritical and supercritical; 2: hydraulic jump can move upstream or downstream; 3: hydraulic jump moves only if the Froude number exceeds 2; 4: hydraulic jump is stationary; 5: a modified implicit technique (LPI) is used to solve mixed flows.
MUD(J)	12	Dynamic routing of mudflow option. MUD= 0: dynamic routing of non-mudflow (water) only; 1: Dynamic routing of mudflow. Set MUD(J)=0.
KFTR(J)	12	Parameter for use of Kalman Filter option. KFTR= 0: switch is off; 1: switch is on.
KLOS(J)	12	Parameter indicating the computation of volume losses in river J. KLOS= 0: the losses will not be computed; 1: the losses will be computed.
IFUT(6)	12	Future input; set IFUT= 0 0 0 0 0 0
XLOS(1,J)	13	Beginning location of the reach(s) where flow loss will occur on river J.
XLOS(2,J)	13	Ending location of the reach(s) where flow loss will occur on river J.
QLOS(J)	13	Percentage of the loss in terms of total active flow amount; (-) for loss and (+) for gain.
ALOS(J)	13	Loss distribution coefficient for river J (0.3-3.0). For a linear loss distribution, set ALOS(J)=1.
XT(I,J)	14	Location of section where computations are made.
DXM(I,J)	15	Minimum computational distance interval between sections.

DATA VARIABLE	INPUT LINE	DEFINITION OF THE VARIABLE
KRCHT(I,J)	16	Parameter for routing method or internal boundary. KRCHT= 0: implicit dynamic; 1: implicit diffusion.
LQ1(K,J)	17	Number of section immediately upstream of lateral flow.
QL(L,K,J)	18	Lateral inflow at cross section.
NGS(K,J)	19	Sequence number of each observed/plotting station
ST1(L,J)	20	Observed stages or discharges at upstream boundary.
T1(L,J)	21	Time array associated with upstream hydrograph.
FLST(I,J)	22	Elevation at which flooding commences
QDI(I,J)	22	Initial discharges
YDI(I,J)	22	Initial water surface elevations
HS(L,I,J)	23	Elevation corresponding to each top width (ft).
BS(L,I,J)	24	Topwidth of active flow portion of cross section (ft).
BSL(L,I,J)	25	Topwidth of active flow portion of left flood plain (ft).
BSR(L,I,J)	26	Topwidth of active flow portion of right flood plain (ft).
BSS(L,I,J)	27	Topwidth of inactive portion of cross section (ft).
SNM(L,I,J)	28	Sinuosity coefficient
FKEC(I,J)	29	Expansion or contraction coefficient
NCM(I,J)	30	Section number of upstream-most station of Manning n
CM(L,I,J)	31	Manning n for channel
CWETL(L,I,J)	32	Wetland friction coefficient for left flood plain
CWETR(L,I,J)	33	Wetland friction coefficient for right flood plain
POREL(L,I,J)	34	Wetland porosity for left flood plain
PORER(L,I,J)	35	Wetland porosity for right flood plain
DIAL(L,I,J)	36	Average stem diameter for left flood plain (ft).
DIAR(L,I,J)	37	Average stem diameter for right flood plain (ft).
MESAGE	38	80-character message describing the data set
RIVER(J)	39	16-character name associated with each river

A.4. DYNAWET Hydrodynamic Module Output

The following is a printing of the text file that is produced by the DYNAWET model. The file has been shortened by only listing the information on the first and last time step.

```
                PROGRAM DYNAWET 1.0 (MODIFIED FLDWAV 1.0.0)

                    ******************************
                    ******************************
                    ***                        ***
                    ***  SUMMARY OF INPUT DATA  ***
                    ***                        ***
                    ******************************
                    ******************************

PROBLEM MBV81898 LEAF-ON STORM FLOW VERIFICATION 8/18/98

      EPSY      THETA         F1     XFACT      DTHYD      DTOUT     METRIC
     0.010      0.500      0.600  5280.000      0.000      0.000          0

       JN         NU      ITMAX     KWARM      KFLP        NET      ICOND    FUTURE DATA
        1         14         10         3         1          0          0    0 0 0

      NYQD        KCG        NCG     KPRES
         0          0          0         0

       NCS        KPL        JNK    KREVRS     NFGRF
         4          2          5         0         0

      IOBS      KTERM         NP      NPST     NPEND
         0          0          0         0         0

       TEH      DTHII     DTHPLT     FRDFR     DTEXP       MDT
     4.000    0.00417    0.08330      0.05   0.00000         0

      NLEV       DHLV      DTHLV
         0    0.00000    0.00000

 RIVER NO.  NBT NPT1 NPT2       EPQJ       COFW      VWIND  WINAGL
    1          4    1   31     0.1000     0.0000     0.0000     0.0000

RIVER NO.      KU     KD    NQL NGAGE NRCM1  NQCM  NSTR  FUTURE DATA
    1           2      4      0      4      3      0     0    0 0 0

RIVER NO.    MIXF   MUD  KFTR  KLOS  FUTURE DATA
    1           2     0     0     1    0 0 0 0 0 0

RIVER     XLOS(1,J)  XLOS(2,J)   QLOS(J) (%)   ALOS(J)
      1         0.04         0.06        -0.50         1.00

 XT(I, 1) I=1,NB( 1)
   0.00000    0.04463    0.06467    0.08802

 DXM(I, 1) I=1,NB( 1)
   0.00446    0.00200    0.00234

 KRCH(I, 1) I=1,NRCH
         0    0    0
```

```
PLOTTING/OBSERVED TIME SERIES FOR RIVER J=  1

    I       NGS   ID
    1         1   MI 0
    2         2   MI 0.045
    3         3   MI 0.065
    4         4   MI 0.088

ST1(K,1), K = 1, NU
      0.03        0.03        0.03        0.03        0.03        0.04        0.26        0.13
      0.09        0.08        0.08        0.07        0.07        0.07

T1(K,1), K = 1, NU
      0.00        0.25        0.50        0.75        1.00        1.25        1.50        1.75
      2.00        2.25        2.50        2.75        3.00        3.25


RIVER NO.  1

 I=    1     FLDSTG=    0.00      YDI=    0.00     QDI=     0.032     AS1=        0.
         HS=          424.27    424.65    424.78    425.20
         BS=             0.0       6.1       6.1       6.1
        BSL=             0.0       0.0       0.0       0.8
        BSR=             0.0       0.0       0.0       7.9
        BSS=             0.0       0.0       0.0       0.0

 I=    2     FLDSTG=    0.00      YDI=    0.00     QDI=     0.000     AS1=        0.
         HS=          414.91    415.06    415.21    416.23
         BS=             0.0       2.9       2.9       2.9
        BSL=             0.0       0.0       0.0      68.6
        BSR=             0.0       0.0       0.0      34.2
        BSS=             0.0       0.0       0.0       0.0

 I=    3     FLDSTG=    0.00      YDI=    0.00     QDI=     0.000     AS1=        0.
         HS=          412.83    413.12    413.41    413.77
         BS=             0.0       2.2       2.2       2.2
        BSL=             0.0       0.0       0.0      47.6
        BSR=             0.0       0.0       0.0      40.3
        BSS=             0.0       0.0       0.0       0.0

 I=    4     FLDSTG=    0.00      YDI=    0.00     QDI=     0.000     AS1=        0.
         HS=          410.76    411.07    411.37    411.52
         BS=             0.0       3.0       3.0       3.0
        BSL=             0.0       0.0       0.0       5.5
        BSR=             0.0       0.0       0.0      12.1
        BSS=             0.0       0.0       0.0       0.0

REACH INFO RIVER NO.  1

        SNM=           1.560     1.560     1.560     1.000
        SNC=           1.560     1.560     1.560     1.000

        SNM=           1.190     1.190     1.190     1.000
        SNC=           1.190     1.190     1.190     1.000

        SNM=           1.250     1.250     1.250     1.000
        SNC=           1.250     1.250     1.250     1.000

 FKEC(I,1), I = 1, NM(1)
         0.00      0.00      0.00

 NCM(K, 1), K=1,NRCM1( 1)
       1    2    3
```

CM (K, 1, 1)=	0.5700	0.5400	0.3800	0.4100
CWETL(K, 1, 1)=	0.0000	0.0000	0.0020	0.0020
CWETR(K, 1, 1)=	0.0000	0.0000	0.0020	0.0020
POREL(K, 1, 1)=	1.0000	1.0000	0.9700	0.9800
PORER(K, 1, 1)=	1.0000	1.0000	0.9700	0.9800
DIAL(K, 1, 1)=	0.0000	0.0000	0.1100	0.1100
DIAR(K, 1, 1)=	0.0000	0.0000	0.1100	0.1100
CM (K, 2, 1)=	0.2500	0.2000	0.1800	0.2000
CWETL(K, 2, 1)=	0.0000	0.0000	0.0050	0.0050
CWETR(K, 2, 1)=	0.0000	0.0000	0.0050	0.0050
POREL(K, 2, 1)=	1.0000	1.0000	0.9600	0.9700
PORER(K, 2, 1)=	1.0000	1.0000	0.9600	0.9700
DIAL(K, 2, 1)=	0.0000	0.0000	0.0250	0.0250
DIAR(K, 2, 1)=	0.0000	0.0000	0.0250	0.0250
CM (K, 3, 1)=	0.0900	0.0900	0.0300	0.0100
CWETL(K, 3, 1)=	0.0000	0.0000	0.0020	0.0020
CWETR(K, 3, 1)=	0.0000	0.0000	0.0050	0.0050
POREL(K, 3, 1)=	1.0000	1.0000	0.9700	0.9800
PORER(K, 3, 1)=	1.0000	1.0000	0.9600	0.9700
DIAL(K, 3, 1)=	0.1000	0.1000	0.1000	0.1000
DIAR(K, 3, 1)=	0.1000	0.1000	0.1000	0.1000

0

METHOD OF ROUTING FOR THIS RIVER SYSTEM:

RIVER NO. 1
L= 1 KRTYP= 0 KRT1= 1 KRTN= 4 IMPLICIT DYNAMIC ROUTING

SUMMARY OF ARRAY SIZES

NO. OF RIVERS IN THE SYSTEM	1
MAXIMUM NO. OF CROSS SECTIONS ON ANY RIVER	32
NO. OF COMPUTATIONAL TIME STEPS	961
MAXIMUM NO. OF GAGING STATIONS ON ANY RIVER	4
MAXIMUM NO. OF ROUTING TECHNIQUES IN THE SYSTEM	1
NO. OF SETS OF POINTS IN THE D/S RATING CURVE TABLE	1
MAXIMUM NO. OF MANNING N REACHES ON ANY RIVER	32
NO. OF SETS OF POINTS IN THE MANNING N TABLE	4
NO. OF SETS OF POINTS IN THE BS VS HSS TABLE	4
MAXIMUM NO. OF LATERAL FLOW HYDROGRAPHS ON ANY RIVER	1
MAXIMUM NO. OF REACHES ON ANY RIVER	4
MAXIMUM NO. OF EQUATIONS TO BE SOLVED (K2*2)	64
MAXIMUM NO. OF INTERNAL BOUNDARIES ON ANY RIVER	1
TOTAL NO. OF LEVEE REACHES IN THE SYSTEM	1
MAXIMUM NO. OF MULTIPLE GATES ON ANY RIVER	1
NO. OF DAMS WHICH HAVE MULTIPLE GATES	0
NO. OF POINTS IN THE MOVABLE GATE TIME SERIES	1
NO. OF INTERPOLATED LEVEE REACHES IN THE SYSTEM	1
MAXIMUM NO. OF ACTUAL CROSS SECTIONS ON ANY RIVER	4
TOTAL NO. OF HYDROGRAPH POINTS USED IN FLDGRF PROGRAM	1922

****
****
*** ***
*** SUMMARY OF OUTPUT DATA ***
*** ***
****
****

RIVER NO	SECT NO	X MILE	BED ELEV. FEET	REACH NO	LENGTH MILE	SLOPE FPM	ROUTING	STRUCT.
1	1	0.000	424.270	1	0.04	209.71	IMP(MIX)	
1	2	0.045	414.910	2	0.02	103.82	IMP(MIX)	
1	3	0.065	412.830	3	0.02	88.65	IMP(MIX)	
1	4	0.088	410.760					

NEW INPUT CROSS SECTION NO. AFTER INTERPOLATION

RIVER NO. 1
NN= 1 11 21 31

RIVER NO. 1
NGS= 1 11 21 31

L= 1 KRTYP= 0 KRT1= 1 KRTN= 31

(SLOP(I,J),I=1,N) FOR RIVER NO. 1

0.039718 0.039718 0.039717 0.039718 0.039718 0.039718 0.039718 0.039717
0.039718 0.039718 0.019664 0.019664 0.019661 0.019664 0.019664 0.019664
0.019664 0.019661 0.019664 0.019664 0.016790 0.016790 0.016790 0.016790
0.016787 0.016790 0.016790 0.016790 0.016790 0.016790 0.016790

GENERATING CONVEYANCE CURVE

J= 1 I= 1 L= 30 ERQK= 2.58 NKC(I,J)= 30

HKC(L,I,J)=	424.27	424.27	424.28	424.28	424.29	424.29	424.30	424.30
HKC(L,I,J)=	424.31	424.31	424.32	424.33	424.35	424.36	424.38	424.40
HKC(L,I,J)=	424.43	424.47	424.51	424.57	424.63	424.66	424.71	424.77
HKC(L,I,J)=	424.88	424.89	424.95	425.02	425.10	425.20		
QKC(L,I,J)=	0.	0.	0.	0.	0.	0.	0.	0.
QKC(L,I,J)=	0.	0.	0.	0.	0.	0.	0.	0.
QKC(L,I,J)=	0.	0.	0.	0.	1.	1.	2.	3.
QKC(L,I,J)=	4.	5.	8.	13.	21.	34.		
BEV(L,I,J)=	1.860	192.567	46.882	21.755	12.961	8.830	6.679	5.346
BEV(L,I,J)=	4.480	3.887	3.149	2.724	2.360	2.155	1.996	1.884
BEV(L,I,J)=	1.810	1.756	1.723	1.701	1.685	1.681	1.675	1.671
BEV(L,I,J)=	1.686	1.677	1.791	1.881	1.904	1.870		

SNM(K, 1, 1)=	1.56	1.56	1.56	1.13
SNM(K, 2, 1)=	1.56	1.56	1.56	1.07
SNM(K, 3, 1)=	1.56	1.56	1.56	1.04
SNM(K, 4, 1)=	1.56	1.56	1.56	1.03
SNM(K, 5, 1)=	1.56	1.56	1.56	1.02
SNM(K, 6, 1)=	1.56	1.56	1.56	1.01
SNM(K, 7, 1)=	1.56	1.56	1.56	1.01
SNM(K, 8, 1)=	1.56	1.56	1.56	1.01
SNM(K, 9, 1)=	1.56	1.56	1.56	1.01
SNM(K, 10, 1)=	1.56	1.56	1.56	1.00
SNM(K, 11, 1)=	1.19	1.19	1.19	1.01
SNM(K, 12, 1)=	1.19	1.19	1.19	1.01
SNM(K, 13, 1)=	1.19	1.19	1.19	1.01
SNM(K, 14, 1)=	1.19	1.19	1.19	1.01
SNM(K, 15, 1)=	1.19	1.19	1.19	1.01
SNM(K, 16, 1)=	1.19	1.19	1.19	1.01
SNM(K, 17, 1)=	1.19	1.19	1.19	1.02
SNM(K, 18, 1)=	1.19	1.19	1.19	1.02
SNM(K, 19, 1)=	1.19	1.19	1.19	1.02
SNM(K, 20, 1)=	1.19	1.19	1.19	1.02

```
 SNM(K, 21, 1)=      1.25      1.25      1.25      1.06
 SNM(K, 22, 1)=      1.25      1.25      1.25      1.07
 SNM(K, 23, 1)=      1.25      1.25      1.25      1.07
 SNM(K, 24, 1)=      1.25      1.25      1.25      1.08
 SNM(K, 25, 1)=      1.25      1.25      1.25      1.08
 SNM(K, 26, 1)=      1.25      1.25      1.25      1.09
 SNM(K, 27, 1)=      1.25      1.25      1.25      1.09
 SNM(K, 28, 1)=      1.25      1.25      1.25      1.10
 SNM(K, 29, 1)=      1.25      1.25      1.25      1.10
 SNM(K, 30, 1)=      1.25      1.25      1.25      1.11
 SNM(K, 31, 1)=      1.25      1.25      1.25      1.11

ERQMX=  2.57 3.08 3.08 3.09 3.08 3.70 3.70 3.71 3.69 3.71* 2.57 2.58 2.57 2.57 2.57 2.57 2.58 2.57 2.57 2.58
ERQMX=  3.08 3.08 3.09 3.09 3.09 3.09 3.08 3.09 3.09 3.08* 3.08

 SNC(K,  1, 1)=      1.56      1.56      1.56      1.14
 SNC(K,  2, 1)=      1.56      1.56      1.56      1.09
 SNC(K,  3, 1)=      1.56      1.56      1.56      1.06
 SNC(K,  4, 1)=      1.56      1.56      1.56      1.08
 SNC(K,  5, 1)=      1.56      1.56      1.56      1.16
 SNC(K,  6, 1)=      1.56      1.56      1.56      1.15
 SNC(K,  7, 1)=      1.56      1.56      1.56      1.14
 SNC(K,  8, 1)=      1.56      1.56      1.56      1.12
 SNC(K,  9, 1)=      1.56      1.56      1.56      1.11
 SNC(K, 10, 1)=      1.56      1.56      1.56      1.01
 SNC(K, 11, 1)=      1.19      1.19      1.19      1.00
 SNC(K, 12, 1)=      1.19      1.19      1.19      1.04
 SNC(K, 13, 1)=      1.19      1.19      1.19      1.05
 SNC(K, 14, 1)=      1.19      1.19      1.19      1.05
 SNC(K, 15, 1)=      1.19      1.19      1.19      1.06
 SNC(K, 16, 1)=      1.19      1.19      1.19      1.06
 SNC(K, 17, 1)=      1.19      1.19      1.19      1.07
 SNC(K, 18, 1)=      1.19      1.19      1.19      1.08
 SNC(K, 19, 1)=      1.19      1.19      1.19      1.09
 SNC(K, 20, 1)=      1.19      1.19      1.19      1.02
 SNC(K, 21, 1)=      1.25      1.25      1.25      1.03
 SNC(K, 22, 1)=      1.25      1.25      1.25      1.14
 SNC(K, 23, 1)=      1.25      1.25      1.25      1.15
 SNC(K, 24, 1)=      1.25      1.25      1.25      1.15
 SNC(K, 25, 1)=      1.25      1.25      1.25      1.16
 SNC(K, 26, 1)=      1.25      1.25      1.25      1.16
 SNC(K, 27, 1)=      1.25      1.25      1.25      1.17
 SNC(K, 28, 1)=      1.25      1.25      1.25      1.17
 SNC(K, 29, 1)=      1.25      1.25      1.25      1.18
 SNC(K, 30, 1)=      1.25      1.25      1.25      1.14
 SNC(K, 31, 1)=      1.25      1.25      1.25      1.11

      QDI(I, 1)
0.03180   0.00000   0.00000   0.00000   0.00000   0.00000   0.00000   0.00000
0.00000   0.00000   0.00000   0.00000   0.00000   0.00000   0.00000   0.00000
0.00000   0.00000   0.00000   0.00000   0.00000   0.00000   0.00000   0.00000
0.00000   0.00000   0.00000   0.00000   0.00000   0.00000   0.00000

      YDI(I, 1)
0.00000   0.00000   0.00000   0.00000   0.00000   0.00000   0.00000   0.00000
0.00000   0.00000   0.00000   0.00000   0.00000   0.00000   0.00000   0.00000
0.00000   0.00000   0.00000   0.00000   0.00000   0.00000   0.00000   0.00000
0.00000   0.00000   0.00000   0.00000   0.00000   0.00000   0.00000

** COMPUTE INITIAL FLOW, NORMAL AND INITIAL DEPTH FOR RIVER NO  1  **
  (QDI(I,1),I=1,N)
0.03180   0.03180   0.03180   0.03180   0.03180   0.03180   0.03180   0.03180
0.03180   0.03180   0.03180   0.03180   0.03180   0.03180   0.03180   0.03180
0.03180   0.03180   0.03180   0.03180   0.03180   0.03180   0.03180   0.03180
0.03180   0.03180   0.03180   0.03180   0.03180   0.03180   0.03180
```

```
INITIAL DISCHARGES:
        (QDI FOR RIVER NO.  1
 0.03180   0.03180   0.03180   0.03180   0.03180   0.03180   0.03180   0.03180
 0.03180   0.03180   0.03180   0.03180   0.03180   0.03180   0.03180   0.03180
 0.03180   0.03180   0.03180   0.03180   0.03180   0.03180   0.03180   0.03180
 0.03180   0.03180   0.03180   0.03180   0.03180   0.03180   0.03180

** COMPUTE NORMAL/CRITICAL DEPTH **
I=   1  X=  0.000  YN=  424.48  DEPN=  0.21  YC=  424.33  DEPC=  0.06  IFR= 0  ITN=  7  ITC=  7
I=   2  X=  0.004  YN=  423.53  DEPN=  0.20  YC=  423.40  DEPC=  0.06  IFR= 0  ITN=  7  ITC=  7
I=   3  X=  0.008  YN=  422.60  DEPN=  0.20  YC=  422.46  DEPC=  0.06  IFR= 0  ITN=  7  ITC=  7
I=   4  X=  0.013  YN=  421.66  DEPN=  0.20  YC=  421.53  DEPC=  0.06  IFR= 0  ITN=  8  ITC=  8
I=   5  X=  0.018  YN=  420.73  DEPN=  0.20  YC=  420.59  DEPC=  0.06  IFR= 0  ITN=  8  ITC=  8
I=   6  X=  0.022  YN=  419.79  DEPN=  0.20  YC=  419.65  DEPC=  0.06  IFR= 0  ITN=  8  ITC=  8
I=   7  X=  0.027  YN=  418.85  DEPN=  0.19  YC=  418.72  DEPC=  0.06  IFR= 0  ITN=  8  ITC=  8
I=   8  X=  0.031  YN=  417.91  DEPN=  0.20  YC=  417.78  DEPC=  0.06  IFR= 0  ITN=  8  ITC=  8
I=   9  X=  0.036  YN=  416.97  DEPN=  0.19  YC=  416.84  DEPC=  0.06  IFR= 0  ITN=  8  ITC=  8
I=  10  X=  0.040  YN=  416.03  DEPN=  0.18  YC=  415.90  DEPC=  0.06  IFR= 0  ITN=  8  ITC=  8
I=  11  X=  0.045  YN=  415.05  DEPN=  0.14  YC=  414.97  DEPC=  0.06  IFR= 0  ITN=  8  ITC=  8
I=  12  X=  0.047  YN=  414.85  DEPN=  0.15  YC=  414.76  DEPC=  0.06  IFR= 0  ITN=  8  ITC=  8
I=  13  X=  0.049  YN=  414.65  DEPN=  0.16  YC=  414.56  DEPC=  0.07  IFR= 0  ITN=  8  ITC=  8
I=  14  X=  0.051  YN=  414.45  DEPN=  0.16  YC=  414.35  DEPC=  0.07  IFR= 0  ITN=  8  ITC=  8
I=  15  X=  0.053  YN=  414.24  DEPN=  0.17  YC=  414.15  DEPC=  0.07  IFR= 0  ITN=  8  ITC=  8
I=  16  X=  0.055  YN=  414.04  DEPN=  0.17  YC=  413.94  DEPC=  0.07  IFR= 0  ITN=  8  ITC=  8
I=  17  X=  0.057  YN=  413.84  DEPN=  0.18  YC=  413.74  DEPC=  0.07  IFR= 0  ITN=  8  ITC=  8
I=  18  X=  0.059  YN=  413.64  DEPN=  0.19  YC=  413.53  DEPC=  0.08  IFR= 0  ITN=  8  ITC=  8
I=  19  X=  0.061  YN=  413.44  DEPN=  0.19  YC=  413.32  DEPC=  0.08  IFR= 0  ITN=  7  ITC=  7
I=  20  X=  0.063  YN=  413.24  DEPN=  0.20  YC=  413.12  DEPC=  0.08  IFR= 0  ITN=  7  ITC=  7
I=  21  X=  0.065  YN=  412.98  DEPN=  0.15  YC=  412.91  DEPC=  0.08  IFR= 0  ITN=  7  ITC=  7
I=  22  X=  0.067  YN=  412.78  DEPN=  0.15  YC=  412.71  DEPC=  0.08  IFR= 0  ITN=  7  ITC=  7
I=  23  X=  0.069  YN=  412.57  DEPN=  0.15  YC=  412.50  DEPC=  0.08  IFR= 0  ITN=  7  ITC=  7
I=  24  X=  0.072  YN=  412.36  DEPN=  0.15  YC=  412.29  DEPC=  0.08  IFR= 0  ITN=  7  ITC=  7
I=  25  X=  0.074  YN=  412.15  DEPN=  0.15  YC=  412.08  DEPC=  0.08  IFR= 0  ITN=  7  ITC=  7
I=  26  X=  0.076  YN=  411.94  DEPN=  0.14  YC=  411.88  DEPC=  0.08  IFR= 0  ITN=  7  ITC=  7
I=  27  X=  0.079  YN=  411.73  DEPN=  0.15  YC=  411.67  DEPC=  0.08  IFR= 0  ITN=  7  ITC=  7
I=  28  X=  0.081  YN=  411.52  DEPN=  0.14  YC=  411.46  DEPC=  0.08  IFR= 0  ITN=  7  ITC=  7
I=  29  X=  0.083  YN=  411.31  DEPN=  0.14  YC=  411.25  DEPC=  0.08  IFR= 0  ITN=  7  ITC=  7
I=  30  X=  0.086  YN=  411.11  DEPN=  0.14  YC=  411.04  DEPC=  0.08  IFR= 0  ITN=  7  ITC=  7
I=  31  X=  0.088  YN=  410.90  DEPN=  0.14  YC=  410.85  DEPC=  0.07  IFR= 0  ITN=  7  ITC=  7

        (IFR(I,J),I=1,N)
 0    0    0    0    0    0    0    0    0    0
 0    0    0    0    0    0    0    0    0    0
 0    0    0    0    0    0    0    0    0    0
 0

WATER ELEVATION AT SECTION N=  31  IS     410.90

 BACKWATER     INN= 31     YNN=    410.90     DEP=     0.14
      I= 30    QIL=     0.    YIL=    411.11    DEP=     0.14    ITB= 10
      I= 29    QIL=     0.    YIL=    411.32    DEP=     0.14    ITB= 10
      I= 28    QIL=     0.    YIL=    411.52    DEP=     0.14    ITB= 10
      I= 27    QIL=     0.    YIL=    411.73    DEP=     0.14    ITB= 10
      I= 26    QIL=     0.    YIL=    411.94    DEP=     0.15    ITB= 10
      I= 25    QIL=     0.    YIL=    412.15    DEP=     0.15    ITB= 10
      I= 24    QIL=     0.    YIL=    412.36    DEP=     0.15    ITB= 10
      I= 23    QIL=     0.    YIL=    412.57    DEP=     0.15    ITB= 10
      I= 22    QIL=     0.    YIL=    412.77    DEP=     0.15    ITB= 10
      I= 21    QIL=     0.    YIL=    412.98    DEP=     0.15    ITB= 10
      I= 20    QIL=     0.    YIL=    413.22    DEP=     0.18    ITB= 10
      I= 19    QIL=     0.    YIL=    413.45    DEP=     0.20    ITB=  9
      I= 18    QIL=     0.    YIL=    413.64    DEP=     0.18    ITB= 10
      I= 17    QIL=     0.    YIL=    413.85    DEP=     0.18    ITB= 10
      I= 16    QIL=     0.    YIL=    414.04    DEP=     0.17    ITB= 10
      I= 15    QIL=     0.    YIL=    414.25    DEP=     0.17    ITB=  9
      I= 14    QIL=     0.    YIL=    414.45    DEP=     0.16    ITB=  9
      I= 13    QIL=     0.    YIL=    414.65    DEP=     0.16    ITB=  9
      I= 12    QIL=     0.    YIL=    414.85    DEP=     0.15    ITB=  9
      I= 11    QIL=     0.    YIL=    415.05    DEP=     0.14    ITB= 10
      I= 10    QIL=     0.    YIL=    416.00    DEP=     0.15    ITB=  8
```

I=	9	QIL=	0.	YIL=	416.99	DEP=	0.21	ITB=	8
I=	8	QIL=	0.	YIL=	417.88	DEP=	0.17	ITB=	9
I=	7	QIL=	0.	YIL=	418.87	DEP=	0.22	ITB=	8
I=	6	QIL=	0.	YIL=	419.77	DEP=	0.18	ITB=	8
I=	5	QIL=	0.	YIL=	420.74	DEP=	0.22	ITB=	7
I=	4	QIL=	0.	YIL=	421.65	DEP=	0.19	ITB=	7
I=	3	QIL=	0.	YIL=	422.61	DEP=	0.22	ITB=	7
I=	2	QIL=	0.	YIL=	423.52	DEP=	0.19	ITB=	8
I=	1	QIL=	0.	YIL=	424.48	DEP=	0.21	ITB=	6

INITIAL WATER ELEVATION:

YDI FOR RIVER NO. 1

424.48224 423.52499 422.61316 421.64774 420.74176 419.76599 418.87253 417.88373
416.99387 415.99927 415.05322 414.85153 414.65051 414.44797 414.24756 414.04382
413.84546 413.63861 413.44669 413.22192 412.98352 412.77484 412.56616 412.35767
412.14914 411.94095 411.73248 411.52472 411.31607 411.10907 410.89957

WATER ELEVATION FOR LOW FILTER:

YUMN FOR RIVER 1

424.48224 423.52499 422.61316 421.64774 420.74176 419.76599 418.87253 417.88373
416.99387 415.99927 415.05322 414.85153 414.65051 414.44797 414.24756 414.04382
413.84546 413.63861 413.44669 413.22192 412.98352 412.77484 412.56616 412.35767
412.14914 411.94095 411.73248 411.52472 411.31607 411.10907 410.89957

INITIAL CONDITIONS FOR RIVER NO. 1

I	DISTANCE MILE	FLOW CFS	WSEL FT	DEPTH FT	MIN WSEL FT	BOTTOM FT
1	0.000	0.	424.482	0.212	424.482	424.270
2	0.004	0.	423.525	0.191	423.525	423.334
3	0.009	0.	422.613	0.215	422.613	422.398
4	0.013	0.	421.648	0.186	421.648	421.462
5	0.018	0.	420.742	0.216	420.742	420.526
6	0.022	0.	419.766	0.176	419.766	419.590
7	0.027	0.	418.873	0.219	418.873	418.654
8	0.031	0.	417.884	0.166	417.884	417.718
9	0.036	0.	416.994	0.212	416.994	416.782
10	0.040	0.	415.999	0.153	415.999	415.846
11	0.045	0.	415.053	0.143	415.053	414.910
12	0.047	0.	414.852	0.150	414.852	414.702
13	0.049	0.	414.651	0.157	414.651	414.494
14	0.051	0.	414.448	0.162	414.448	414.286
15	0.053	0.	414.248	0.170	414.248	414.078
16	0.055	0.	414.044	0.174	414.044	413.870
17	0.057	0.	413.845	0.183	413.845	413.662
18	0.059	0.	413.639	0.185	413.639	413.454
19	0.061	0.	413.447	0.201	413.447	413.246
20	0.063	0.	413.222	0.184	413.222	413.038
21	0.065	0.	412.984	0.154	412.984	412.830
22	0.067	0.	412.775	0.152	412.775	412.623
23	0.069	0.	412.566	0.150	412.566	412.416
24	0.072	0.	412.358	0.149	412.358	412.209
25	0.074	0.	412.149	0.147	412.149	412.002
26	0.076	0.	411.941	0.146	411.941	411.795
27	0.079	0.	411.732	0.144	411.732	411.588
28	0.081	0.	411.525	0.144	411.525	411.381
29	0.083	0.	411.316	0.142	411.316	411.174
30	0.086	0.	411.109	0.142	411.109	410.967
31	0.088	0.	410.900	0.140	410.900	410.760

INITIAL CONDITIONS AS READ IN

```
 TT =   0.00000 HRS      DTH =   0.00417 HRS      ITMX=  0

 RIVER=   1     QU(1)=      0.000     YU(1)=     424.48     QU(N)=      0.000     YU(N)=     410.90
        FRMX=   0.226  IFRMX=   21          FRMN=   0.041  IFRMN=    7
```

INITIAL CONDITIONS IMPROVED BY SOLVING UNSTEADY FLOW EQUATIONS WITH BOUNDARIES HELD CONSTANT

```
 TT =   0.00000 HRS      DTH =   0.00417 HRS      ITMX=  0

 RIVER=   1     QU(1)=      0.000     YU(1)=     424.48     QU(N)=      0.000     YU(N)=     410.90
        FRMX=   0.226  IFRMX=   21          FRMN=   0.041  IFRMN=    9

 TT =   0.00000 HRS      DTH =   0.00417 HRS      ITMX=  0

 RIVER=   1     QU(1)=      0.000     YU(1)=     424.48     QU(N)=      0.000     YU(N)=     410.90
        FRMX=   0.226  IFRMX=   21          FRMN=   0.041  IFRMN=    9

 TT =   0.00000 HRS      DTH =   0.00417 HRS      ITMX=  0

 RIVER=   1     QU(1)=      0.000     YU(1)=     424.48     QU(N)=      0.000     YU(N)=     410.90
        FRMX=   0.226  IFRMX=   21          FRMN=   0.042  IFRMN=    9

 TT =   0.00417 HRS      DTH =   0.00417 HRS      ITMX=  0

 RIVER=   1     QU(1)=      0.000     YU(1)=     424.48     QU(N)=      0.000     YU(N)=     410.90
        FRMX=   0.226  IFRMX=   21          FRMN=   0.041  IFRMN=    9

 TT =   0.00833 HRS      DTH =   0.00417 HRS      ITMX=  0

 RIVER=   1     QU(1)=      0.000     YU(1)=     424.48     QU(N)=      0.000     YU(N)=     410.90
        FRMX=   0.226  IFRMX=   21          FRMN=   0.042  IFRMN=    9
.
.
.
.
 TT =   3.99991 HRS      DTH =   0.00417 HRS      ITMX=  0

 RIVER=   1     QU(1)=      0.000     YU(1)=     424.48     QU(N)=      0.000     YU(N)=     410.93
        FRMX=   0.231  IFRMX=   29          FRMN=   0.043  IFRMN=    7
```

TOTAL INFLOW (1000 CF)		TOTAL OUTFLOW (1000 CF)		TOTAL VOLUME	CONTINUITY ERROR
RIVER	TRIBUTARIES	RIVER	TRIBUTARIES	CHANGE(1000 CUFT)	(PERCENT)
0.98	0.00	1.01	0.00	0.02	-4.97

TOTAL VOLUME/ACTIVE VOLUME CHANGE (%) OF RIVER 1 = 3.20 6.04

TOTAL ITERATIONS FOR EACH OF 1 RIVERS.
79

TOTAL TIME= 4.00 TOTAL NO. OF TIME STEPS: KTIME= 49 NUMTIM= 961

PROFILE OF CRESTS AND TIMES
* ORIGINAL CRESS-SECTION
\# PEAK STAGE EXCEEDED MAX HS

RVR NO.	SEC NO.	LOCATION MILE	BOTTOM FEET	TIME MAX WSEL(HR)	MAX WSEL FEET	TIME MAX FLOW(CFS)	MAX FLOW CFS	MAX VL (FPS)	MAX VC (FPS)	MAX VR (FPS)
1	1*	0.000	424.27	1.49976	424.63	1.49976	0.2632	0.0000	0.1881	0.0000
1	2	0.004	423.33	1.52476	423.74	1.52476	0.2563	0.0000	0.1948	0.0000
1	3	0.009	422.40	1.55392	422.80	1.54975	0.2544	0.0000	0.2006	0.0000
1	4	0.013	421.46	1.57892	421.85	1.57475	0.2527	0.0000	0.2132	0.0000
1	5	0.018	420.53	1.61641	420.91	1.59558	0.2517	0.0000	0.2167	0.0000
1	6	0.022	419.59	1.65390	419.96	1.61641	0.2502	0.0000	0.2360	0.0000
1	7	0.027	418.65	1.70390	419.04	1.64557	0.2488	0.0000	0.2276	0.0000
1	8	0.031	417.72	1.65807	418.07	1.67057	0.2460	0.0000	0.2537	0.0000
1	9	0.036	416.78	1.71639	417.16	1.69556	0.2434	7.9230	-0.3198	7.9230
1	10	0.040	415.85	1.66307	416.24	1.71639	0.2438	0.0000	0.3581	0.0000
1	11*	0.045	414.91	1.73306	415.21	1.72889	0.2444	0.0000	0.3788	0.0000
1	12	0.047	414.70	1.73722	415.01	1.73722	0.2442	0.0000	0.3818	0.0000
1	13	0.049	414.49	1.74556	414.81	1.74139	0.2438	0.0000	0.3847	0.0000
1	14	0.051	414.29	1.74972	414.62	1.74972	0.2433	0.0000	0.3838	0.0000
1	15	0.053	414.08	1.75389	414.42	1.75389	0.2429	0.0000	0.3855	0.0000
1	16	0.055	413.87	1.75805	414.22	1.76222	0.2426	0.0000	0.3907	0.0000
1	17	0.057	413.66	1.76639	414.03	1.76639	0.2421	0.0000	0.3996	0.0000
1	18	0.059	413.45	1.77472	413.83	1.77055	0.2414	0.0000	0.3985	0.0000
1	19	0.061	413.25	1.77888	413.64	1.77888	0.2411	0.0000	0.3976	0.0000
1	20	0.063	413.04	1.78305	413.43	1.78305	0.2406	0.0000	0.4790	0.0000
1	21*	0.065	412.83	1.78722	413.15	1.78305	0.2405	0.0000	0.6420	0.0000
1	22	0.067	412.62	1.78722	412.94	1.78722	0.2404	0.0000	0.6298	0.0000
1	23	0.069	412.42	1.79138	412.73	1.79555	0.2402	0.0000	0.6170	0.0000
1	24	0.072	412.21	1.79971	412.52	1.79138	0.2401	0.0000	0.6064	0.0000
1	25	0.074	412.00	1.79555	412.31	1.79971	0.2402	0.0000	0.5935	0.0000
1	26	0.076	411.80	1.80388	412.10	1.80388	0.2398	0.0000	0.5826	0.0000
1	27	0.079	411.59	1.81221	411.90	1.81221	0.2392	0.0000	0.5718	0.0000
1	28	0.081	411.38	1.81638	411.69	1.81638	0.2386	0.0000	0.5658	0.0000
1	29	0.083	411.17	1.82888	411.48	1.82471	0.2374	0.0000	0.5599	0.0000
1	30	0.086	410.97	1.83304	411.27	1.83304	0.2359	0.0000	0.5543	0.0000
1	31*	0.088	410.76	1.84137	411.06	1.84137	0.2350	0.0000	0.5544	0.0000

KTIME	TII(KTIME)	COMPUTED STAGES FOR RIVER= 1 SECTION=	1	11	21	31
1	0.000	424.48223877	415.05340576	412.98358154	410.9[illegible]0121460	
2	0.083	424.48223877	415.05410767	412.98361206	410.9[illegible]0145874	
3	0.167	424.48223877	415.05435181	412.98480225	410.9[illegible]0145874	
4	0.250	424.48223877	415.05422974	412.98489380	410.9[illegible]0182495	
5	0.333	424.48223877	415.05404663	412.98498535	410.9[illegible]0203857	
6	0.417	424.48223877	415.05413818	412.98471069	410.9[illegible]0216064	
7	0.500	424.48223877	415.05401611	412.98486328	410.9[illegible]0200806	
8	0.583	424.48223877	415.05444336	412.98477173	410.9[illegible]0200806	
9	0.666	424.48223877	415.05505371	412.98483276	410.9[illegible]0194702	
10	0.750	424.48223877	415.05578613	412.98538208	410.9[illegible]0203857	
11	0.833	424.48223877	415.05621338	412.98629761	410.9[illegible]0264893	
12	0.916	424.48223877	415.05633545	412.98712158	410.9[illegible]0353394	
13	1.000	424.48223877	415.05670166	412.98736572	410.9[illegible]0441895	
14	1.083	424.48501587	415.05673218	412.98776245	410.9[illegible]0463257	
15	1.166	424.48815918	415.05664062	412.98797607	410.9[illegible]0493774	
16	1.250	424.49124146	415.05618286	412.98797607	410.9[illegible]0512085	
17	1.333	424.59292603	415.05615234	412.98791504	410.9[illegible]0512085	
18	1.416	424.65646362	415.05331421	412.98666382	410.9[illegible]0505981	
19	1.499	424.68817139	415.05572510	412.98712158	410.9[illegible]0441895	
20	1.583	424.67141724	415.05322266	412.98794556	410.9[illegible]0454102	
21	1.666	424.65075684	415.07180786	412.99383545	410.9[illegible]0457153	
22	1.749	424.63137817	415.20611572	413.10522461	410.9[illegible]0728760	
23	1.833	424.61370850	415.18692017	413.14111328	411.0[illegible]422974	
24	1.916	424.59692383	415.17102051	413.12899780	411.0[illegible]776001	
25	1.999	424.57928467	415.15597534	413.11837769	411.0[illegible]186035	
26	2.082	424.57455444	415.14328003	413.10223389	411.01[illegible]800537	
27	2.166	424.57110596	415.13372803	413.08911133	411.00[illegible]329590	
28	2.249	424.56762695	415.12332153	413.07943726	410.99[illegible]508667	
29	2.332	424.56552124	415.11541748	413.06945801	410.98[illegible]809814	
30	2.416	424.56323242	415.11163330	413.06158447	410.97[illegible]845459	

31	2.499	424.56103516	415.10848999	413.05761719	410.97009277
32	2.582	424.55899048	415.10592651	413.05413818	410.96572876
33	2.666	424.55697632	415.10375977	413.05123901	410.96194458
34	2.749	424.55502319	415.10244751	413.04794312	410.95895386
35	2.832	424.55313110	415.10125732	413.04598999	410.95663452
36	2.916	424.55130005	415.10034180	413.04434204	410.95526123
37	2.999	424.54946899	415.09939575	413.04296875	410.95401001
38	3.082	424.54922485	415.09829712	413.04168701	410.95297241
39	3.165	424.54904175	415.09692383	413.04031372	410.95202637
40	3.249	424.54888916	415.09573364	413.03878784	410.95092773
41	3.332	424.48822021	415.09805298	413.03726196	410.94982910
42	3.415	424.48947144	415.09725952	413.03768921	410.94888306
43	3.499	424.48718262	415.08569336	413.03707886	410.94827271
44	3.582	424.49099731	415.10052490	413.02780151	410.94866943
45	3.665	424.48944092	415.09524536	413.04205322	410.94256592
46	3.749	424.48739624	415.08392334	413.03729248	410.95220947
47	3.832	424.48535156	415.07424927	413.02584839	410.94815063
48	3.915	424.48379517	415.06695557	413.01483154	410.94015503
49	3.998	424.48321533	415.06317139	413.00521851	410.92797852

KTIME	TII(KTIME)	COMPUTED DISCHARGE FOR RIVER= 1 SECTION=	1	11	21	31
1	0.000	0.03180000	0.03203979	0.03180854	0.03204552	
2	0.083	0.03180000	0.03250651	0.03184777	0.03218579	
3	0.167	0.03180000	0.03266372	0.03254285	0.03218883	
4	0.250	0.03180000	0.03258393	0.03259371	0.03243386	
5	0.333	0.03180000	0.03245726	0.03262788	0.03254515	
6	0.417	0.03180000	0.03252985	0.03248163	0.03260616	
7	0.500	0.03180000	0.03241925	0.03258150	0.03251398	
8	0.583	0.03180000	0.03275009	0.03252158	0.03251356	
9	0.666	0.03180000	0.03321439	0.03255020	0.03249895	
10	0.750	0.03180000	0.03376783	0.03288781	0.03254836	
11	0.833	0.03180000	0.03405721	0.03342075	0.03286410	
12	0.916	0.03180000	0.03415414	0.03390675	0.03333937	
13	1.000	0.03180000	0.03441971	0.03405043	0.03382928	
14	1.083	0.03329220	0.03443146	0.03428568	0.03401678	
15	1.166	0.03479160	0.03436494	0.03439970	0.03424222	
16	1.250	0.03629100	0.03401273	0.03440822	0.03438719	
17	1.333	0.11151554	0.03409943	0.03437288	0.03438726	
18	1.416	0.18718527	0.03200267	0.03362034	0.03434838	
19	1.499	0.26285499	0.03347719	0.03385432	0.03381214	
20	1.583	0.21953590	0.03180000	0.03443910	0.03392460	
21	1.666	0.17535359	0.05149367	0.03783369	0.03398385	
22	1.749	0.13117127	0.24141918	0.16031146	0.03622576	
23	1.833	0.11616328	0.20699315	0.22723395	0.23289265	
24	1.916	0.10140252	0.17945977	0.19209523	0.21470658	
25	1.999	0.08664176	0.15194309	0.17142257	0.18575144	
26	2.082	0.08395900	0.13241610	0.14466287	0.16336372	
27	2.166	0.08139336	0.11986856	0.12885648	0.13986881	
28	2.249	0.07882772	0.10621671	0.11701380	0.12669420	
29	2.332	0.07758047	0.09593499	0.10477010	0.11519313	
30	2.416	0.07634763	0.09091335	0.09515301	0.10328253	
31	2.499	0.07511479	0.08655296	0.09031208	0.09421530	
32	2.582	0.07391487	0.08299308	0.08604454	0.08940938	
33	2.666	0.07271535	0.07999594	0.08265691	0.08527579	
34	2.749	0.07151583	0.07841574	0.07977466	0.08199376	
35	2.832	0.07034919	0.07692945	0.07818997	0.07946151	
36	2.916	0.06918299	0.07579909	0.07678096	0.07796496	
37	2.999	0.06801679	0.07468212	0.07562802	0.07658123	
38	3.082	0.06800000	0.07354939	0.07457205	0.07543959	
39	3.165	0.06800000	0.07221717	0.07336840	0.07439233	
40	3.249	0.06800000	0.07105020	0.07210346	0.07319969	
41	3.332	0.03180000	0.07374767	0.07077636	0.07197772	
42	3.415	0.03180000	0.07298393	0.07125930	0.07095671	

43	3.499	0.03180000	0.06094920	0.07090411	0.07024091
44	3.582	0.03180000	0.07631940	0.06276899	0.07079626
45	3.665	0.03180000	0.07037183	0.07504055	0.06396312
46	3.749	0.03180000	0.05906069	0.07069998	0.07467164
47	3.832	0.03180000	0.04945311	0.06109414	0.07002667
48	3.915	0.03180000	0.04204746	0.05180875	0.06109163
49	3.998	0.03180000	0.03892675	0.04440961	0.05151887

KTIME TII(KTIME) COMPUTED VELOCITY (FT/SEC) FOR RIVER= 1 SECTION= 1 11 21 31

1	0.000	0.08751680	0.16116999	0.35547400	0.33215079
2	0.083	0.08751680	0.16192888	0.35577181	0.33245400
3	0.167	0.08751680	0.16216038	0.35796785	0.33248574
4	0.250	0.08751680	0.16203949	0.35810292	0.33328915
5	0.333	0.08751680	0.16182332	0.35804898	0.33342594
6	0.417	0.08751680	0.16197668	0.35771376	0.33348012
7	0.500	0.08751680	0.16169715	0.35811371	0.33325031
8	0.583	0.08751680	0.16238868	0.35787624	0.33324614
9	0.666	0.08751680	0.16331284	0.35791135	0.33338141
10	0.750	0.08751680	0.16437173	0.35908026	0.33346441
11	0.833	0.08751680	0.16480105	0.36063799	0.33382702
12	0.916	0.08751680	0.16500121	0.36204433	0.33450213
13	1.000	0.08751680	0.16545425	0.36246237	0.33526367
14	1.083	0.08928473	0.16544612	0.36313459	0.33611807
15	1.166	0.09063702	0.16533354	0.36332375	0.33691397
16	1.250	0.09192772	0.16463745	0.36343247	0.33749112
17	1.333	0.13267088	0.16523024	0.36335748	0.33749196
18	1.416	0.15553427	0.16128039	0.36099771	0.33739027
19	1.499	0.18805698	0.16298285	0.36146581	0.33504468
20	1.583	0.16930656	0.16037309	0.36388925	0.33556575
21	1.666	0.14981817	0.20731372	0.37128949	0.33617213
22	1.749	0.12443553	0.37640309	0.55860329	0.34562922
23	1.833	0.12188692	0.35332900	0.62150544	0.55613685
24	1.916	0.11759174	0.33255938	0.56671405	0.53581792
25	1.999	0.11224476	0.30622429	0.54321283	0.51944286
26	2.082	0.11222043	0.28844681	0.51456350	0.50703520
27	2.166	0.11129613	0.27783415	0.50585049	0.48826623
28	2.249	0.11032123	0.26471528	0.49566686	0.47368997
29	2.332	0.11014004	0.25355330	0.48157236	0.45751116
30	2.416	0.11008801	0.24755126	0.46758467	0.44722641
31	2.499	0.10992843	0.24166414	0.45948532	0.44110146
32	2.582	0.10970820	0.23660150	0.45148814	0.43659180
33	2.666	0.10947074	0.23225464	0.44521508	0.43218046
34	2.749	0.10912162	0.23021576	0.44272575	0.42814341
35	2.832	0.10878071	0.22812256	0.44178650	0.42467970
36	2.916	0.10837397	0.22657956	0.44052771	0.42258698
37	2.999	0.10797075	0.22509885	0.43949533	0.42048213
38	3.082	0.10812479	0.22386056	0.43865430	0.41877362
39	3.165	0.10826674	0.22247213	0.43730739	0.41694349
40	3.249	0.10838524	0.22122641	0.43595117	0.41496301
41	3.332	0.08273880	0.22494271	0.43425885	0.41277668
42	3.415	0.08182115	0.22426581	0.43545714	0.41104525
43	3.499	0.08357795	0.20874883	0.43596128	0.40950111
44	3.582	0.08071768	0.22791755	0.42282423	0.41116902
45	3.665	0.08188944	0.21999030	0.43989432	0.39656568
46	3.749	0.08343722	0.20567569	0.43360698	0.41782084
47	3.832	0.08502930	0.19091928	0.41967621	0.40878689
48	3.915	0.08624728	0.17680344	0.39961642	0.38883600
49	3.998	0.08671699	0.17168276	0.38129604	0.37731960

KTIME	TII(KTIME)	COMPUTED DISTANCES (FT) FOR RIVER= 1 SECTION= 1	11	21	31
1	0.000	0.00000000	235.65988159	105.78038788	123.29138184
2	0.083	0.00000000	235.65988159	105.78038788	123.29138184
3	0.167	0.00000000	235.65988159	105.78038788	123.29138184
4	0.250	0.00000000	235.65988159	105.78038788	123.29138184
5	0.333	0.00000000	235.65988159	105.78038788	123.29138184
6	0.417	0.00000000	235.65988159	105.78038788	123.29138184
7	0.500	0.00000000	235.65988159	105.78038788	123.29138184
8	0.583	0.00000000	235.65988159	105.78038788	123.29138184
9	0.666	0.00000000	235.65988159	105.78038788	123.29138184
10	0.750	0.00000000	235.65988159	105.78038788	123.29138184
11	0.833	0.00000000	235.65988159	105.78038788	123.29138184
12	0.916	0.00000000	235.65988159	105.78038788	123.29138184
13	1.000	0.00000000	235.65988159	105.78038788	123.29138184
14	1.083	0.00000000	235.65988159	105.78038788	123.29138184
15	1.166	0.00000000	235.65988159	105.78038788	123.29138184
16	1.250	0.00000000	235.65988159	105.78038788	123.29138184
17	1.333	0.00000000	235.65988159	105.78038788	123.29138184
18	1.416	0.00000000	235.65988159	105.78038788	123.29138184
19	1.499	0.00000000	235.65988159	105.78038788	123.29138184
20	1.583	0.00000000	235.65988159	105.78038788	123.29138184
21	1.666	0.00000000	235.65988159	105.78038788	123.29138184
22	1.749	0.00000000	235.65988159	105.78038788	123.29138184
23	1.833	0.00000000	235.65988159	105.78038788	123.29138184
24	1.916	0.00000000	235.65988159	105.78038788	123.29138184
25	1.999	0.00000000	235.65988159	105.78038788	123.29138184
26	2.082	0.00000000	235.65988159	105.78038788	123.29138184
27	2.166	0.00000000	235.65988159	105.78038788	123.29138184
28	2.249	0.00000000	235.65988159	105.78038788	123.29138184
29	2.332	0.00000000	235.65988159	105.78038788	123.29138184
30	2.416	0.00000000	235.65988159	105.78038788	123.29138184
31	2.499	0.00000000	235.65988159	105.78038788	123.29138184
32	2.582	0.00000000	235.65988159	105.78038788	123.29138184
33	2.666	0.00000000	235.65988159	105.78038788	123.29138184
34	2.749	0.00000000	235.65988159	105.78038788	123.29138184
35	2.832	0.00000000	235.65988159	105.78038788	123.29138184
36	2.916	0.00000000	235.65988159	105.78038788	123.29138184
37	2.999	0.00000000	235.65988159	105.78038788	123.29138184
38	3.082	0.00000000	235.65988159	105.78038788	123.29138184
39	3.165	0.00000000	235.65988159	105.78038788	123.29138184
40	3.249	0.00000000	235.65988159	105.78038788	123.29138184
41	3.332	0.00000000	235.65988159	105.78038788	123.29138184
42	3.415	0.00000000	235.65988159	105.78038788	123.29138184
43	3.499	0.00000000	235.65988159	105.78038788	123.29138184
44	3.582	0.00000000	235.65988159	105.78038788	123.29138184
45	3.665	0.00000000	235.65988159	105.78038788	123.29138184
46	3.749	0.00000000	235.65988159	105.78038788	123.29138184
47	3.832	0.00000000	235.65988159	105.78038788	123.29138184
48	3.915	0.00000000	235.65988159	105.78038788	123.29138184
49	3.998	0.00000000	235.65988159	105.78038788	123.29138184

KTIME	TII(KTIME)	RETENTION TIMES (MIN) FOR RIVER= 1 SECTION= 1	11	21	31
1	0.000	0.00000000	24.36970139	4.95959330	6.18651676
2	0.083	0.00000000	24.25549316	4.95544147	6.18087435
3	0.167	0.00000000	24.22086525	4.92504120	6.18028450
4	0.250	0.00000000	24.23893547	4.92318392	6.16538620
5	0.333	0.00000000	24.27131462	4.92392540	6.16285706
6	0.417	0.00000000	24.24833488	4.92853975	6.16185570
7	0.500	0.00000000	24.29025269	4.92303562	6.16610479
8	0.583	0.00000000	24.18681335	4.92630196	6.16618204
9	0.666	0.00000000	24.04994392	4.92581892	6.16368008
10	0.750	0.00000000	23.89501381	4.90978384	6.16214609
11	0.833	0.00000000	23.83276558	4.88857651	6.15545273

12	0.916	0.00000000	23.80385399	4.86958742	6.14302921
13	1.000	0.00000000	23.73867416	4.86397123	6.12907553
14	1.083	0.00000000	23.73984146	4.85496712	6.11349583
15	1.166	0.00000000	23.75600624	4.85243940	6.09905338
16	1.250	0.00000000	23.85644722	4.85098791	6.08862352
17	1.333	0.00000000	23.77085876	4.85198879	6.08860826
18	1.416	0.00000000	24.35301971	4.88370562	6.09044361
19	1.499	0.00000000	24.09863853	4.87738085	6.13308144
20	1.583	0.00000000	24.49079704	4.84489870	6.12355804
21	1.666	0.00000000	18.94551277	4.74833393	6.11251259
22	1.749	0.00000000	10.43473053	3.15609765	5.94526243
23	1.833	0.00000000	11.11616802	2.83667111	3.69487548
24	1.916	0.00000000	11.81041622	3.11092782	3.83499002
25	1.999	0.00000000	12.82610416	3.24551702	3.95588541
26	2.082	0.00000000	13.61659908	3.42621756	4.05269003
27	2.166	0.00000000	14.13672447	3.48523235	4.20847511
28	2.249	0.00000000	14.83731747	3.55683756	4.33797741
29	2.332	0.00000000	15.49048901	3.66093779	4.49137974
30	2.416	0.00000000	15.86606598	3.77045393	4.59466696
31	2.499	0.00000000	16.25257492	3.83691573	4.65846634
32	2.582	0.00000000	16.60033798	3.90487885	4.70658493
33	2.666	0.00000000	16.91102791	3.95989847	4.75462580
34	2.749	0.00000000	17.06079865	3.98216391	4.79945803
35	2.832	0.00000000	17.21734428	3.99062991	4.83860302
36	2.916	0.00000000	17.33459473	4.00203323	4.86256456
37	2.999	0.00000000	17.44862175	4.01143408	4.88690519
38	3.082	0.00000000	17.54513931	4.01912498	4.90684271
39	3.165	0.00000000	17.65463638	4.03150415	4.92838097
40	3.249	0.00000000	17.75404930	4.04404593	4.95190239
41	3.332	0.00000000	17.46073341	4.05980539	4.97813082
42	3.415	0.00000000	17.51343536	4.04863358	4.99910021
43	3.499	0.00000000	18.81526566	4.04395199	5.01795053
44	3.582	0.00000000	17.23283195	4.16959667	4.99759531
45	3.665	0.00000000	17.85380936	4.00779533	5.18162918
46	3.749	0.00000000	19.09639740	4.06590891	4.91803217
47	3.832	0.00000000	20.57238388	4.20087290	5.02671766
48	3.915	0.00000000	22.21486664	4.41174698	5.28463507
49	3.998	0.00000000	22.87745476	4.62372112	5.44593048

A.5. DYNAWET Calibration

The following figures present the results from the calibration runs for the four events used. Based on these figures, the model was able to be calibrated so that the simulations replicated the actual observations closely.

A.5.1. Leaf-off Calibration results

The results of the calibration for the leaf-off events are presented in Figures A.6a,b,c and A.7a,b,c. For site MBF, the model closely matched the observed data for most of the event. The error for both events was less than 0.050 feet. Results for site MBW1 indicated an under-prediction error (not exceeding 0.100 feet) for the receding limb of the March 9, 1998 event and a slight over-prediction for the April 19, 1998 event. Site MBW2 indicated an under prediction for the rising limb of the March 9, 1998 event (not exceeding 0.100 feet) and a slight delay in the simulated data for the April 19, 1998 event.

A.5.2. Leaf-on Calibration results

The results of the calibration for the leaf-on events are presented in Figures A.8a,b,c and A.9a,b,c. The simulated data closely matched the observed data within 0.025 feet for site MBF. Site MBW1 stage was under-predicted (not exceeding 0.050 feet) during the rising and receding limbs during channel flow conditions for the July 5,1998 event, but over-predicted (not exceeding 0.075 feet) these portions of the hydrograph for the August 26,1998 event. For site MBW2, the data matched closely (within 0.050 feet) for the leaf-on calibration but over-predicted for the beginning and end of the hydrograph for the July 5, 1998 event.

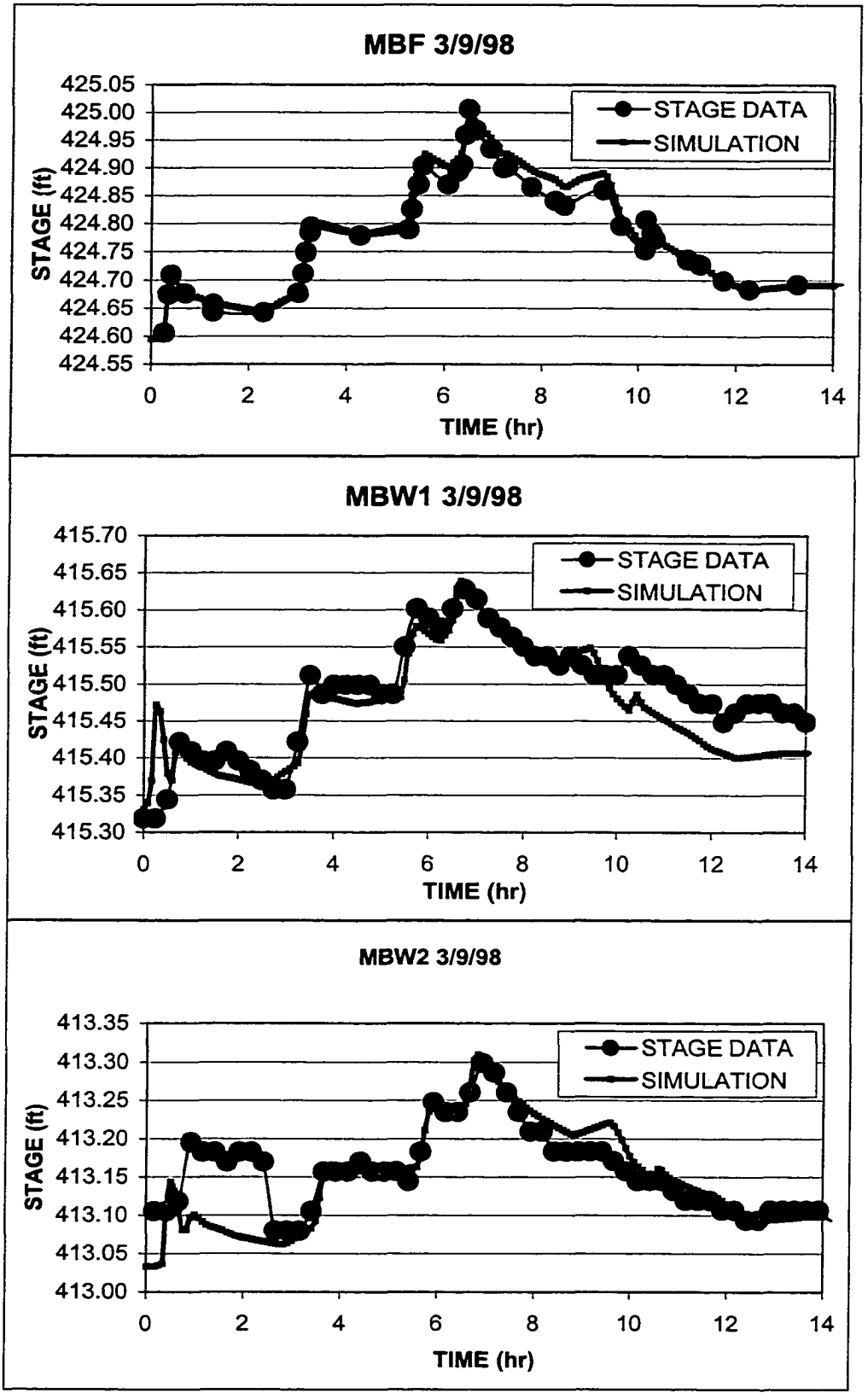

Figures A.6 a,b,c. Plots of simulation and stage data at each monitoring station for peak leaf-off storm event calibration on 3/9/98.

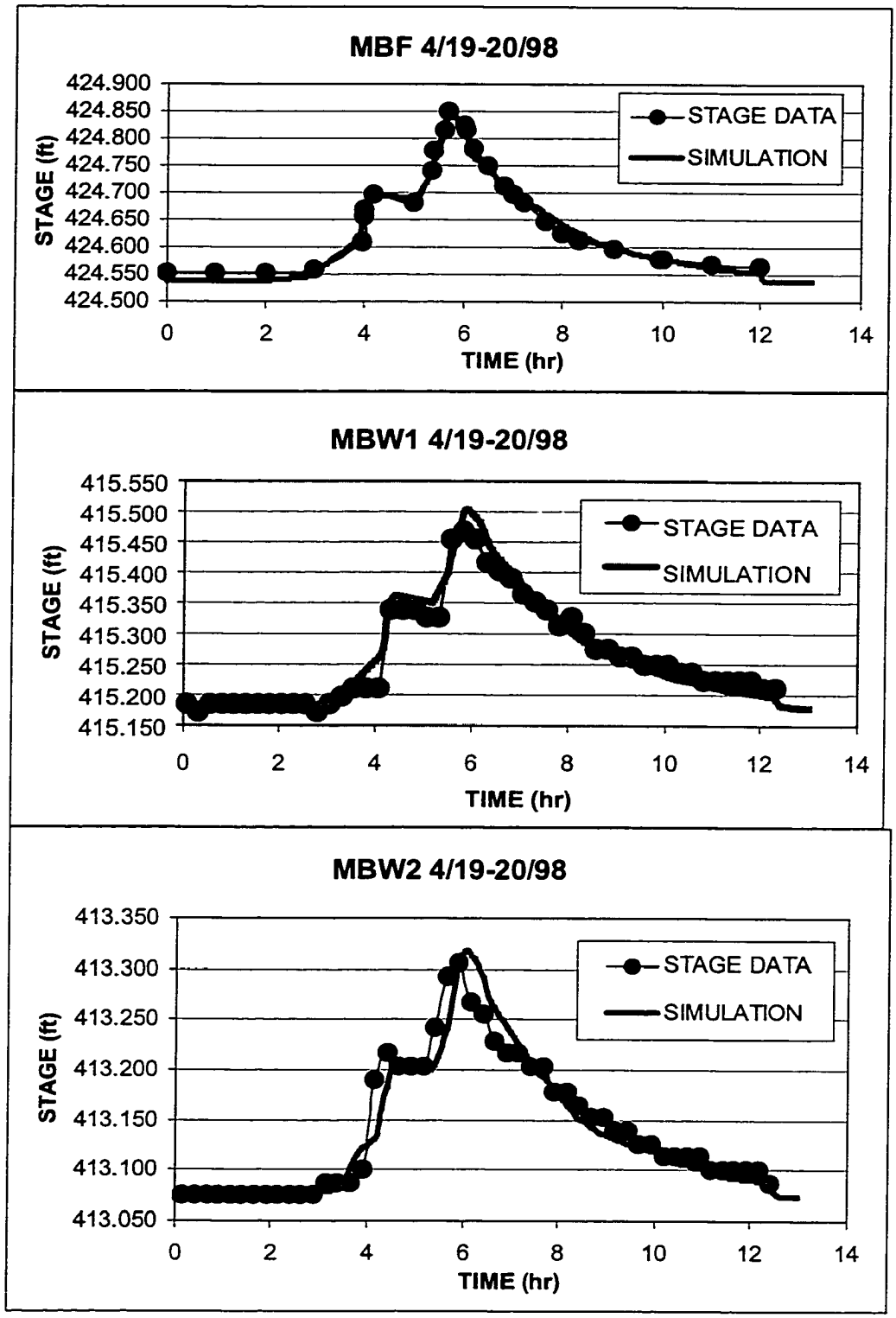

Figures A.7 a,b,c. Plots of simulation and stage data at each monitoring station for low leaf-off storm event calibration on 4/19-20/98

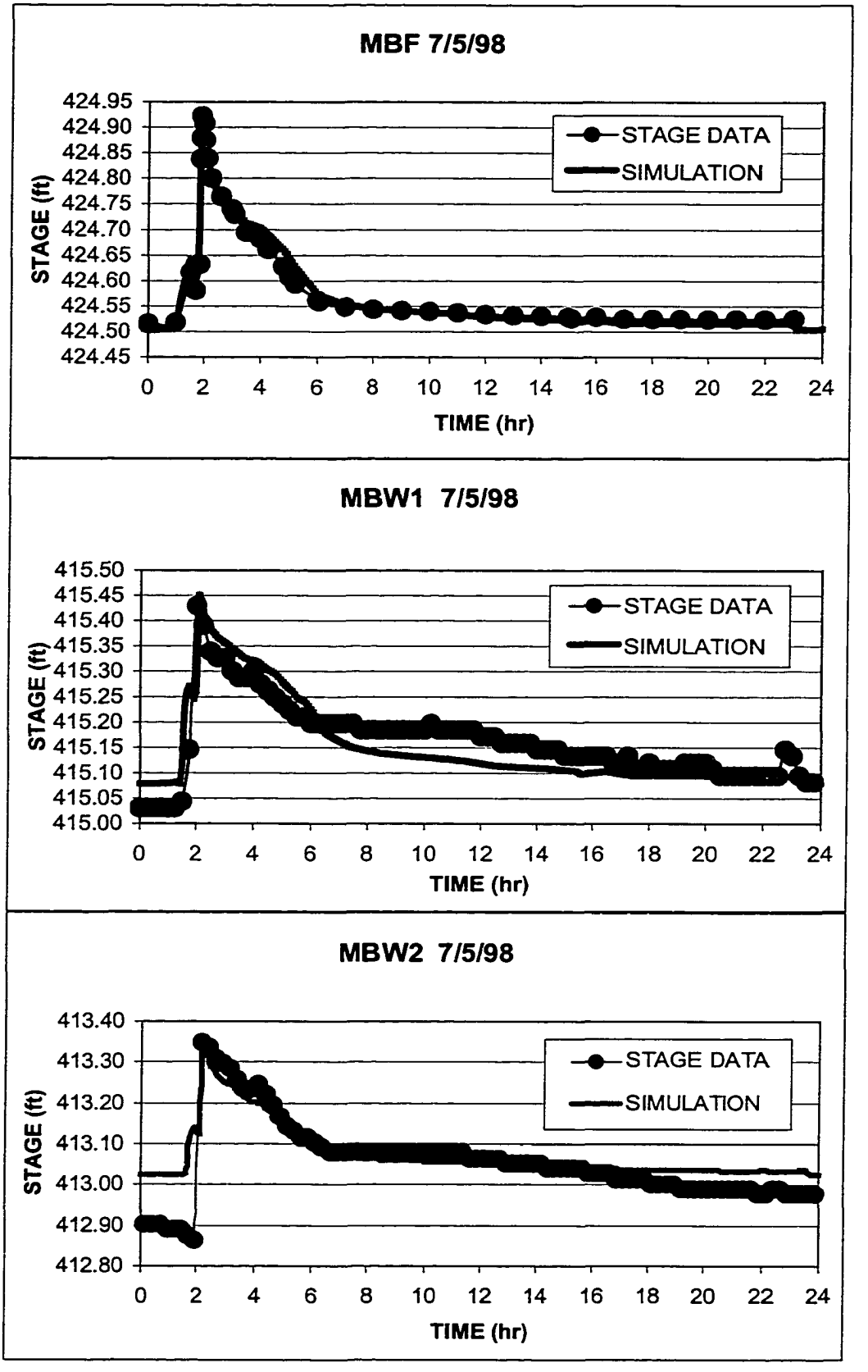

Figures A.8 a,b,c. Plots of simulation and stage data at each monitoring station for peak leaf-on storm event calibration on 7/5/98

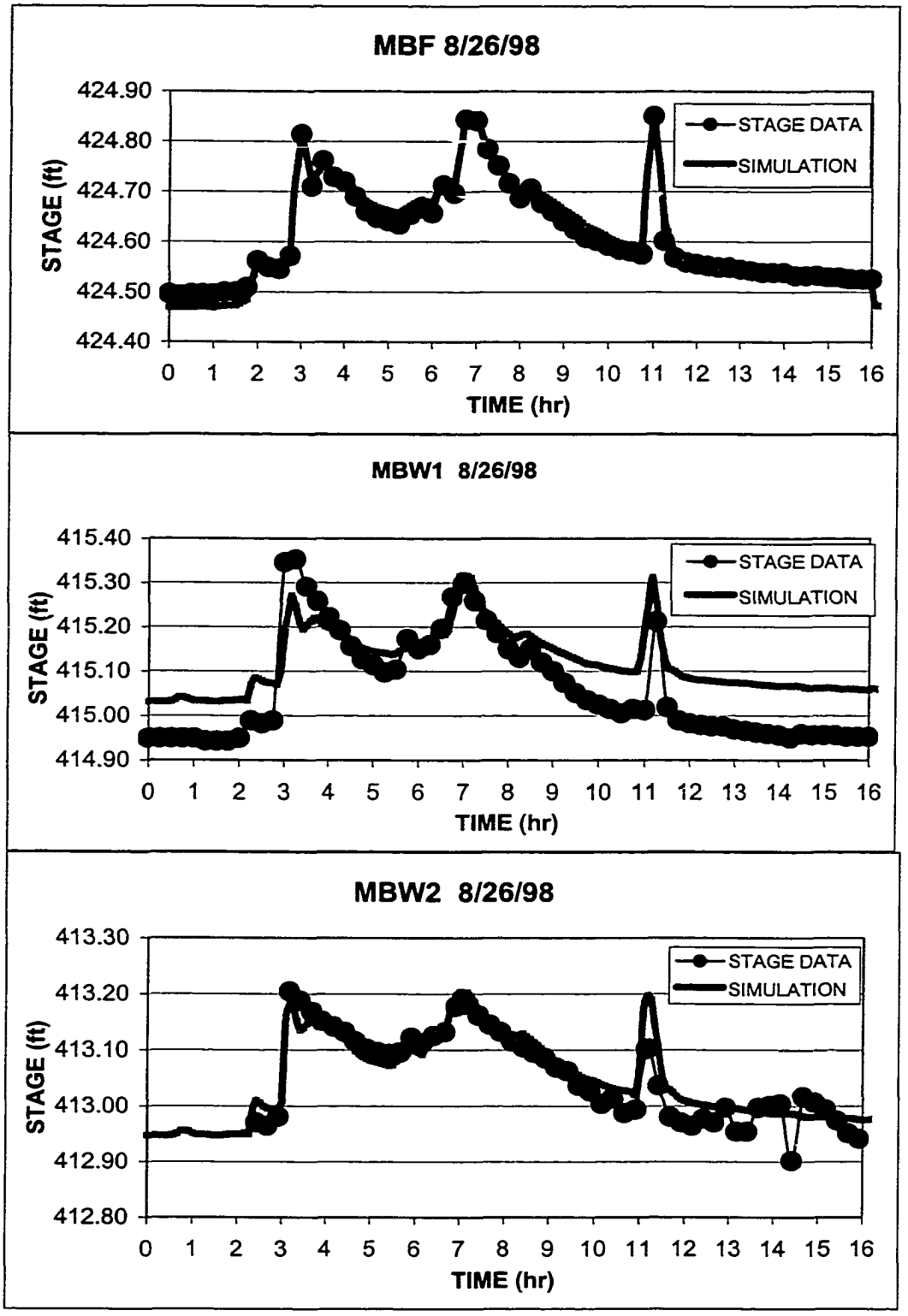

Figures A.9 a,b,c. Plots of simulation and stage data at each monitoring station for low leaf-on storm event calibration on 8/26/98.

A.6. Wetland Particle Model Program

The following Fortran code represents the Wetland Particle Model. Comments are incorporated to provide reference to the program's construction.

PROGRAM MAIN

```
PROGRAM MAIN

CC      **********************************************************************
CC      **********************************************************************
CC       PARTICLE MODEL FOR USE WITH
CC      DYNAMIC ROUTING MODEL (DYNAWET)
CC      FOR NATURALLY OCCURRING WETLANDS
C
C       THE PARTICLE TRANSPORT IS DETERMINED AT VARIOUS LOCATIONS AND TIMES
C       ALONG A ONE DIMENSIONAL WETLAND WITH THE USE OF EQUATIONS THAT
C       SIMULATE A PLUG FLOW REACTOR ALONG WITH A SERIES OF CONTINUOUSLY
C       STIRRED REACTORS.
C
C       DEVELOPED BY DAVID A. STERN
C               JANUARY 2000

CC      **********************************************************************
CC      **********************************************************************

        DIMENSION C(1000,1000),CI(1000,1000),T(1000,1000)
        DIMENSION PORT(1000),TC(1000),TP(1000),CIN(1000),CE(1000)

        PRINT 1
        WRITE (IPR,1)
    1   FORMAT(17X,'PARTICLE MODEL FOR USE WITH'/,
        .16X,'DYNAMIC ROUTING MODEL (DYNAWET)'/,
        .15X,'FOR NATURALLY OCCURRING WETLANDS'///)

CC      ************ OPEN INPUT AND OUTPUT FILES ************************
        IN=155
        IPR=165

        OPEN(IN,FILE='IN.TXT',STATUS='OLD')
        OPEN(IPR,FILE='OUT.TXT')

CC      ************ WRITE STARTING TIME AND DATE **********************
        CALL GETDAT(IYR,IMON,IDAY)
        CALL GETTIM(IHR1,IMIN1,ISEC1,I100TH)
```

```
      WRITE(*,90)
 90   FORMAT(1X,'*****************************************')
      WRITE(*,91) IMON,IDAY,IYR,IHR1,IMIN1,ISEC1
 91   FORMAT(1X,'MODEL RUN START TIME: 'I2,'/',I2.2,'/',I4.4,
      .2X,I2.2,1H:,I2.2,1H:,I2.2)
CC    ***********************************************************************

      PRINT 2
      WRITE (IPR,2)
  2   FORMAT(//5X,'************ ECHO OF INPUT DATA ************'/,
      .'*************************************************************'/)


CC    ***********************************************************************
CC    ************** READ IN INPUT DATA *********************************
CC    ***********************************************************************

CC    ********** READ IN INTEGER INPUT PARAMETERS ******************
      READ(IN,10) NT,NX
10    FORMAT(2I5)
      PRINT 15,NT,NX
      WRITE(IPR,15) NT,NX
 15   FORMAT(/'TOTAL TIME STEPS =',I5,/'TOTAL SEGMENTS =',2X,I5/)

CC    ********** READ IN REAL NUMBER INPUT PARAMETERS *************
      READ(IN,20) RKP,RKC
20    FORMAT(2F10.6)
      PRINT 25,RKP,RKC
      WRITE(IPR,25) RKP,RKC
 25   FORMAT(/F10.4,5X,'= PLUG FLOW REDUCTION RATE',/
      .F10.4,5X,'= CONTINUOUS STIRRED TANK REACTOR REDUCTION RATE',/)

CC    ********** READ INPUT CONCENTRATION ARRAY ********************
      PRINT 31
      WRITE(IPR,31)
 31   FORMAT(/1X,'TIME STEP',5X,'INPUT CONCENTRATION')

   DO 30 JJ=1,NT
      READ (IN,21) CIN(JJ)
21    FORMAT(F15.3)
      PRINT 32, JJ,CIN(JJ)
      WRITE(IPR,32) JJ,CIN(JJ)
 32   FORMAT(I5,5X,F15.3)
 30   CONTINUE

CC    ********** READ IN INPUT ARRAYS *********************************
      DO 60 K=1,NX
      READ (IN,34) PORT(K),TC(K),TP(K)
34    FORMAT(3F10.6)
      PRINT 35, K,PORT(K),TC(K),TP(K)
      WRITE(IPR,35) K, PORT(K),TC(K),TP(K)
```

```
 35     FORMAT(/1X,'SEGMENT NUMBER: ',I5,
        ./F10.4,5X,'= PROPORTION PFR',
        ./F10.4,5X,'= CSTR CENTROID TIME',
        ./F10.4,5X,'= CSTR PEAK TIME'/)

CC      ******** READ IN RETENTION TIMES FROM DYNAWET ***************
        READ (IN,50) (T(K,L),L=1,NT)
50      FORMAT(F10.6)
        DO 42 LL=1,NT
        PRINT 45, LL,T(K,LL)
        WRITE(IPR,45) LL,T(K,LL)
 45     FORMAT(1X,'TIME STEP ='I5,5X,'RETENTION TIME =',F10.4)
42      CONTINUE
60      CONTINUE

CC      ***********************************************************
CC      ***********************************************************
        PRINT 3
        WRITE (IPR,3)
 3      FORMAT(//5X,'************ OUTPUT DATA ************'/,
        .'************************************************************'/,
        . 'TIME STEP'3X,'SEGMENT',5X,'CONCENTRATION',2X,'# OF CSTRS')

CC      ***********************************************************
CC      ***************** CALCULATE PARTICLE REDUCTION *****************
CC      ***********************************************************

        I=1
        J=1
        DO 80 J=1,NT
        DO 70 I=1,NX

        PDA= RKP*T(I,J)
        CDA= RKC*T(I,J)
        RN=TC(I)/(TC(I)-TP(I))

        CI(I,J)=COUT
        IF (I.EQ.1) CI(I,J)=CIN(J)

CC      ****************** REDUCTION EQUATION ***************************

        C(I,J)=(CI(I,J)*EXP(-PDA/PORT(I)))/((1+((CDA/(1-PORT(I))/RN))**RN))

CC      ***********************************************************

        COUT=C(I,J)

CC      ***********************************************************
CC      ************** PRINT OUTPUT DATA ******************************
CC      ***********************************************************
```

```
      PRINT 55,J,I,COUT,RN
      WRITE(IPR,55) J,I,COUT,RN
 55   FORMAT(I5,5X,I5,5X,F15.5,6X,F4.2)

70    CONTINUE
80    CONTINUE

CC    ************ WRITE ENDING TIME **********************************

      CALL GETTIM(IHR2,IMIN2,ISEC2,I100TH)
      WRITE(*,92) IHR2,IMIN2,ISEC2
 92   FORMAT(//1X,'END TIME IS     ',I2.2,1H:,I2.2,1H:,I2.2)

      ISEC=ISEC2
      IMIN=IMIN2
      IHR=IHR2
      IF(ISEC1.GT.ISEC2) THEN
      ISEC=ISEC2+60
      IMIN=IMIN2-1
      ENDIF
      IF(IMIN1.GT.IMIN) THEN
      IMIN=IMIN+60
      IHR=IHR-1
      ENDIF
      IF(IHR1.GT.IHR) IHR=IHR+24
      IHR=IHR-IHR1
      IMIN=IMIN-IMIN1
      ISEC=ISEC-ISEC1
      WRITE(*,*)
      WRITE(*,93) IHR,IMIN,ISEC
 93   FORMAT(/1X,'TOTAL RUNTIME IS ',I2.2,1H:,I2.2,1H:,I2.2)
      WRITE(*,90)
      STOP
      END
```

A.7. Input and Output for the Wetland Particle Model

The following text represents the printout for the input and output files for the Wetland Particle Module. The input file is accompanied with a table explaining the input values. The output file is self-explanatory.

A.7.1. WPM Input File

```
9,2
.005, .005
10000.
12000.
14000.
15000.
13000.
12500.
11500.
11000.
10000.
0.5, 14., 10.
27.7148
27.71391
27.71391
26.63289
20.28914
20.82164
21.44146
21.37036
26.71032
0.5, 16., 10.
3.63521
3.63437
3.63437
3.62454
2.26545
2.80618
2.90435
2.97736
```

Table A.2. Variable Definition Table for the WPM Input File

Input Line(s)	Value	Variable	Definition
1	9	NT	Total number of time steps.
1	2	XT	Total number of segments.
2	0.005	RKP	PFR reduction rate.
2	0.005	RKC	CSTR reduction rate.
3 through 11		CIN(NT)	Input concentration for each time step up to NT.
12	0.5	PORT(1)	Portion of transport behavior attributed to PFR in first segment (S1) .
12	14.0	TC(1)	Observed time of centroid for CSTR in S1.
12	10.0	TP(1)	Observed time of peak for CSTR in S1.
13 through 21		T(1,NT)	Retention times (from DYNAWET output) for S1 for NT time steps.
22		PORT(2)	Portion of transport behavior attributed to PFR in second segment (S2) .
22		TC(2)	Observed time of centroid for CSTR in S2.
22		TP(2)	Observed time of peak for CSTR in S2.
23 through 31		T(2,NT)	Retention times (from DYNAWET output) for S2 for NT time steps.

A.7.2. WPM Output File

PARTICLE MODEL FOR USE WITH
DYNAMIC ROUTING MODEL (DYNAWET)
FOR NATURALLY OCCURRING WETLANDS

********** ECHO OF INPUT DATA **********
****

TOTAL TIME STEPS = 9
TOTAL SEGMENTS = 2

0.0050 = PLUG FLOW REDUCTION RATE
0.0050 = CONTINUOUS STIRRED TANK REACTOR REDUCTION RATE

TIME STEP	INPUT CONCENTRATION
1	10000.000
2	12000.000
3	14000.000
4	15000.000
5	13000.000
6	12500.000
7	11500.000
8	11000.000
9	10000.000

SEGMENT NUMBER: 1
0.5000 = PROPORTION PFR
14.0000 = CSTR CENTROID TIME
10.0000 = CSTR PEAK TIME

TIME STEP = 1 RETENTION TIME = 27.7148
TIME STEP = 2 RETENTION TIME = 27.7139
TIME STEP = 3 RETENTION TIME = 27.7139
TIME STEP = 4 RETENTION TIME = 26.6329
TIME STEP = 5 RETENTION TIME = 20.2891
TIME STEP = 6 RETENTION TIME = 20.8216
TIME STEP = 7 RETENTION TIME = 21.4415
TIME STEP = 8 RETENTION TIME = 21.3704
TIME STEP = 9 RETENTION TIME = 26.7103

SEGMENT NUMBER: 2
0.5000 = PROPORTION PFR
16.0000 = CSTR CENTROID TIME
10.0000 = CSTR PEAK TIME

TIME STEP = 1 RETENTION TIME = 3.6352
TIME STEP = 2 RETENTION TIME = 3.6344
TIME STEP = 3 RETENTION TIME = 3.6344
TIME STEP = 4 RETENTION TIME = 3.6245
TIME STEP = 5 RETENTION TIME = 2.2655
TIME STEP = 6 RETENTION TIME = 2.8062
TIME STEP = 7 RETENTION TIME = 2.9044
TIME STEP = 8 RETENTION TIME = 2.9774
TIME STEP = 9 RETENTION TIME = 3.4512

********** OUTPUT DATA **********

TIME STEP	SEGMENT	CONCENTRATION	# OF CSTRS
1	1	7578.36475	3.50
1	2	7307.74463	2.67
2	1	9094.11816	3.50
2	2	8769.44531	2.67
3	1	10609.80469	3.50
3	2	10231.01953	2.67
4	1	11491.41016	3.50
4	2	11082.24121	2.67
5	1	10612.27148	3.50
5	2	10374.52734	2.67
6	1	10149.87012	3.50
6	2	9868.95313	2.67
7	1	9280.12988	3.50
7	2	9014.42578	2.67
8	1	8882.96484	3.50
8	2	8622.33203	2.67
9	1	7655.00049	3.50
9	2	7395.24805	2.67

BIBLIOGRAPHY

Abbott, M.B. and F. Ionescu. 1967. "On the Numerical Computation of Nearly Horizontal Flows." *J.Hydraul Res* 5(2):97-117.

Amein, M., C.S. Fang and S. Ching. 1970. " Implicit Flood Routing in Natural Channels." *Asce Proceedings, Journal Of The Hydraulics Division* 96(Hy12):2481-500.

Amein, M. and H.L. Chu. 1975. " Implicit Numerical Modeling of Unsteady Flows." *J.Hydraul.Div., Am.Soc.Civ.Eng.* 101(Hy6):717-31.

APHA, AWWA and WPCF. 1998. Standard Methods for the Examination of Water and Wastewater. 20th. Washington, D.C.: American Public Health Association.

ASTM (American Society for Testing and Materials). 1992. "Method D 5613-94:Standard Test Method for Open-Channel Measurement of Time of Travel Using Dye Tracers." In: ASTM (American Society for Testing and Materials), Annual Book of ASTM Standards, Section 11 Water and Environmental Technology. ASTM, Philadelphia, Pa., p. 736-45.

Baltzer, R.A. and C. Lai. 1968. "Computer simulation of unsteady flows in waterways." *J.Hydraul.Div., Am.Soc.Civ.Eng.* 94(Hy4):1083-117.

Brinson, M.M. 1993. A Hydrogeomorphic Classification for Wetlands. U.S. Army Corps of Engineers, Washington, D.C. Wetlands Research Program, Technical Report WRP-DE-4.

Chaudhry, Y.M. and D.N. Contractor. 1973. "Application of the Implicit Method to Surges in Channels". *Water Resources Research* 9(6):1605-12.

Chow, V.T. 1959. Open-Channel Hydraulics. McGraw-Hill, New York, New York. 680 pp.

Chow, V.T., D.R. Maidment and L.W. Mays. 1988. Applied Hydrology. McGraw Hill, New York, New York. 572 pp.

Costanza, R. and F.H. Sklar. 1985. "Articulation, Accuracy and Effectiveness of Mathematical Models: a Review of Freshwater Wetland Applications." *Ecological Modelling* 27(1/2):45-68.

Cowardin, L.M., V. Carter, F.C. Golet and E.T. LaRoe. 1979. Classification of Wetlands and Deepwater Habitats of the United States. U.S. Fish and Wildlife Service Biological Services Program Report FWS/OBS - 79/31., Washington, DC. pp.103.

Danckwerts, P.V. 1953. "Continuous Flow Systems:Distribution of Residence Times." *Chem.Eng.Sci.* 2(1):1-13.

DeLong, LL. 1986. Extension of the Unsteady One-dimensional Open-channel Flow Equations for Flow Simulation in Meandering Channels with Flood Plains. USGS Water Supply Paper 2290. U.S. Geological Survey, Denver, CO. 101 pp.

DeLong, LL. 1989. "Mass Conservation: 1-d Open Channel Flow Equations." *J.Hydraul.Eng.* 115(2):263-9.

Elder, J.F. 1987. "Indicator Bacteria Concentrations as Affected by Hydrologic Variables in the Apalachicola River, Florida." *Water, Air, and Soil Pollution* WAPLAC 32(3):407-16.

Engman, E.T. 1989. "Applicability of Manning 's n Values for Shallow Overland Flow." *Proceedings of the International Conference on Channel Flow and Catchment Runoff: Centennial of Manning 's Formula and Kuichling 's Rational Formula.* University of Virginia, Charlottesville VA. 299 pp.

Fenzl, R.N. 1962. Hydraulic Resistance of Broad Shallow Vegetated Channels. Doctoral Dissertation, University of California at Davis, California.

Fisher, P.J. 1990. "Hydraulic Characteristics of Constructed Wetalnds at Richmond. NSW, Australia." In:. Constructed Wetlands in Water Pollution Control. P.F.Cooper, B.C.Findlater, editors Oxford, U.K.:Pergamon Press. p 21-31.

Fread, D.L. and Smith GF. 1978. "Calibration Technique for 1-D Unsteady Flow Models" *Journal of the Hydraulics Division, American Society of Civil Engineers* 104(HY7):1027-1044

Fread, D.L. and T.E.Harbaugh. 1971. "Open-channel Profiles by Newton's Iteration Technique." *Journal of Hydrology* 13(1):70-80.

Fread, D.L. 1973. "Technique for Implicit Dynamic Routing in Rivers with Tributaries." *Water Resources Research* 9(4):918-26.

Fread, D.L. 1974. Numerical Properties of Implicit Four-point Finite Difference Equations of Unsteady Flow. HRL-45, NOAA Technical Memorandum NWS HYDRO-18, Hydrologic Research Laboratory, National Weather Service, Silver Springs, MD. 38 pp.

Fread, D.L. 1976. "Flood Routing in Meandering Rivers with Flood Plains." In Proceedings for: *Rivers '76, Symposium on Inland Watersways for Navigation,Flood Control, and Water Diversions, August 10-12, 1976. Fort Collins, Colo.*, Colorado State University, Fort Collins, Colo. Volume I, p16-35.

Fread, D.L. 1985. "Channel Routing". In: Hydrological Forecasting, (Eds: M.G. Anderson and T.P. Burt), John Wiley and Sons, New York, New York. Chapter 14, p 437-503.

Fread, D.L. and J.M.Lewis. 1998. NWS FLDWAV Model: Theoretical Description, User Documentation. Hydrologic Research Laboratory, Office of Hydrology, National Weather Service, NOAA, Silver Springs, MD. 335 pp.

Gupta RS. 1989. Hydrology and Hydraulic Systems. Prentice-Hall Inc. Englewood Cliffs, NJ. 739 pp.

Hall, B.R. and G.E. Freeman. 1994. "Study of Hydraulic Roughness in Wetland Vegetation Takes New Look at Manning's n." *Wetlands Res. Program Bull.* 4(1):1-4.

Hammer, D.A. and R.K. Bastian. 1989. "Wetlands Ecosystems: Natural Water Purifiers". In: Constructed Wetlands for Wastewater Treatment, Municipal, Industrial, and Agricultural (Ed. D.A. Hammer), Lewis Publishers, Chelsea, Michigan. p 5-19.

Hammer, D.E. and R.H. Kadlec. 1983. Design Principals for Wetland Treatment Systems. U.S. EPA. Report 600/2-83-026, USEPA Office of Research and Development Ada, Ohio.

Hammer, D.E. and R.H. Kadlec. 1986. "A Model for Wetland Surface Water Dynamics." *Water Resources Research* 22(13):1951-1958.

Hargesheimer, E.E., C.M. Lewis, and C.M. Yentsch. 1992. Evaluation of Particle Counting as a Measure of Treatment Plant Performance.: AWWA Research Foundation and American Water Works Association, Denver, CO. 319 pp.

Jadhav, R.S. 1994. Modeling Hydraulic Performance of Free Water Surface Constructed Wetlands." Masters Thesis, University of Cincinnati, Cincinnati, Ohio. 82 pp.

Jadhav, R.S. and S.G. Buchberger. 1995. "Effects of Vegetation on Flow Through Free Water Surface Wetlands." *Ecol.Eng.* 5(4):481-96.

Jarosewich, M. 1987. "Rapid Assessment of the Hydraulics and Hydrology of Wetlands for Wastewater Treatment." In Proceedings: *National Wetland Symposium on Wetland Hydology September 16-18, 1987, Chicago Illinois*, Association of State Wetland Managers Inc. Berne, New York. p 185-191.

Johnston, C.A., T. Johnson, M. Kuehl, D. Taylor, and J Westman. 1990. The Effects of Freshwater Wetlands on Water Quality: Compliation of Literature Values. USEPA, Corvallis Research Laboratory, Corvallis, OR. 178 pp.

Kadlec, R.H., D.E. Hammer, In-Sik Nam, and J.O. Wilkes. 1981. "The Hydrology of Overland Flow in Wetlands." *Chem.Eng.Commun.* 9:331-44.

Kadlec, R.H. 1990. "Overland Flow in Wetlands: Vegetation Resistance." *J.Hydraul Eng.* 116(5):691-706.

Kadlec, R.H. 1994. "Detention and Mixing in Free Water Wetlands." *Ecol.Eng.* 3(4):1-36.

Kadlec, R.H. and R.L. Knight. 1996. Treatment Wetlands. Lewis Publishers, Boca Raton, FL. 848 pp.

Levenspiel, O. 1999. Chemical Reaction Engineering. Third ed. John Wiley & Sons, Inc. New York, NY. 668 pp.

Liggett, J.A. and J.A. Cunge. 1975. "Numerical Methods of Solution of the Unsteady Flow Equations." In: Unsteady Flow in Open Channels. (Eds: K. Mahmood and V.Yevjevich). Water Resources Pub., Fort Collins, Co. Chp. 4, p 89-182.

MacVicar, T.K. 1985. A Wet Season Field Test of Experimental Water Deliveries to Northeast Shark River Slough. Report 85-3. South Florida Water Management District, West Palm Beach, FL.

Mierau, R. and P. Trimble. 1988. Hydrologic Characteristics of the Kissimmee River Floodplain Boney Marsh Experimental Area. South Florida Water Management District, West Palm Beach, FL.

Miller, D.C. 1987. "Predicting the Impact of Vegetation on Storm Surges" In: *Wetland Hydrology: Proceedings of the National Wetland Symposium, Chicago, Illinois, September 16-18,1987.* Association of State Wetland Managers, Inc. Berne, New York. p 113-119.

Mitsch, W.J. and B.C. Reeder. 1991. "Modelling Nutrient Retention of a Freshwater Coastal Wetland." *Ecological Modelling* 54:151-87.

Mitsch, W.J. and J.G. Gosselink. 1993. Wetlands. Second edition. Van Nostrand Reinhold. New York. 722 pp.

Novotny, V., K.R. Imhoff, M. Olthof and P.A. Krenkel. 1989. Handbook of Urban Drainage and Wastewater Disposal. John Wiley and Sons. New York. 390pp.

Pilgrim, D.J., T.J. Schulz, and I.D. Pilgrim. 1992. "Tracer Investigation of Flow Patterns in Two Field Scale Constructed Wetlands with Subsurface Flow". *Proceedings of 3rd International Conference on Wetland Systems for Water Pollution Control.* Sydney, Australia.

Preissmann, A. 1961. "Propagation of Translatory Waves in Channels and Rivers". In: *Proceedings, First Congress of French Association for Computation.* Grenoble, France. p 433-442.

Price, R.K. 974 Jul 1. Comparison of Four Numerical Methods for Flood Routing [Abstract]. *Journal Of The Hydraulics Division, ASCE* 100(Hy 7):879-99.

Roberson, J.A., C.T. Crowe. 1990. Engineering Fluid Mechanics. forth edition. Boston: Houghton Mifflin Co. 0-395-38124.

Roig LC, I.P.King. 1992. "Continuum Model for Flows in Emergent Marsh Vegetation." In: *Proceedings of the 2nd International conference on Estuarine and Coastal Modeling, November 13-15,1992*, ASCE :pp 268-279..

Saint-Venant Bd. 1871. Theory of Unsteady Water Flow, with Application to River Floods and to Propagation of Tides in River Channels. Computes Rendus, (Translated into English by U.S.Corps of Engrs., No.49-g,Waterways Experiment Station, Vicksburg, Miss., 1949.) 73:148-54,-237-40.

Schueler TR. 1992. Design of Stormwater Wetland Systems: Guidelines for Creating Diverse and Effective Wetlands in thr Mid-Atlantic Region. Washington, D.C.: Metropolitan Washington Council of Governments.

Shih SF, A.C.Federico, J.F.Milleson, M.Rosen. 1979. "Sampling Programs for Evaluating Upland Marsh to Improve Water Quality". *Trans.ASAE* 22:828-33.

Shih SF, G.S.Rahi. 1982. Seasonal Variations of Manning's roughness coefficient in a Subtropical Marsh. *Trans.ASAE* 25:116-20.

Shilton AN, and J.N.Prasad. 1996. "Tracer Studies of a Gravel Bed Wetland". *Wat.Sci.Tech.* 34(3-4):421-5.

Smith RH. 1978. Development of a Dynamic Flood Routing Model for Small Meandering Rivers. University of Missouri.

Stairs, D. B. and J. A. Moore. 1994. "Flow Characteristics of Constructed Wetlands: Tracer Studies of the Hydraulic Regime". In: *Proceedings of 4th International Conference on Wetland Systems for Water Pollution Control.* Guangzhou, China.

Stern, D.A., L.L.Janus; R.Khanbilvardi; J.C.Alair; W.R.Richardson,P.B.McCann; Y.A.Gorokhovich 1998. "Estimating Flow Velocities through a Natural Wetland." In: *Water resources Engineering '98, Proceedings of the International Water Resources Engineering Conference. August 1998.* ASCE, Reston, Va. p 502-507

Stowell, R., G.Tchobanoglous, J.Colt, and A.Knight. 1979. The Use of Aquatic Plants and Animals for the Treatment of Wastewater. Departments of Civil Engineering and Land, Air and Water Resources, University of California, Davis, CA. 639 pp.

Strelkoff, T. 1970. "Numerical Solution of Saint-Venant Equations". *J.Hydraul.Div., Am.Soc.Civ.Eng.* 96(HY1):223-52.

Tiner, R.W. 1997. Keys to Landscape Position and Landform Descriptors for U.S. Wetlands (Operational Draft). U.S. Fish and Wildlife Service, Northeast Region, Hadley, MA. 11 pp.

Turner Designs Inc., 1981. Model 10 Operational Manual. Turner Designs Inc. Sunnyvale, CA. 35 pp.

U.S. Army Corps of Engineers. 1995. CE-QUAL-RIV1: A Dynamic, One-Dimensional (Longitudinal) Water Quality Model for Streams User's Manual. Report EL-95-2 United States Army Corps of Engineers, Waterways Experimental Station. Vicksburg, MS.

U.S. Environmental Protection Agency. 1985. Freshwater Wetlands for Wastewater Management, Environmental Assessment Handbook. Atlanta, GA.: EPA Region IV. EPA-904/9-85-135.

U.S. Environmental Protection Agency. 1989. Drinking Water; National Primary Drinking Water Regulations; Filtration, Disinfection, Turbidity, *Giardia lamblia*, Virures, *Legionella*, and Heterotrophic Bacteria; Final Rule. *Federal Regulation* 54:27486-541.

U.S. Geological Survey. 1997. Full Equations (FEQ) model for the solution of the full, dynamic equations of motion for one-dimensional unsteady flow in open channels and through control structures. U.S. Geological Survey Water-Resources Investigations Report 97-4037 Franz DD, and C.S.Melching Authors. Reston, VA. 205pp.

Wilson, J.F., E.D.Cobb, F.A.Kilpatrick. 1986. Fluorometric Procedures for Dye Tracing. U.S. Geological Survey Denver, CO .